Freie Universität Berlin

Fachbereich Erziehungswissenschaft
und Psychologie

LANGUAGES
OF
EMOTION

Neural Correlates of Joy and Fear Evoked by Musical Stimulation: Extensive Investigations of Network Differences and Modulations by fMRI Scanner Noise, fMRI Magnetic Field Strength and a Physiological Measure of Emotional Personality

Dissertation

zur Erlangung des akademischen Grades

Doktor der Philosophie (Dr. phil.)

Doctor of Philosophy (Ph.D.)

vorgelegt von

BSc/MSc Stavros Skouras

in Berlin, 2013

Supervisor:

Prof. Dr. Stefan Koelsch

Erstgutachter:

Prof. Dr. Malek Bajbouj

Zweitgutachter:

Prof. Dr. Hauke Heekeren

Datum der (letzten) mündlichen Prüfung: 17/12/2013

Acknowledgements

I would like to give special thanks to all the people who have believed in me and supported me through my doctoral studies:

- my family; especially Gella, Thanos, Spyros, Nikos and Lella
- my supervisors; especially Stefan Koelsch
- the members of the Neurocognition of Music research group; especially Sebastian Jentschke, Aleksandra Gulka, Moritz Lehne, Regula von Schintling, Kamila Borowiak, Vienna Doenni, Yu Fukuda, Matts Kuessner and Corinna Bonhage.
- faculty members from the University of Sussex that assisted in various ways; especially Brendan Weekes, Hugo Critchley, Marcus Gray, Alan Garnham, Ben Dyson and Chris Darwin.
- The radiographers involved in the fMRI experiments; especially Christian Kainz and Jan Bush
- The LIPSIA team; especially Karsten Mueller and Erik Tuerke

Contents

English Summary 1

Deutsche Zusammenfassung 2

List of Figures and Tables 3

1. Introduction and Synopsis 3

1.1 On the use of Music in Neuroscience . . . 3

1.2 On Quantifying Emotions through fMRI. . . 4

1.3 Synopsis of the thesis . . . 6

1.4 fMRI and the Statistical Analysis Methods Utilized . . . 12

- 1.4.1 General Linear Modeling . . . 12
- 1.4.2 Eigenvector Centrality Mapping . . . 13
- 1.4.3 Functional Connectivity . . . 13
- 1.4.4 Psychophysiological Interaction . . . 13

1.5 References . . . 14

2. Neural correlates of music-evoked fear and joy:
The roles of auditory cortex and superficial amygdala 19

2.0 Abstract . . . 20

2.1 Introduction . . . 21

- 2.1.1 Summary of Hypotheses . . . 27

2.2 Methods . . . 28

- 2.2.1 Participants . . . 28
- 2.2.2 Stimuli and Procedure . . . 29
- 2.2.3 MR Scanning . . . 35
- 2.2.4 Data Analysis . . . 35
  - 2.2.4.1 Temporal Interaction Analysis . . . 36
  - 2.2.4.2 Psychophysiological Interaction . . . 37

2.3 Results . . . 38

- 2.3.1 Behavioral Data . . . 38

    2.3.2 fMRI Data 39
2.4 Discussion 49
    2.4.1 Summary of Results 49
    2.4.2 Auditory cortex and emotional processing 50
    2.4.3 Superficial amygdala and its role for joy and fear 54
    2.4.4 Primary somatosensory cortex (S1) 58
2.5 Conclusions 59
2.6 Acknowledgements 60
2.7 References 61
2.8 Supplementary Material 72

3. Eigenvector Centrality Mapping of sustained emotion 73

3.0 Abstract 74
3.1 Introduction 75
3.2 Materials and Methods 80
    3.2.1 Participants 80
    3.2.2 Stimuli 80
    3.2.3 Procedure 81
    3.2.4 MR Scanning 82
    3.2.5 Data Analysis 83
3.3 Results 85
    3.3.1 Behavioral Data 85
    3.3.2 fMRI Data 85
        3.3.2.1 Functional Connectivity Analysis 88
3.4 Discussion 91
3.5 Conclusions 98
3.6 Acknowledgements 99
3.7 References 99
3.8 Supplementary Material 109

4. Superficial Amygdala and Hippocampal Activity During Affective Music Listening at 3 T but not 1.5 T fMRI 111
4.0 Abstract 112
4.1 Introduction 113
4.2 Methods 116
  4.2.1 Participants 116
  4.2.2 Stimuli 117
  4.2.3 Procedure 118
  4.2.4 MR Scanning 120
  4.2.5 Behavioral Data Analysis 120
  4.2.6 fMRI Data Analysis 121
4.3 Results 122
  4.3.1 Behavioral Results 122
  4.3.2 fMRI Results 123
4.4 Discussion 125
4.5 Acknowledgements 128
4.6 References 129
4.7 Supplemental Material 136
5. Scanner noise interaction with affective neural processes 137
5.0 Abstract 138
5.1 Introduction 139
5.2 Methods 144
  5.2.1 Participants 144
  5.2.2 Stimuli 145
  5.2.3 Procedure 146
  5.2.4 MR Scanning 147
  5.2.5 Data Analysis 149
5.3 Results 151

5.3.1 Behavioral Data 151
5.3.2 fMRI Data. 153
5.4 Discussion 157
5.5 Conclusion 163
5.6 References 164
5.7 Supplementary Material 179

6. Neural correlates of emotional personality:

A structural and functional magnetic resonance imaging study 181

6.0 Abstract 181
6.1 Introduction 183
6.1.1 Physiological measures of personality 187
6.1.2 The present study 191
6.2 Experiment 1: Functional MRI using Eigenvector Centrality Mapping (ECM) 193
6.2.1 Materials and Methods 193
6.2.1.1 Participants 193
6.2.1.2 Experimental procedure 194
6.2.1.3 MR Scanning 197
6.2.1.4 ECG data analysis 197
6.2.1.5 Functional MRI data analysis 198
6.2.1.6 Comparison of NEO and ECG data 200
6.2.2 Results 201
6.2.2.1 Relations between cardiac (ECG) and psychological (NEO) data 201
6.2.2.2 Relations between behavioral ratings and ECG / NEO data 201
6.2.2.3 Psychological (NEO) measures and ECM data 203
6.2.2.4 Physiological (cardiac) measures and ECM data 207
6.2.3 Discussion 208
6.2.3.1 Functional MR data and psychological (NEO) measures 208
6.2.3.2 Functional MR data and physiological Ek measure 210

6.2.3.3 Emotion-specificity of ECM results 212
6.3 Experiment 2: Structural MRI using Voxel Based Morphometry (VBM) 213
6.3.1 Materials and Methods 214
6.3.1.1 Participants 214
6.3.1.2 Experimental procedure 214
6.3.1.3 MR Scanning 215
6.3.1.4 Structural MRI data analysis 215
6.3.2 Results 217
6.3.2.1 Relations between ECG and NEO data 217
6.3.2.2 Psychological (NEO) measures and VBM data 217
6.3.2.3 Physiological (cardiac) measures and VBM data 218
6.3.3 Discussion 220
6.3.3.1 Structural MR data and psychological (NEO) measures 220
6.3.3.2 Structural MR data and physiological Ek measure 221
6.4 General Discussion 221
6.4.1 Summary of results 221
6.4.2 Relations between cardiac and NEO measures 222
6.4.3 The functional significance of the hippocampal formation for emotional personality 225
6.4.4 Limitations 229
6.5 Conclusions 230
6.6 Acknowledgments 231
6.7 References 232
6.8 Supplementary Material 251

Appendix 257

Selbständigkeitserklärung 257
Publications related to the thesis 258
Curriculum Vitae 259

List of Figures and Tables

Figure 1.1: Summary of most important findings from the thesis 11

Fig. 2.1: Experimental design 34

Table 2.1: Descriptive statistics of behavioral data 40

Figure 2.2: Behavioral ratings of participants on the four emotion scales used in the present study 40

Table 2.2: Results of General Linear Model (GLM) contrasts 41

Figure 2.3: FMRI results 42

Figure 2.4: Timelines depicting average BOLD signal intensity in the regions that significantly differed in the GLM contrast joy vs fear 44

Table 2.3: Results of the interaction contrast of emotion (joy vs. fear) × time (1st half vs. 2nd half of each trial) 46

Table 2.4: Results of PPI analysis 48

Figure 3.1: Experimental design 78

Table 3.1: Descriptive statistics of behavioral data 86

Figure 3.2: Behavioral ratings 86

Table 3.2: Results of the ECM contrast emotion (joy > fear) 87

Table 3.3: Results of the emotion-specific functional connectivity analyses (contrast: joy > fear) 89

Figure 3.3: fMRI results 90

Figure 3.4: Summary of results 92

Table 4.1: Descriptive statistics, ANOVA and post-hoc t-tests for behavioral data 122

Table 4.2: Results of GLM contrast joy > fear 124

Figure 4.1: fMRI Results 124

Figure 5.1: Experimental design 148

Figure 5.2: Behavioral ratings of participants on the four emotion scales used 152

Table 5.1: fMRI results 155

Figure 5.3: fMRI results 156

Table 6.1: Overview of personality-related functional and structural brain differences reported in studies using subjective measures of personality 186

Figure 6.1. Illustration of procedure and data analysis 188

Box 6.1: Modulatory influence of psychological factors on regional cardiac activity . . . 190

Table 6.2: Results of agreeableness regression 204

Table 6.3: Results of the ECM constrasts high vs low 205

Figure 6.2. Experiment 1: Functional neuroimaging data (ECM) 206

Figure 6.3. Experiment 2: Structural neuroimaging data (VBM) 219

English Summary

The research conducted for the present doctoral dissertation aimed to expand the knowledge on the neural correlates of joy and fear as well as to investigate the extent to which such correlates can be influenced by fMRI magnetic field strength, fMRI scanner noise and the Eκ physiological index taken to reflect emotional personality. To this purpose, a specialized psychoacoustically balanced stimulus set comprising of happy, neutral and fearful musical excerpts was created and utilized in five fMRI experiments.

The findings suggest the superficial amygdala to be the brain structure exhibiting the greatest increases in activity and centrality during joy, compared to fear. Moreover, this difference in activity is influenced by fMRI magnetic field strength, being statistically significant at 3 Tesla but not at 1.5 Tesla.

Findings also suggest the auditory cortex to be significantly more active during joy than fear. Additionally to the amygdala, the auditory cortex was found to posess an important role related to the processing of emotions elicited through musical stimulation. The auditory cortex was found to exhibit emotion-specific functional connectivity with a variety of visual, parietal, and limbic/paralimbic structures.

Furthermore, the centrality of the auditory cortex was found to be greater in participants with higher values of the Eκ index. The findings also suggested that together with the visual cortex, the auditory cortex is the locus of a statistical interaction effect between scanner noise and emotion.

Deutsche Zusammenfassung

Die im Rahmen dieser Doktorarbeit durchgeführten Studien verfolgen das Ziel, neue Erkenntnisse über die neuronalen Korrelate von Freude und Furcht zu gewinnen. Außerdem untersuchen sie die Beeinflussung dieser Korrelate durch die magnetische Feldstärke und den Lärmpegel des Magnetresonanztomographen sowie durch das physiologische Maß emotionaler Persönlichkeitsmerkmale Ek. Zu diesem Zweck wurden spezielle, psychoakustisch ausbalancierte Stimuli aus fröhlichen, neutralen und furchteinflößenden Musikausschnitten zusammengestellt und in fünf fMRT-Experimenten verwendet.

Die Ergebnisse deuten darauf hin, dass die Amygdala die Hirnstruktur mit der größten Zunahme an Aktivität und Zentralität während des Erlebens von Furcht im Vergleich zu Freude ist. Dieser Aktivitätsunterschied wird durch die magnetische Feldstärke des Magnetresonanztomographen beeinflusst und ist für 3 Tesla aber nicht für 1,5 Tesla statistisch signifikant.

Die Ergebnisse zeigen außerdem, dass der auditorische Kortex bei Freude signifikant stärker aktiviert ist als bei Furcht. Ferner scheint der auditorische Kortex neben der Amygdala eine wichtige Rolle in durch Musik evozierter emotionaler Verarbeitung zu spielen und weist eine emotionsspezifische funktionale Konnektivität mit einer Vielzahl visueller, parietaler und limbischer/paralimbischer Strukturen auf.

Desweiteren gibt es einen positiven Zusammenhang zwischen der Zentralität des auditorischen Kortex' und den Werten des Ek-Index'. Die Ergebnisse zeigen zudem einen statistischen Interaktionseffekt im auditorischen Kortex (und im visuellen Kortex) zwischen dem Lärmpegel des Magnetresonanztomographen und Emotion.

Introduction and Synopsis

The present work extends across a wide scope of neuroscientific fields, such as affective neuroscience, auditory cognitive neuroscience, applied functional network connectivity theory, magnetic resonance imaging methods optimization and personality research. Extensive literature reviews covering the topics relevant to each chapter are presented therein. The purpose of the present introduction is to provide an overview of the findings and to clarify their novelty and complementarity, binding them together to form a broad perspective that encompasses all the research questions addressed. Special effort has been put into avoiding the use of the highly technical terminology, characterizing the rest of the chapters, with the aim of making this overview accessible to all psychologists.

1.1 On the use of Music in Neuroscience

Using music to conduct neuroscientific research is often assumed to be pertaining to unraveling the neural processes through which music exerts its indisputable effects on psychological states (Gabrielsson, Juslin, 2003; Västfjäll 2002). This is a common misconception as the aim in this research field is not understanding “musical” neural processes per se. “Musical neuroscientists” are using music rather as the preferred medium of stimulation in much the same way other neuroscientists use words, pictures and videos. Using music can be very fruitful for gaining insight into basic cognitive processes as well as pathological conditions, as demonstrated by advances made over the past 20 years.

The musical approach to the study of cognition has allowed for a more accurate understanding of language processes by determining what is unique to language processing and what is shared with music processing (Patel 2003, 2009, 2012). In turn this increased understanding has shaped new methods of treating patients, specifically by using singing to facilitate the rehabilitation of stroke patients with impaired verbal abilities (Schlaug et al. 2008, 2010; Norton et al. 2009). Beyond furthering the understanding of basic cognitive processes such as attention and memory (Janata et al. 2002; Koelsch et al. 2009), using music to study the brain and human psychology generally, is also beginning to help with some of the most challenging psychiatric and neurological contemporary challenges such as Parkinson's disease (Bernatzky et al. 2004 ; Wan et al. 2010), Dementia (Sarkamo, 2012 ; Bertelli, 2011), Schizophrenia (Silverman 2003, Ulrich et al. 2007; Peng 2010; Yang 1998) and Depression (Osuch et al. 2009; Aust et al. 2013).

1.2 On Quantifying Emotions through fMRI

The quantification of emotions is in essence an effort to encode the activity of the psyche into statistically meaningful terms, to capture subtle conscious and subconscious processes in 4D images of brain activity representing timeseries of observations of values of miniscule points of measurement.

Emotional experiences were traditionally thought of as comprising the most intimate realm of our conscious life and were considered to be private and characteristic to the human species. Yet, evidence is accumulating to suggest that even small animals such as rodents, posess and express at least three distinct emotional states: joy, fear, and neutral (the absence of fear or joy); that these emotions are hardwired into the organisms' genetics, serving an evolutionary role by facilitating adaptation through learning and motivating appropriate behaviours such as avoiding dangerous environments or revisiting sources of nutrition and warmth (Panksepp, Burgdorf, 2003).

In human psychology, the emotional components of cognition are of profound importance as impaired emotional functioning is an early marker of practically every psychopathological state (Mannie et al. 2007; Hoekert et al. 2007; Connan et al. 2003; Leppännen et al. 2006; Kang et al. 2012). It is therefore important to understand these emotional processes and musical stimulation is a useful tool as the reason music has been used throughout the centuries is primarily to induce transient emotional experiences (Perlovsky, 2009).

The present work has been focused towards the aim of furthering scientific understanding of the neural processes associated with the two most biologically important emotions: joy and fear. The predominant psychological importance of joy and fear over other emotions is reflected in the fact that they are the two main emotions implicated in behavioural learning through conditioning.

1.3 Synopsis of the thesis

Through 5 research articles, detailed emotional networks activated during emotional music listening have been identified. Moreover, the first steps in the investigation of as yet underexplored ways in which emotional functioning can be influenced by factors such as personality, fMRI scanner noise and fMRI magnetic field strength have been made.

The first study (Chapter 2) utilized General Linear Modelling (GLM) and Psychophysiological Interaction (PPI) analyses to investigate differences in neural activity between joy and fear. The study emphasised on the temporal evolution of these emotions and the emotion-specific patterns of functional connectivity, during 30 seconds of emotional music listening.

The second study (Chapter 3) utilized Eigenvector Centrality Mapping (ECM) and Functional Connectivity (FC) analyses to investigate differences in network centrality across longer periods of musical stimulation in the range of a few minutes. ECM differences are taken to reflect differences in the computational importance of specific areas under different experimental conditions. FC unveiled the networks responsible for the observed differences in centrality.

In cohort, the first two studies serve to show the importance of the superficial amygdala (SF) for the manifestation of the emotional state of joy. The first study shows that an initial burst of SF activity can serve to differentiate joy from fear. The second study shows that even after this initial burst, the SF maintains a crucial computational role in the manifestation of joy, by exhibiting an increase in centrality and in the influence it exerts on the activity across the rest of the brain.

The third study (Chapter 4) shows that the observed significant difference in SF activity between music-elicited joy and fear is observable only when the most advanced commercially available imaging equipment, featuring very strong magnetic fields (3 Tesla), is utilized. As this technology is relatively recent, the finding alerts one to the possibility of previous research having missed the significance of the SF.

The fourth study (Chapter 5) shows that the auditory cortex (AC) is similarly influenced in its responsiveness to affective stimuli by the presence of scanner noise. As scanner noise decreases, the ability of the AC to differentiate between subtle affective states becomes more precise.

In cohort, the third and fourth studies show that the power to distinguish between emotional states based on brain data is limited by technological constraints. These constraints seem to have the most impact on precisely the brain regions that have the most potential in offering the discriminative information of interest.

The fifth study (Chapter 6) suggests that AC activity is more central and influential on overall brain functioning in more emotional individuals. This is in good accordance with the results from the first study. In cohort, the first and fifth studies show that increased activity in the AC is essential to the appreciation of joy that is driven by auditory stimulation and that the brains of individuals who are of a more emotional personality are likely to be neurally configured in a way that maximises the impact of AC activity on their brain state during music listening.

In summary, the present work serves to extend the current knowledge of affective functioning of the human brain by revealing detailed emotion-specific interactions between several important brain regions. Furthermore, the present research is adding to the literature information regarding the temporal nature of affective experiences, the structure of the functional networks underlying affective experiences and certain technological factors that are influencing the images of neural functioning that can be constructed at present time.

Beyond the unified picture that the studies reveal when viewed in cohort, each one allows for additional conclusions to be drawn, representing specific advances of scientific knowledge. The first study (Chapter 2) demonstrates that the role of the AC extends beyond low level perceptual processing of acoustic information to encompass a principal role in emotional processing of music. A second conclusion that can be drawn from the first study is that the SF amygdala plays a critical role during music listening by exhibiting notable decreases in activity and further modulating activity in the visual cortex during fear, most likely reflecting alertness in the presence of danger. This expands the current perspective on the selectivity of the SF for processing social stimuli by contributing the first solid evidence that besides pictures of faces, appropriate music can also serve as a social stimulus. A study aiming to investigate this in detail is underway.

The second study (Chapter 3) represents an important expansion of current knowledge on neural networks underlying sustained emotional experience, lasting several minutes, and is the first to use Eigenvector Centrality Mapping for the analysis of neural networks underlying emotion. An important novel observation from this experiement is that both SF and laterobasal amygdala are central to emotional processes throughout sustained periods of time and not only during the initial stage of stimulus assessment, as previously considered. Moreover, the study is furthering scientific evidence regarding the functional specialization of amygdalar nuclei by suggesting that it is the SF amygdala that is related to the rewarding attribute of the emotional experience of joy, through functional connectivity between SF and nucleus accumbens (NAc), and the laterobasal amygdala that is related to the subjective feeling component of emotion, through functional connectivity with sensory areas. In addition, the study demonstrates the involvement of the hypothalamus, thalamus and hippocampus in sustained emotional experience, providing novel fMRI evidence regarding slow endocrine changes during emotional experiences. Furthermore, the second study also reveals the prominence of the striatal complex as a central node involved in emotive sensorimotor functioning.

The third study (Chapter 4) is the first to offer evidence raising concern regading the existence of false negatives, under 1.5 T in the superficial amygdala and hippocampus, in past research. The study is also important in posing the question of whether different magnetic field strengths can be optimal for recording and monitoring activity in different brain regions (e.g. 3 T for SF amygdala and 1.5 T for cuneus) due to the differing region-specific properties that can affect the contrast-to-noise ratio across the brain. These are important contributions to the literature of methodological issues in fMRI research because they regard questions that have not received fitting experimental attention to date.

The fourth study (Chapter 5) furthers scientific knowledge by demonstrating statistically that the effects of scanner noise are not only limited to auditory, motor, visual, attentional and memory processes, as previously evidenced, but extend further to include emotional functioning. This finding is particularly important in raising awareness of the influence of scanner noise on observed brain function across the discipline of cognitive neuroscience and particularly among affective neuroscientists, as well as in motivating future investment of research efforts towards the eradication of scanner noise.

Finally, the fifth study (Chapter 6) represents several scientific steps forward in the investigation of human brain function. It is the first study to investigate personality-characteristic computational hubs in the brain by using Eigenvector Centrality Mapping. It is also the first study to compare psychometric and physiological measures of personality with regards to their efficacy and relation to brain anatomy and function. Results implicate two brain structures of particular significance in contemporary research, the amygdala and nucleus accumbens, in the expression of neuroticism and aggreeableness respectively, and serve to corrobotate that reliable information regarding brain activity resides in the electrocardiograph. Moreover, the study indicates that the role of the hippocampal formation extends beyond its well established role for cognition to include a new role contributing both functionally as well as anatomically to the expression of human emotional personality. These steps delineate important new perspectives with significant potential for future clinical applications.

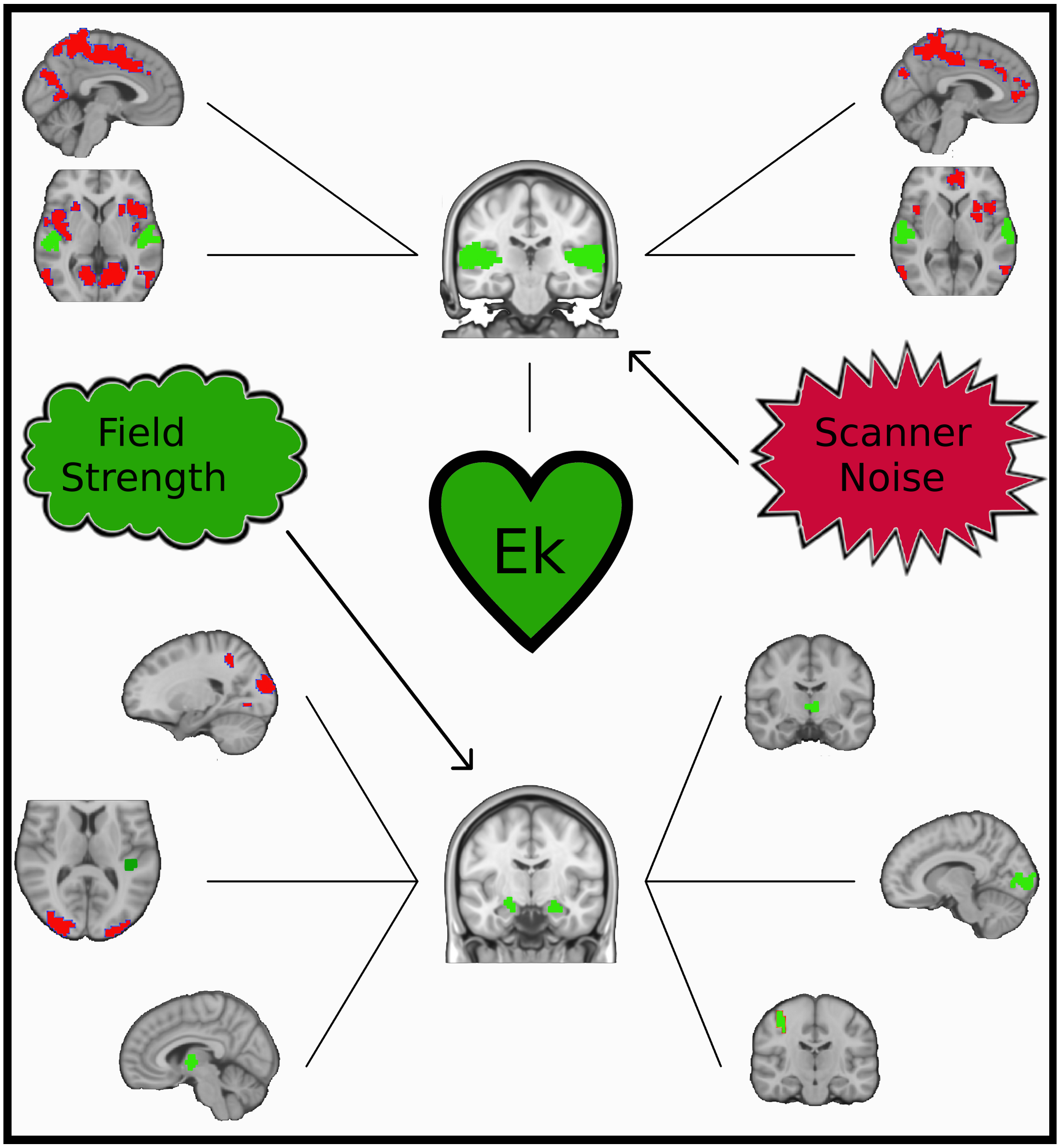

Figure 1.1: Summary of most important findings from the thesis. In the central column, green brain regions are significantly more active during music-elicited joy than during fear. Lines represent correlations. In the outer columns, green brain regions correlate with the ones in the central column during music-elicited joy and red areas correlate with them during fear. Arrows represent causal influences on the observability of emotional differences due to technological factors. Dark green and red shapes represent positive and negative influences respectively. Increased field strength increases the observability of emotion-specific differences in amygdalar activity. Increased scanner noise diminishes the observability of emotion-specific differences in auditory cortex activity. Increased values of the Eκ cardiac index correlate with increased network centrality of the auditory cortex during affective music listening.

1.4 fMRI and the Statistical Analysis Methods Utilized

fMRI was the method chosen for conducting all experiments. fMRI is a modern technology that allows for the measurement and monitoring of changes in oxygen consumption inside the brain with a temporal resolution in the range of seconds. This is accomplished through the use of functional magnetic tomographers, often referred to as “scanners”, that are able to create precisely controlled magnetic fields to momentarily excite brain matter and construct 3D images of brain activity from the resulting electromagnetic energy emitted. The most common fMRI scanners used at present are operating at magnetic field strengths of either 1.5 or 3 Tesla (see Chapter 4). A side-effect of the operation of fMRI scanners is a repetative audible loud sound referred to as “scanner noise” (see Chapter 5) that compromises the conditions of measurement.

1.4.1 General Linear Modelling (GLM)

The most common statistical approach to analysing fMRI data is that of using information regarding the design of an experiment in order construct a model that describes the brain activity in each measured location in terms of a linear equation that features a weighted variable for each experimental factor. The model features a convolution of the experimental design with the haemodynamic response function; which is itself a model of the time taken for the required quantity of blood, containing oxygen and glucose, to reach active neuronal populations. The GLM approach allows for the creation of contrast images that reveal the significant differences in neural activity between different experimental conditions (see Chapters 2, 4 and 5).

1.4.2 Eigenvector Centrality Mapping (ECM)

ECM is a data-driven, model-free mathematical method that was recently adapted for use with fMRI data (Lohmann et al. 2010). ECM attributes a value to each measured location in the brain such that a region receives a large value if it is strongly correlated with many other regions that are themselves central within the network. ECM produces a map in which each location has a value that indicates its centrality. These maps can be used for subsequent statistical tests much like contrast images in standard GLM analyses. For ECM to be applicable, it is important that the data are obtained during long trials (in the range of minutes) featuring continuous sampling (see Chapters 3 and 6).

1.4.3 Functional Connectivity (FC)

FC is a kind of seed-based correlation analysis (Lowe, 2010; Friston, 1994). It computes functional correlations from a user-specified seed location to all other locations in the brain. As with ECM, it is important that the data are characterized by temporal continuity. Under appropriate conditions, images resulting from functional connectivity analysis can be subjected to further statistical analyses (see Chapter 3).

1.4.4 Psychophysiological Interaction

PPI is essentially a hybrid between GLM and FC. It reveals the interaction effect between a physiological covariate, e.g. the timecourse of activity at a specified seed-region, and a psychological experimental factor (Friston et al. 1997). This is accomplished by computing the interaction term between an experimental factor and the physiological covariate of interest, e.g. the activity in a particular brain area, and including the interaction term as a variable in a GLM. By specifying the contrast of interest appropriately, one can obtain a picture of the brain activity that correlates with the computed interaction term. Similarly to ECM and FC, temporal continuity of the data is essential for PPI (see Chapter 1).

1.5 References

Bernatzky G, Bernatzky P, Hesse HP, Staffen W, Ladurner G (2004): Stimulating music increases motor coordination in patients afflicted with Morbus Parkinson. Neuroscience letters, 361(1):4-8.

Bertelli R (2011): Why is it that research into the effects of music on dementia with Lewy bodies is so urgently needed? European Review, 2(2):58-73.

Connan F, Campbell I, Katzman M, Lightman S, Treasure J (2003): A neurodevelopmental model for anorexia nervosa. Physiol Behav 79(1):13–24.

Gabrielsson A, Juslin PN (2003): Emotional expression in music. In: Davidson RJ, Scherer KR, Goldsmith HH, editors. Handbook of Affective Sciences. New York, USA: Oxford University Press. P 503–534.

Hoekert M, Kahn R, Pijnenborg M, Aleman A (2007): Impaired recognition and expression of emotional prosody in schizophrenia: review and meta-analysis. Schizophrenia Research 96(1):135–145.

Janata, Petr and Tillmann, Barbara and Bharucha, Jamshed J (2002): Listening to polyphonic music recruits domain-general attention and working memory circuits. Cognitive, Affective and Behavioral Neuroscience, 2(2):121-140.

Kang J, Namkoong K, Yoo S, Jhung K, Kim S (2012): Abnormalities of emotional awareness and perception in patients with obsessive–compulsive disorder. Journal of Affective Disorders, 141:286-293.

Koelsch S, Schulze K, Sammler D, Fritz T, Müller K, Gruber O (2009): Functional architecture of verbal and tonal working memory: an FMRI study. Human brain mapping, 30(3):859-873.

Leppänen J (2006): Emotional information processing in mood disorders: a review of behavioral and neuroimaging findings. Current Opinion in Psychiatry, 19(1):34-39.

Mannie Z, Bristow G, Harmer C, Cowen P (2007): Impaired emotional categorisation in young people at increased familial risk of depression. Neuropsychologia, 45(13):2975–2980.

Norton A, Zipse L, Marchina S, Schlaug G (2009): Melodic Intonation Therapy. Annals of the New York Academy of Sciences, 1169(1):431-436.

Panksepp J, Burgdorf J (1999): Laughing rats? Playful tickling arouses high frequency ultrasonic chirping in young rodents. In: Hameroff SR, Kaszniak AW, Chalmers DJ, editors. Toward a science of consciousness III: The Third Tucson Discussions and Debates, Volume 3. Cambridge, MA, USA: MIT Press. P 231-244.

Knutson B, Burgdorf J, Panksepp J (2002): Ultrasonic vocalizations as indices of affective states in rats. Psychological bulletin, 128(6):961-977.

Panksepp J, Burgdorf J (2003): “Laughing” rats and the evolutionary antecedents of human joy? Physiology and Behavior, 79(3):533-547

Patel AD (2009): Music and the brain: Three links to language. In: Hallam S, Cross I, Thau M, editors. The Oxford handbook of music psychology 1st ed. Oxford, UK: Oxford University Press. P 208-216.

Patel, AD (2003): Language, music, syntax and the brain. Nature neuroscience, 6(7):674-681.

Patel AD (2012): Advancing the comparative study of linguistic and musical syntactic processing. In Rebuschat P, Rohrmeier M, Hawkins JA, Cross I. Language and Music as Cognitive Systems. 1st ed. Oxford: Oxford University Press. P 248-253.

Peng SM, Koo M, Kuo JC (2010): Effect of group music activity as an adjunctive therapy on psychotic symptoms in patients with acute schizophrenia. Archives of psychiatric nursing, 24(6):429-434.

Perlovsky L (2010): Musical emotions: Functions, origins, evolution. Physics of Life Reviews, 7(1):2-27.

Särkämö T, Laitinen S, Tervaniemi M, Numminen A, Kurki M, Rantanen P (2012): Music, Emotion, and Dementia Insight From Neuroscientific and Clinical Research. Music and Medicine, 4(3):153-162.

Schlaug G, Marchina S, Norton A (2008): From singing to speaking: Why singing may lead to recovery of expressive language function in patients with Broca's aphasia. Music perception, 25(4):315-323.

Schlaug G, Norton A, Marchina S, Zipse L, Wan CY (2010): From singing to speaking: facilitating recovery from nonfluent aphasia. Future neurology, 5(5):657-665.

Silverman MJ (2003): The influence of music on the symptoms of psychosis: a meta-analysis. Journal of Music therapy, 40(1):27-40.

Ulrich G, Houtmans T, Gold C (2007): The additional therapeutic effect of group music therapy for schizophrenic patients: a randomized study. Acta Psychiatrica Scandinavica, 116(5):362-370

Västfjäll D (2002): Emotion induction through music: A review of the musical mood induction procedure. Musicae Scientiae, Special Issue:173-211.

Wan CY, Rüber T, Hohmann A, Schlaug G (2010): The therapeutic effects of singing in neurological disorders. Music perception, 27(4):287-295.

Yang WY, Li Z, Weng YZ, Zhang HY, Ma B (1998): Psychosocial rehabilitation effects of music therapy in chronic schizophrenia, Hong Kong Journal of Psychiatry, 8(1):38-40.

The roles of superficial amygdala and auditory cortex in music-evoked fear and joy

Koelsch S*, Skouras S*, Fritz T, Herrera P, Bonhage C, Küssner MB, Jacobs AM

* authors with equal contribution

Published in NeuroImage, Volume 81, November 2013. Pages 49-60.
http://dx.doi.org/10.1016/j.neuroimage.2013.05.008

2.0 Abstract

This study investigates neural correlates of music-evoked fear and joy with fMRI. Studies on neural correlates of music-evoked fear are scant, and there are only a few studies on neural correlates of joy in general. Eighteen individuals listened to excerpts of fear-evoking, joy-evoking, as well as neutral music and rated their own emotional state in terms of valence, arousal, fear, and joy. Results show that BOLD signal intensity increased during joy, and decreased during fear (compared to the neutral condition) in bilateral auditory cortex (AC) and bilateral superficial amygdala (SF). In the right primary somatosensory cortex (area 3b) BOLD signals increased during exposure to fear-evoking music. While emotion-specific activity in AC increased with increasing duration of each trial, SF responded phasically in the beginning of the stimulus, and then SF activity declined. Psychophysiological Interaction (PPI) analysis revealed extensive emotion-specific functional connectivity of AC with insula, cingulate cortex, as well as with visual, and parietal attentional structures. These findings show that the auditory cortex functions as a central hub of an affective-attentional network that is more extensive than previously believed. PPI analyses also showed functional connectivity of SF with AC during the joy condition, taken to reflect that SF is sensitive to social signals with positive valence. During fear music, SF showed functional connectivity with visual cortex and area 7 of the superior parietal lobule, taken to reflect increased visual alertness and an involuntary shift of attention during the perception of auditory signals of danger.

2.1 Introduction

Of all emotions, fear is the one that has been investigated most intensely in affective neuroscience over the last decades. However, there is scarcity of functional neuroimaging studies on fear with music, and neural correlates of music-evoked fear have thus remained elusive. This stands in gross contrast to a long musical tradition of using musical means to evoke fear in the listener. The earliest theoretical treatise on such means is the Affektenlehre (“theory of affects”) of the Baroque, which prescribed musical methods and figures for imitating, or portraying (and thus, according to the Affektenlehre, summoning) emotions, including fear (Mattheson, 1739/1999). Among countless well-known examples of fear-evoking (Western) music are Handel's Messiah (“And He Shall Purify”), Mozart's Idomeneo, the thunderstorm portrayed in Beethoven's sixth symphony, Berlioz' Songe d'une nuit du Sabbat, Herrmann's music for Psycho, and Penderecki's Polymorphia.

Nevertheless, only two previous functional neuroimaging studies have investigated brain responses to fear-evoking music. One of these studies explored how fear music can enhance feelings of fear evoked by images (Baumgartner et al., 2006), but that study did not present fear music alone, thus leaving open the question as to which activation patterns would be evoked by fearful music alone (i.e., without negative visual images). The other study investigated how music evoking fear or joy can change the perception of neutral film clips (Eldar et al., 2007). The latter study also investigated brain responses evoked by the fear music alone (without film clips), compared to a baseline condition, in selected regions of interest (amygdala, anterior hippocampal formation, prefrontal cortex, and auditory cortex). However, no effects of fear music were observed without film-clips (nor effects of joy or neutral music without film-clips), neither in the amygdala, nor in the hippocampus or the prefrontal cortex. In addition, a study by Lerner et al. (2009) showed that listening to fear-evoking music with closed eyes (compared to listening with open eyes), evoked greater activation than open eyes in the amygdala/anterior hippocampal formation and anterior temporal poles (this effect of eyes open/closed was not observed when listening to neutral music). Main effects of fear compared to neutral music were not reported in that study. Finally, a recent study by Trost et al. (2012) reported brain activations due to music-evoked “tension” (characterized by feelings of high arousal and low valence), under which the authors also subsumed “feelings of anxiety and suspense induced by scary music” (brain activations included bilateral superior temporal gyrus, right parahippocampal gyrus, motor and premotor areas, cerebellum, right caudate nucleus, and precuneus). Notably, the concept of “tension” also includes emotional phenomena not related to fear, such as emotional reactions to unexpected musical events (Huron, 2006), and, therefore, Trost et al. (2012) argued that it is not clear whether the observed brain activations were due to fear responses, or to more general feelings of tension and unease. Thus, there are no functional neuroimaging data available that would allow us to draw conclusions about neural correlates of music-evoked fear.

With regard to lesion studies, Gosselin et al. (2005) showed impaired recognition of scary music in epileptic patients following unilateral medial temporal lobe excision (including the amygdala). In that study, both patients with left or right medial temporal lobe resections showed impaired recognition of scary, but not happy or sad, music. Corroborating this finding, data from a patient with bilateral damage restricted to the amygdala showed a selective impairment in the recognition of scary and sad music (Gosselin et al., 2007), indicating that the recognition of fear expressed by music involves the amygdala. These findings are reminiscent of findings reporting similar impairment for the recognition of fearful faces (reviewed in Peretz, 2010), suggesting that scary music and fearful faces are processed, at least in part, by common cerebral structures. Supporting this assumption, patients with unilateral anteromedial temporal lobe excision were found to be impaired in the recognition of both scary music and fearful faces (Gosselin et al., 2011), with results in both tasks being correlated. This suggested a multimodal representation of fear within the amygdala (although recognition of fearful faces was preserved in some patients, while their recognition of scary music was impaired). However, due to the size of the lesions in the reported studies, it remains unclear which nuclei of the amygdaloid complex played a role in the reported findings.

Functional neuroimaging studies on fear evoked by visual stimuli, recall/imagery, or auditory (but not musical) stimuli have also implicated the amygdaloid complex (LeDoux, 2000), in particular the basolateral amygdala (BL), as well as a range of functionally connected structures in fear responses (e.g., Phan et al., 2002). Such structures include the auditory cortex in auditory fear conditioning paradigms (LeDoux, 2000), as well as a large array of both cortical and subcortical structures, such as cingulate and insular cortex, hippocampus, parahippocampal cortex, orbitofrontal cortex, dorsolateral prefrontal cortex, striate (visual) cortex, basal ganglia, cerebellum, as well as brainstem regions such as the periaqueductal gray (Roy et al., 2009; Stein et al., 2007; Williams et al., 2006).

Based on the reported findings, we aimed to investigate the role of the amygdaloid complex and the auditory cortex, including their functional connections, for fear evoked by music. The cultural practice of using music to evoke fear makes music an important means to investigate neural circuits underlying fear (Eerola and Vuoskoski, 2011), in addition to the vast number of studies using visual stimuli to investigate neural correlates of fear. Besides fear stimuli, the present study also used joyful and neutral music. Joy was chosen as positive emotion because, on the one hand, both joy and fear are considered as “basic emotions” (Ekman, 1999), and both the expression of joy as well as of fear in Western music can be recognized universally (Fritz et al., 2009). On the other hand, other than, e.g. peaceful music (which is also perceived as positive, e.g. Vieillard et al., 2008), arousal levels evoked by joy music can well be matched with those evoked by fear music. Similarly, musical and acoustical parameters such as tempo and pitch variation can well be matched between joy and fear music. Moreover, joyful music was chosen to replicate results of previous studies. Although only a few previous functional neuroimaging studies specifically used “happy” (Brattico et al., 2011; Brown et al., 2004; Mitterschiffthaler et al., 2007) or “joyful” (Koelsch et al., 2006; Mueller et al., 2011) music, these studies, along with other studies investigating musical frissons (Blood and Zatorre, 2001; Salimpoor et al., 2011), or music evoking emotional responses with positive valence and high arousal (Trost et al., 2012) indicate a number of relatively consistent features, namely stronger BOLD signal intensity (a) in the auditory cortex (Brattico et al., 2011; Koelsch et al., 2006; Mitterschiffthaler et al., 2007; Mueller et al., 2011; Trost et al., 2012), (b) the ventral striatum (Blood and Zatorre, 2001; Brown et al., 2004; Koelsch et al., 2006; Menon and Levitin, 2005; Mitterschiffthaler et al., 2007; Trost et al., 2012), (c) the anterior insula (Blood and Zatorre, 2001; Brown et al., 2004; Koelsch et al., 2006), and (d) the anterior cingulate cortex (Blood and Zatorre, 2001; Janata, 2009; Mitterschiffthaler et al., 2007). Moreover, (e) several studies on music evoked emotions showed signal changes in the anterior hippocampal formation in response to stimuli with positive emotional valence (e.g., Blood and Zatorre, 2001; Mueller et al., 2011; Trost et al., 2012). Based on these findings, we hypothesized increased BOLD signals in response to joy stimuli (compared to neutral or fear stimuli) in the auditory cortex, ventral striatum, insula, ACC, and hippocampal formation.

Another aspect of our study was the investigation of the temporal dynamics of emotion across time. To our knowledge, only two previous functional neuroimaging studies have investigated the temporal dynamics of neural correlates of emotion (for habituation-effects across an experimental session see Mutschler et al., 2010). A study by Salimpoor et al. (2011) reported that BOLD signal intensity increased (a) in the dorsal striatum during the anticipation of a music-evoked frisson, and (b) in the ventral striatum during the experience of the frisson (notably, additional PET data showed that these signal increases were related to dopaminergic synaptic activity in these structures). Another study (Koelsch et al., 2006), in which stimuli of

60 s were split into two 30-second halves, showed that significant signal differences between pleasant and unpleasant music were most pronounced during the second half of the trials. The structures with such temporal dynamics of activation included the auditory cortex, inferior fronto-lateral areas (area 45 and the posterior part of the inferior frontal sulcus), anterior insula, the amygdaloid complex (probably basolateral amygdala), hippocampal formation, temporal poles, and parahippocampal cortex (a similar trend was observed in the ventral striatum).

Particular care was taken with regard to the acoustic parameters of our stimuli: numerous acoustical features of the stimuli were measured, which allowed us (1) to match joy, fear, and neutral stimuli with regard to numerous acoustical parameters (e.g., pitch variation, tempo, intensity, and spectral flux), and (2) to introduce acoustical factors that differed between conditions as regressors of no interest in the analysis of fMRI data. Provided that no crucial acoustical features were missed, this enabled us to investigate the role of the auditory cortex with regard to its emotion-specific interfacing with limbic/paralimbic structures. Previous work has implicated auditory association cortex (auditory parabelt), as well as its connections with the lateral amygdala, in fear conditioning (LeDoux, 2000). However, auditory parabelt regions project to numerous limbic/paralimbic structures (such as orbitofrontal cortex, insula, and cingulate cortex; e.g. Petrides and Pandya, 1988; Smiley et al., 2007; Yukie, 1995), and the role of these auditory projections for emotional processes, and thus the role that the auditory cortex plays for emotional processes, is largely unknown.

2.1.1 Summary of hypotheses

Motivated by the reported findings, we tested whether music-evoked fear, as compared to neutral or joy stimuli, would elicit signal changes in the basolateral nucleus of the amygdaloid complex. For joy, as compared to neutral or fear, we expected stronger BOLD signal intensity in the ventral striatum, auditory cortex, hippocampal formation, insula, and cingulate cortex. Finally, to explore neural networks underlying joy and fear, we performed a Psychophysiological Interaction (PPI) analysis using the peak voxels indicated by the contrast analysis between conditions as seed voxels. More specifically, we were interested in emotion-specific functional connectivity between amygdaloid complex and auditory cortex, between auditory cortex and insula, as well as between auditory cortex and cingulate cortex.

2.2 Methods

2.2.1 Participants

18 individuals (aged 20–31 years, M = 23.78, SD = 3.54, 9 females) took part in the experiment. All participants had normal hearing (as assessed with standard pure tone audiometry) and were right-handed (according to self-report). None of the participants was a professional musician, nor a music student. Seven participants had no formal musical training, eight participants had once received music lessons (mean duration of formal training was 2.81 years, SD = 2.36, instruments were: flute, drums, piano, violin, guitar and melodica) but had not played their instruments for several years (M = 8.83, SD = 7.52), and three participants had learned a musical instrument that they were still playing (mean duration of formal training was 12.5 years, SD = 3.5, instruments were: guitar, violin, piano and electric bass). Exclusion criteria were left-handedness, professional musicianship, past diagnosis of a neurological or psychiatric disorder, a score of ≥13 on Beck's Depression Inventory (BDI; Beck et al., 1993), excessive consumption of alcohol or caffeine during the 24 h prior to testing, and poor sleep during the previous night. All subjects gave written informed consent. The study was conducted according to the Declaration of Helsinki and approved by the ethics committee of the School of Life Sciences and the Psychology Department of the University of Sussex.

2.2.2 Stimuli and procedure

Musical stimuli were selected to evoke (a) feelings of joy, (b) feelings of fear, or (c) neither joy nor fear (henceforth referred to as neutral stimuli). There were n = 8 stimuli per category (the complete list of joy and fear stimuli is provided in Supplementary Table S1). Joy stimuli had been used in previous studies (e.g., Fritz et al., 2009; Koelsch et al., 2010a, 2011; Mueller et al., 2011) and consisted of CD-recorded pieces from various epochs and styles (classical music, Irish jigs, jazz, reggae, South American and Balkan music). Fear-evoking musical stimuli were excerpts from soundtracks of suspense movies and video games. To increase the fear-evoking effect of the fear stimuli, their relatively high acoustic roughness (see also next paragraph) was further increased: from each fear excerpt, two copies were obtained and pitch-shifted, one copy was shifted one semitone higher, the other copy a tritone lower (see also Fritz et al., 2009; Koelsch et al., 2006). Then, all three versions of one excerpt (original pitch, one semitone higher, and a tritone lower) were rendered as a single wav-file (pitch-shift and rendering was performed using Ableton Live, version 8.0.4, Ableton AG, Berlin, Germany). Neutral stimuli were sequences of isochronous tones, for which the pitch classes were randomly selected from a pentatonic scale. These tone sequences were generated using the MIDI (musical instrument digital interface) toolbox for Matlab (Eerola and Toiviainen, 2004). Importantly, for each joy–fear stimulus pair (see below), a neutral control stimulus was generated that matched joy and fear stimuli with regard to tempo, F0 range (i.e., range of the fundamental frequency), and instrumentation (using the two main instruments or instrument groups of the respective joy-fear pair). To create stimuli that sounded like musical compositions played with real instruments (similar to the joy and fear stimuli), the tones from the MIDI sequences were set to trigger instrument samples from a high quality natural instrument library (X-Sample Chamber Ensemble, Winkler & Stahl GbR, Detmold, Germany) and from the Ableton Instrument library (Ableton AG, Berlin, Germany). Stimuli were then rendered as wav-files using Ableton Live. Using Praat (version 5.0.29; Boersma, 2002), all excerpts (joy, fear, and neutral) were edited so that they all had the same length (30 s), 1.5 s fade-in/fade-out ramps, and the same RMS power.

Importantly, joy and fear stimuli were chosen such that each joyful excerpt had a fearful counterpart that matched with regard to tempo (beats per minute), mean fundamental frequency, variation of fundamental frequency, pitch centroid value, spectral complexity, and spectral flux. This was confirmed by an acoustic analysis of the stimuli using ‘Essentia’, an in-house library for extracting audio and music features from audio files (http://mtg.upf.edu/technologies/essentia). The Essentia software was also used to specify acoustical differences between stimuli with regard to other acoustical factors: 177 acoustical descriptors were extracted frame-by-frame (frame length = 21.5 ms, 50% overlap), averaged along the entire duration of the file, and then compared between conditions (joy, neutral, fear) using one-way ANOVAs. Bonferroni-corrected significance-level was 0.05/177 = 0.00028 (lowering this threshold for one-sided tests, i.e. 0.00056, did not change any of the results). The extracted features represent acoustic and musical features used in music information retrieval, i.e., different combinations of them are used for predictive models of musically relevant categorizations such as genre detection, instrument detection, key and mode detection, or emotional expression. Although these features have mostly been validated in machine-learning contexts (Huq et al., 2010; Kim et al., 2010; Laurier, 2011), it is possible that they also play a role for human auditory perception. In addition, many of the used parameters have been validated in perceptual experiments, such as features related to spectral complexity, F0, and F0 variations (Agrawal et al., 2012; Alluri et al., 2012; Coutinho and Dibben, 2012; Juslin and Laukka, 2003; Kumar et al., 2012), sensory dissonance (Coutinho and Dibben, 2012; Koelsch et al., 2006; Plomp and Levelt, 1965; Vassilakis and Kendall, 2010), spectral flux (Coutinho and Dibben, 2012; Menon et al., 2002), spectral centroid (Coutinho and Dibben, 2012), spectral crest (Laurier, 2011), temporal modulation frequencies (Kumar et al., 2012), key strength (Alluri et al., 2012; Krumhansl, 1990), and pulse clarity (Alluri et al., 2012). Significant effects of condition were indicated for the following acoustic factors (with F-values in parentheses, degrees of freedom: 2, 21):

(a) Mean (72.3) and variance (13.8) of F0 salience (this measure is highest for single tones, intermediate for chords, and lowest for noises; note that mean F0 and variance of F0 did not differ between joy, fear, and neutral stimuli). The mean F0 salience was highest for neutral, intermediate for joy, and lowest for fear stimuli ($p < .0001$ in all pairwise comparisons). This reflects that both joy and fear (but not neutral) stimuli contained numerous harmonies, and that fear (but not joy) stimuli contained numerous percussive sounds, as well as hissing and whooshing noises.

(b) Mean (41.3) and variance (28.0) of sensory dissonance. Sensory dissonance was lowest for neutral, intermediate for joy, and highest for fear stimuli. Mean sensory dissonance differed significantly between joy and neutral ($p < .0001$), between fear and neutral ($p < .0001$), and between joy and fear stimuli ($p < .05$).

(c) Mean chord strength (25.2) and key strength (14.7); these factors measure how strongly a sound resembles the sound of a chord, and how clearly the sounds of a stimulus can be attributed to a key. Chord strength was higher for joy compared to fear stimuli ($p < .0001$), as well as for joy compared to neutral stimuli ($p < .0006$), whereas fear and neutral stimuli did not differ significantly from each other. Key strength was higher for joy compared to fear stimuli ($p < .0001$), and neutral compared to fear stimuli ($p = .01$); joy and neutral stimuli did not differ significantly from each other ($p > .15$).

(d) Mean (30.0) and variance (16.4) of spectral flux (a measure of spectral variation within sounds), mean (30.0) spectral crest (a measure of the inhomogeneity, or noisiness, of the spectrum) and mean (10.6) spectral complexity (which correlates with the amount of different timbres that are present in a piece). Mean spectral flux, spectral crest, and spectral complexity were lowest for neutral stimuli (with significant differences between neutral and joy, as well as between neutral and fear stimuli, $p < .05$ in each test), and did not differ significantly between joy and fear stimuli ($p > .2$ in each test).

Prior to the MRI session, participants were presented with short (12 s) versions of each stimulus to obtain familiarity ratings: Participants rated their familiarity with each piece on a four-point scale (ranging from “To my knowledge I have never heard this piece before”, to “I know this piece, and I know who composed or performed it”). Participants were then trained on the rating procedure, using 12 s long excerpts of musical pieces that did not belong to the stimulus set used in the fMRI scanning session.

During the fMRI scanning session, stimuli were presented in a pseudo-random order so that no more than two stimuli of each stimulus category (joy, fear, neutral) followed each other. Participants were asked to listen to the musical stimuli with their eyes closed (see also Lerner et al., 2009). Each musical stimulus was followed by an interval of 2 s in which a beep tone of 350 Hz and 1 s duration signaled participants to open their eyes and to commence the rating procedure. During the rating procedure, participants indicated how they felt at the end of each excerpt with regard to valence (‘pleasantness’), ‘arousal’, ‘joy’ and ‘fear’. That is, participants provided ratings about how they felt, and not about which emotion each stimulus was supposed to express (Gabrielson and Juslin, 2003; Juslin and Västfjäll, 2008). Ratings were obtained with 6-point Likert scales (ranging from “not at all” to “very much”). The time interval for the rating procedure was 12 s and each rating period was followed by a 4 s rest period (during which participants closed their eyes again), amounting to a total length of 48 s per trial (see Fig. 1). The entire stimulus set was presented twice during the fMRI scanning session. Musical stimuli were presented using Presentation (version 13.0, Neurobehavioral systems, Albany, CA, USA) via MRI compatible headphones (under which participants wore earplugs). Instructions and rating screens were delivered through MRI compatible liquid crystal display goggles (Resonance Technology Inc., Northridge, CA, USA) with integrated eye-tracker that allowed us to guarantee that participants opened and closed their eyes according to the instruction.

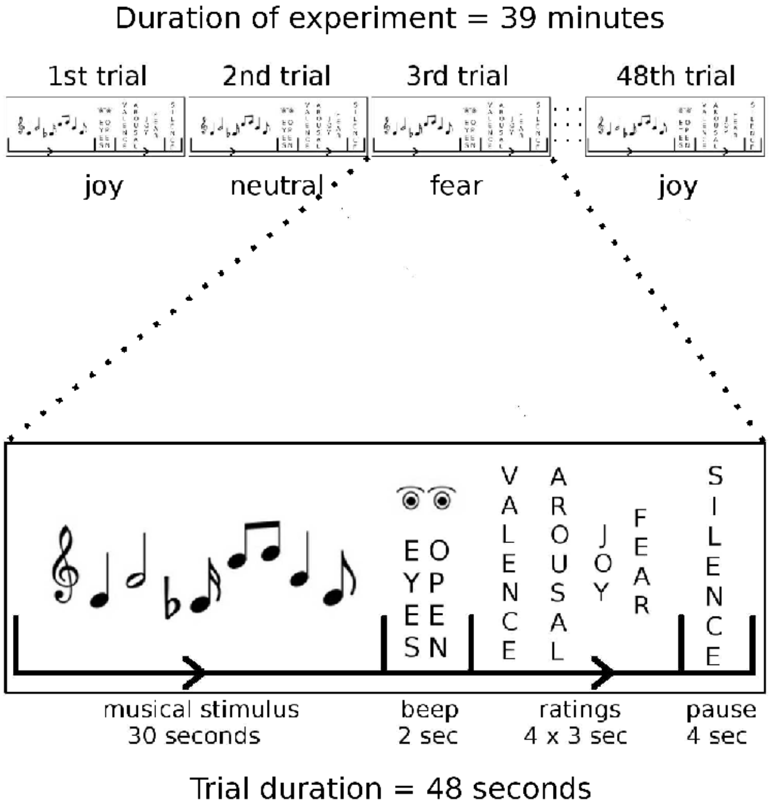

Figure 2.1: Experimental design. In each trial, a music stimulus was presented for 30 s. Music stimuli were pseudorandomly either a joy, a fear, or a neutral stimulus. Participants listened to the music with their eyes closed. Then, a beep tone signaled to open the eyes and to commence the rating procedure. Four ratings (felt valence, arousal, joy, and fear) were obtained in 12 s, followed by a 4 s pause (during which participants closed their eyes again). Trial duration was 48 s, the experiment comprised of 48 trials.

2.2.3 MR scanning

Scanning was performed with a 3 T Siemens Magnetom TrioTim. Prior to the functional MR measurements, a high-resolution (1 × 1 × 1 mm) T1-weighted anatomical reference image was acquired from each participant using a rapid acquisition gradient echo (MP-RAGE) sequence. Continuous Echo Planar Imaging (EPI) was used with a TE of 30 ms and a TR of 2000 ms. Slice-acquisition was interleaved within the TR interval. The matrix acquired was 64 × 64 voxels with a field of view of 192 mm, resulting in an in-plane resolution of 3 mm. Slice thickness was 3 mm with an interslice gap of 0.6 mm (37 slices, whole brain coverage). The acquisition window was tilted at an angle of 30° relative to the AC-PC line in order to minimize susceptibility artifacts in the orbitofrontal cortex (Deichmann et al., 2002, 2003; Weiskopf et al., 2007). Given the duration of our stimuli (30 s), a continuous scanning design was required to perform the PPI analysis (so that enough data points were available for meaningful correlation estimations, see below).

2.2.4 Data analysis

FMRI data were processed using LIPSIA 2.1 (Lohmann et al., 2001). Data were corrected for slicetime acquisition and normalized into MNI-space-registered images with isotropic voxels of 3 cubic millimeters. A temporal highpass filter with a cutoff frequency of 1/90 Hz was applied to remove low frequency drifts in the fMRI time series, and a spatial smoothing was performed using a 3D Gaussian kernel and a filter size of 6 mm FWHM.

A mixed effects block design GLM analysis was employed (Friston et al., 2007). Valence ratings, arousal ratings, familiarity ratings, psychoacoustic parameters that differed significantly between conditions (see Stimuli and procedure), and realignment parameters were included in the design matrix as covariates of no interest (Johnstone et al., 2006). Then, one-sample t-tests were calculated voxel-wise for the contrast between fear vs. joy, and corrected for multiple comparisons by the use of cluster-size and cluster-value thresholds obtained by Monte Carlo simulations with a significance level of $p < 0.05$ (Lohmann et al., 2008). The significant clusters identified in this analysis were used as regions of interest (ROIs) to compare the average signal intensity (averaged across all voxels in each cluster) within those clusters between fear and neutral, as well as between joy and neutral. In addition, to explore the temporal nature of the significant differences in activity between fear and joy, for each peak voxel of each significant cluster, the timecourse of activity was determined by computing the voxel intensity separately for each scan (i.e., with a temporal resolution of 2 s) and for each condition.

2.2.4.1 Temporal interaction analysis

To investigate possible interactions between emotion and time we split the data from each trial into first half (seconds 1 to 15) and second half (seconds 16 to 30), and calculated a statistical parametric map based on the interaction between emotion (two levels: joy, fear) and time (two levels: first half, second half). A first-level interaction contrast was calculated for each subject, and the contrast images were then used for voxel-wise one-sample t-tests at the second level (corrected for multiple comparisons by the use of cluster-size and cluster-value thresholds obtained by Monte Carlo simulations with a significance level of $p < .0.05$) to identify clusters of voxels for which the emotion × time interaction was significantly different from zero.

2.2.4.2 Psychophysiological Interaction

The timecourses of activity at the peak voxels identified in the contrast joy vs. fear, averaged together with the timecourses from adjacent voxels, were used as seeds for Psychophysiological Interaction (PPI) analyses to identify target regions for which the covariation of activity between seed and target regions was significantly different between experimental conditions. At the first level, contrasts were calculated for each subject based on the interaction term between emotion (joy vs. fear) and each seed voxel's timecourse of activity (Friston et al., 1997). For each seed voxel, the contrast images from all subjects were used in voxel-wise one-sample t-tests at the second level (corrected for multiple comparisons by the use of cluster-size and cluster-value thresholds obtained by Monte Carlo simulations with a significance level of $p < .0.05$) to identify clusters of voxels for which the psychophysiological interaction effect was significant.

2.3 Results

2.3.1 Behavioral data

Behavioral data are summarized in Fig. 2 and Table 1. Valence (pleasantness) ratings were lower for fear than for joy stimuli ($t(15) = 42.29$, $p < 0.0001$), higher for joy than for neutral stimuli ($t(15) = 16.10$, $p < 0.0001$), and did not differ significantly between neutral and fear stimuli ($t(15) = -1.94$, $p=.072$). Arousal ratings were higher for fear than for neutral stimuli ($t(15) = 11.84$, $p < 0.0001$), higher for joy than for neutral stimuli ($t(15) = 12.26$, $p < 0.0001$), and did not differ between joy and fear stimuli ($t(15)= .94$, $p=.36$). Joy ratings were lowest for fear stimuli, and highest for joy stimuli, with ratings for neutral stimuli being in between. Joy ratings differed significantly between fear and neutral stimuli ($t(15) = 9.03$, $p < 0.0001$), fear and joy stimuli ($t(15) = 32.32$, $p < 0.0001$), and between joy and neutral stimuli ($t(15) = 16.73$, $p < 0.0001$). Correspondingly, fear ratings were highest for fear stimuli, lowest for joy stimuli, with ratings for neutral stimuli being in between. Although the degree of experienced fear was relatively moderate (4.02 on a scale from 1 to 6), fear ratings differed significantly between fear and neutral stimuli ($t(15) = 17.71$, $p < 0.0001$), fear and joy stimuli ($t(15) = 33.16$, $p < 0.0001$), and between joy and neutral stimuli ($t(15) = 9.93$, $p < 0.0001$). Average familiarity ratings were highest for joy stimuli, lowest for neutral stimuli, with ratings for fear stimuli being in between. Familiarity ratings differed significantly between joy and fear stimuli ($t(7) = 3.659$, $p < 0.05$), fear and neutral stimuli ($t(7) = 4.41$, $p < 0.01$), and between joy and neutral stimuli ($t(7) = 5.06$, $p < 0.0005$). Due to the differences in the behavioral ratings between stimulus categories with regard to valence, arousal, and familiarity, each participant's valence, arousal, and familiarity ratings were used in the fMRI data analysis as regressors of no interest (see Data analysis). Therefore, these variables (valence, arousal, and familiarity) did not contribute to the fMRI results presented in the following.

2.3.2 fMRI data

The statistical parametric maps (SPMs) of the contrast joy > fear (corrected for multiple comparisons, $p < .05$) revealed significant BOLD signal differences in the auditory cortex (AC) bilaterally, and in the superficial amygdala (SF) bilaterally (see also Table 2 and Fig. 3a). The activation of the AC covered auditory core, belt, and parabelt regions bilaterally. The voxels with maximum z-values were located along Heschl's gyrus (HG), with the peak voxel in the left AC being located on the postero-lateral rim of HG (30% TE 1.2 according to Morosan et al., 2001), and the peak voxel in the right AC being located more medially on HG (90% TE 1.0 according to Morosan et al., 2001). In both left and right amygdala, the peak voxel was located in SF (left: 80% probability, right: 90% probability according to the cytoarchitectonic probability map by Amunts et al., 2005). The signal differences in SF extended bilaterally into the hippocampal-amygdaloid transition area (HATA, Amunts et al., 2005). The opposite contrast (fear > joy) showed signal differences in the anterior bank of the right postcentral gyrus (area 3b of the primary somatosensory cortex,

Table 2.1: Descriptive statistics of behavioral data (mean, with standard deviation in parentheses). Range of valence, arousal, joy, and fear scales was 1 to 6, range of the familiarity scale was 1 to 4. For statistical tests see main text.

	Fear	Neutral	Joy
Valence	2.43 (0.20)	2.69 (0.48)	4.84 (0.21)
Arousal	3.97 (0.21)	3.03 (0.22)	4.05 (0.21)
Joyfulness	1.62 (0.16)	2.40 (0.29)	4.83 (0.42)
Fearfulness	4.02 (0.23)	2.22 (0.30)	1.31 (0.17)
Familiarity	1.44 (0.11)	1.17 (0.10)	2.01 (0.42)

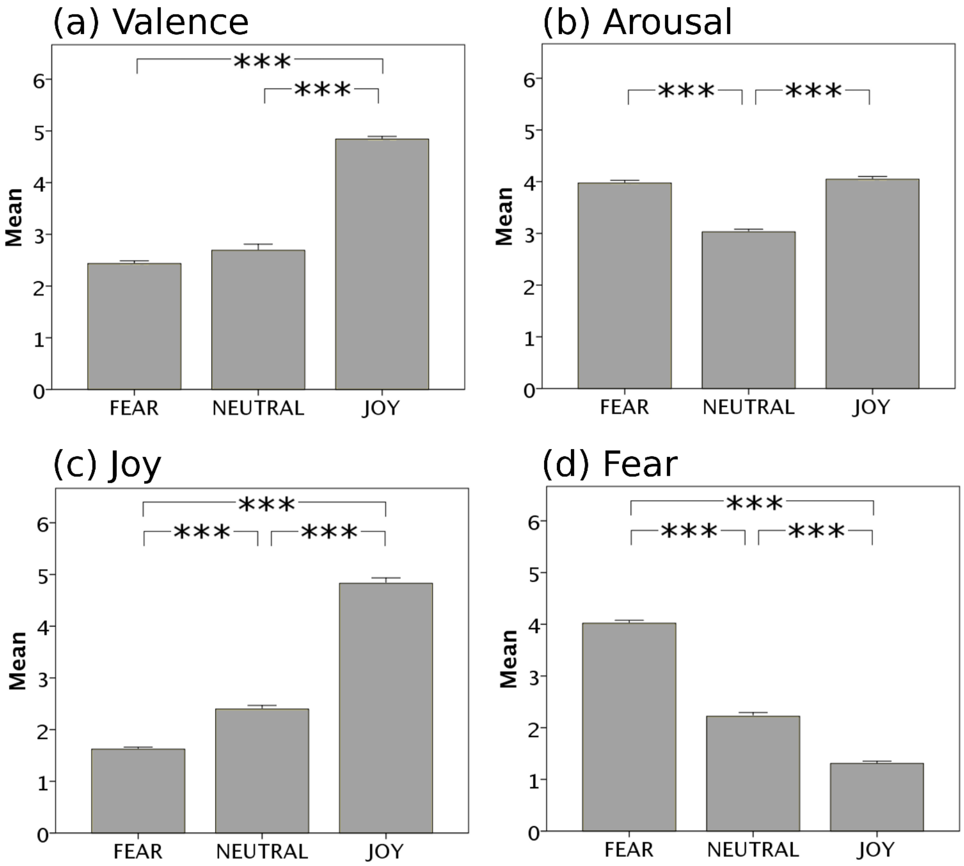

Figure 2.2: Behavioral ratings of participants on the four emotion scales used in the present study. (a) valence, (b) arousal, (c) joy, and (d) fear. Range of scales was 1 to 6. Ratings are depicted separately for each stimulus category (fear, neutral, joy). Note that joy stimuli were rated as more pleasant than fear and neutral stimuli (valence/pleasantness ratings for fear and neutral stimuli did not differ from each other). Also note that arousal ratings of joy and fear stimuli did not differ from each other, and that both joy and fear stimuli were rated as more arousing than neutral stimuli.

S1, the peak voxel was located with 80% probability in this area according to Geyer et al., 1999). Contrasts with the neutral condition did not yield any additional activations (see also Table 2 and next section), except activations in the visual cortex for both joy > neutral (left V1, MNI-coordinate: −1, −82, −5; left V4: −33, −82, −14; right V2: 32, −99, 3) and fear > neutral (left V2, MNI-coordinate: −8, −95, 25; right V2: 23, −93, 26).

Table 2.2: Results of General Linear Model (GLM) contrasts, corrected for multiple comparisons (p < .05): (a) joy > fear, (b) fear > joy. The two outermost right columns provide the p-values for comparisons involving the neutral condition within the significant clusters identified in the GLM analysis (region of interest analysis). The diamonds in the outermost right column indicate that differences between fear and neutral were due to higher signal intensity during neutral than during fear. Abbreviations: ROI: region of interest; l: left; r: right; n.s.: not significant.

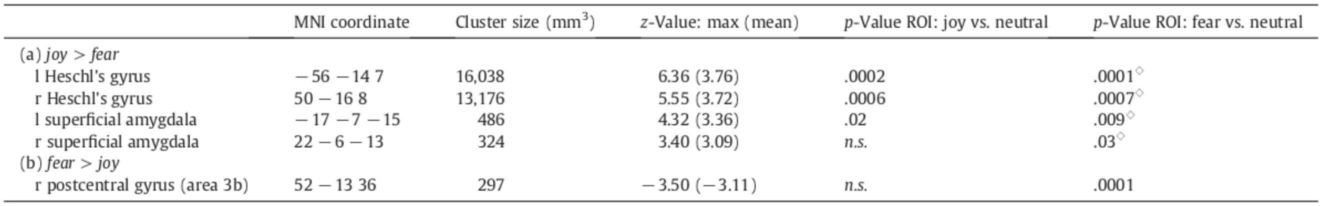

	MNI coordinate	Cluster size (mm^3)	z-Value: max (mean)	p-Value ROI: joy vs. neutral	p-Value ROI: fear vs. neutral
(a) *joy > fear*					
l Heschl's gyrus	− 56 − 14 7	16,038	6.36 (3.76)	.0002	.0001$^{\diamond}$
r Heschl's gyrus	50 − 16 8	13,176	5.55 (3.72)	.0006	.0007$^{\diamond}$
l superficial amygdala	− 17 − 7 − 15	486	4.32 (3.36)	.02	.009$^{\diamond}$
r superficial amygdala	22 − 6 − 13	324	3.40 (3.09)	*n.s.*	.03$^{\diamond}$
(b) *fear > joy*					
r postcentral gyrus (area 3b)	52 − 13 36	297	− 3.50 (− 3.11)	*n.s.*	.0001

ROI analysis

To specify whether the observed differences between fear and joy were due to signal increase or decrease compared to the neutral control condition, ROI analyses were conducted for the significant clusters identified in the GLM analysis (AC, SF, S1), comparing the mean signal intensity of the voxels in each cluster between fear and neutral, as well as between joy and neutral. Results of these analyses (corrected for multiple comparisons, p < .05) showed that, compared to the neutral condition, there was stronger signal intensity during joy and weaker signal intensity during fear in the AC bilaterally as well as in the left SF (see also Table 2). In the

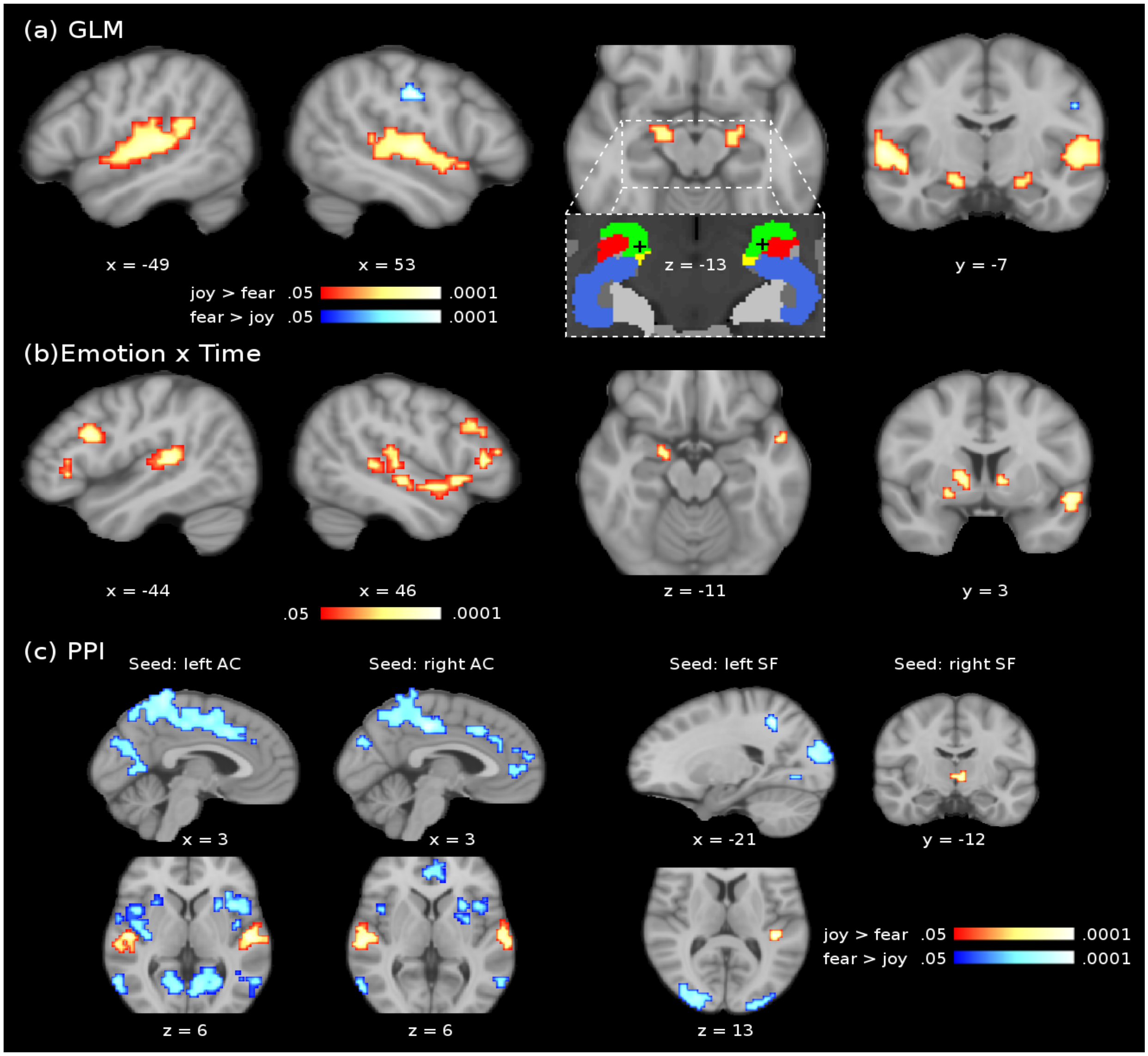

Figure 2.3: FMRI results (all corrected for multiple comparisons, p < .05). (a) shows the statistical parametric maps (SPMs) of the direct contrast between joy and fear stimuli, red: joy > fear, blue: fear > joy. The SPMs show stronger BOLD signals during joy (compared to fear) in the auditory cortex (AC), and the SF bilaterally. Stronger BOLD signals during fear (compared to joy) were yielded in area 3b of the primary sensory cortex. The inset shows the coordinates of the peak voxels in the SF (indicated by the black crosses) projected on the cytoarchitectonic probability map according to Eickhoff et al. (2005); green: superficial amygdala, red: basolateral amygdala, yellow: hippocampal-amygdaloid transition area, blue: hippocampus (cornu ammonis). (b) shows the interaction contrast between emotion (joy vs. fear) and time (1st half of each trial vs. 2nd half of each trial). Significant interactions were indicated in the auditory cortex bilaterally, the left SF, left area 45 (pars triangularis of the inferior frontal gyrus), inferior frontal sulcus, and ventral pallidum/ventral striatum. (c) shows results of the Psychophysiological Interaction Analysis (PPI) for the regions that significantly differed in the SPM contrast between fear and joy, seed voxels were located in left AC (Heschl's gyrus), right AC (Heschl's gyrus), left SF, and right SF. Red/yellow colors indicate regions that exhibited stronger functional connectivity with the seed regions during the joy than during the fear condition. Blue colors indicate regions that exhibited stronger functional connectivity with the seed regions during the fear than during the joy condition.

right SF, signal intensity was weaker during fear compared to neutral (with no difference between joy and neutral). In the right S1, signal intensity was stronger during fear compared to neutral (joy and neutral did not differ from each other).

Timelines

To explore the temporal dynamics of the observed differences, the signal intensity of the peak voxel of each significant cluster (AC, SF, S1) was computed separately for each scan (i.e., with a temporal resolution of 2 s) in each condition. These timelines are shown in Fig. 4. In the AC, the auditory stimuli evoked a signal increase (in all conditions), with the signal intensity being generally highest for joy, lowest for fear, and intermediate for neutral (see next paragraph for statistical analysis).

The most pronounced differences between conditions emerged at, and after around 10 s after stimulus onset. In SF, joy stimuli evoked a signal increase bilaterally, while fear stimuli evoked a signal increase only in the right SF. In the left SF, differences in signal intensity between fear and joy were particularly strong during the first half of the stimuli (and a similar trend is observable in the right SF). Differences between conditions emerged several seconds after stimulus onset, were most pronounced at around 10 s, and vanished towards the end of the stimuli (see next paragraph for statistical analysis). In the right S1, all conditions evoked an initial signal decrease, followed by a signal increase (which was strongest for fear stimuli), and a decline of signal intensity towards the end of the stimuli.

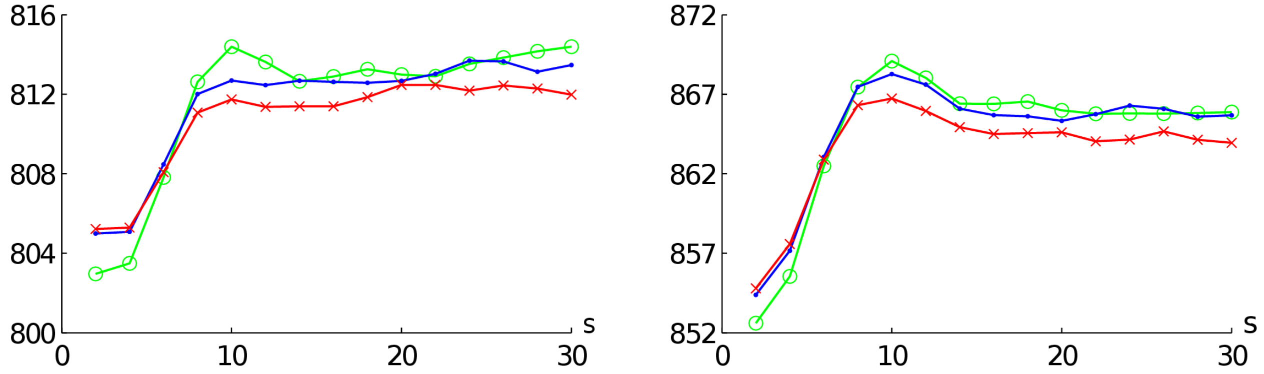

(a) Left auditory cortex

(b) Right auditory cortex

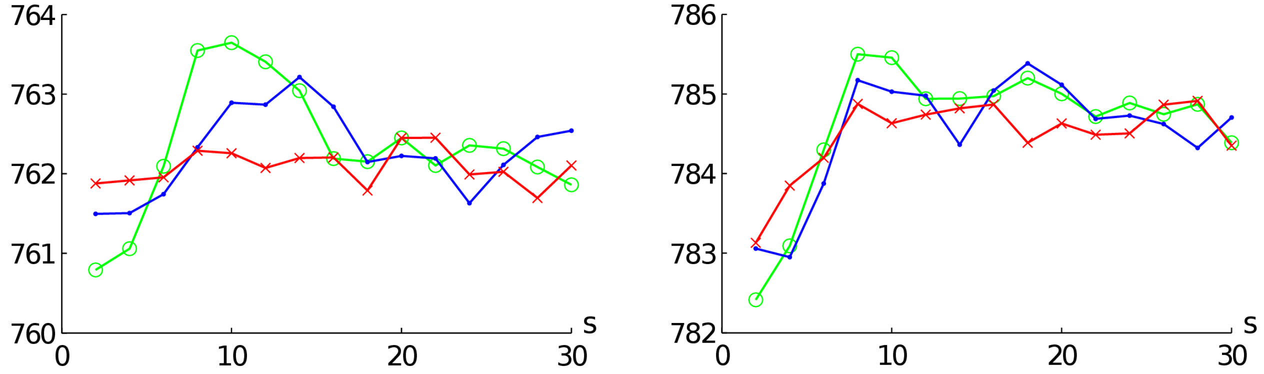

(c) Left superficial amygdala

(d) Right superficial amygdala

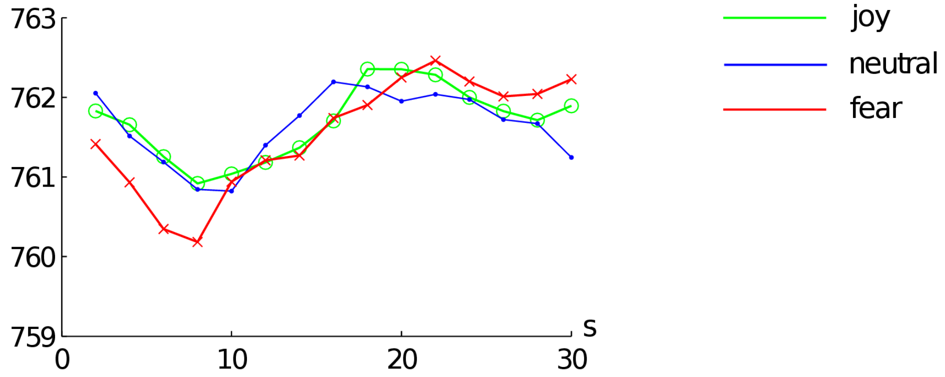

(e) Right somatosensory cortex (S1)

Figure 2.4: Timelines depicting average BOLD signal intensity in the regions that significantly differed in the GLM contrast joy vs. fear. The ordinate represents values of voxel intensity, the abscissa represents time (in seconds), zero corresponds to the onset of trials.

Temporal interaction analysis

To statistically test the temporal dynamics observed in the timelines, and to further explore the temporal dynamics of differences between conditions in other structures (see Introduction), a temporal interaction analysis was computed with factors emotion (two levels: joy and fear) and time (two levels: first half and second half of each stimulus, see Materials and methods). Results (corrected for multiple comparisons, $p < .05$) are listed in Table 3 and summarized in Fig. 3b. Significant interactions were observed in the AC bilaterally, and in the left SF. This confirms the observations based on the timelines that differences in the AC were more pronounced during the second half, and in the SF during the first half of trials. Moreover, according to the hypotheses (see Introduction), significant emotion × time interactions were observed bilaterally (a) in the posterior portion of the inferior frontal sulcus (IFS), (b) the anterior part of Broca's area (BA 45/46), and (c) in the ventral pallidum/ventral striatum (see also Fig. 3b). These interactions were due to more pronounced differences between conditions in the second compared to the first half. No interactions were observed in the hippocampus, parahippocampal gyrus, temporal poles, nor in the Rolandic operculum.

PPI analysis

Finally, we conducted a Psychophysiological Interaction (PPI) analysis (for details see Materials and methods). Seed regions were the peak voxels (as well as the directly adjacent voxels) identified in the GLM analysis in the direct contrast between fear and joy stimuli. Results of this analysis (corrected for multiple

Table 2.3: **Results of the interaction contrast of emotion (joy vs. fear) × time (1st half vs. 2nd half of each trial), corrected for multiple comparisons** ($p < .05$). Abbreviations: AC: auditory cortex; FOp: frontal operculum; SF: superficial amygdala STG: superior temporal gyrus; l: left; r: right.

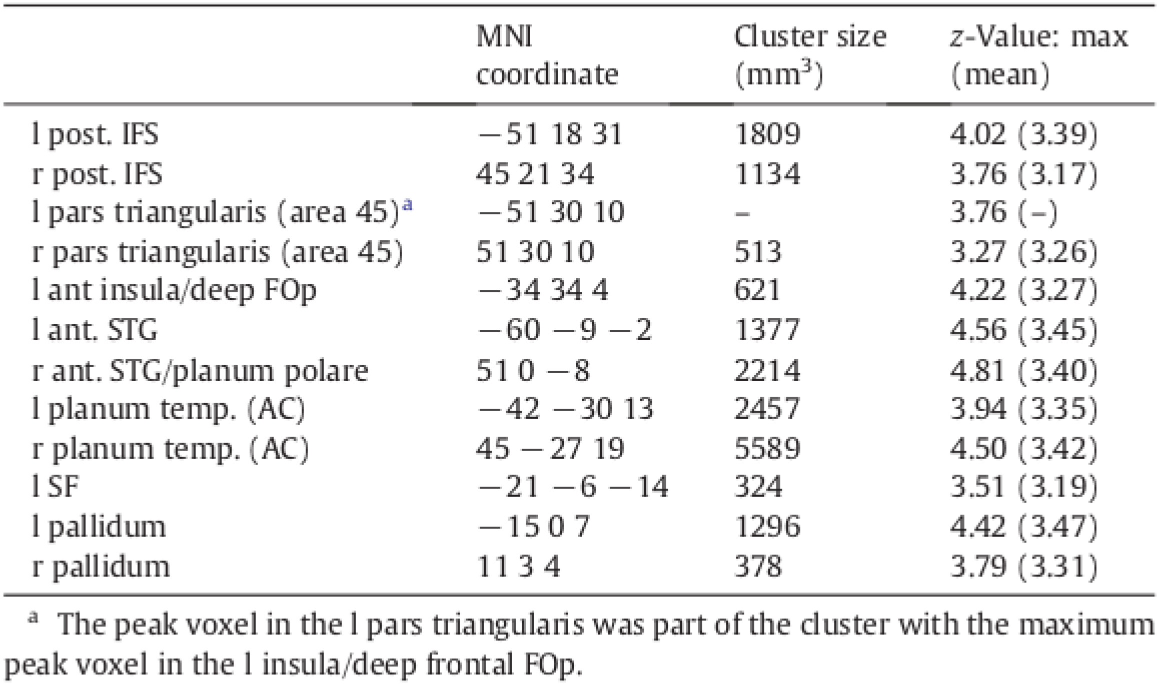

	MNI coordinate	Cluster size (mm^3)	*z*-Value: max (mean)
l post. IFS	−51 18 31	1809	4.02 (3.39)
r post. IFS	45 21 34	1134	3.76 (3.17)
l pars triangularis (area 45)[a]	−51 30 10	–	3.76 (–)
r pars triangularis (area 45)	51 30 10	513	3.27 (3.26)
l ant insula/deep FOp	−34 34 4	621	4.22 (3.27)
l ant. STG	−60 −9 −2	1377	4.56 (3.45)
r ant. STG/planum polare	51 0 −8	2214	4.81 (3.40)
l planum temp. (AC)	−42 −30 13	2457	3.94 (3.35)
r planum temp. (AC)	45 −27 19	5589	4.50 (3.42)
l SF	−21 −6 −14	324	3.51 (3.19)
l pallidum	−15 0 7	1296	4.42 (3.47)
r pallidum	11 3 4	378	3.79 (3.31)

[a] The peak voxel in the l pars triangularis was part of the cluster with the maximum peak voxel in the l insula/deep frontal FOp.

comparisons, $p < 0.05$), are listed in Table 4 and summarized in Fig. 3c.

Both left and right AC showed stronger functional connectivity during joy (compared to fear) with both ipsilateral and contralateral AC. In specific, the left posterior-lateral auditory belt showed stronger functional connectivity during joy with both left and right primary auditory cortex (left: 80%, right: 100% probability for TE 1.0 according to Morosan et al., 2001), as well as with lateral auditory belt-regions of both hemispheres. The right auditory core region showed stronger functional connectivity during joy with lateral auditory belt regions of both hemispheres (TE 2 according to Morosan et al., 2001, no probabilistic maps are available for this region). During fear (compared to joy), both left and right AC showed stronger functional connectivity with the cuneus (areas 17 and 18), the median wall of the precuneus (areas 5 and 7), and almost the entire cingulate sulcus (CS), from the pre-genual CS to the ascending branch of the (posterior) CS. Moreover, both left and right AC showed stronger functional connectivity during fear with the anterior insula bilaterally, and the left (but not the right) AC showed stronger functional connectivity during fear with the fundus of the central sulcus and the anterior bank of postcentral gyrus (areas 3a & b of S1).

The left SF showed stronger functional connectivity during joy (compared to fear) with right posterior HG (posterior auditory core and belt regions, 80% TE 1.1 according to Morosan et al., 2001). During fear (compared to joy), the left SF showed stronger functional connectivity with cuneus (V1–V4), and area 7a of the superior parietal lobule (precuneus) bilaterally (left: 70%, right: 40% probability according to Scheperjans et al., 2008). The right SF showed stronger functional connectivity during joy (compared to fear) with the mediodorsal nucleus of the thalamus (43% th-temporal according to Eickhoff et al., 2005). The S1 region did not show any significant PPI results in our data.

Table 2.4: Results of PPI analysis (corrected for multiple comparisons, p < .05), separately for the seed voxels in: (a) left AC (Heschl's gyrus), (b) right AC (Heschl's gyrus), (c) left SF, and (d) right SF (the PPI analysis with S1 as seed region did not indicate any results). Positive z-values (outermost right column) indicate stronger functional connectivity during joy compared to fear, whereas negative z-values indicate stronger functional connectivity during fear compared to joy. Abbreviations: AC: auditory cortex; FOp: frontal operculum; HG: Heschl's gyrus; ITS: inferior temporal sulcus; MD: mediodorsal; MTG: middle temporal gyrus; PAC: primary auditory cortex; SF: superficial amygdala; SFS: superior frontal sulcus; SPL: superior parietal lobule; STG: superior temporal gyrus; l: left; r: right.

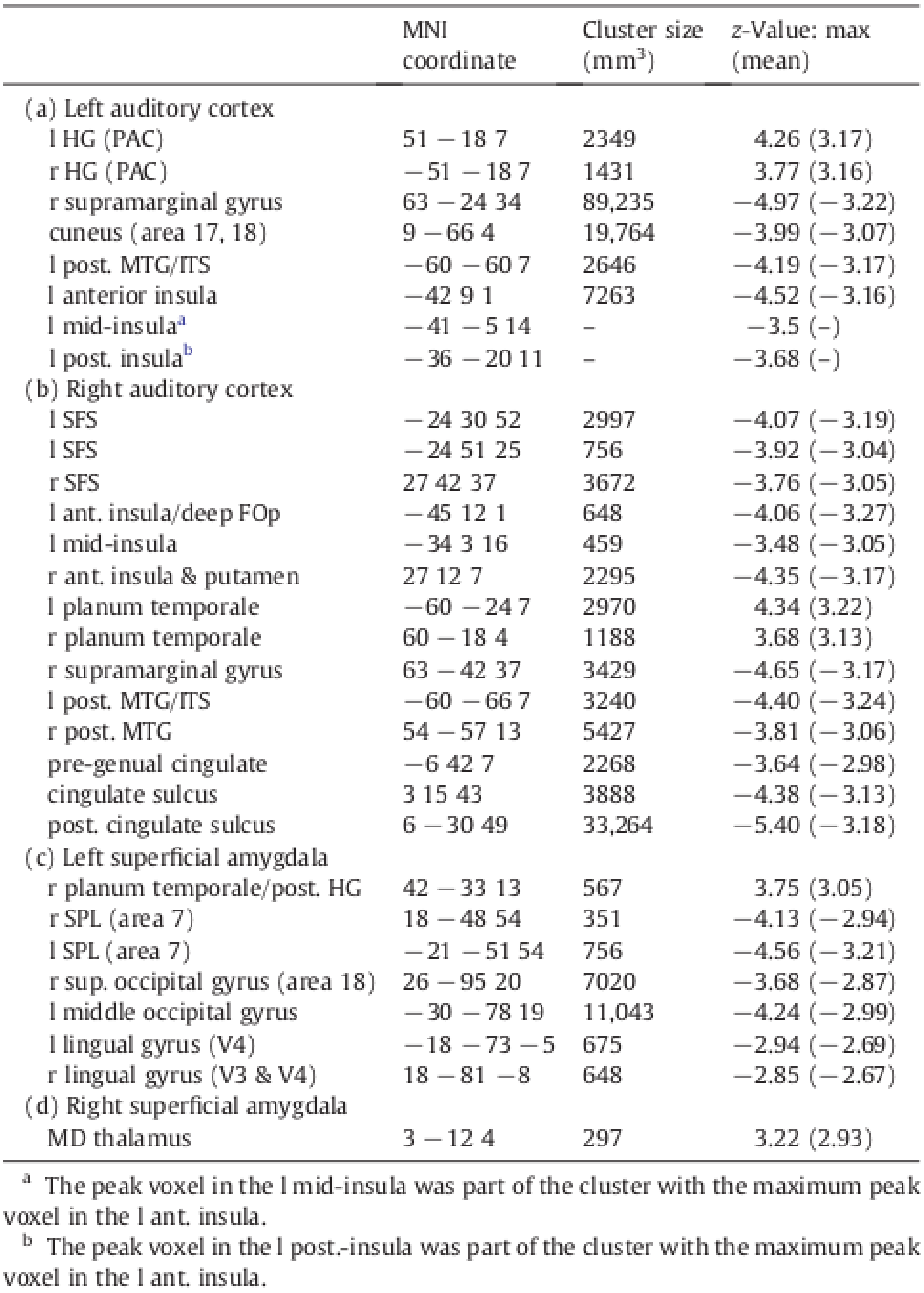

	MNI coordinate	Cluster size (mm^3)	*z*-Value: max (mean)
(a) Left auditory cortex			
l HG (PAC)	51 −18 7	2349	4.26 (3.17)
r HG (PAC)	−51 −18 7	1431	3.77 (3.16)
r supramarginal gyrus	63 −24 34	89,235	−4.97 (−3.22)
cuneus (area 17, 18)	9 −66 4	19,764	−3.99 (−3.07)
l post. MTG/ITS	−60 −60 7	2646	−4.19 (−3.17)
l anterior insula	−42 9 1	7263	−4.52 (−3.16)
l mid-insula[a]	−41 −5 14	–	−3.5 (–)
l post. insula[b]	−36 −20 11	–	−3.68 (–)
(b) Right auditory cortex			
l SFS	−24 30 52	2997	−4.07 (−3.19)
l SFS	−24 51 25	756	−3.92 (−3.04)
r SFS	27 42 37	3672	−3.76 (−3.05)
l ant. insula/deep FOp	−45 12 1	648	−4.06 (−3.27)
l mid-insula	−34 3 16	459	−3.48 (−3.05)
r ant. insula & putamen	27 12 7	2295	−4.35 (−3.17)
l planum temporale	−60 −24 7	2970	4.34 (3.22)
r planum temporale	60 −18 4	1188	3.68 (3.13)
r supramarginal gyrus	63 −42 37	3429	−4.65 (−3.17)
l post. MTG/ITS	−60 −66 7	3240	−4.40 (−3.24)
r post. MTG	54 −57 13	5427	−3.81 (−3.06)
pre-genual cingulate	−6 42 7	2268	−3.64 (−2.98)
cingulate sulcus	3 15 43	3888	−4.38 (−3.13)
post. cingulate sulcus	6 −30 49	33,264	−5.40 (−3.18)
(c) Left superficial amygdala			
r planum temporale/post. HG	42 −33 13	567	3.75 (3.05)
r SPL (area 7)	18 −48 54	351	−4.13 (−2.94)
l SPL (area 7)	−21 −51 54	756	−4.56 (−3.21)
r sup. occipital gyrus (area 18)	26 −95 20	7020	−3.68 (−2.87)
l middle occipital gyrus	−30 −78 19	11,043	−4.24 (−2.99)
l lingual gyrus (V4)	−18 −73 −5	675	−2.94 (−2.69)
r lingual gyrus (V3 & V4)	18 −81 −8	648	−2.85 (−2.67)
(d) Right superficial amygdala			
MD thalamus	3 −12 4	297	3.22 (2.93)

[a] The peak voxel in the l mid-insula was part of the cluster with the maximum peak voxel in the l ant. insula.

[b] The peak voxel in the l post.-insula was part of the cluster with the maximum peak voxel in the l ant. insula.

2.4 Discussion

2.4.1 Summary of results

The contrast analysis showed that BOLD signals in the auditory cortex (AC) bilaterally were strongest during joy, weakest during fear, with neutral in between. A similar pattern was observed for the superficial amygdala (SF), except that joy vs. neutral did not differ from each other in the right SF. In S1, fear evoked stronger BOLD signals than both neutral and joy (joy vs. neutral did not differ). In AC bilaterally, responses were stronger during the second half of each trial (and the same phenomenon was observed in area 45, the IFS, and the ventral pallidum/ventral striatum). By contrast, BOLD signals in the left SF were stronger during the first half. PPI results showed that both left and right AC showed stronger functional connectivity during joy (compared to fear) with both the ipsilateral and the contralateral AC. During fear (compared to joy), both left and right AC showed stronger functional connectivity with the cuneus (areas 17 and 18), the median wall of the precuneus (areas 5 and 7), and almost the entire cingulate sulcus (CS). Moreover, both left and right AC showed stronger functional connectivity during fear with the anterior insula bilaterally, and the left (but not the right) AC showed stronger functional connectivity during fear with areas 3a & b of S1. The left SF showed stronger functional connectivity during joy (compared to fear) with right posterior Heschl's gyrus. During fear (compared to joy), the left SF showed stronger functional connectivity with cuneus (V1–V4), and area 7a of the superior parietal lobule (precuneus) bilaterally. The right SF showed stronger functional connectivity during joy (compared to fear) with the mediodorsal nucleus of the thalamus.

2.4.2 Auditory cortex and emotional processing

Pronounced emotion-specific effects were observed in the auditory cortex: In the General Linear Model (GLM) contrast, BOLD responses in the entire supratemporal cortex (auditory core, belt, and parabelt) were stronger for joy than neutral stimuli, and stronger for neutral than fear stimuli. As will be argued in the following, these results indicate a prominent role of the auditory cortex in the emotional processing of auditory information. Importantly, there are five reasons as to why the activity differences between conditions cannot simply be due to acoustical factors: (1) the values of acoustical descriptors that significantly differed between conditions were included as covariates of no interest, and should therefore not have contributed to differences between conditions observed in the GLM contrasts. (2) However, even if this procedure did not cancel out acoustical differences between conditions, joy and fear stimuli did not differ with regard to their intensity, mean F0 frequency, variation of F0 frequency, pitch centroid value, spectral complexity, and spectral flux. (3) F0 salience and chord strength differed significantly between joy and fear stimuli, as well as between joy and neutral stimuli (F0 salience was highest for neutral, intermediate for joy, and lowest for fear stimuli; chord strength was highest for joy stimuli, and did not differ between neutral and fear stimuli). Nevertheless, in the GLM, BOLD signal intensity in the auditory cortex was stronger in response to joy compared to neutral, and during neutral compared to fear stimuli; this pattern does not correlate with the pattern of F0 salience (being strongest for neutral stimuli) or the pattern of chord strength (which did not differ between neutral and fear stimuli). (4) Key-strength showed differences between joy and fear, as well as between fear and neutral stimuli, but not between joy and neutral stimuli. Again, this pattern is not consistent with the pattern of BOLD responses observed in the auditory cortex. Although not well known, it is highly likely that extraction of the key of tonal music (including extraction of a tonal center) involves both posterior and anterior supratemporal cortex bilaterally (e.g., Koelsch, 2011; Liegeois-Chauvel et al., 1998; Patterson et al., 2002; Peretz and Zatorre, 2005). Therefore, the interactions of the auditory cortex with limbic/paralimbic brain structures are likely to be due to emotional processes, rather than being merely due to cognitive processes related to the key-strength of sounds. (5) Although fear stimuli had a higher degree of sensory dissonance than joy stimuli, activity changes in the auditory cortex are unlikely to be due to this difference only, because neutral stimuli were even more consonant than joy stimuli. The pattern of BOLD signal intensity observed in the GLM contrast is, thus, not related to the degree of sensory dissonance of the stimuli.

Instead, the observed pattern of BOLD signal intensity in the AC corresponds to the emotion ratings for joy (and inversely for fear, respectively), indicating that activity of the auditory cortex is related to the emotional quality of auditory information: Compared to neutral, BOLD signals had a higher intensity during the joy condition, and a lower intensity during the fear condition. In other words, we observed an actual increase in BOLD activity during listening to joy stimuli and an actual decrease during listening to fear stimuli (compared to neutral stimuli). With regard to the pronounced regional activity in the auditory cortex during the joy-evoking music (as indicated by the GLMs), it is likely that this was in part due to a more detailed acoustical analysis of the joyful music, which was probably related to a voluntary shift of attention: participants had a preference for the joy stimuli (as indicated by the valence ratings), and therefore probably paid more voluntary attention to those stimuli, leading to a stronger auditory cortex activation (Jäncke et al., 1999). Similar findings have previously been reported for pleasant compared to unpleasant music (Koelsch et al., 2006; Mueller et al., 2011) or pleasant vs. unpleasant sounds from the International Affective Digitized Sound System (IADS, Plichta et al., 2011). However, it is unlikely that merely preference (and, correspondingly, voluntary shifts of attention) explains this effect, because the preference of participants was comparable between fear and neutral music (again, as indicated by the valence ratings), and yet BOLD signal intensity differed between fear and neutral.

The role of the auditory cortex in the emotional processing of auditory information is further highlighted by the PPI results involving auditory seed regions: These results revealed emotion-specific functional connectivity (a) between auditory cortical areas and cingulate, as well as insular cortex during joy stimuli, and (b) between auditory areas and parietal, as well as visual cortex (V1–V5) during fear stimuli. Both cingulate and insular cortex are involved in emotional processes, in particular with regard to autonomic regulation as well as the production of subjective feelings (Craig, 2009; Medford and Critchley, 2010). In addition, the cingulate cortex has been implicated in the coordination of autonomic activity, behavior, motor expression, as well as cognitive processes in response to emotionally salient stimuli (Koelsch et al., 2010b; Medford and Critchley, 2010).

With regard to the marked functional connectivity between auditory areas and parietal as well as visual cortex, anatomical studies indicate that core, belt and parabelt regions project to V1 and V2 of visual cortex, and that neurons in V2 project back into these auditory regions (reviewed in Smiley et al., 2007). The observed functional connectivity between these areas in the present study highlights the role of auditory–visual interactions, in particular during emotional states of fear. The functional significance of such interactions is probably increased visual alertness in the face of danger signaled by auditory information (probably including involuntary shifts of attention). Our results are the first to show that the auditory cortex is a central hub of an affective-attentional network that is more extensive than previously believed, involving functional connectivity of auditory association cortex with a diverse range of visual, attentional, and limbic/paralimbic structures. This finding also supports the notion that multisensory interactions in the cerebral cortex are not limited to established polysensory regions, but that “interactions with other sensory systems also take place in auditory cortex” (Smiley et al., 2007). Notably, this latter conclusion holds even if such multisensory interactions were due to acoustical features which were possibly not accounted for by the computational feature extraction (and not necessarily related to emotional responses).

Many of the observed emotion-specific functional connections parallel anatomical connections previously described in monkeys (as described below). Our results provide information about the emotion-specific nature of such connections. With regard to functional connections to the insula, our results parallel connections between posterior AC and neighboring granular insula in macaque monkeys (Smiley et al., 2007), taken as a likely source of somatosensory input into the AC (Smiley et al., 2007). In addition, we observed functional connectivity not only with posterior, but also with mid- and anterior insula. This indicates clear functional connectivity between AC and the insula in humans, possibly reflecting sensory-limbic interactions that are more pronounced in humans than in monkeys. Such sensory-limbic interactions are also apparent in the extensive functional connectivity between AC and cingulate cortex. Previous studies with monkeys showed anatomical connections between (lateral) auditory belt and posterior cingulate cortex (Yukie, 1995). Our data suggest more extensive functional connections between auditory cortex and cingulate cortex in humans that also include anterior cingulate regions.

2.4.3 Superficial amygdala and its role for joy and fear

The superficial amygdala (SF) showed higher BOLD signal values bilaterally during joy compared to the fear stimuli. These findings corroborate previous reports of (right) SF activation in response to pleasant joyful music (compared to unpleasant music-like noise, Mueller et al., 2011). Due to its dense anatomical connections to the ventral striatum (from which it evolved phylogenetically, Nieuwenhuys et al., 2008), the superior amygdaloid complex has so far been implicated in positive emotion and hedonic processes (Nieuwenhuys et al., 2008), in line with our results. In addition, the superior amygdaloid complex has reciprocal connections to the orbitofrontal cortex (Bach et al., 2011) and plays a role for olfactory processes (Heimer and Van Hoesen, 2006; Price, 2003). Further functional connections include the caudate, cingulate cortex, insula, and hippocampus (Roy et al., 2009). Interestingly, a study by Goossens et al. (2009) suggested that the SF is particularly sensitive to social stimuli. Thus, in the present study, the joyful music possibly evoked activity within the SF due to the extraction of the social significance of the joyful music (but see also below). Such significance emerges from several social functions of music, including communication, coordination of movements, cooperation, and social cohesion (summarized in Koelsch, 2010). The fear stimuli, on the other hand, had no socially incentive value (being a signal of threat, and thus motivating withdrawal), probably resulting in decreased neuronal activity within the SF bilaterally (compared to joy and neutral stimuli). The fact that fear stimuli evoked significantly weaker responses in the right SF compared to a neutral control condition, and virtually no signal change in the left SF, suggests that the pattern of SF response to an auditory signal codes the emotional quality of that stimulus (i.e., whether the stimulus is an incentive social signal, or a signal of threat). Note that it is unlikely that SF simply codes valence (or arousal), for two reasons: first, to our knowledge, no previous study using stimuli that are perceived as rewarding, but do not have a social component (such as monetary rewards) reported SF activation, and second, valence as well as arousal ratings were used as regressors of no interest in the statistical modeling of the data, and are thus unlikely to contribute to the present fMRI results.

The PPI results reveal that functional connectivity between (left) SF and auditory regions was stronger during joy than during fear stimuli. Although previous studies have shown anatomical and functional connections between the basolateral (BL) amygdala and AC that are involved in fear conditioning (LeDoux, 2000), the significance of functional connectivity of the SF has remained elusive. As argued above, such connectivity is perhaps related to the social significance of stimuli, in contrast to the connectivity between BL and AC, which appears to be important for the conditioning of (auditory) signals of danger. It has recently been proposed (Kumar et al., 2012) that amygdala activity affects AC activity as a function of the emotional valence of stimuli (and that AC provides limbic/paralimbic structures with information about the acoustic quality of sounds). Thus, the functional connectivity between (left) SF and AC observed in the present study is in part consistent with the results by Kumar et al. (2012), because the stronger AC activity during joy (compared to fear) might be related to amygdalar activity (note that the functional connectivity between SF and AC was stronger during joy than fear, and that joy also evoked stronger BOLD signals than fear in AC). The neural pathway that originates in SF and modulates AC activity remains to be specified; as will be discussed below, such a pathway probably involves thalamic nuclei, including the medio-dorsal thalamus. Notably, the study by Kumar et al. (2012) presented unpleasant stimuli only, thus our results suggest that amygdala activity is also related to AC activity in response to pleasant auditory stimuli.

In addition to joy, SF is also involved in fear responses, as indicated by the increased functional connectivity of the (left) SF with area 7 and with visual areas during fear (compared to joy), possibly related to the elicitation of increased visual alertness during fear-evoking auditory information. Finally, the right SF showed increased functional connectivity during joy with the medio-dorsal thalamus (MD). A diffusion-tensor-imaging study by Behrens et al. (2003) reported a fiber tract extending anteriorly and inferiorly along the medial wall of the thalamus, then turning laterally into the amygdala. A similar path has been documented for non-human primates, via the inferior thalamic peduncle (Aggleton and Mishkin, 1984). In the study by Behrens et al. (2003), this pathway was small, and the authors were thus not confident that their result was valid. However, our results suggest that this pathway from MD to the (superficial) amygdala exists, and that it plays a specific role for positive emotion. Perhaps this thalamic nucleus is part of the pathway by which AC activity is regulated as an effect of SF activity.

Contrary to our hypothesis, no activity changes were observed between conditions in the hippocampal formation. However, the activity changes observed in the SF spread into the hippocampal-amygdaloid transition area, and perhaps stronger signal changes in the hippocampal formation would have been obtained in a less noisy environment: Mueller et al. (2011) reported that significant signal changes in the hippocampal formation (evoked by pleasant joyful music contrasted to unpleasant music-like noise) were observed only with interleaved silent steady state scanning, or with sparse temporal scanning; no signal change was observed in the hippocampus during continuous scanning in that study.

2.4.4 Primary somatosensory cortex (S1)

Stronger BOLD signals were measured in right area 3b of S1 during fear than during joy (or neutral) in voxels that correspond to the cortical representation of the face in S1 (Blakemore et al., 2005; Moulton et al., 2009). Previous experiments have reported that the recognition of emotions from visually presented facial expressions requires right somatosensory-related cortices, including the face representation in S1 (Adolphs et al., 2000). That finding corroborated the notion that individuals recognize another individual's emotional state by internally generating somatosensory representations that simulate how the other individual would feel when displaying a certain emotional (facial) expression. Our data suggest that such somatosensory-driven simulations are also activated by auditory information with emotional valence, such as music (probably also affective prosody). This notion is consistent with data indicating facial mimicry in response to happiness or sadness expressed by music (Lundqvist et al., 2009). It is also possible that somatosensory activity reflects mapping of an evoked emotional state during the emergence of feelings with the aid of somatosensory representations (e.g., of proprioceptive information during visually evoked emotions, Rudrauf et al., 2009). Again, our results suggest that such mapping can be activated by auditory information with emotional valence. The reason as to why, in our study, S1 representations were activated more strongly in response to fear than to joy remains to be specified.

2.5 Conclusions

This study has two main conclusions: First, during music listening, the auditory cortex has emotion-specific functional interactions with a diverse range of visual, parietal, and limbic/paralimbic structures; this demonstrates that the auditory cortex is a central relay of an affective-attentional network that is more extensive than previously believed. This finding also implicates that the auditory cortex is involved in sensory-limbic and multisensory interactions that resemble those of established polysensory regions. Second, our results suggest that the superficial amygdala (SF) is sensitive for incentive social signals (including music), but at the same time also involved in fear responses: in concert with the auditory cortex, the SF appears to elicit increased visual alertness in the face of danger signaled by auditory information. Fear music may thus activate phylogenetically old mechanisms that engage the visual localization of potentially threatening objects. It is tempting to speculate that the corresponding increase of activity in visual areas during listening to fear-evoking music leads to more intense visual imagery (compared, e.g., to joyful music), particularly when listening to music with closed eyes (as in the present study). Such increased visual imagery during fear-evoking music might be an important factor contributing to the emotional experience, and the esthetic appeal, of fear-evoking music.

2.6 Acknowledgment

This research was funded by the German Research Foundation (Deutsche Forschungsgemeinschaft, DFG) and the Cluster of Excellence “Languages of Emotion”.

2.7 References

Adolphs, R., Damasio, H., Tranel, D., Cooper, G., Damasio, A., 2000. A role for somatosensory cortices in the visual recognition of emotion as revealed by three-dimensional lesion mapping. J. Neurosci. 20, 2683–2690.

Aggleton, J., Mishkin, M., 1984. Projections of the amygdala to the thalamus in the cynomolgus monkey. J. Comp. Neurol. 222, 56–68.

Agrawal, D., Timm, L., Viola, F.C., Debener, S., Buechner, A., Dengler, R., Wittfoth, M., 2012. ERP evidence for the recognition of emotional prosody through simulated cochlear implant strategies. BMC Neurosci. 13, 113.

Alluri, V., Toiviainen, P., Jääskeläinen, I.P., Glereanc, E., Sams, M., Brattico, E., 2012. Large-scale brain networks emerge from dynamic processing of musical timbre, key and rhythm. NeuroImage 59, 3677–3689.

Amunts, K., Kedo, O., Kindler, M., Pieperhoff, P., Mohlberg, H., Shah, N., Habel, U., Schneider, F., Zilles, K., 2005. Cytoarchitectonic mapping of the human amygdala, hippocampal region and entorhinal cortex: intersubject variability and probability maps. Anat. Embryol. 210, 343–352.

Bach, D., Behrens, T., Garrido, L., Weiskopf, N., Dolan, R., 2011. Deep and superficial amygdala nuclei projections revealed in vivo by probabilistic tractography. J. Neurosci. 31, 618–623.

Baumgartner, T., Lutz, K., Schmidt, C., Jäncke, L., 2006. The emotional power of music: how music enhances the feeling of affective pictures. Brain Res. 1075, 151–164.

Beck, A., Steer, R., Brown, G., 1993. Beck Depression Inventory. Psychological Corporation, San Antonio, TX.

Behrens, T., Johansen-Berg, H., Woolrich, M., Smith, S., Wheeler-Kingshott, C., Boulby, P., Barker, G., Sillery, E., Sheehan, K., Ciccarelli, O., et al., 2003. Non-invasive mapping of connections between human thalamus and cortex using diffusion imaging. Nat. Neurosci. 6, 750–757.

Blakemore, S., Bristow, D., Bird, G., Frith, C., Ward, J., 2005. Somatosensory activations during the observation of touch and a case of vision–touch synaesthesia. Brain 128, 1571–1583.

Blood, A., Zatorre, R., 2001. Intensely pleasurable responses to music correlate with activity in brain regions implicated in reward and emotion. Proc. Natl. Acad. Sci. 98, 11818–11823.

Boersma, P., 2002. Praat, a system for doing phonetics by computer. Glot Int. 5 (9/10), 341–345.

Brattico, E., Alluri, V., Bogert, B., Jacobsen, T., Vartiainen, N., Nieminen, S., Tervaniemi, M., 2011. A functional MRI study of happy and sad emotions in music with and without lyrics. Front. Psychol. 2, 1–16.

Brown, S., Martinez, M., Parsons, L., 2004. Passive music listening spontaneously engages limbic and paralimbic systems. NeuroReport 15, 2033–2037.

Coutinho, E., Dibben, N., 2012. Psychoacoustic cues to emotion in speech prosody and music. Cogn. Emot. 1–27.

Craig, A., 2009. How do you feel—now? The anterior insula and human awareness. Nat. Rev. Neurosci. 10, 59–70.

Deichmann, R., Josephs, O., Hutton, C., Corfield, D., Turner, R., 2002. Compensation of susceptibility-induced bold sensitivity losses in echo-planar fMRI imaging. NeuroImage 15, 120–135.

Deichmann, R., Gottfried, J., Hutton, C., Turner, R., 2003. Optimized EPI for fMRI studies of the orbitofrontal cortex. NeuroImage 19, 430–441.

Eerola, T., Toiviainen, P., 2004. Mir in matlab: the midi toolbox. Proceedings of the International Conference on Music Information Retrieval, pp. 22–27 (Citeseer).

Eerola, T., Vuoskoski, J.K., 2011. A comparison of the discrete and dimensional models of emotion in music. Psychol. Music. 39, 18–49.

Eickhoff, S., Stephan, K., Mohlberg, H., Grefkes, C., Fink, G., Amunts, K., Zilles, K., 2005. A new SPM toolbox for combining probabilistic cytoarchitectonic maps and functional imaging data. NeuroImage 25, 1325–1335.

Ekman, P., 1999. Basic emotions. In: Dalgleish, T., Power, M. (Eds.), Handbook of Cognition and Emotion. Wiley Online Library, pp. 45–60.

Eldar, E., Ganor, O., Admon, R., Bleich, A., Hendler, T., 2007. Feeling the real world: limbic response to music depends on related content. Cereb. Cortex 17, 2828–2840.

Friston, K., Buechel, C., Fink, G., Morris, J., Rolls, E., Dolan, R., 1997. Psychophysiological and modulatory interactions in neuroimaging. NeuroImage 6, 218–229.

Friston, K., Ashburner, J., Kiebel, S., Nichols, T., Penny, W., 2007. Statistical Parametric Mapping: the Analysis of Functional Brain Images. Elsevier Academic Press, London.

Fritz, T., Jentschke, S., Gosselin, N., Sammler, D., Peretz, I., Turner, R., Friederici, A.D., Koelsch, S., 2009. Universal recognition of three basic emotions in music. Curr. Biol. 19, 573–576.

Gabrielson, A., Juslin, P., 2003. Emotional expression in music. In: Davidson, R., Scherer, K., Goldsmith, H. (Eds.), Handbook of Affective Sciences. Oxford University Press, New York, pp. 503–534.

Geyer, S., Schleicher, A., Zilles, K., 1999. Areas 3a, 3b, and 1 of human primary somato-sensory cortex: 1. microstructural organization and interindividual variability. NeuroImage 10, 63–83.

Goossens, L., Kukolja, J., Onur, O., Fink, G., Maier, W., Griez, E., Schruers, K., Hurlemann, R., 2009. Selective processing of social stimuli in the superficial amygdala. Hum. Brain Mapp. 30, 3332–3338.

Gosselin, N., Peretz, I., Noulhiane, M., Hasboun, D., Beckett, C., Baulac, M., Samson, S., 2005. Impaired recognition of scary music following unilateral temporal lobe excision. Brain 128, 628–640.

Gosselin, N., Peretz, I., Johnsen, E., Adolphs, R., 2007. Amygdala damage impairs emotion recognition from music. Neuropsychologia 45, 236–244.

Gosselin, N., Peretz, I., Hasboun, D., Baulac, M., Samson, S., 2011. Impaired recognition of musical emotions and facial expressions following anteromedial temporal lobe excision. Cortex 47, 1116–1125.

Heimer, L., Van Hoesen, G., 2006. The limbic lobe and its output channels: implications for emotional functions and adaptive behavior. Neurosci. Biobehav. Rev. 30, 126–147.

Huq, A., Bello, J.P., Rowe, R., 2010. Automated music emotion recognition: a systematic evaluation. J. New Music Res. 39, 227–244.

Huron, D., 2006. Sweet Anticipation: Music and the Psychology of Expectation. The MIT Press.

Janata, P., 2009. The neural architecture of music-evoked autobiographical memories. Cereb. Cortex 19, 2579–2594.

Jäncke, L., Mirzazade, S., Shah, N.J., 1999. Attention modulates activity in the primary and the secondary auditory cortex: a functional magnetic resonance imaging study in human subjects. Neurosci. Lett. 266, 125–128.

Johnstone, T., Ores Walsh, K., Greischar, L., Alexander, A., Fox, A., Davidson, R., Oakes, T., 2006. Motion correction and the use of motion covariates in multiple-subject fMRI analysis. Hum. Brain Mapp. 27, 779–788.

Juslin, P., Laukka, P., 2003. Communication of emotions in vocal expression and music performance: different channels, same code? Psychol. Bull. 129, 770–814.

Juslin, P., Västfjäll, D., 2008. Emotional responses to music: the need to consider underlying mechanisms. Behav. Brain Sci. 31, 559–575.

Kim, Y.E., Schmidt, E.M., Migneco, R., Morton, B.G., Richardson, P., Scott, J., Speck, J.A., Turnbull, D., 2010. Music emotion recognition: a state of the art review. In Proc. ISMIR, pp. 255–266 (Citeseer).

Koelsch, S., 2010. Towards a neural basis of music-evoked emotions. Trends Cogn. Sci. 14, 131–137.

Koelsch, S., 2011. Towards a neural basis of music perception—a review and updated model. Front. Psychol. 2, 1–20.

Koelsch, S., Fritz, T., Cramon, D.Y., Müller, K., Friederici, A.D., 2006. Investigating emotion with music: an fMRI study. Hum. Brain Mapp. 27, 239–250.

Koelsch, S., Offermanns, K., Franzke, P., 2010. Music in the treatment of affective disorders: an exploratory investigation of a new method for music–therapeutic research. Music. Percept. 27, 307–316.

Koelsch, S., Siebel, W.A., Fritz, T., 2010. Functional neuroimaging of emotion with music. In: Juslin, P., Sloboda, J. (Eds.), Handbook of Music and emotion: Theory, Re search, Applications. Oxford University Press Oxford, Oxford, pp. 313–346.

Koelsch, S., Fuermetz, J., Sack, U., Bauer, K., Hohenadel, M., Wiegel, M., Kaisers, U., Heinke, W., 2011. Effects of music listening on cortisol levels and propofol consumption during spinal anesthesia. Front. Psychol. 2, 1–9.

Krumhansl, C., 1990. Cognitive Foundations of Musical Pitch. Oxford University Press, USA.

Kumar, S., von Kriegstein, K., Friston, K., Griffiths, T.D., 2012. Features versus feelings: dissociable representations of the acoustic features and valence of aversive sounds. J. Neurosci. 32, 14184–14192.

Laurier, C., 2011. Automatic Classification of Musical Mood by Content-Based Analysis. Ph.D. thesis Universitat Pompeu Fabra, Barcelona.

LeDoux, J., 2000. Emotion circuits in the brain. Ann. Rev. Neurosci. 23, 155–184.

Lerner, Y., Papo, D., Zhdanov, A., Belozersky, L., Hendler, T., 2009. Eyes wide shut: amygdala mediates eyes-closed effect on emotional experience with music. PLoS One 4, e6230.

Liegeois-Chauvel, C., Peretz, I., Babaie, M., Laguitton, V., Chauvel, P., 1998. Contribution of different cortical areas in the temporal lobes to music processing. Brain 121, 1853–1867.

Lohmann, G., Müller, K., Bosch, V., Mentzel, H., Hessler, S., Chen, L., von Cramon, D.Y., 2001. Lipsia — a new software system for the evaluation of functional magnet resonance images of the human brain. Comput. Med. Imaging Graph. 25, 449–457 (See also at http://www.cns.mpg.de/lipsia).

Lohmann, G., Neumann, J., Müller, K., Lepsien, J., Turner, R., 2008. The multiple comparison problem in fMRI — a new method based on anatomical priors. Workshop on Analysis of Functional Medical Images, New York University, pp. 179–187.

Lundqvist, L., Carlsson, F., Hilmersson, P., Juslin, P., 2009. Emotional responses to music: experience, expression, and physiology. Psychol. Music. 37, 61–90.

Mattheson, J., 1739/1999. Der vollkommene Capellmeister. Bärenreiter, London.

Medford, N., Critchley, H., 2010. Conjoint activity of anterior insular and anterior cingulate cortex: awareness and response. Brain Struct. Funct. 214, 535–549.

Menon, V., Levitin, D., 2005. The rewards of music listening: response and physiological connectivity of the mesolimbic system. NeuroImage 28, 175–184.

Menon, V., Levitin, D., Smith, B., Lembke, A., Krasnow, B., Glazer, D., Glover, G., McAdams, S., 2002. Neural correlates of timbre change in harmonic sounds. NeuroImage 17, 1742–1754.

Mitterschiffthaler, M.T., Fu, C.H., Dalton, J.A., Andrew, C.M., Williams, S.C., 2007. A functional MRI study of happy and sad affective states evoked by classical music. Hum. Brain Mapp. 28, 1150–1162.

Morosan, P., Rademacher, J., Schleicher, A., Amunts, K., Schormann, T., Zilles, K., 2001. Human primary auditory cortex: cytoarchitectonic subdivisions and mapping into a spatial reference system. NeuroImage 13, 684–701.

Moulton, E., Pendse, G., Morris, S., Aiello-Lammens, M., Becerra, L., Borsook, D., 2009. Segmentally arranged somatotopy within the face representation of human primary somatosensory cortex. Hum. Brain Mapp. 30, 757–765.

Mueller, K., Mildner, T., Fritz, T., Lepsien, J., Schwarzbauer, C., Schroeter, M., Möller, H., 2011. Investigating brain response to music: a comparison of different fMRI acquisition schemes. NeuroImage 54, 337–343.

Mutschler, I., Wieckhorst, B., Speck, O., Schulze-Bonhage, A., Hennig, J., Seifritz, E., Ball, T., 2010. Time scales of auditory habituation in the amygdala and cerebral cortex. Cereb. Cortex 20, 2531–2539.

Nieuwenhuys, R., Voogd, J., Huijzen, C.V., 2008. The Human Central Nervous System. Springer, Berlin.

2.8 Supplementary Material

Supplementary Table 1: List of Stimuli

Composer / artist	Title	ASIN Nr.
Joy-evoking		
Joël Francisco Perri	El Canto de Mi Antara	B002BEXEHO
Craobh Rua	The Luck Penny	B000003NHN
Scotch Mist	Shetland Tune	n/a
Alfredo de Angelis	Pregonera	B001P5LDTQ
Orchestra Paraschiv Oprea	Batuta de la Adancata	B00000DTI6
Louis Armstrong	St. Louis Blues	B006CBVRJY
Niccolò Paganini	Violin Concerto No. 1, 3rd movement	B000001GHC
Jonathan Richman	Egyptian Reggae	B00580D1IU
Fear-evoking		
Danny Elfman	The Killing	B00000JC9R
Michael Giacchino	Monsters Are Such Interesting People (from: Lost)	B000EHSVDM
Michael Giacchino	Just Another Day on the Beach (from: Lost)	B000I2IQ9M
Michael Giacchino	Charlie's Dream (from: Lost)	B000I2IQ9M
Takeshi Miura et al.	Pulsating Right Arm (from: Biohazard Code)	B00005HWMB
Seiko Kobuchi	Boss Battle (from: Biohazard Zero)	n/a
Masami Ueda & Saori Maeda	Cold Sweat (from: Biohazard 3)	B000058A7Y
Akihiko Matsumoto et al.	Freezer Burn (from: Resident Evil Outbreak)	B00019257G

Eigenvector Centrality Mapping of Sustained Emotion

Stefan Koelsch & Stavros Skouras

Both authors contributed equally to this ms

http://dx.doi.org/10.1002/hbm.22416

To be published in Human Brain Mapping.

3.0 Abstract

Due to methodological constraints, functional neuroimaging in affective neuroscience has focused on brief emotional episodes. This fMRI study computed Eigenvector Centrality Mapping (identifying computational hubs within networks of inter-connected structures) and Functional Connectivity (FC) analysis to reveal neural networks underlying sustained emotions. Sustained emotions were evoked using joyful or fearful music, presented in four minute trials. Results show that superficial amygdala (SF), laterobasal amygdala (LB), hypothalamus, and striatum function as computational hubs during sustained joy. SF showed FC during joy with the nucleus accumbens (Nac), suggesting that SF and Nac modulate approach-avoidance behavior in response to social cues such as music. The striatum exhibited FC during joy with premotor cortex, areas 1 and 7a, hippocampus, insula and cingulate cortex, showing that sensorimotor, attentional, and emotional processes converge in the striatum during music perception. The hypothalamus showed FC during joy with hippocampus and mediodorsal thalamus, suggesting that hypothalamic endocrine activity is modulated by hippocampal and thalamic activity during sustained periods of music-evoked emotion. This fMRI study is the first to reveal a functional architecture of sustained emotion, indicating that emotions measured on a scale of minutes involve different neural correlates than those measured on a scale of seconds.

3.1 Introduction

The majority of research in affective neuroscience has focussed on initial reactions to external or internal stimuli. While this is an ecologically valid approach for emotions such as surprise, or recognition of emotional expressions, the majority of emotions experienced by humans in everyday life usually span over longer time periods, in the range of minutes or even longer (e.g., joy, worry, fear, or sadness). Although only few functional neuroimaging studies are available on this topic, several lines of evidence indicate that neural activity underlying emotion changes over time: Firstly, it appears that activity levels in limbic/paralimbic structures change significantly over time, which might be related, at least in part, to different functional connections between brain structures constituting a network underlying that emotion. For example, combining positron emission tomography (PET) and fMRI data, Salimpoor et al. (2011) showed that during the anticipation of a music-evoked frisson (involving exceptionally strong feelings of pleasantness and reward) dopamine availability increased in the dorsal striatum, whereas during the experience of the frisson itself, dopamine availability increased in the ventral striatum (probably the nucleus accumbens). Consistent with this finding, an fMRI study with musical stimuli of 1 min duration showed that BOLD signal values in amygdala, ventral striatum, hippocampus, parahippocampal gyrus and temporal pole were significantly higher during the second half of each musical stimulus (seconds 30 to 60) compared to the first half (Koelsch et al., 2006). Secondly, while autonomic responses to emotional stimuli are relatively quick (within the range of seconds), endocrine changes are considerably slower (usually within the range of minutes, or even longer, see e.g. Gotthardt et al., 1995). Therefore, neural activity initiating and monitoring such endocrine processes might go unnoticed when investigating initial reactions to stimuli only. That is, neural correlates of emotional experiences that usually last longer than just a few seconds can change over time, and there is lack of knowledge regarding neural correlates of emotional states that last several minutes. The present study investigates this issue, thus exploring a blind spot in the current view on neural correlates of emotion.

Investigating neural correlates of emotional states that span longer time intervals (such as minutes) using fMRI is challenging because traditional analysis methods require modelling of the hemodynamic response function. To achieve a reasonable statistical power, this requires a sufficient number of trials per experimental condition (usually at least about 20), and thus relatively short stimuli. For example, previous fMRI experiments with musical stimuli used stimulus durations between 12 and 24 s (Eldar et al., 2007; Menon and Levitin, 2005; Ball et al., 2007), or 44 s up to maximally 1 min (Baumgartner et al., 2006; Trost et al., 2012; Koelsch et al., 2006; Mitterschiffthaler et al., 2007). Functional neuroimaging studies using films (Hasson et al., 2004; Goldin et al., 2005) or a story (Wallentin et al., 2011) have used longer stimuli (up to 30 min, see Hasson et al., 2004), but to achieve a high statistical power these studies used continuous emotion regressors (Goldin et al., 2005), or continuous inter-subject correlations (Hasson et al., 2004), which inform us about neural correlates of changing emotional experience, rather than about sustained emotional states. It should be mentioned that, in contrast to fMRI, PET studies typically use longer time intervals to evoke and measure emotion, often around 60 s or longer (for a review of PET studies on emotion see, e.g., Costafreda et al., 2008). However, regarding functional connectivity, or similar analyses involving correlational computations between voxels of the time-series of a scanning session, fMRI can be more informative than PET due to fMRI’s higher spatial and temporal resolution (Poeppel et al., 2008).

To overcome the methodological barrier constraining the duration of experimental stimuli used in fMRI research, we used a new data-driven and model-free approach, the Eigenvector Centrality Mapping (ECM, Lohmann et al., 2010). ECM attributes a centrality value to each voxel in the brain such that a voxel receives a large value if it is strongly correlated with many other nodes that are themselves central within the network (Google’s Page-Rank algorithm is a variant of eigenvector centrality). ECM thus exploits small-world properties of the human brain (Sporns and Honey, 2006), and indicates the ”computational hubs” of neural networks distributed across different macroscopic brain structures (Tomasi and Volkow, 2011). Because ECM is based on correlations between timeseries, it can be applied for timeseries as long as several minutes (with the upper limit being the maximal length of a scanning session). For example, a previous study with a within-subjects design compared data of 7.6-minutes resting state scans of subjects when they were in states of hunger or satiety (Lohmann et al., 2010, that study reported that centrality values were higher during the hungry state in the posterior cingulate cortex and the precuneus). ECM is thus reminiscent of resting-state fMRI, except that ECM can also be computed for separate experimental conditions (i.e., not necessarily on resting state data), such as different emotion conditions. Hence, ECM can be used to identify emotion-specific computational hubs, beyond the computational hubs involved in resting state activity.

In the present study, we used for the first time ECM to investigate neural correlates of emotion. We employed three experimental conditions in which musical stimuli evoked either joy, or fear, or neither joy nor fear (”neutral” condition). Each condition consisted of one single trial of 4 min duration (Figure 1). That is, there were three trials per participant, each with a duration of four minutes: one joy, one fear, and one neutral trial (ordering of trials was counterbalanced across subjects).

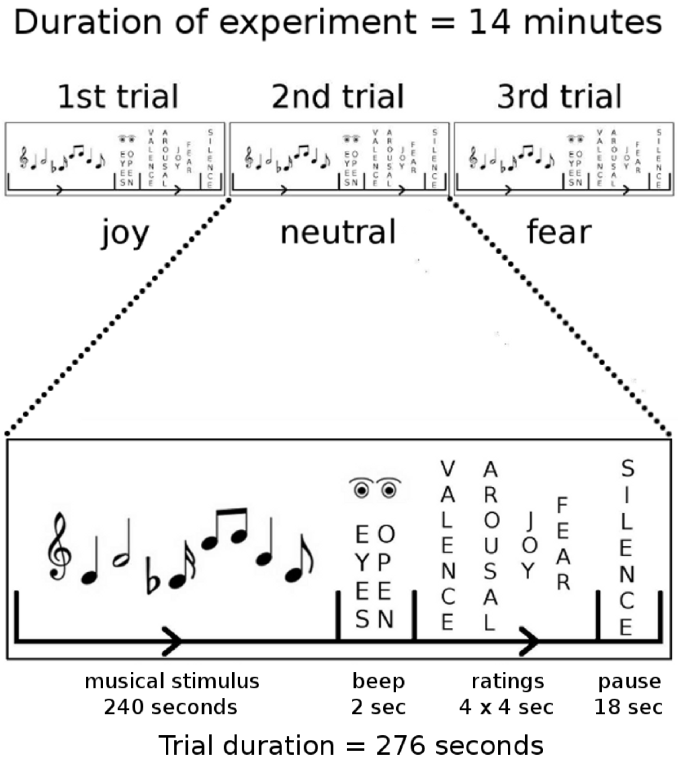

Figure 3.1: Experimental design. Three trials, each with a duration of several minutes, were presented to each subject. Each trial consisted of a music stimulus that was presented for 4 minutes (either joy, fear, or neutral, ordering was counterbalanced across subjects). Participants listened to the music with their eyes closed. The presentation of music was followed by a beep tone signalling to open the eyes and to commence the rating procedure. Four ratings (felt valence, arousal, joy, and fear) were obtained in 16 s.

Computational hubs identified in the contrasts between conditions were then used as seed regions for functional connectivity (FC) analysis. FC was computed separately for each condition, and FC maps were compared between conditions to identify emotion-specific functional connections between the identified ECM hubs and other brain structures.

This enabled us to investigate brain networks underlying joy and fear on the time-scale of minutes. Previous studies implicated the amygdala, in particular the lateral and basolateral nuclei, in the evaluation of both positive and negative stimuli (LeDoux, 2000; Paton et al., 2006; Murray, 2007; Holland and Gallagher, 2004), and the central amygdala in initiating behavioural, autonomic, and endocrine responses to such stimuli (LeDoux, 2000). These studies investigated phasic emotional responses – whether the amygdala also plays a role for tonic emotions has remained unknown. Therefore, we aimed at testing whether the direct contrast of ECMs between the joy and the fear condition in our study (calculated for several minutes of emotional experience) would show differences in these structures. In addition, we expected differences between conditions in neural structures involved in endocrine changes, specifically hypothalamus and hippocampus (which has dense bidirectional connections with the hypothalamus, and is substantially involved in the modulation of hypothalamic endocrine activity, O’Mara, 2005).

3.2 Materials and Methods

3.2.1 Participants

20 individuals (aged 21 – 38 years, M = 25.55, SD = 4.80, 10 females) took part in the experiment (for details see Supplementary Methods). Participants had normal hearing (as assessed with standard pure tone audiometry) and were right-handed (according to self-report). None of the participants was a professional musician or a music student. Exclusion criteria were past diagnosis of a neurological or psychiatric disorder, a score on Beck's Depression Inventory (Beck et al., 1993) of more than 12 points, excessive consumption of alcohol or caffeine during the 24 hours prior to testing, and poor sleep during the previous night. All subjects gave written informed consent, the study was conducted according to the Declaration of Helsinki and approved by the ethics committee of the School of Life Sciences and the Psychology Department of the University of Sussex.

3.2.2 Stimuli

Musical stimuli were selected to evoke (a) joy (CD-recorded pieces of joyful music from various epochs and styles), (b) fear (excerpts from soundtracks of suspense movies and video games), or (c) neither joy nor fear (henceforth referred to as neutral stimuli). None of the stimuli contained vocals. Details about the stimuli are provided in the Supplementary Materials and Supplementary Table S1. There were n = 8 stimuli per category, each with a duration of 30 s, concatenated into musically versatile stimulus blocks of 4 min duration per category (see Figure 1). Importantly, joy, fear, and neutral stimuli were balanced across experimental conditions with regard to tempo (beats per minute), mean F0 pitch, F0 pitch range, F0 pitch variation, pitch centroid values, spectral complexity, and spectral flux. A detailed acoustic analysis of the stimuli is provided in the Supplementary Materials. In brief, 177 acoustical descriptors were extracted and compared between conditions (joy, neutral, fear) using one-way ANOVAs. Significant effects of condition were indicated for ten acoustical factors (mean and variance of F0 salience, mean and variance of sensory dissonance, mean chord strength, mean key strength, mean and variance of spectral flux, mean spectral crest, and mean spectral complexity). To compensate for these acoustical differences, the values of these psychoacoustic parameters were used in the fMRI data analysis as regressors of no interest (see Data Analysis for details).

3.2.3 Procedure

Each participant listened to three different blocks, or trials, of musical stimuli (each trial lasting 4 min): One joy trial, one fear trial, and one neutral trial (see Figure 1). Ordering of trials was counterbalanced across subjects. Participants were asked to listen to the musical stimuli with their eyes closed. Each block of musical stimuli was followed by an interval of 2 s in which a sine-wave tone of 350 Hz and 1 s duration signaled participants to open their eyes and to commence the rating procedure. During the rating procedure, participants indicated how they felt at the end of each trial with regard to valence (pleasantness), arousal, joy, and fear. That is, participants provided ratings about how they actually felt, and not about which emotion they thought each block of stimuli was supposed to express (Gabrielson and Juslin, 2003). Ratings were obtained with 6-point Likert scales (ranging from ”not at all” to ”very much”). The time interval for the rating procedure was 16 s. The total length of the fMRI experiment thus amounted to about 14 min. Musical stimuli were presented using Presentation (version 13.0, Neurobehavioral systems, Albany, CA, USA) via MRI compatible headphones (under which participants wore earplugs). Instructions and rating screens were delivered through MRI compatible liquid crystal display goggles (Resonance Technology Inc., Northridge, CA, USA).

3.2.4 MR Scanning

Scanning was performed with a 3T Siemens Magnetom TrioTim. Prior to the functional MR measurements, a high-resolution (1x1x1 mm) T1-weighted anatomical reference image was acquired from each participant using a rapid acquisition gradient echo (MP-RAGE) sequence. Continuous Echo Planar Imaging (EPI) was used with a TE of 30 ms and a TR of 2,000 ms. Slice-acquisition was interleaved within the TR interval. The matrix acquired was 64x64 voxels with a Field Of View (FOV) of 192 mm, resulting in an in-plane resolution of 3 mm. Slice thickness was 3 mm with an interslice gap of 0.6 mm (37 slices, whole brain coverage). The acquisition window was tilted at an angle of 30 degrees relative to the AC-PC line in order to minimize susceptibility artifacts in the orbitofrontal cortex (Deichmann et al., 2002, 2003; Weiskopf et al., 2007). Given the analyses methods employed, a continuous scanning design was preferable for optimum correlation estimations (see Data Analysis for details).

3.2.5 Data Analysis

FMRI data were processed using LIPSIA 2.1 (Lohmann et al., 2001). Data were corrected for slicetime acquisition and normalized into MNI-space-registered images with isotropic voxels of 3 cubic millimeters. A temporal highpass filter with a cutoff frequency of 1/90 Hz was applied to remove low frequency drifts in the fMRI time series, and a spatial smoothing was performed using a 3D Gaussian kernel and a filter size of 6 mm FWHM.

The mean signal value per scan was computed and regressed out of each participant's data. Similarly, the movement parameters of each participant were regressed out of the entire fMRI timeseries acquired. In addition, the psychoacoustic parameters that had been identified to differ significantly between experimental conditions (see Supplemental Materials for details) were regressed out of each respective experimental condition. Thus, variance that could be explained by any of these factors was removed from the fMRI timeseries.

Functional MR data were analyzed using Eigenvector Centrality Mapping (ECM, Lohmann et al., 2010). On the first-level of statistical estimations, whole-brain ECM was computed separately for each participant, and separately for each trial (i.e., separately for the 4 minute block of each condition). On the second level of the ECM analysis, ECMs were compared between experimental conditions using voxel-wise paired sample t−tests. Results were corrected for multiple comparisons by the use of cluster-size and cluster-value thresholds obtained by Monte Carlo simulations with a significance level of $p < 0.05$ (Lohmann et al., 2008).

The ECM clusters identified by these analyses were then used as seeds for functional connectivity analyses: Each significant cluster identified by the ECM analysis was used as a functional connectivity seed, by computing the amount of correlation of the average timecourse of activity within each cluster with the activity in all other voxels. Functional connectivity maps were calculated separately for each experimental condition and for each participant, and then normalized across subjects. Subsequently, the normalized maps were compared between experimental conditions using paired t−tests corrected for multiple comparisons by the use of cluster-size and cluster-value thresholds obtained by Monte Carlo simulations with a significance level of $p < 0.05$ (Lohmann et al., 2008).

3.3 Results

3.3.1 Behavioral Data

Behavioral data are summarized in Table 1 and Figure 2. Joy ratings were higher for joy than neutral stimuli ($t(19) = 4.92$, $p < 0.0001$), and tended to be higher for neutral than fear stimuli ($t(19) = 2.55$, $p < 0.05$). Fear ratings were higher for fear than joy stimuli ($t(19) = 5.75$, $p < 0.0001$), but did not differ between fear and neutral stimuli ($p > .7$). Valence (pleasantness) ratings were higher for joy than neutral stimuli ($t(19) = 4.30$, $p < 0.001$), and higher for joy than fear stimuli ($t(19) = 6.79$, $p < 0.0001$), but did not differ significantly between neutral and fear stimuli ($p = .59$). Arousal ratings did not differ between joy and fear stimuli ($p = 1$), but tended to be higher for joy than neutral stimuli ($t(19) = 2.11$, $p < 0.05$), and higher for fear than neutral stimuli ($t(19) = 2.45$, $p < 0.05$).

3.3.2 fMRI data

Eigenvector centrality maps (ECMs) were computed separately for each emotion condition, and compared between conditions using voxel-wise t−tests (corrected for multiple comparisons, $p < .05$, see Materials and Methods for details). Results of these tests are listed in Table 2 and shown in Figure 3a. The contrast joy > fear showed significantly higher centrality values during joy (compared to fear) in the left superficial (SF) amygdala (extending into the hippocampal-amygdaloid

Table 3.1: Descriptive statistics of behavioral data (for test statistics see main text). Scales ranged from 1 ("not at all") to 6 ("very much").

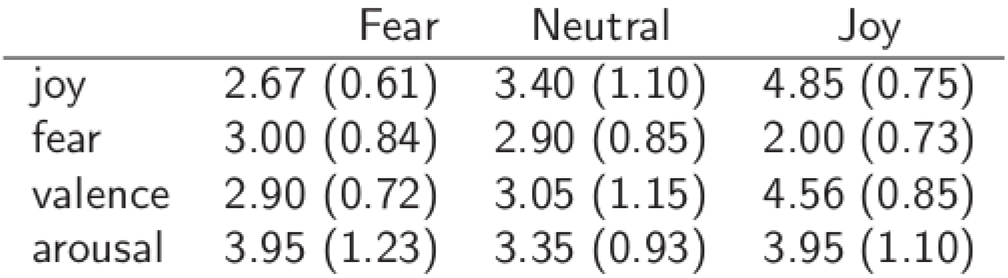

	Fear	Neutral	Joy
joy	2.67 (0.61)	3.40 (1.10)	4.85 (0.75)
fear	3.00 (0.84)	2.90 (0.85)	2.00 (0.73)
valence	2.90 (0.72)	3.05 (1.15)	4.56 (0.85)
arousal	3.95 (1.23)	3.35 (0.93)	3.95 (1.10)

(a) Valence

(b) Arousal

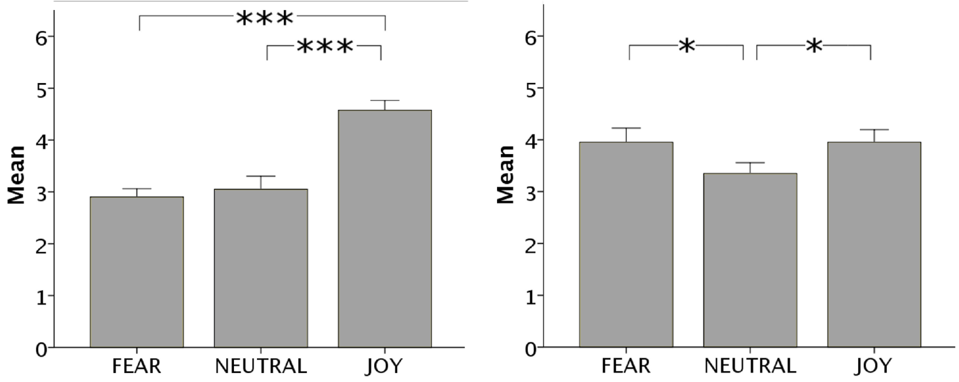

(c) Joy

(d) Fear

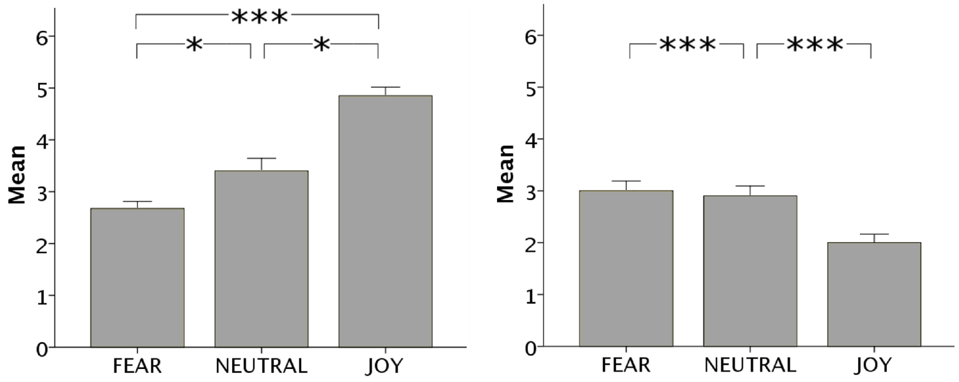

Figure 3.2: **Behavioral ratings.** Participants rated their emotional state on four scales: (a) valence, (b) arousal, (c) joy, and (d) fear. Average ratings are depicted separately for each stimulus category (fear, neutral, joy). Scales ranged from 1 ("not at all") to 6 ("very much"). Note that joy stimuli were rated as more pleasant than fear and neutral ones (valence/pleasantness ratings of fear and neutral did not differ from each other). Also note that arousal ratings of joy and fear stimuli did not differ from each other (and both joy and fear stimuli were rated as more arousing than neutral stimuli).

transition area) and the right laterobasal (LB) group of the amygdala (extending into the superficial group of the amygdala). In the left hemisphere, a cluster of significantly activated voxels protracted from the striatum (putamen and caudate nucleus) into the claustrum and the piriform cortex. Morever, significant ECM clusters were observed in the hypothalamus bilaterally. The opposite contrast (fear > joy) did not reveal any significantly activated clusters. Note that values of acoustic descriptors that differed between conditions were introduced as regressors of no interest during the pre-processing (see Data Analysis for details). Therefore, it is unlikely that acoustical differences between stimuli contributed to the present results.

Table 3.2: Results of the ECM contrast emotion (joy > fear), corrected for multiple comparisons ($p < .05$). Percentages in brackets indicate anatomical probabilities according to the SPM Anatomy Toolbox (Eickhoff et al., 2005).

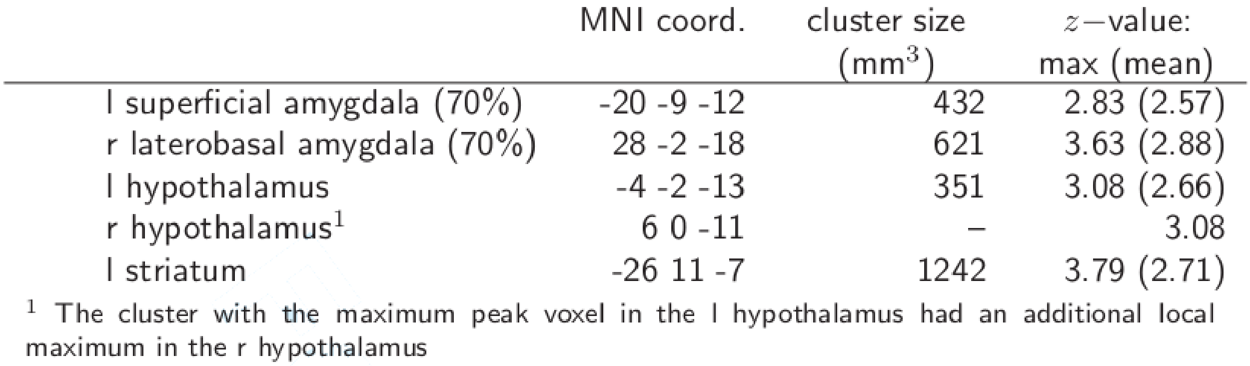

	MNI coord.	cluster size (mm^3)	$z-$value: max (mean)
l superficial amygdala (70%)	-20 -9 -12	432	2.83 (2.57)
r laterobasal amygdala (70%)	28 -2 -18	621	3.63 (2.88)
l hypothalamus	-4 -2 -13	351	3.08 (2.66)
r hypothalamus[1]	6 0 -11	–	3.08
l striatum	-26 11 -7	1242	3.79 (2.71)

[1] The cluster with the maximum peak voxel in the l hypothalamus had an additional local maximum in the r hypothalamus

Comparisons with the neutral condition showed that, in the left SF as well as in the hypothalamus, centrality values were significantly higher for joy than for neutral ($p < .05$ for each structure, corrected for multiple comparisons), and nominally (but not significantly) lower in the fear compared to the neutral condition. In the right LB, centrality values were nominally higher for joy than for neutral, and higher for neutral than for fear stimuli, but these differences were statistically not significant. In the striatum, centrality values tended to be higher for joy than for neutral ($z = 3.01$), and were nominally higher for neutral than for fear, but none of these differences was statistically significant when corrected for multiple comparisons.

3.3.2.1 Functional Connectivity analysis

The ECM clusters were then used as seed regions for functional connectivity analysis, and functional connectivity maps were compared between experimental conditions (that is, for each ECM cluster, the average timecourse of activity was used as seed time-series in functional connectivity analyses to identify target regions for which the covariation of activity between seed and target regions was significantly different between experimental conditions, see Data Analysis for details). Results (corrected for multiple comparisons, $p < 0.05$) are listed in Table 3 and summarized in Figures 3b & 4).

The left superficial amygdala (SF) showed stronger functional connectivity during joy than during fear stimuli with the left medial thalamic region (MTR, the maximum was located in the paraventricular nucleus of the thalamus). The right

Table 3.3: Results of the emotion-specific functional connectivity analyses (contrast: joy > fear), corrected for multiple comparisons ($p < .05$). Seed-voxels used for the functional connectivity analyses are the peak voxels of the ECM results (ECM contrast joy > fear; seed regions are indicated by italic font in the outermost left column). For example, the superficial amygdala (which showed higher centrality values during joy compared to fear) showed increased functional connectivity with the thalamus during joy (compared to fear). Percentages in brackets indicate anatomical probabilities according to the SPM Anatomy Toolbox (Eickhoff et al., 2005). Abbreviations: CA: cornu ammonis of hippocampal formation; IPS: intraparietal sulcus; LB: laterobasal group of amygdala; MCC: midcingulate cortex; SF: superficial group of amygdala; SMA: supplementary motor area; SPL: superior parietal lobule; SUB: subiculum of hippocampal formation; l: left; r: right.

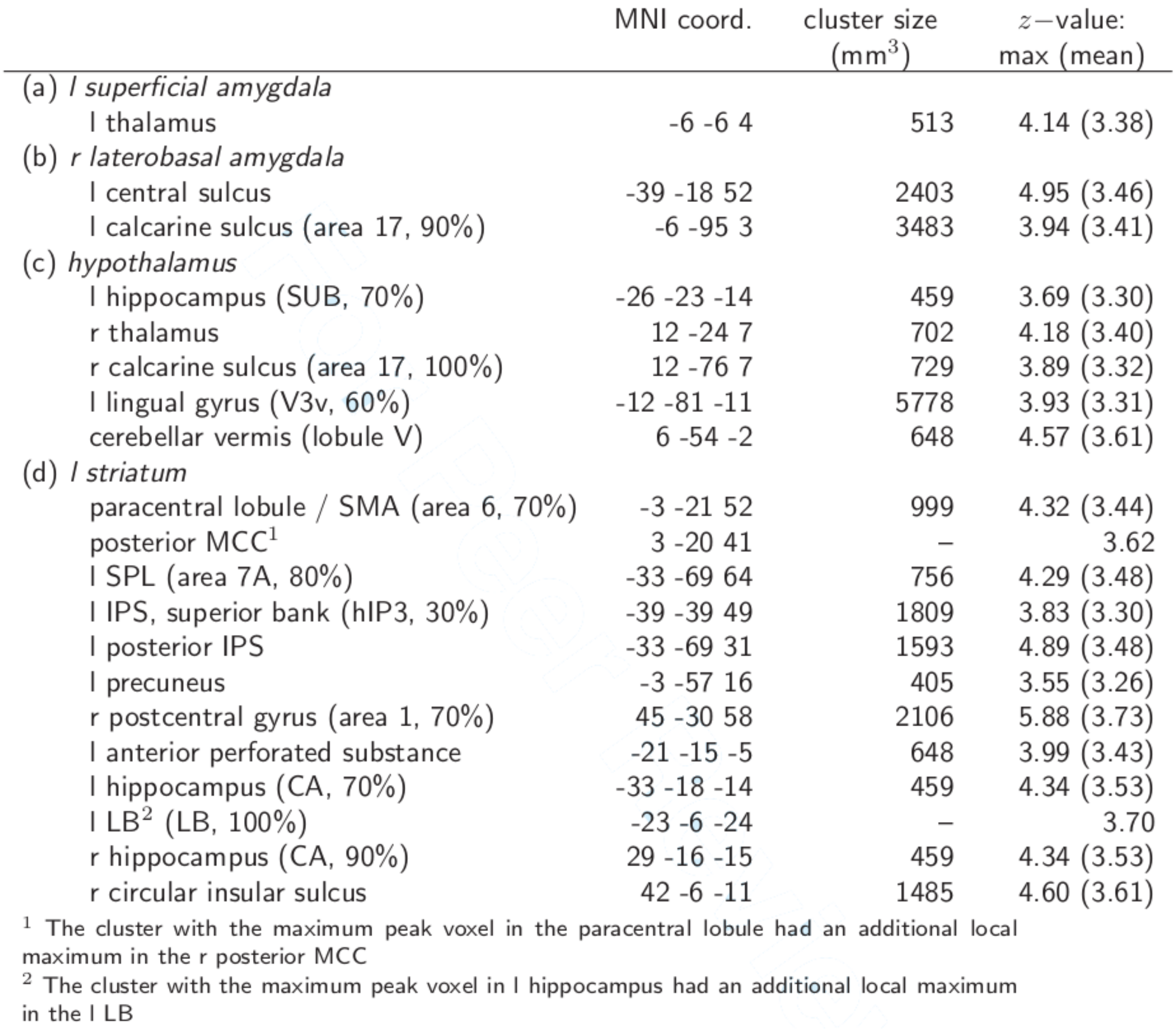

	MNI coord.	cluster size (mm^3)	z−value: max (mean)
(a) *l superficial amygdala*			
l thalamus	-6 -6 4	513	4.14 (3.38)
(b) *r laterobasal amygdala*			
l central sulcus	-39 -18 52	2403	4.95 (3.46)
l calcarine sulcus (area 17, 90%)	-6 -95 3	3483	3.94 (3.41)
(c) *hypothalamus*			
l hippocampus (SUB, 70%)	-26 -23 -14	459	3.69 (3.30)
r thalamus	12 -24 7	702	4.18 (3.40)
r calcarine sulcus (area 17, 100%)	12 -76 7	729	3.89 (3.32)
l lingual gyrus (V3v, 60%)	-12 -81 -11	5778	3.93 (3.31)
cerebellar vermis (lobule V)	6 -54 -2	648	4.57 (3.61)
(d) *l striatum*			
paracentral lobule / SMA (area 6, 70%)	-3 -21 52	999	4.32 (3.44)
posterior MCC[1]	3 -20 41	–	3.62
l SPL (area 7A, 80%)	-33 -69 64	756	4.29 (3.48)
l IPS, superior bank (hIP3, 30%)	-39 -39 49	1809	3.83 (3.30)
l posterior IPS	-33 -69 31	1593	4.89 (3.48)
l precuneus	-3 -57 16	405	3.55 (3.26)
r postcentral gyrus (area 1, 70%)	45 -30 58	2106	5.88 (3.73)
l anterior perforated substance	-21 -15 -5	648	3.99 (3.43)
l hippocampus (CA, 70%)	-33 -18 -14	459	4.34 (3.53)
l LB[2] (LB, 100%)	-23 -6 -24	–	3.70
r hippocampus (CA, 90%)	29 -16 -15	459	4.34 (3.53)
r circular insular sulcus	42 -6 -11	1485	4.60 (3.61)

[1] The cluster with the maximum peak voxel in the paracentral lobule had an additional local maximum in the r posterior MCC

[2] The cluster with the maximum peak voxel in l hippocampus had an additional local maximum in the l LB

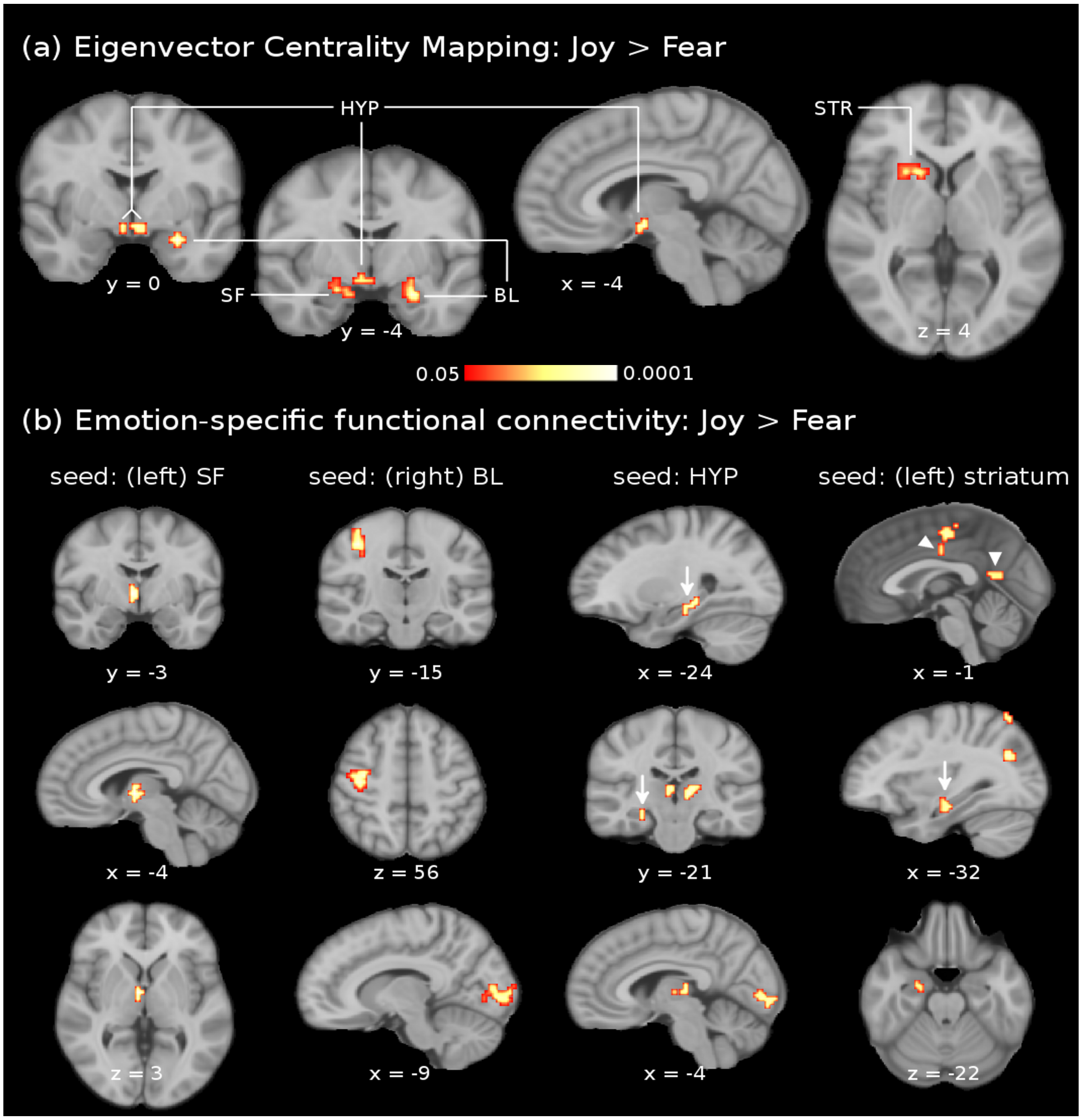

Figure 3.3: fMRI results. (a) shows the comparison of Eigenvector Centrality Maps (ECM) between joy and fear (joy > fear). Clusters of significantly higher centrality values during joy than fear were indicated in the hypothalamus (HYP), left superficial amygdala (SF), right laterobasal amygdala (LB) and left striatum (STR). These four clusters were used as seed regions for functional connectivity analyses. The results of the comparison of functional connectivity maps between joy and fear (joy > fear) are shown in (b), separately for the four seed regions (left SF: outermost left, right BL: middle left column, hypothalamus: middle right column, left striatum: outermost right column). Scale for (b) is the same as for (a). The left SF showed emotion-specific functional connectivity (stronger during joy than fear) with the hypothalamus. The right BL showed stronger functional connectivity during joy than fear with somatosensory cortex (area 3b) and primary visual cortex (V1, bottom image of left middle column). The hypothalamus showed emotion-specific functional connectivity with the hippocampal formation (arrows), thalamus and primary visual cortex (V1, bottom image of right middle column). The left striatum showed stronger functional connectivity during joy than fear in supplementary motor area, midcingulate cortex and posterior cingulate cortex (arrow-heads), hippocampal formation (arrow), and laterobasal amygdala (bottom image of outermost right column). Images are shown in neurological convention, all results are corrected for multiple comparisons ($p < .05$).

laterobasal amygdala (LB) showed stronger functional connectivity during joy than during fear stimuli with the left central sulcus (area 3b according to Geyer et al., 1999) and with primary visual cortex (area 17). The hypothalamus showed stronger functional connectivity during joy than during fear stimuli with the left hippocampus, the right thalamus, V1, V3v, and the cerebellum. Finally, the left striatum exhibited significantly stronger functional connectivity during joy than during fear stimuli with left LB, both left and right hippocampus, left anterior perforated substance, right circular insular sulcus, posterior midcingulate cortex (area p24b' according to Palomero-Gallagher et al., 2009), supplementary motor area (SMA), postcentral gyrus (area 1), the medial bank of the left intraparietal sulcus (IPS, area hIP3 according to Scheperjans et al., 2008), left lateral superior parietal lobule (area 7A according to Scheperjans et al., 2008), and posterior cingulate cortex (area v23 according to Palomero-Gallagher et al., 2009). None of the comparisons showed stronger functional connectivity during fear (compared to joy).

3.4 Discussion

Our data reveal a neural network underlying sustained positive emotion with the (left) superficial group of the amygdala (SF), the (right) laterobasal group of the amygdala (LB), hypothalamus, and the striatum as computational hubs, as well as a number of functionally connected cortical and subcortical structures (summarized in Figure 4). These structures include hippocampus, medial thalamus, cerebellum, and neocortical structures involved in attention, sensorimotor processes and vision. Out of these structures, thalamus, hippocampus, and (primary) visual cortex were functionally connected to more than one computational hub, thus constituting second-order computational hubs.

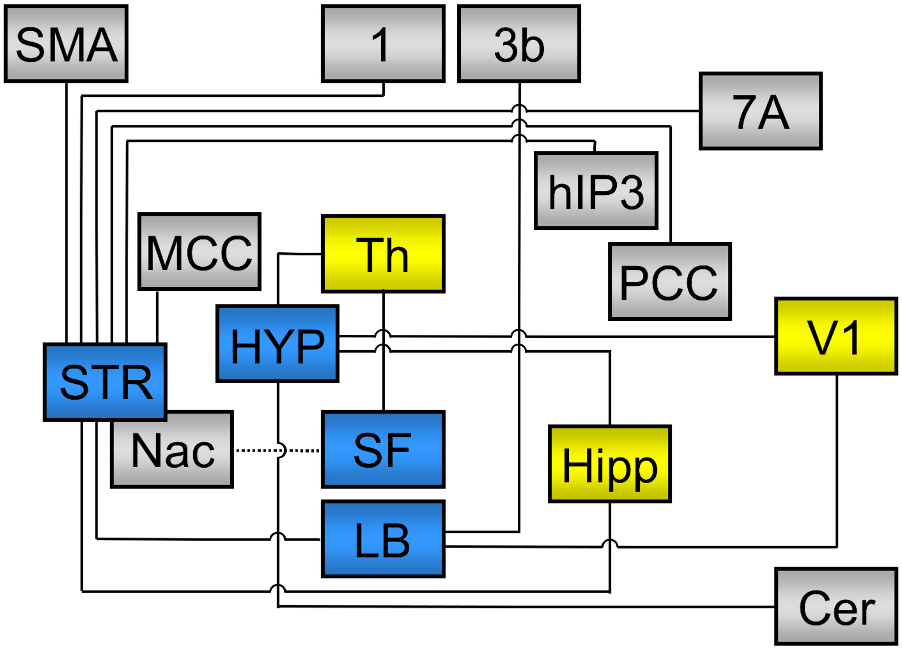

Figure 3.4: Summary of results.
Blue rectangles indicate computational hubs (joy > fear) as indicated by the ECM, lines indicate functional connections to other structures as indicated by the emotion-specific (joy > fear) functional connectivity analysis. The dotted line connecting SF and Nac indicates that this result was yielded by the uncorrected z-map (see main text). Yellow boxes indicate structures that are functionally connected to more than one ECM hub. Cer: cerebellum: Hipp: hippocampal formation; HYP: hypothalamus; LB: laterobasal group of amygdala; MCC: middle cingulate cortex; Nac: nucleus accumbens; PCC: posterior cingulate cortex; SF: superficial group of amygdala; SMA: supplementary motor area; STR: striatum; Th: Thalamus.

The involvement of SF (consisting of anterior amygdaloid area, amygdalopyriform transition area, cortical nuclei, and amygdaloid-hippocampal area according, e.g., to Amunts et al., 2005) indicates that SF plays a central role during sustained periods of emotional experience. Hence, other than previously believed, SF is not only active during the initial stages of stimulus evaluation. Our data corroborate the notion that SF is involved in the evaluation of signals with social relevance (Bzdok et al., 2012), and indicate that SF is particularly sensitive for positive social signals, including joy expressed by music: On the one hand, SF is sensitive to social stimuli, as indicated by an fMRI study by Goossens et al. (2009) in which signal changes in the SF were observed in response to faces, but not to houses. On the other hand, trustworthiness as well as attractiveness judgments of faces overlap in the SF (Bzdok et al., 2011). It has previously been argued that individuals perceive music as a stimulus with social significance due to its communicative properties (Cross and Morley, 2008; Steinbeis and Koelsch, 2008; Koelsch, 2010), and the finding that SF exhibits stronger activity in response to joy than fear (and neutral) stimuli indicates that neural activity in SF also codes whether social signals are incentive or aversive.

The SF showed functional connectivity with the medial thalamic region (MTR) which was specific for joy. Both amygdala and thalamus possess evaluative and mnemonic functions, and efferents to the MTR enable the amygdala to influence neural activity in large regions of the (prefrontal) cortex (Aggleton and Mishkin, 1984). In addition, both amygdala and MTR show high density of opiate receptors (Wamsley et al., 1982), and it is interesting to note that both SF and MTR (in particular the paraventricular nucleus of the thalamus) project to the nucleus accumbens (Nac; Bzdok et al., 2012; Li and Kirouac, 2008). Such connections have been proposed to modulate approach-avoidance behavior towards social cues in human interaction (Bzdok et al., 2011), and based on the studies showing projections between SF and Nac (Bzdok et al., 2012; Li and Kirouac, 2008) we also investigated possible emotion-specific functional connectivity between SF (used as seed region) and Nac in our data, using a lower statistical threshold (uncorrected z−maps thresholded at $p < .001$ and a voxel-extent of five voxels). This revealed functional connectivity between SF and ventral striatum / Nac that was stronger during joy than during fear (see Supplemental Figure S1, see also dashed line in Figure 4). Taken together, these results indicate that, in humans, SF and Nac modulate approach-avoidance behavior in response to social cues, and that functional connectivity between SF, MTR and Nac is modulated by the emotional valence of stimuli.

The (right) laterobasal group of the amygdala (LB, consisting of lateral, basolateral, basomedial and paralaminar nuclei Amunts et al., 2005) also showed higher centrality values during joy. These data are the first to show that LB plays a central role for emotions lasting over the course of minutes. LB is conceived of as the main amygdalar input structure for auditory information (as well as for sensory information from other modalities), and involved in the evaluation and learning of both positive and negative stimuli (LeDoux, 2000; Critchley et al., 2002; Vuilleumier, 2005; Paton et al., 2006; Murray, 2007; Holland and Gallagher, 2004). Note that LB has been implicated in learning and encoding of stimuli signalling reward (Paton et al., 2006; Murray, 2007) and the generation of reward expectancies that guide goal-directed behavior (Holland and Gallagher, 2004). Thus, activation of LB in the present study was likely to be due to the coding of the reward value of pleasant music. Of particular interest is also the functional connectivity between LB and sensory cortex (probably area 3b). LB is connected to sensory areas (both directly and indirectly, Murray, 2007; Shi and Cassell, 1999), and this connection may well be related to sensory aspects, and thus to the subjective feeling component, of emotion (Harrison et al., 2010; Herwig et al., 2010; Gray et al., 2007).

The hypothalamus also showed higher centrality values during joy (compared to fear). This indicates that the hypothalamus is involved in joy, in particular during longer emotional periods. Activation of the hypothalamus in the present study was probably due to endocrine changes, and the fact that hypothalamic activation is rarely observed in fMRI studies on emotion is presumably due to the fact that such changes are relatively slow (and thus go unnoticed in experiments with shorter stimulus durations). Future endocrinological studies could aim at specifying hormones released during experiences of joy (studies on endocrine effects of music are reviewed in Koelsch and Stegemann, 2012).

Importantly, the hypothalamus showed emotion-specific functional connectivity (stronger for joy than for fear) with the subiculum of the hippocampal formation. This finding is well in accordance with the observations that the subiculum has dense bidirectional connections with the hypothalamus (O’Mara, 2005). These connections include projections from the subiculum to the medial preoptic area, the ventromedial and dorsomedial nuclei, and ventral premammillary as well as medial mammillary nuclei (O’Mara, 2005). The functional significance of these connections is thought to be modulation of hypothalamus-pituitary-andrenal (HPA) axis activity (in particular inhibition of HPA-axis activity mediated by GABAergic neurones, O’Mara, 2005). Thus, the subiculum is substantially involved in terminating or limiting HPA axis activity in response to stress. The present results hence indicate that the hippocampal formation plays a role for modulating hypothalamic endocrine activity during sustained periods of music-evoked positive emotion; this finding has important implications for the application of music therapy to reduce stress and stress responses in both clinical and non-clinical settings (reviewed in Koelsch and Stegemann, 2012).

The (left) striatum was identified as another computational hub (in the comparison joy > fear). Notably, compared to SF, LB, and hypothalamus, the striatum showed by far the largest number of emotion-specific functional connections with other structures, including (left) LB and (left) anterior perforated substance, bilatera hippocampus, posterior middle cingulate cortex, right circular insular sulcus, supplementary motor area (SMA), area 1, medial bank of the left intraparietal sulcus (area hIP3), left lateral superior parietal lobule (area 7A), and posterior cingulate cortex (PCC, area v23). The observation of these extensive functional connections of the striatum with other cerebral structures is consistent with anatomical studies showing that the entire neocortex, including sensorimotor and parietal association cortex, sends fibres to both the caudate nucleus and the putamen (Nieuwenhuys et al., 2008). In addition, the basolateral nucleus of the amygdala (Russchen et al., 1985), hippocampus (Parent and Hazrati, 1995; Haber et al., 1990) as well as cingulate cortex (Parent and Hazrati, 1995; Haber et al., 1990) send projections to the ventral striatum including, but not limited to, the nucleus accumbens. Although sensorimotor, association, and limbic cortical areas project in a segregated manner onto three distinct striatal regions (referred to as associative, sensorimotor and limbic striatal territories, Parent and Hazrati, 1995), it is striking that the region identified as striatal computational hub in our study is located at the borders of all three of these territories (c.f. Parent and Hazrati, 1995). Hence, our data on emotion-specific functional connections of the striatum are in remarkable agreement with anatomical projections to the striatum, and indicate that such projections play a role for emotional processes.

Previous music and language research implicated the striatum mainly in motor-related processes (for an exception see Salimpoor et al., 2011). The role of the striatum for emotional processes has first been discussed by MacLean (1972), who proposed that the striatal complex is part of a storage mechanism for learned emotive behaviors, a notion that is corroborated by the the functional connections of the striatum with sensorimotor and limibic structures in the present study. MacLean (1972) also proposed that the striatal complex plays a role for behavior involving conspecific recognition and communication in the form of rudimentary, non-verbal signalling. Our results emphasize the significant role of the striatum for emotional processes, and show that the striatum functions as a computational hub in which sensorimotor, attentional, and emotional processes converge during the perception of positive music.

3.5 Conclusions

The present fMRI study is the first using Eigenvector Centrality Mapping for the analysis of neural networks underlying emotion, and the first to reveal the functional neuroarchitecture of sustained emotion (evoked and measured over the course of several minutes). The data show that both superficial (SF) and laterobasal (LB) nuclear groups of the amygdala play a role throughout sustained periods of joy and are (other than previously believed) not only active during the initial stages of stimulus evaluation. Results corroborate the recent notion that SF is involved in the evaluation of signals with social relevance, and they indicate that SF is particularly sensitive for social signals with positive valence, such as joy expressed by music. The functional connectivity between SF and nucleus accumbens (Nac) probably modulates approach-avoidance behavior in response to social cues, whereas the functional connectivity between LB and sensory areas appears to be related to sensory aspects, and thus to the subjective feeling component, of emotion. Our data on sustained emotions also indicate emotion-specific functional connectivity between hypothalamus and hippocampus, which is likely to be due to the modulation of hypothalamus-pituitary-andrenal (HPA) axis activity (in particular inhibition of HPA-axis activity) during extended periods of emotional experience. Of the four observed computational hubs, the striatal complex had by far the largest number of emotion-specific functional connections to other structures. This highlights the role of the striatal complex in emotion, in particular with regard to emotive sensorimotor functions. Our results are important because they expand our knowledge on neural networks underlying sustained emotional experience.

3.6 Acknowledgements

The authors declare that they have no conflict of interest. The authors thank Vienna Doenni and Yu Fukuda for their assistance during the data collection.

3.7 References

Aggleton J, Mishkin M. 1984. Projections of the amygdala to the thalamus in the cynomolgus monkey. The Journal of comparative neurology. 222:56–68.

Amunts K, Kedo O, Kindler M, Pieperhoff P, Mohlberg H, Shah N, Habel U, Schneider F, Zilles K. 2005. Cytoarchitectonic mapping of the human amygdala, hippocampal region and entorhinal cortex: intersubject variability and probability maps. Anatomy and embryology. 210:343–352.

Ball T, Rahm B, Eickhoff S, Schulze-Bonhage A, Speck O, Mutschler I. 2007. Response properties of human amygdala subregions: Evidence based on functional MRI combined with probabilistic anatomical maps. PLoS One. 2:e307.

Baumgartner T, Lutz K, Schmidt C, J¨ancke L. 2006. The emotional power of music: how music enhances the feeling of affective pictures. Brain Research. 1075:151–164.

Beck A, Steer R, Brown G. 1993. Beck depression inventory. San Antonio, TX: Psychological Corporation. Bzdok D, Laird A, Zilles K, Fox P, Eickhoff S. 2012. An investigation of the structural, connectional, and functional subspecialization in the human amygdala. Human Brain Mapping.

Bzdok D, Langner R, Caspers S, Kurth F, Habel U, Zilles K, Laird A, Eickhoff S. 2011. ALE metaanalysis on facial judgments of trustworthiness and attractiveness. Brain Structure and Function. 215:209–223.

Costafreda S, Brammer M, David A, Fu C, et al. 2008. Predictors of amygdala activation during the processing of emotional stimuli: a meta-analysis of 385 pet and fmri studies. Brain Research Reviews. 58:57–70.

Critchley H, Mathias C, Dolan R. 2002. Fear conditioning in humans: the influence of awareness and autonomic arousal on functional neuroanatomy. Neuron. 33:653–663.

Cross I, Morley I. 2008. The evolution of music: Theories, definitions and the nature of the evidence. In S Malloch, C Trevarthen, editors, Communicative musicality: Exploring the basis of human companionship, pages 61–82. Oxford: Oxford University Press.

Deichmann R, Gottfried J, Hutton C, Turner R. 2003. Optimized EPI for fMRI studies of the orbitofrontal cortex. Neuroimage. 19:430–441.

Deichmann R, Josephs O, Hutton C, Corfield D, Turner R. 2002. Compensation of susceptibility-induced bold sensitivity losses in echo-planar fMRI imaging. Neuroimage. 15:120–135.

Eerola T, Toiviainen P. 2004. Mir in matlab: The midi toolbox. In Proceedings of the International Conference on Music Information Retrieval, pages 22–27. Citeseer.

Eickhoff S, Stephan K, Mohlberg H, Grefkes C, Fink G, Amunts K, Zilles K. 2005. A new spm toolbox for combining probabilistic cytoarchitectonic maps and functional imaging data. Neuroimage. 25:1325–1335.

Eldar E, Ganor O, Admon R, Bleich A, Hendler T. 2007. Feeling the real world: limbic response to music depends on related content. Cerebral Cortex. 17:2828–2840.

Fritz T, Jentschke S, Gosselin N, Sammler D, Peretz I, Turner R, Friederici AD, Koelsch S. 2009. Universal recognition of three basic emotions in music. Current Biology. 19:573–576.

Gabrielson A, Juslin P. 2003. Emotional expression in music. In R Davidson, K Scherer, H Goldsmith, editors, Handbook of Affective Sciences, pages 503–534. New York: Oxford University Press.

Geyer S, Schleicher A, Zilles K. 1999. Areas 3a, 3b, and 1 of human primary somatosensory cortex: 1. microstructural organization and interindividual variability. Neuroimage. 10:63–83.

Goldin P, Hutcherson C, Ochsner K, Glover G, Gabrieli J, Gross J, et al. 2005. The neural bases of amusement and sadness: a comparison of block contrast and subject-specific emotion intensity regression approaches. Neuroimage. 27:26–36.

Goossens L, Kukolja J, Onur O, Fink G, Maier W, Griez E, Schruers K, Hurlemann R. 2009. Selective processing of social stimuli in the superficial amygdala. Human brain mapping. 30:3332–3338.

Gotthardt U, Schweiger U, Fahrenberg J, Lauer C, Holsboer F, Heuser I. 1995. Cortisol, ACTH, and cardiovascular response to a cognitive challenge paradigm in aging and depression. American Journal of Physiology-Regulatory, Integrative and Comparative Physiology. 268:R865–R873.

Gray M, Harrison N, Wiens S, Critchley H. 2007. Modulation of emotional appraisal by false physiological feedback during fMRI. PLoS One. 2:e546.

Haber S, Lynd E, Klein C, Groenewegen H. 1990. Topographic organization of the ventral striatal efferent projections in the rhesus monkey: an anterograde tracing study. The Journal of comparative neurology. 293:282–298.

Harrison N, Gray M, Gianaros P, Critchley H. 2010. The embodiment of emotional feelings in the brain. The Journal of Neuroscience. 30:12878–12884.

Hasson U, Nir Y, Levy I, Fuhrmann G, Malach R. 2004. Intersubject synchronization of cortical activity during natural vision. Science. 303:1634–1640.

Herwig U, Kaffenberger T, J¨ancke L, Br¨uhl A. 2010. Self-related awareness and emotion regulation. Neuroimage. 50:734.

Holland P, Gallagher M. 2004. Amygdala–frontal interactions and reward expectancy. Current opinion in neurobiology. 14:148–155.

Koelsch S. 2010. Towards a neural basis of music-evoked emotions. Trends in Cognitive Sciences. 14:131–137.

Koelsch S, Fritz T, Cramon DY, M¨uller K, Friederici AD. 2006. Investigating emotion with music: An fMRI study. Human Brain Mapping. 27:239–250.

Koelsch S, Fuermetz J, Sack U, Bauer K, Hohenadel M, Wiegel M, Kaisers U, Heinke W. 2011. Effects of music listening on cortisol levels and propofol consumption during spinal anesthesia. Frontiers in Psychology. 2:1–9.

Koelsch S, Offermanns K, Franzke P. 2010. Music in the Treatment of Affective Disorders: An Exploratory Investigation of a New Method for Music-Therapeutic Research. Music Perception. 27:307–316.

Koelsch S, Stegemann T. 2012. The brain and positive biological effects in healthy and clinical populations. In R MacDonald, D Kreutz, L Mitchell, editors, Music, Health and Well-Being, pages 436–456. Oxford: Oxford University Press.

LeDoux J. 2000. Emotion circuits in the brain. Ann Rev Neurosci. 23:155 – 184.

Li S, Kirouac G. 2008. Projections from the paraventricular nucleus of the thalamus to the forebrain, with special emphasis on the extended amygdala. The Journal of comparative neurology. 506:263–287.

Lohmann G, Margulies D, Horstmann A, Pleger B, Lepsien J, Goldhahn D, Schloegl H, Stumvoll M, Villringer A, Turner R. 2010. Eigenvector Centrality Mapping for Analyzing Connectivity Patterns in fMRI Data of the Human Brain. PLoS-one. 5:e10232.

Lohmann G, M¨uller K, Bosch V, Mentzel H, Hessler S, Chen L, von Cramon DY. 2001. Lipsia - a new software system for the evaluation of functional magnet resonance images of the human brain. Computerized Medical Imaging and Graphics. 25:449–457. See also at http://www.cns.mpg.de/lipsia.

Lohmann G, Neumann J, M¨uller K, Lepsien J, Turner R. 2008. The multiple comparison problem in fMRI – a new method based on anatomical priors. In Workshop on Analysis of Functional Medical Images, New York University, pages 179–187.

MacLean P. 1972. Cerebral evolution and emotional processes: new findings on the striatal complex. Annals of the New York Academy of Sciences. 193:137–149.

Menon V, Levitin D. 2005. The rewards of music listening: response and physiological connectivity of the mesolimbic system. Neuroimage. 28:175–184.

Mitterschiffthaler MT, Fu CH, Dalton JA, Andrew CM, Williams SC. 2007. A functional MRI study of happy and sad affective states evoked by classical music. Human Brain Mapping. 28:1150–1162.

Murray E. 2007. The amygdala, reward and emotion. Trends in cognitive sciences. 11:489–497.

Nieuwenhuys R, Voogd J, Huijzen CV. 2008. The Human Central Nervous System. Berlin: Springer. O'Mara S. 2005. The subiculum: what it does, what it might do, and what neuroanatomy has yet to tell us. Journal of anatomy. 207:271–282.

Palomero-Gallagher N, Vogt B, Schleicher A, Mayberg H, Zilles K. 2009. Receptor architecture of human cingulate cortex: Evaluation of the four-region neurobiological model. Human brain mapping. 30:2336–2355.

Parent A, Hazrati L. 1995. Functional anatomy of the basal ganglia. i. the cortico-basal gangliathalamo-cortical loop. Brain Research Reviews. 20:91–127.

Paton J, Belova M, Morrison S, Salzman C. 2006. The primate amygdala represents the positive and negative value of visual stimuli during learning. Nature. 439:865–870.

Poeppel T, Krause B, et al. 2008. Functional imaging of memory processes in humans: positron emission tomography and functional magnetic resonance imaging. Methods. 44:315.

Russchen F, Bakst I, Amaral D, Price J. 1985. The amygdalostriatal projections in the monkey. An anterograde tracing study. Brain research. 329:241–257.

Salimpoor V, Benovoy M, Larcher K, Dagher A, Zatorre R. 2011. Anatomically distinct dopaminerelease during anticipation and experience of peak emotion to music. Nature neuroscience. 14:257–262.

Scheperjans F, Eickhoff S, H¨omke L, Mohlberg H, Hermann K, Amunts K, Zilles K. 2008. Probabilistic maps, morphometry, and variability of cytoarchitectonic areas in the human superior parietal cortex. Cerebral Cortex. 18:2141–2157.

Shi C, Cassell M. 1999. Cascade projections from somatosensory cortex to the rat basolateral amygdala via the parietal insular cortex. The Journal of comparative neurology. 399:469–491.

Sporns O, Honey C. 2006. Small worlds inside big brains. Proceedings of the National Academy of Sciences. 103:19219.

Steinbeis N, Koelsch S. 2008. Understanding the intentions behind man-made products elicits neural activity in areas dedicated to mental state attribution. Cerebral Cortex. 19:619–623.

Tomasi D, Volkow N. 2011. Association between functional connectivity hubs and brain networks. Cerebral Cortex. 21:2003–2013.

Trost W, Ethofer T, Zentner M, Vuilleumier P. 2012. Mapping aesthetic musical emotions in the brain. Cerebral Cortex.

Vuilleumier P. 2005. How brains beware: neural mechanisms of emotional attention. Trends in cognitive sciences. 9:585–594.

Wallentin M, Nielsen A, Vuust P, Dohn A, Roepstorff A, Lund T. 2011. Amygdala and heart rate variability responses from listening to emotionally intense parts of a story. Neuroimage. 58:963–973.

Wamsley J, Zarbin M, Young W, Kuhar M. 1982. Distribution of opiate receptors in the monkey brain: an autoradiographic study. Neuroscience. 7:595–613.

Weiskopf N, Hutton C, Josephs O, Turner R, Deichmann R. 2007. Optimized epi for fMRI studies of the orbitofrontal cortex: compensation of susceptibility-induced gradients in the readout direction. Magnetic Resonance Materials in Physics, Biology and Medicine. 20:39–49.

3.8 Supplementary Material

Stimuli

Joy stimuli had been used in previous studies (Fritz et al., 2009; Koelsch et al., 2010, 2011) and consisted of CD-recorded pieces from various epochs and styles (classical music, Irish jigs, jazz, reggae, South American and Balkan music). Fear stimuli were excerpts from soundtracks of suspense movies and video games (the complete list of joy and fear stimuli is provided in Supplementary Table S1). To increase the fearfulness of the fear stimuli, their comparably high acoustic roughness (as determined with ’Essentia’, a library for extracting audio and music features from audio files, see Supplementary Materials) was further increased by creating dissonant versions, where each musical excerpt was audible in three different pitches simultaneously (original pitch, one semitone higher, and a tritone lower, as in previous studies (Koelsch et al., 2006; Fritz et al., 2009). The pitch-shifted, additional counterparts of each excerpt were created so that only their pitch differed, while their tempo remained equal. The original excerpt together with the two pitch-shifted counterparts was then rendered as a single wav-file using Ableton Live (version 8.0.4, Ableton Inc., New York, USA).

Neutral stimuli were sequences of isochronous tones, for which the pitch classes were randomly selected from a pentatonic scale. These tone sequences were coded in MIDI (musical instrument digital interface) and generated using the MIDI toolbox for Matlab (Eerola and Toiviainen, 2004). To create stimuli that sounded like musical compositions played with real instruments (similar to the joy and fear stimuli), the tones from the MIDI sequences were set to trigger instrument samples from a high quality natural instrument library (X-Sample Chamber Ensemble, Winkler & Stahl GbR, Detmold, Germany) and from the Ableton Instrument library (Ableton Inc., New York, USA). Stimuli were then rendered as wav-files using Ableton Live. Using Praat (version 5.0.29; Boersma, 2002), all excerpts (joy, fear, and neutral) were edited so that they all had the same length (30 s), 1.5 s fade-in/fade-out ramps, and the same average RMS power.

Acoustical analysis of stimuli

Acoustic analysis of the stimuli was performed using ’Essentia’, a library for extracting audio and music features from audio files (http://mtg.upf.edu/technologies/essentia): 177 acoustical descriptors were extracted frame-by-frame (frame length = 21.5 ms, 50% overlap), averaged along the entire duration of the file, and then compared between conditions (joy, neutral, fear) using one-way ANOVAs. Significant effects of condition (Bonferroni-corrected significance-level was $p < .001$) were indicated for the following acoustic factors (with F−values in parentheses, degrees of freedom: 2, 21): (a) Mean (72.3) and variance (13.8) of F0 salience (this measure is highest for single tones, intermediate for chords, and lowest for noises; note that mean F0 and variance of F0 did not differ between joy, fear, and neutral stimuli). The mean F0 salience was highest for neutral, intermediate for joy, and lowest for fear stimuli ($p < .001$ in all pairwise comparisons). This reflects that both joy and fear (but not neutral) stimuli contained numerous harmonies, and that fear (but not joy) stimuli contained numerous percussive sounds, as well as hissing and whooshing noises. (b) Mean (41.3) and variance (28.0) of sensory dissonance. Sensory dissonance was lowest for neutral, intermediate for joy, and highest for fear stimuli. Mean sensory dissonance differed significantly between joy and neutral (p < .001), between fear and neutral (p < .001), and between joy and fear stimuli (p < .05). (c) Mean chord strength (25.2) and key strength (14.7); these factors measure how strongly a sound resembles the sound of a chord, and how clearly the sounds of a stimulus can be attributed to a key. Chord strength was larger for joy compared to fear, as well as for joy compared to neutral sounds (p < .001 in each test), whereas fear and neutral stimuli did not differ significantly from each other. Key strength was larger for joy compared to fear (p < .001), and for neutral compared to fear sounds (p = .01); joy and neutral stimuli did not differ significantly from each other (p > .15). (d) Mean (30.0) and variance (16.4) of spectral flux, mean spectral crest (30.0) and mean spectral complexity (10.6). Mean spectral flux, spectral crest, and spectral complexity were lowest for neutral stimuli (with significant differences between neutral and joy, as well as between neutral and fear stimuli, p < .05 in each test), and did not differ significantly between joy and fear stimuli (p > .2 in each test). To compensate for these acoustical differences, the values of these psychoacoustic parameters were used in the fMRI data analysis as regressors of no interest (see Data Analysis of main text for details).

Supplementary Results

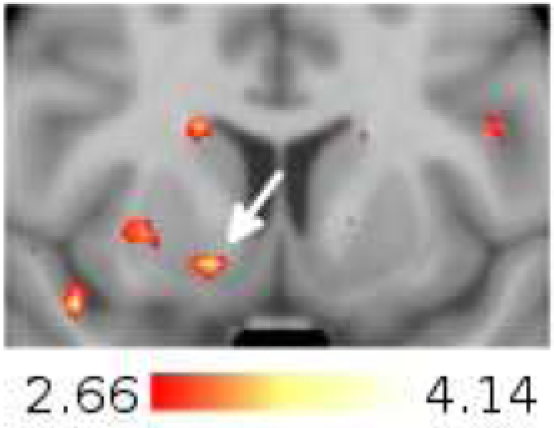

Supplemental Figure S1. Uncorrected statistical parametric map of the comparison of functional connectivity between joy and fear (joy > fear) using the superficial (SF) group of the amygdala as seed region. With a statistical threshold of p < .001 and a voxel-extent of five voxels, SF shows significant functional connectivity with the nucleus accumbens (arrow) that was stronger during joy than during fear.

Superficial Amygdala and Hippocampal Activity During Affective Music Listening at 3 T but not 1.5 T fMRI

Stavros Skouras, Marcus Gray, Hugo Critchley, Stefan Koelsch

(publication under review in Human Brain Mapping)

4.0 Abstract

The purpose of this study was to compare 3 T and 1.5 T fMRI results during emotional music listening. Stimuli comprised of psychoacoustically balanced instrumental musical pieces, with three different affective expressions (fear-neutral-joy). Participants (N=32) were split into two groups, one subjected to fMRI scanning using 3 T and another group scanned using 1.5 T. Whole brain t-tests (corrected for multiple comparisons) compared joy and fear in each of the two groups. The 3T group showed significant activity differences between joy and fear localized in bilateral superficial amygdala, bilateral hippocampus and bilateral auditory cortex. The 1.5 T group showed significant activity differences between joy and fear localized in bilateral auditory cortex and cuneus. This is the first study to compare results obtained under different field strengths with regards to affective processes elicited by means of auditory/musical stimulation. The findings raise concern over false negatives in the superficial amygdala and hippocampus in affective studies conducted under 1.5 T and caution that imaging improvements due to increasing magnetic field strength can be influenced by region-specific characteristics.

4.1 Introduction

Over the past decade, fMRI scanning at 3 T has evolved from being a promising new technology to being a standard technology used in cognitive neuroscientific studies. Although it is generally accepted that increasing magnetic field strength has led to improved neuroimaging quality there is certain controversy surrounding the matter, as the comparison with the 1.5 T predecessor is not trivial nor well documented (Wardlaw et al., 2012). Moreover, there exist no published studies comparing field strength effects with regards to affective processes elicited by means of auditory stimulation, because the vast majority of published studies are focused on differences during sensory and motor tasks.

As an early review suggests, the increase from 1.5 T to 3 T is accompanied by improved detection of activity in terms of both volume and reliability (Voss et al. 2006). This is due to increased signal-to-noise ratio (SNR) and contrast-to-noise ratio (CNR) which in theory can be exchanged for increased spatial and/or temporal resolution. However, the authors caution that factors other than field strength might underlie these effects (Voss et al. 2006). A more recent review takes an opposing stance, implying that the merits of 3 T scanning are exaggerated, particularly because the actual SNR improvement from 1.5 T to 3 T is only 25% of what was theoretically expected (Wardlaw et al. 2012). Furthermore, there seem to be more artefacts occurring at 3 T, particularly in regions near the base of the skull. The authors also caution that other factors, which are uncontrolled across studies, may be influencing the overall pattern of observations and that their review is compromised by underspecified report practises characterizing the literature on the subject (Wardlaw et al. 2012).

Relatively few studies have made explicit comparisons between 1.5 T and 3 T using human subjects. One of these studies used no experimental task (Triantafyllou et al., 2005), three studies used motor tasks (Fera et al., 2003; Yongbi et al., 2001; Hoenig et al., 2005), one study used a visual task (Okada et al., 2005) and one study used sensorymotor (visual) stimulation (Krüger et al., 2001). Only one study used a cognitive task (Hoenig et al., 2005), only two studies used auditory tasks (Rabe et al., 2006; Han, Talavage, 2011) and only one used an affective (visual) task (Krasnow et al., 2003).

The only published study making comparisons between 1.5 T and 3 T while utilizing cognitive rather than sensory or motor tasks (Hoenig et al., 2005), suggests that the improved sensitivity associated with imaging at 3 T can lead beyond the identification of stronger activity in a particular region, to the identification of additional activity in regions that are not observable when imaging at 1.5 T. Results from the only related comparative study to date utilizing an affective task (Krasnow et al., 2003) suggest that imaging at 3 T is also preferable for subcortical regions. That study limited the analysis of the data from the affective task to the amygdala and found a non-significant trend for stronger amygdala activity at 3 T relative to 1.5 T (Krasnow et al. 2003). Paradoxically, higher signal drop-out in the amygdala under 3 T was also observed alhough this finding did not reach significance (Krasnow et al. 2003). The interested reader should note that susceptibility artifacts and signal drop-out due to 3 T imaging can be mitigated by use of spiral in-out acquisition sequences (Preston et al., 2004).

Only two prior studies related to field strength have used an auditory task. The first one investigated whether habituation effects during auditory sine-wave stimulation differ between 1.5 T and 3 T and found only marginal, non-significant differences (Rabe et al., 2006). The second study utilized a task involving passively listening to 750 ms of an auditory stimulus every 12 or 24 s and made no explicit comparison between the two field strengths, focusing instead on showing that increasing the number of fMRI datasets by combining 1.5 T and 3 T datasets is preferable to using a fewer number of only 3 T datasets (Han, Talavage, 2011).

In the present study we use emotional music to address whether there is any noticeable difference in the detectability of emotion-related contrasts, as established with 3 T fMRI. Our recent studies show that during music-elicited joy, the superficial amygdala is the structure with the strongest increase in activity (Koelsch et al., 2013) as well as centrality (see Chapter 3). We aim to test whether the detectability of this structure is enhanced or diminished when scanning at 1.5 T.

4.2 Methods

4.2.1 Participants

32 individuals (aged 19 – 28 years, M = 22.93, SD = 2.75, 18 females) took part in the experiment. All participants had normal hearing (as assessed with standard pure tone audiometry) and were right-handed (according to self-report). None of the participants was a professional musician or a music student; 16 participants had no or only minimal formal musical training and 16 participants were amateur musicians who had learned at least one musical instrument (mean duration of formal training was 2.78 years). The participants were split into two groups of 16 subjects each; a group that underwent 3 T scanning (aged 19 – 28 years, M = 22.94, SD = 2.72, 9 females, mean duration of formal training 3.62 years, SD = 5.04) and a group that underwent 1.5 T scanning (aged 19 – 28 years, M = 22.92, SD = 2.90, 9 females, mean duration of formal training 1.94 years, SD = 2.35).

Independent samples t-tests showed that the two groups did not differ with regards to age (p = 0.98) and formal musical training (p = 0.24). Exclusion criteria were left-handedness, professional musicianship, a score on Beck's Depression Inventory (Beck, Steer, 1993) of 13 or more points, consumption of alcohol or caffeine exceeding one litre during the 24 hours prior to testing, poor sleep during the previous night, past diagnosis of a neurological or psychiatric disorder, and abnormal brain anatomy. All subjects gave written informed consent. The study was conducted according to the Declaration of Helsinki and approved by the ethics committee of the School of Life Sciences and the Psychology Department of the University of Sussex.

4.2.2 Stimuli

The stimuli utilized have been described in detail elsewhere (Koelsch et al., 2013). Briefly, musical stimuli were selected to evoke (a) feelings of joy, (b) feelings of fear, or (c) neither joy nor fear (henceforth referred to as neutral stimuli). There were n = 8 stimuli per category. Musical stimuli evoked the intended feelings in the sample studied (see Behavioral Data). Joyful stimuli had been used in previous studies (e.g., Fritz et al., 2009; Koelsch et al., 2010, 2011) and consisted of CD-recorded pieces from various epochs and styles (classical music, Irish jigs, jazz, reggae, South American and Balkan music). Fearful musical stimuli were excerpts from soundtracks of suspense movies and video games. The complete list of joyful and fearful stimuli is provided in Supplementary Table S1. Neutral stimuli were created using the MIDI toolbox for Matlab (Eerola, Toiviainen, 2004) and Ableton Live (version 8.0.4, Ableton Inc., New York, USA). Neutral stimuli comprised of sequences of isochronous tones, for which the pitch classes were randomly selected from a pentatonic scale and the timbres where chosen from a high quality natural instrument library (X-Sample Chamber Ensemble, Winkler, Stahl GbR, Detmold, Germany). Stimuli were edited using Praat (version 5.0.29; Boersma, 2002), so that they all had the same length (30 s), 1.5 s fade-in/fade-out ramps, and the same RMS power. All stimuli were matched across conditions in triplets (joy-neutral-fear) with regard to tempo (beats per minute), mean F0 pitch, F0 pitch variation, pitch centroid value, spectral complexity, and spectral flux. This was confirmed by an acoustic analysis of the stimuli using ’Essentia’, an in-house library for extracting audio and music features from audio files (http://mtg.upf.edu/technologies/essentia). The Essentia software was also used to test for differences between stimuli with regard to another 177 acoustical factors. Ten psychoacoustic factors were found to differ significantly between experimental conditions ($p < 0.001$, corrected for multiple comparisons). These factors were mean and variance of F0 salience, mean and variance of sensory dissonance, mean chord strength and key strength, mean and variance of spectral flux, mean spectral crest and mean spectral complexity (for details see Koelsch et al., 2013). The values of these factors associated with each stimulus were used in the fMRI data analysis as additional regressors of the general linear model’s (GLM) design matrix (see also Data Analysis).

4.2.3 Procedure

Prior to the MRI session, participants were presented with short (12 s) versions of each stimulus to obtain familiarity ratings (for the importance of this see Pereira et al., 2011). Participants rated their familiarity with each piece on a four-point scale (ranging from "To my knowledge I have never heard this piece before", to "I know this piece, and I know who composed, or performed it"). Familiarity ratings from six participants who stated at least once that they knew the name of the piece or the composer of one of the neutral pieces that were created for the purposes of the study were not considered in the analysis of familiarity ratings. Participants were then trained on the rating procedure, using 12 s long excerpts of musical pieces that did not belong to the stimulus set used in the fMRI scanning session.

During the fMRI scanning session, stimuli were presented in a pseudo-random order so that no more than two stimuli of each stimulus category (joy, fear, neutral) followed each other. The task of the participants was to listen to the musical stimuli with their eyes closed and to rate their emotional state after each musical stimulus. Each musical stimulus was followed by an interval of 2 s in which a beep tone of 350 Hz and 1 s duration signalled participants to open their eyes and to commence the rating procedure. During the rating procedure, participants indicated how they felt at the end of each excerpt with regard to valence ('pleasantness'), 'arousal', 'joy' and 'fear'. That is, participants offered ratings on how they felt, and not about which emotion each song was supposed to express (for the importance of this see Gabrielsson, Juslin, 2003). Ratings were obtained with 6-point Likert scales (ranging from "not at all" to "very much"). The time interval for the rating procedure was 12 s and each rating period was followed by approximately 3 s of rest. The entire stimulus set was presented twice during the fMRI scanning session.

Musical stimuli were presented using Presentation (version 13.0, Neurobehavioral systems, Albany, CA, USA) via MRI compatible headphones (MR confon, Magdeburg, Germany for the 1.5 T group and Resonance Technology Inc, Salt Lake City, USA for the 3 T group), under which participants wore earplugs. Instructions and rating screens were delivered through MRI compatible liquid crystal display goggles (Resonance Technology Inc., Northridge, CA, USA) to the 3 T group and through a mirror screen to the 1.5 T group.

4.2.4 MR Scanning

Images were acquired using a 1.5 T Magnetom Avanto and a 3 T Siemens Magnetom TrioTim (Siemens AG, Erlangen, Germany), both featuring 12-channel coils. Prior to the functional MR measurements, a high-resolution (1x1x1 mm) T1-weighted anatomical reference image was acquired from each participant using a rapid acquisition gradient echo (MP-RAGE) sequence.

During the functional MR measurements, both groups underwent Echo Planar Imaging (EPI) with a TE of 30 ms and a TR of 2 s. Slice-acquisition was interleaved within the TR interval. The matrix acquired was 64x64 voxels with a Field Of View (FOV) of 192 mm, resulting in an in-plane resolution of 3 mm. Slice thickness was 3 mm with an interslice gap of 0.6 mm (37 slices, whole brain coverage). The acquisition window was tilted at an angle of 30 degrees relative to the AC-PC line to minimize susceptibility artifacts in the orbitofrontal cortex (Deichmann et al., 2002, 2003; Weiskopf et al., 2007).

4.2.5 Behavioral data analysis

Standardized behavioral ratings were subjected to a 2-way mixed ANOVA with factors emotion (fear, neutral, joy) and field strength (1.5 T, 3 T), with the planned contrasts emotion, and emotion x field strength. The latter contrast was computed to guarantee that differences in activation between groups were not simply due to one group responding differently than the other to any of the stimulus categories.

4.2.6 fMRI data analysis

FMRI data were processed using LIPSIA 2.1 (Lohmann et al., 2001). Data were corrected for slicetime acquisition and normalized into MNI-space-registered images with isotropic voxels of 3 cubic millimeters. A temporal highpass filter with a cutoff frequency of 1/90 Hz was applied to remove low frequency drifts in the fMRI time series, and a spatial smoothing was performed using a 3D Gaussian kernel and a filter size of 6 mm FWHM. A mixed effects block design GLM analysis was employed (Friston, 2007). Valence ratings, arousal ratings, familiarity ratings, psychoacoustic parameters that differed significantly between conditions (see Stimuli) and realignment parameters were included in the design matrix as covariates of no interest (Johnstone et al., 2006). On the first level, parametric contrasts were calculated to show brain regions where signal intensity is stronger for joy than for fear. One sample t-tests were utilized at the second level to calculate the group z-map for each of the two groups. Findings were corrected for multiple comparisons by the use of cluster-size and cluster-value thresholds obtained by Monte Carlo simulations with a significance level of $p < 0.05$ (Lohmann et al., 2008). For each significant cluster identified in the contrast between joy and fear of each group, a two sample t-test was calculated based on the peak coordinate in order to test whether the values obtained at different field strengths are significantly different.

4.3 Results

4.3.1 Behavioral results

ANOVA showed a significant effect of emotion on ratings of valence, arousal, happiness, fearfulness and familiarity ($p < 0.001$ in all analyses, see Table 1). Arousal ratings were highest for joy, intermediate for fear, and lowest for neutral stimuli ($p < .001$ in all pairwise comparisons, see also Table 1). Both valence (pleasantness) and joy ratings were highest for joy, intermediate for neutral, and lowest for fear stimuli ($p < .05$ in all pairwise comparisons, see also Table 1). Fearfulness ratings were highest for fear, intermediate for neutral, and lowest for joy stimuli ($p < .001$ in all pairwise comparisons, see also Table 1). Due to the differences in the behavioral ratings between stimulus categories with regard to valence, arousal, and familiarity, each participant's valence, arousal, and familiarity ratings were used in the fMRI data analysis as regressors of no interest (see Data Analysis). Therefore, these variables (valence, arousal, and familiarity) did not contribute to the fMRI results presented in the following.

Table 4.1: Descriptive statistics, ANOVA and post-hoc t-tests for behavioral data. Three asterisks signify significance at the 0.001 level and one asterisk signifies significance at the 0.05 level (corrected for multiple comparison's using the Bonferroni method).

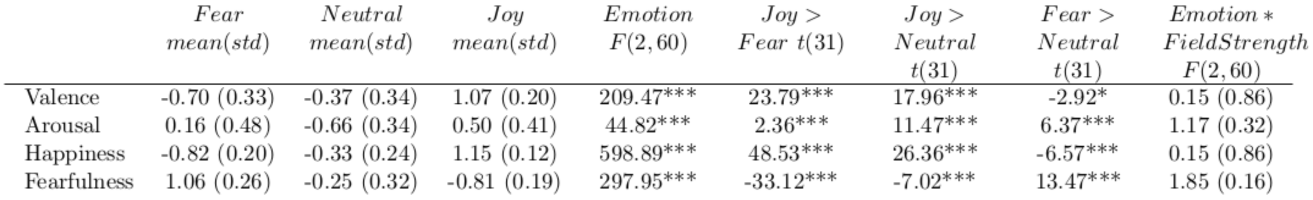

	$Fear$ $mean(std)$	$Neutral$ $mean(std)$	Joy $mean(std)$	$Emotion$ $F(2,60)$	$Joy >$ $Fear$ $t(31)$	$Joy >$ $Neutral$ $t(31)$	$Fear >$ $Neutral$ $t(31)$	$Emotion *$ $FieldStrength$ $F(2,60)$
Valence	-0.70 (0.33)	-0.37 (0.34)	1.07 (0.20)	209.47***	23.79***	17.96***	-2.92*	0.15 (0.86)
Arousal	0.16 (0.48)	-0.66 (0.34)	0.50 (0.41)	44.82***	2.36***	11.47***	6.37***	1.17 (0.32)
Happiness	-0.82 (0.20)	-0.33 (0.24)	1.15 (0.12)	598.89***	48.53***	26.36***	-6.57***	0.15 (0.86)
Fearfulness	1.06 (0.26)	-0.25 (0.32)	-0.81 (0.19)	297.95***	-33.12***	-7.02***	13.47***	1.85 (0.16)

4.3.2 fMRI results

For the 3 T group, the statistical parametric map (SPM) of the joy > fear contrast (corrected for multiple comparisons, $p < .05$) revealed significant BOLD signal differences in the auditory cortex (AC) bilaterally, as well as in the hippocampus and superficial amygdala bilaterally (see also Table 2a and Figure 1a). For the 1.5 T group, the SPM of the joy > fear contrast (corrected for multiple comparisons, $p < .05$) revealed significant BOLD signal differences in the auditory cortex (AC), and the visual cortex, centred around the calcarine fissure (see also Table 2 and Figure 1a). For each peak voxel identified in the joy > fear contrast of each group, two samples t-tests showed that the reported activations significantly differed between groups (all tests $p < .05$) except in OP4 bilaterally and right auditory cortex. In the auditory cortex, which is the only region that was significant for both groups, the volume increase observed from 1.5 to 3T was 58% in the right and 17% in the left hemisphere. The SPM of the interaction between emotion (joy, fear) and group (1.5 T, 3 T) was limited to the clusters centred on the auditory cortex (corrected for multiple comparisons, $p < .05$).

Table 4.2: Results of GLM contrast joy > fear (corrected for multiple comparisons, p < .05), separately for the 3 T group (a) and the 1.5 T group (b). The rightmost column shows the uncorrected significance of the difference between 3 T and 1.5 T at the peak coordinate.

	MNI coordinate	cluster size (mm^3)	$z-$value: max (mean)	$3T > 1.5T$: $z-$score ($p-$value)
(a) 3 Tesla: $joy > fear$				
Left Superior Temporal Gyrus	-60 -9 7	13419	6.03 (3.59)	1.122 (n.s.)
Right Superior Temporal Gyrus	48 -21 4	10584	5.36 (3.53)	2.056 ($p < 0.05$)
Left Hippocampus (HATA)	-18 -12 -11	378	3.90 (3.18)	1.957 ($p < 0.05$)
Hipp (CA/FD)	18 -15 -11	351	3.46 (3.03)	1.924 ($p < 0.05$)
(b) 1.5 Tesla: $joy > fear$				
Right Heschls Gyrus	48 -18 10	6102	4.22 (3.10)	0.269 (n.s.)
Cuneus (BA 18)	6 -99 13	3321	4.30 (3.21)	-2.69 ($p < 0.01$)
Left Superior Temporal Gyrus	-60 -12 7	1755	3.65 (3.07)	1.102 (n.s.)
Right Middle Occipital Gyrus	33 -96 1	648	3.64 (3.06)	-3.10 ($p < 0.001$)

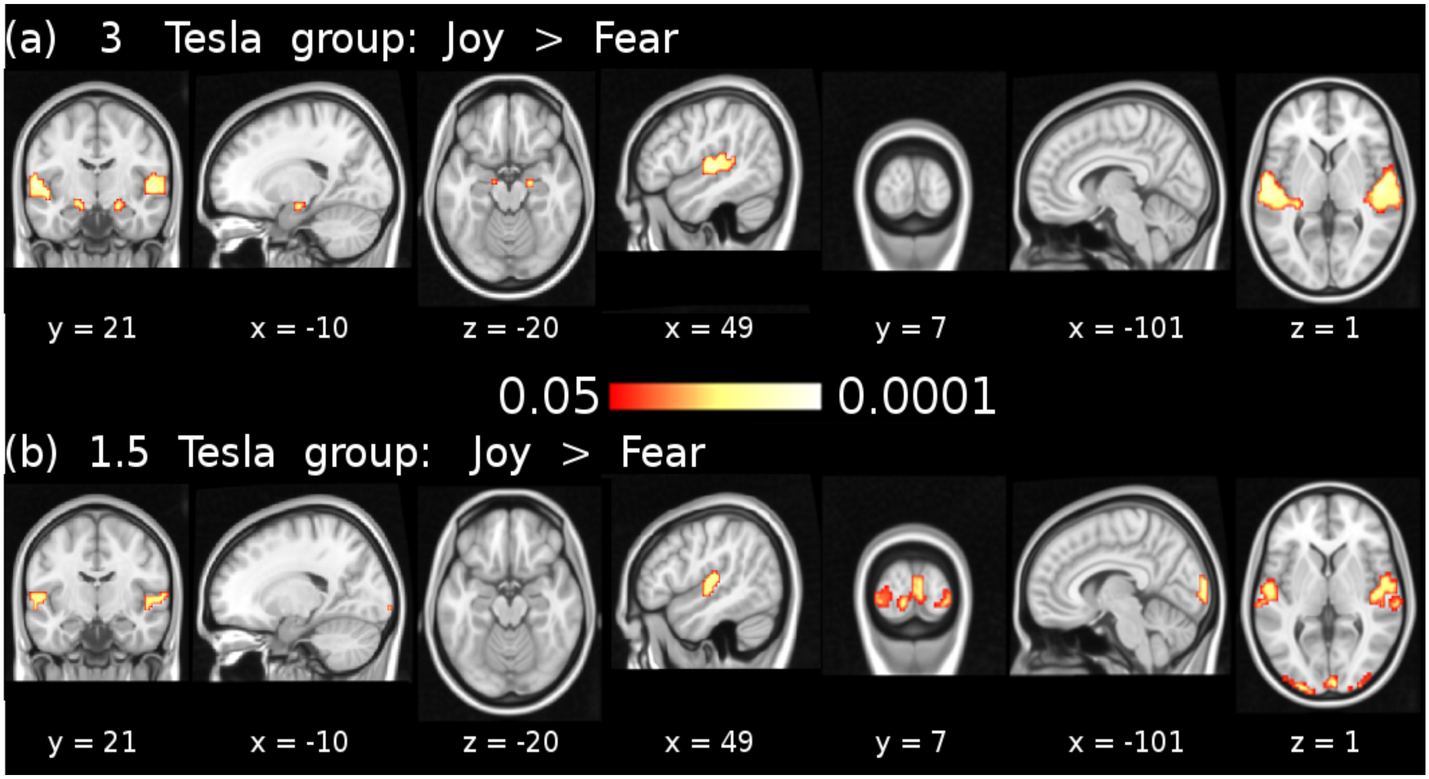

Figure 4.1: fMRI Results. (a) Results of GLM contrast joy > fear for the 3 T group, corrected for multiple comparisons (p < .05). (b) Results of GLM contrast joy > fear for the 1.5 T group, corrected for multiple comparisons (p < .05).

4.4 Discussion

The present study is the first to make an explicit comparison between results obtained utilizing different field strengths with regards to affective processes elicited by means of auditory stimulation. While comparing music-elicited joy and fear, the group scanned at 3 T showed significant differences in bilateral auditory cortex, bilateral hippocampus and bilateral superficial amygdala. The group scanned at 1.5 showed significant differences in bilateral auditory cortex and cuneus. The results suggest that 3 T is better suited to detecting activity in the limbic system, especially when relatively small structures, like the superficial amygdala are involved.

Regarding the subcortical activity observed only in the 3 T group, the present findings are in line with the only previous study utilizing an affective task for comparing between field strengths (Krasnow et al. 2003) as well as with evidence from another independent study performed at 3 T (see Chapter 3), that showed bilateral superficial amygdala and hippocampus to consist the neural hubs with the most significant increase in eigenvector centrality during joy, compared to fear. Therefore, this activity represents a finding that is replicable at 3 T, even when using a different design and analysis method. This difference in activity between joy and fear is not observable at 1.5 T presumably because it concerns activation of a miniscule amygdalar nucleus that might require the increased contrast-to-noise ratio featured by 3 T, to appear as significantly differing between experimental conditions in a whole-brain analysis. This interpretation is supported by the fact that most fMRI studies that have reported results localized in the superficial amygdala have been conducted at 3 T (e.g. Goossens et al., 2009; Bach et al., 2011; Roy et al., 2009) and raises concerns regarding false negatives in the superficial amygdala and hippocampus in affective experiments conducted with 1.5 T MRI.

Regarding the observed activity in the auditory cortex, the location of the peak coordinates are within a few millimetres’ distance across the two experimental groups. The fact that the volumes of the significant regions are greater under 3 T is in line with the majority of previous literature utilizing sensory tasks (for a review see Voss et al., 2006) and corroborates the view that 3 T provides increased sensitivity in cortical areas. However, it is important to note that in the present study the activity is related to emotional processing because it represents differences between listening to joyous compared to fearful music and the psychoacoustic properties of our stimuli are modelled and balanced across experimental conditions. This is in line with previous research highlighting the involvement of the auditory cortex in the emotional appreciation of music and is attributed to involuntary neural processes that increase attentiveness to pleasant musical stimuli as well as the level of detail of constructed mental representations of musical content (Jäncke et al., 1999; Koelsch et al., 2005; Plichta et al., 2011; Koelsch et al., 2013).

The visual cortex activity observed in the 1.5 T group was unexpected, so its interpretation is subject to speculation. Several studies corroborate the possibility of such activity to be related to processes of visual imagery (Phan et al., 2002; Lang et al., 1998) and "visual imagery" is considered as an emotion related mechanism during music listening (Juslin, Vastfjall, 2008; Koelsch, 2012). The reason the visual cortex is significantly more active during joy compared to fear, although only for the 1.5 T group, is possibly related to a monoamine receptor increase in the right frontal occipital lobe, induced by frightening music (Zhang et al., 2012).

The main limitation of our study resides in its between-subjects design. An additional limitation relates to the observation that, even though the image acquisition protocol had been optimized to minimize signal loss, the 1.5 T data were generally of poorer quality because they featured more extensive signal loss in the vicinity of the temporal poles. However, none of the regions identified by the analyses were affected by this common phenomenon (Deichmann et al., 2002) which suggests that the presented results are reliable.

These results raise concern for the existence of false negatives under 1.5 T in the superficial amygdala and hippocampus. This is because most previous studies comparing performance between 1.5 T and 3 T fMRI featured effects observable at 1.5 T (for a review see Voss et al., 2006). We examined whether an effect that had been observed at 3 T could be observed at 1.5 T as well and found this not to be the case. We caution that affective experiments conducted at 1.5 T may have featured actual differences in the superficial amygdala and hippocampus that have not been identified due to insufficient contrast-to-noise ratio. Our results also suggest that the increased sensitivity to functional change accomplished by higher field strength is unevenly distributed throughout the brain, such that 3 T does not always identify more activity than 1.5 T. The increased sensitivity within the cuneus observed at 1.5 T corroborates the view that the improvement due to the increase in magnetic field strength is modulated by region-specific characteristics such as local tissue microstructure, local magnetic field distortions and blood vessel distribution (Voss et al., 2006). Further research is necessary to fully map such phenomena and to accommodate their influence on neuroimaging through the optimization of fMRI scanning procedures.

4.5 Acknowledgements

The authors have no conflict of interest. The provision of funding for this project was made by the Psychology Department of the University of Sussex, the Brighton and Sussex Medical School and the RCUK fellowship award of S.K.

4.6 References

Bach D, Behrens T, Garrido L, Weiskopf N, Dolan R (2011): Deep and superficial amygdala nuclei projections revealed in vivo by probabilistic tractography. J Neurosci, 31(2):618–623.

Beck A, Steer R (1993): Beck depression inventory manual. San Antonio: Psychological Corporation.

Deichmann R, Josephs O, Hutton C, Corfield D, Turner R (2002): Compensation of susceptibility-induced BOLD sensitivity losses in echo-planar fMRI imaging. Neuroimage, 15(1):120–135.

Deichmann R, Gottfried J, Hutton C, Turner R (2003): Optimized EPI for fMRI studies of the orbitofrontal cortex. Neuroimage, 19(2):430–441.

Eerola T, Toiviainen P (2004): Mir in matlab: The midi toolbox. In: Proceedings of the International Conference on Music Information Retrieval, pp. 22–27. Universitat Pompeu Fabra Barcelona.

Fera F, Yongbi MN, van Gelderen P, Frank JA, Mattay VS, Duyn JH (2003): EPI-BOLD fMRI of human motor cortex at 1.5 T and 3.0 T: Sensitivity dependence on echo time and acquisition bandwidth. JMRI, 19(1):19–26.

Friston KJ, Stephan K (2007): Modelling brain responses. In: Friston KJ, Ashburner JT, Kiebel SJ, Nichols EN, Penny WD, editors. Statistical parametric mapping: The analysis of functional brain images. 1st ed. London: Elsevier. p 17-31.

Fritz T, Jentschke S, Gosselin N, Sammler D, Peretz I, Turner R, Friederici A, Koelsch S (2009): Universal recognition of three basic emotions in music. CB, 19(7):573–576.

Gabrielson A, Juslin P (2003): Emotional expression in music. In Davidson R, Scherer K, Goldsmith H, editors. Handbook of Affective Sciences. New York: Oxford University Press. p 503–534.

Goossens L, Kukolja J, Onur O, Fink G, Maier W, Griez E, Schruers K, Hurlemann R (2009): Selective processing of social stimuli in the superficial amygdala. HBM, 30(10):3332–3338.

Han K, Talavage T (2011): Effects of combining field strengths on auditory functional MRI group analysis: 1.5 T and 3T. JMRI, 34(6):1480–1488.

Hoenig K, Kuhl C, Scheef L (2005): Functional 3.0-T MR Assessment of Higher Cognitive Function: Are There Advantages over 1.5-T Imaging? Radiology, 234(3):860–868.

Jäncke L, Mirzazade S, Joni Shah N (1999): Attention modulates activity in the primary and the secondary auditory cortex: a functional magnetic resonance imaging study in human subjects. Neurosci Lett , 266(2):
125–128.

Johnstone T, Ores Walsh K, Greischar L, Alexander A, Fox A, Davidson R, Oakes T (2006): Motion correction and the use of motion covariates in multiple-subject fMRI analysis. HBM, 27(10):779–788.

Juslin P, Vastfjall D (2008): Emotional responses to music: The need to consider underlying mechanisms. Behav Brain Sci , 31(5):559.

Koelsch S (2012): Brain and Music. Wiley-Blackwell.

Koelsch S, Skouras S (2013): A neural network of sustained joy: An fMRI study using Eigenvector Centrality Mapping. Currently under review / submitted as supplementary material.

Koelsch S, Fritz T, Cramon Y, Müller K, Friederici A et al. (2005): Investigating emotion with music: an fMRI study. HBM, 27(3):239–250.

Koelsch S, Offermanns K, Franzke P (2010): Music in the treatment of affective disorders: an exploratory investigation of a new method for music-therapeutic research. Music Perception, 27(4):307–316.

Koelsch S, Fuermetz J, Sack U, Bauer K, Hohenadel M, Wiegel M, Kaisers U, Heinke W (2011): Effects of music listening on cortisol levels and propofol consumption during spinal anesthesia. Front Psychol, 2:58

Koelsch S, Skouras S, Fritz T, Herrera P, Bonhage C, Kuessner M, Jacobs A (2013): The roles of superficial amygdala and auditory cortex in music-evoked fear and joy. Neuroimage, 81:49-60

Krasnow B, Tamm L, Greicius MD, Yang TT, Glover GH, Reiss AL, Menon V (2003): Comparison of fMRI activation at 3 and 1.5 T during perceptual, cognitive, and affective processing. Neuroimage, 18(4):813–826.

Krüger G, Kastrup A, Glover GH (2001): Neuroimaging at 1.5 T and 3.0 T: Comparison of oxygenation-sensitive magnetic resonance imaging. Magn Reson Med, 45(4):595–604.

Lang P, Bradley M, Fitzsimmons J, Cuthbert B, Scott J, Moulder B, Nangia V (1998): Emotional arousal and activation of the visual cortex: an fMRI analysis. Psychophysiology, 35(2):199–210.

Lohmann G, Müller K, Bosch V, Mentzel H, Hessler S, Chen L, Zysset S, Von Cramon D (2001): Lipsia - a new software system for the evaluation of functional magnetic resonance images of the human brain. Comput Med Imaging Graph, 25(6):449–457.

Lohmann G, Neumann J, Müller K, Lepsien J, Turner R (2008): The multiple comparison problem in fMRI - A new method based on anatomical priors. In: Proceedings of the First Workshop on Analysis of Functional Medical Images, pp 1–8.

Okada T, Yamada H, Ito H, Yonekura Y, Sadato N (2005): Magnetic field strength increase yields significantly greater contrast-to-noise ratio increase: Measured using BOLD contrast in the primary visual area. Acad Radiol, 12(2):142–147.

Pereira CS, Teixeira J, Figueiredo P, Xavier J, Castro SL, Brattico E et al. (2011): Music and emotions in the brain: familiarity matters. PloS ONE, 6(11):e27241.

Phan KL, Wager T, Taylor SF, Liberzon I (2002): Functional neuroanatomy of emotion: a meta-analysis of emotion activation studies in PET and fMRI. Neuroimage, 16(2):331.

Plichta M, Gerdes A, Alpers G, Harnisch W, Brill S, Wieser M, Fallgatter A. (2011): Auditory cortex activation is modulated by emotion: A functional near-infrared spectroscopy (fNIRS) study. Neuroimage, 55(3):1200–1207.

Preston A, Thomason M, Ochsner K, Cooper J, Glover G (2004): Comparison of spiral-in/out and spiral-out BOLD fMRI at 1.5 and 3 T. Neuroimage, 21(1):291–301.

Rabe K, Michael N, Kugel H, Heindel W, Pfleiderer B (2006): fMRI studies of sensitivity and habituation effects within the auditory cortex at 1.5 T and 3 T.

Roy A, Shehzad Z, Margulies D, Kelly A, Uddin L, Gotimer K, Biswal B, Castellanos F, Milham M (2009): Functional connectivity of the human amygdala using resting state fMRI. Neuroimage, 45(2):614.

Triantafyllou C, Hoge R, Krueger G, Wiggins C, Potthast A, Wiggins G, Wald L (2005): Comparison of physiological noise at 1.5 T, 3 T and 7 T and optimization of fMRI acquisition parameters. Neuroimage, 26(1):243–250.

Voss H, Zevin J, McCandliss B (2006): Functional MR imaging at 3.0 T versus 1.5 T: a practical review. Neuroimaging Clin N Am, 16(2):285–297.

Wardlaw JM, Brindle W, Casado AM, Shuler K, Henderson M, Thomas B, Macfarlane J, Muñoz Maniega S, Lymer K, Morris Z, Pernet C, Nailon W, Ahearn T, Mumuni AN, Mugruza C, McLean J, Chakirova G, Tao YT, Simpson J, Stanfield AC, Johnston H, Parikh J, Royle NA, De Wilde J, Bastin ME, Weir N, Farrall A, Valdes Hernandez MC (2012): A systematic review of the utility of 1.5 versus 3 Tesla magnetic resonance brain imaging in clinical practice and research. Eur Radiol,22(11):2295-2303.

Weiskopf N, Hutton C, Josephs O, Turner R, Deichmann R (2007): Optimized EPI for fMRI studies of the orbitofrontal cortex: compensation of susceptibility-induced gradients in the readout direction. Magnetic Resonance Materials in Physics, Biology and Medicine, 20(1):39–49.

Yongbi M, Fera F, Mattay V, Frank J, Duyn J (2001): Simultaneous BOLD/perfusion measurement using dual-echo FAIR and UNFAIR: sequence comparison at 1.5 T and 3.0 T. Magn Reson Imaging, 19(9): 1159–1165.

Zhang Y, Chen Q, Du F, Hu Y, Chao F, Tian M, Zhang H (2012): Frightening Music Triggers Rapid Changes in Brain Monoamine Receptors: A Pilot PET Study. JNM, 53(10):1573–1578.

4.7 Supplementary Material

Supplementary Table 1: List of Stimuli

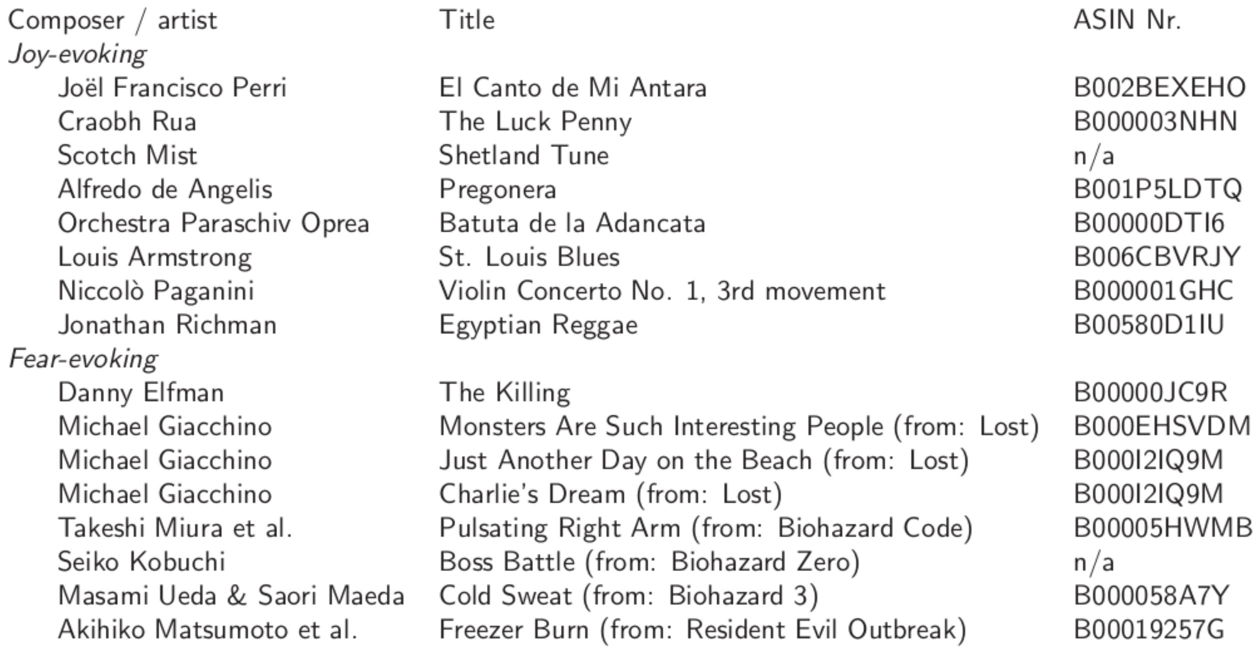

Composer / artist	Title	ASIN Nr.
Joy-evoking		
Joël Francisco Perri	El Canto de Mi Antara	B002BEXEHO
Craobh Rua	The Luck Penny	B000003NHN
Scotch Mist	Shetland Tune	n/a
Alfredo de Angelis	Pregonera	B001P5LDTQ
Orchestra Paraschiv Oprea	Batuta de la Adancata	B00000DTI6
Louis Armstrong	St. Louis Blues	B006CBVRJY
Niccolò Paganini	Violin Concerto No. 1, 3rd movement	B000001GHC
Jonathan Richman	Egyptian Reggae	B00580D1IU
Fear-evoking		
Danny Elfman	The Killing	B00000JC9R
Michael Giacchino	Monsters Are Such Interesting People (from: Lost)	B000EHSVDM
Michael Giacchino	Just Another Day on the Beach (from: Lost)	B000I2IQ9M
Michael Giacchino	Charlie's Dream (from: Lost)	B000I2IQ9M
Takeshi Miura et al.	Pulsating Right Arm (from: Biohazard Code)	B00005HWMB
Seiko Kobuchi	Boss Battle (from: Biohazard Zero)	n/a
Masami Ueda & Saori Maeda	Cold Sweat (from: Biohazard 3)	B000058A7Y
Akihiko Matsumoto et al.	Freezer Burn (from: Resident Evil Outbreak)	B00019257G

MRI scanner noise interaction with affective neural processes

Stavros Skouras, Marcus Gray, Hugo Critchley, Stefan Koelsch

Published in PloS one, *8*(11), e80564.

http://dx.doi.org/10.1371/journal.pone.0080564

5.0 Abstract

The purpose of the present study was the investigation of interaction effects between functional MRI scanner noise and affective neural processes. Stimuli comprised of psychoacoustically balanced musical pieces, expressing three different emotions (fear-neutral-joy). Participants (N=34, 19 female) were split into two groups, one subjected to continuous scanning and another subjected to sparse temporal scanning that features decreased scanner noise. Tests for interaction effects between scanning group (sparse/quieter vs continuous/noisier) and emotion (fear-neutral-joy) were performed. Results revealed interactions between the affective expression of stimuli and scanning group localized in bilateral auditory cortex, insula and calcarine sulcus. Post-hoc comparisons revealed that during sparse scanning, but not during continuous scanning, BOLD signals were significantly stronger for joy than for fear, as well as stronger for fear than for neutral in bilateral auditory cortex. During continuous scanning, but not during sparse scanning, BOLD signals were significantly stronger for joy than for neutral in the left auditory cortex and for joy than for fear in the calcarine sulcus. This is the first study to show a statistical interaction effect between scanner noise and affective processes and extends evidence that suggests scanner noise to be an important factor in functional MRI research that can affect and distort affective brain processes.

5.1 Introduction

The increasing interest of the neuroscientific community in applying research findings towards the development of clinical applications to complement diagnostic, therapeutic and surgical praxis makes the issue of scanner noise particularly pressing. An extensive review (Moelker and Pattynama, 2003) highlighted that the interference of scanner noise on normal brain function can be particularly pronounced during cognitive task performance in neurodegenerative and psychopathological populations, which have greater difficulty in attending to task-related stimuli (Kamio et al. 2001; Bublak et al. 2006). Moreover, interference from scanner noise is especially important in the case of functional MRI (fMRI) utilization for planning of surgical removal of brain tissue, due to the need for accurate functional mapping and the influence of scanner noise on brain activation patterns (Voets et al. 2005; Sunaert et al. 2001; Mueller et al. 1996; Achten et al. 2001). Functional mapping is complicated by the fact that when improving resolution, by means of increasing the strength of the magnetic field utilized during imaging, the intensity of scanner noise also increases, thereby compromising progress in resolution by the increased noise interference (Price et al. 2001; Moelker et al. 2003).

Scanner noise is intrinsically linked to the usual scanning implementation. In brief, magnetic resonance tomographers create strong momentary magnetic fields which cause the axes of the atoms of the objects being scanned to align momentarily and then return to their original orientation, emitting electromagnetic energy that comprises the fMRI datum (Kramer, 1984). The rapid changes of the magnetic forces cause magnetic elements of the apparatus to expand and contract in fast frequencies, resulting in a repetitive audibly loud sound, the scanner noise, which compromises the conditions of measurement (McGury and Frank, 2000) and constitutes a disadvantage of fMRI compared to positron emission tomography, magnetoencephalography and electroencephalography. In principle, the scanner noise is acting as a nuisance stimulus with undesirable effects, such as raising the baseline neural activity in the auditory cortex (Edmister et al. 1999; Bandettini et al. 2005), thereby decreasing the already low signal-to-noise ratio and percent signal change that is due to experimental manipulation (Moelker and Pattynama, 2003; Amaro et al. 2002). Moreover, scanner noise overlaps in acoustic frequency with certain stimuli (Price et al. 2001; Counter et al. 2005; Langers et al. 2004), leading to masking effects (Shah et al. 1999) and an increase in attentional resources required for the disambiguation of signal sources (Cho et al. 1997; Cho et al. 1998, Zhang et al. 2005), as well as nonlinear interactions in the auditory cortex (Langers et al. 2004; Talavage et al. 2004). Scanning protocols that feature a decrease in scanner noise, such as sparse temporal sampling (Gaab et al. 2007a,b; Hall et al. 1999) have been proven to decrease the derogatory effects of scanner noise as demonstrated with fMRI (for reviews see McJury and Frank 2000; Amaro et al 2002), magnetoencephalography (Mathiak et al. 2002), positron emission tomography (Mazard et al. 2002), as well as electroencephalography experimental results which show that during auditory working memory tasks, listening to recordings of scanner noise can differentially alter significantly the amplitude or latency of the P1, N1, N2 and P3 event related potential components (Novitski et al. 2003).

The derogatory effects of scanner noise were considered by most researchers to exert an influence solely on auditory processes treated as being cognitively separable from most experimental tasks, even though numerous studies suggest that the visual and motor cortices can also be influenced (Cho et al. 1998; Zhang et al. 2005; Mazard et al. 2002; Ludwig et al. 1999; Loenneker et al. 2001) and that scanner noise can influence attention as well as memory performance (Novitski et al. 2003; Tomasi et al. 2005). The way effects of scanner noise are modulated in the face of stimuli evoking basic emotions of biological importance, such as joy and fear (Panksepp, 2005), is not known.

Considering the stimuli and methods used in previous studies of scanner noise effects, it is apparent that beyond the consistent impact of scanner noise on the response of the auditory cortex during auditory tasks (reduced percentage of fMRI signal change), there are indications and concerns for more complex scanner noise effects on visual cortex activity (Zhang et al. 2005). The nature of such effects seems to be related to the task performed, with decreases in activity due to scanner noise during simple sensory stimulation (Cho et al. 1998; Zhang et al. 2005; Ludwig et al. 1999; Loenneker et al. 2001) and an increase in activity due to scanner noise during more elaborate cognitive tasks involving mental imagery (Mazard et al. 2002). The visual, motor and auditory cortices are brain regions where effects can manifest due to emotional factors (Warren et al. 2006; Vuilleumier et al. 2001; Lang et al. 1998; Phan et al. 2002; Fox et al. 1991; Plichta et al. 2011). Because no measure of valence, arousal nor intensity of emotional experiences was obtained during any of the previous studies on scanner noise effects, one cannot preclude the possibility that differences were due to affective factors that were uncontrolled within and across studies.

A recent study (Mueller et al. 2011) used consonant (pleasant) and dissonant (unpleasant) versions of 10 second-long musical excerpts, showing that decreasing scanner noise when contrasting responses between pleasant and unpleasant music leads to enhanced detectability of activity in limbic structures related to affective processing. That study reported results from three experiments concerning the sensitivity of continuous temporal scanning, sparse temporal scanning and interleaved silent steady state scanning techniques. Interleaved silent steady state showed stronger activation than sparse temporal scanning, and sparse temporal scanning showed stronger activation than continuous temporal scanning in auditory cortex, amygdala and hippocampal formation. However, no statistical comparison was made between the data obtained using the three different acquisition schemes. Therefore, no previous study has explicitly computed statistical interaction effects between scanner noise and emotion.

The present study aims to investigate for the possible existence of brain regions where the pattern of affective responses can be altered or even reversed due to scanner noise. Understanding the brain mechanisms implementing emotional experiences is important because they seem to be related to brain processes that are particularly vulnerable to stress (O’Mara, 2005; Warner-Schmidt and Duman, 2006; Weniger et al. 2009; Plevier et al. 2001) and impaired emotional functioning can be seen as a marker of most psychopathologies (Mannie et al. 2007; Hoekert et al. 2007; Connan et al. 2003; Leppännen et al.

2006; Kang et al. 2012). Moreover, behavioral interventions that target the emotional constituents of cognition can be successful in alleviating depressive symptomatology (Goldman et al. 2006) and reduction of emotional stress has beneficial effects on immune system function (Cohen and Pressman, 2006; Steptoe et al. 2005; Tosevski and Milovancevic, 2006; Chesney et al. 2005). Musical stimulation, being emotional and acoustic, provides a well-suited medium for the investigation of interference by an acoustic distractor, such as scanner noise, on affective processing.

To address the question of possible interactions between emotion and scanner noise, a stimulus set was utilized, consisting of fearful, neutral and joyous musical pieces. An independent pilot study using the same stimuli (Koelsch et al. 2013) showed that the auditory cortex and amygdala, which are the brain regions with the most significant difference in activity between the extremes of this biologically relevant affective spectrum, exhibit a linear increase in activity from fear to joy. The present study tests for an interaction effect between the two-level factor temporal scanning protocol used (sparse vs continuous, that corresponds to reduced vs constant scanner noise, respectively) and the three-level linear factor emotion (fear-neutral-joy).

It was hypothesized that the auditory cortex would show an interaction effect because it has been found to be most responsive to such acoustic emotional stimulus sets (Plichta et al. 2011; Mueller et al. 2011), and to be susceptible to acoustic interference due to scanner noise in all related published studies (for reviews see McJury and Frank, 2000; Amaro et al. 2002). Moreover, the present study tested whether the visual and motor cortices would also show interaction effects due to emotional factors that had not been accounted for across previous studies. The study also tested whether limbic structures such as the amygdala and hippocampal formation are influenced by scanner noise. Given the large variety of areas contributing to emotional phenomena, a whole-brain approach was employed.

5.2 Methods

5.2.1 Participants

34 individuals (aged 19 – 36 years, M = 23.78, SD = 4.98, 19 females) took part in the experiment. All participants had normal hearing (as assessed with standard pure tone audiometry) and were right-handed (according to self-report). None of the participants was a professional musician or a music student; 19 participants had no or only minimal formal musical training and 15 participants were amateur musicians who had learned at least one musical instrument (mean duration of formal training was 2.6 years). The participants were split into two groups of 17 subjects each; a group that underwent sparse temporal scanning (aged 19 – 36 years, M = 24.53, SD = 6.28, 9 females, mean duration of formal musical training 3.19 years, SD = 3.35) and a group that underwent continuous scanning (aged 19 – 28 years, M = 22.92, SD = 2.90, 10 females, mean duration of formal musical training 1.94 years, SD = 2.28). Independent samples t-tests showed that the two groups did not differ with regards to age and formal musical training ($p > 0.05$). Exclusion criteria were left-handedness, professional

musicianship, a score on Beck’s Depression Inventory (Beck and Steer, 2003) of 13 or more points, consumption of alcohol or caffeine exceeding one liter during the 24 hours prior to testing, poor sleep during the previous night, past diagnosis of a neurological or psychiatric disorder, and abnormal brain anatomy. All subjects gave written informed consent. The study was conducted according to the Declaration of Helsinki and approved by the ethics committee of the School of Life Sciences and the Psychology Department of the University of Sussex.

5.2.2 Stimuli

Musical stimuli were selected from CD recordings to evoke joy or fear (see Supplemental Table 3). Neutral pieces, evoking neither joy nor fear were composed algorithmically. There were 8 stimuli per category. Behavioral data (see Results for details) showed that musical stimuli evoked the desired feelings in the sample studied. All stimuli were matched across conditions in triplets (joy-neutral-fear) with regard to tempo (beats per minute), mean fundamental frequency pitch, fundamental frequency pitch variation, pitch centroid value, spectral complexity, and spectral flux. This was confirmed by an acoustic analysis of the stimuli using “Essentia”, an in-house library for extracting audio and music features from audio files (http://mtg.upf.edu/technologies/essentia). The Essentia software was also used to test for differences between stimuli with regard to another 177 acoustical factors. Ten psychoacoustic factors were found to differ significantly between experimental conditions ($p < 0.001$, corrected for multiple comparisons). These factors were mean and variance of fundamental frequency salience, mean and variance of sensory dissonance, mean chord strength and mean key strength, mean and variance of spectral flux, mean spectral crest and mean spectral complexity (for more details see Koelsch et al. 2013). The values of these factors associated with each stimulus were used in the fMRI data analysis as additional regressors of the general linear model’s design matrix (see Data Analysis for details).

5.2.3 Procedure

Prior to the MRI session, participants were presented with short (12 s) versions of each stimulus to obtain familiarity ratings: Participants rated their familiarity with each piece on a four-point scale (ranging from "To my knowledge I have never heard this piece before", to "I know this piece, and I know who composed, or performed it"). One outlier participant, who misinterpreted the familiarity rating scale, was not considered in the analysis of familiarity ratings. Following the familiarity ratings, participants were trained on the emotion rating procedure, using 12 s long excerpts of musical pieces that did not belong to the stimulus set used in the fMRI scanning session. During the fMRI scanning session, stimuli were presented in a pseudo-random order so that no more than two stimuli of each stimulus category (joy, fear, neutral) followed each other. The task of the participants was to listen to the musical stimuli with their eyes closed and to rate their emotional state after each musical stimulus. Each musical stimulus was followed by an interval of 2 s in which a beep tone of 350 Hz and 1 s duration signaled participants to open their eyes and to commence the rating procedure. During the rating procedure, participants indicated how they felt at the end of each excerpt with regard to valence ("pleasantness"), "arousal", "joy" and "fear".

That is, participants rated how they felt, and not which emotion each song was supposed to express (for the importance of this see Gabrielsson and Juslin, 2003). Ratings were obtained with 6-point Likert scales (ranging from "not at all" to "very much"). The time interval for the rating procedure was 12 s and each rating period was followed by approximately 3 s of rest (see Figure 1). The entire stimulus set was presented twice during the fMRI scanning session. Musical stimuli were presented using Presentation (version 13.0, Neurobehavioral systems, Albany, CA, USA) via MRI compatible headphones (under which participants wore earplugs). Instructions and rating screens were delivered through MRI compatible liquid crystal display goggles (Resonance Technology Inc., Northridge, CA, USA).

5.2.4 MR Scanning

Images were acquired using a 1.5 tesla scanner (Magnetom Avanto, Siemens AG, Erlangen, Germany) equipped with a standard 12-channel head coil. Prior to the fMRI measurements, a high-resolution (1x1x1 mm) T1-weighted anatomical reference image was acquired from each participant using a rapid acquisition gradient echo sequence. During the fMRI measurements, the continuous scanning group (N=17) underwent Echo Planar Imaging with an echo time of 30 ms and a repetition time of 2 seconds. Slice-acquisition was interleaved within the repetition time interval. The matrix acquired was 64x64 voxels with a Field Of View of 192 mm, resulting in an in-plane resolution of 3 mm. Slice thickness was 3 mm with an interslice gap of 0.6 mm (37 slices, whole brain coverage). The acquisition window was tilted at an angle of 30 degrees relative to the line between the anterior and posterior commissures to minimize susceptibility artifacts in the orbitofrontal cortex (Deichmann et al. 2002,2003; Weiskopf et al. 2007). All scanning parameters were identical for the sparse scanning group (N=17) apart from the introduction of a 4 s delay between volume acquisitions.

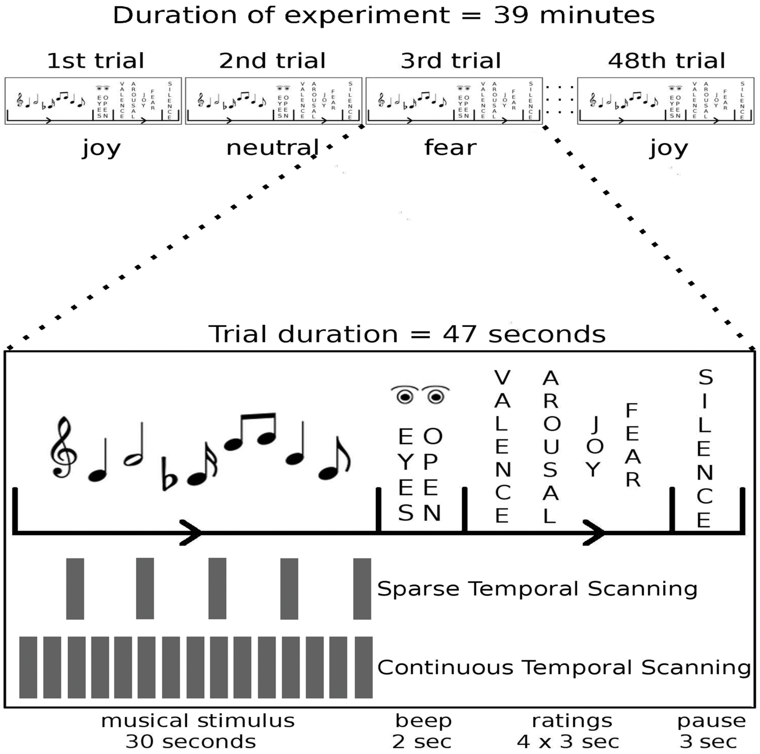

Figure 5.1: Experimental design. In each trial, a music stimulus (either joy, fear, or neutral) was presented in pseudorandom order for 30 s. Participants listened to the music with their eyes closed. Then, a beep tone signaled to open the eyes and to commence the rating procedure. Four ratings (felt valence, arousal, joy, and fear) were obtained in 12 s, followed by a few seconds of pause. Trial duration was approximately 47 s, the experiment comprised of 48 trials. Grey bars indicate volume acquisitions for sparse and continuous scanning groups (TR = 2 s).

5.2.5 Data Analysis

fMRI data were processed using LIPSIA 2.1 (Lohmann, 2001). Data were corrected for slicetime acquisition and normalized into MNI-space-registered images with isotropic voxels of 3 cubic millimeters. A temporal highpass filter with a cutoff frequency of 1/90 Hz was applied to remove low frequency drifts in the fMRI time series, and a spatial smoothing was performed using a 3D Gaussian kernel and a filter size of 6 mm Full Width at Half Maximum. A mixed effects block design general linear model analysis was employed (Friston and Stephan, 2007). Valence ratings, arousal ratings, familiarity ratings, ten important psychoacoustic parameters (see Stimuli) and realignment parameters were entered in the design matrix as covariates of no interest (Johnstone et al. 2006). On the first level, parametric contrasts were calculated to show brain regions where activity correlates with increases/decreases along the emotional spectrum from fear to joy. Two sample t-tests were utilized at the second level to compare the contrast images from the first level between the two groups, computing the interaction effects between the parametric factor emotion (with levels fear, neutral, joy) and scanning group (with levels sparse/quieter and continuous/noisier). Findings were corrected for multiple comparisons by the use of cluster-size and cluster-value thresholds obtained by Monte Carlo simulations with a significance level of $p < 0.05$ (Lohmann et al. 2008). Additionally, to certify that interaction effects in the auditory cortex are due to scanner noise modifying affective responses rather than modifying psychoacoustic processes, the same procedure was used to compute z−maps of interaction effects between scanning group and each of the ten important psychoacoustic parameters (see Stimuli).

To clarify the nature of the interaction effects between scanning group and emotion, z−maps were computed and examined for each scanning group separately, for each combination of stimulus categories (i.e. joy vs fear, joy vs neutral, fear vs neutral). The computed z−maps were corrected for multiple comparisons by the use of cluster-size and cluster-value thresholds obtained by Monte Carlo simulations with a significance level of $p < 0.05$ (Lohmann et al. 2008). The conjunction of each z-map with the z-map of the interaction effect was also computed based on the absolute z-values.

5.3 Results

5.3.1 Behavioral Data

Behavioral data are summarized in Figure 2 and Supplemental Tables 1 and 2. All reported results were corrected for multiple comparisons. Valence (pleasantness) ratings were lower for fear than for joy stimuli ($t(33) = 14.50$, $p < 0.0001$), higher for joy than for neutral stimuli ($t(33) = 10.68$, $p < 0.0001$), but did not differ significantly between neutral and fear stimuli ($t(33) = 1.82$, $P = 0.077$).

Arousal ratings were lowest for neutral stimuli, and highest for joy stimuli, with ratings for fear stimuli being in between. Arousal ratings differed significantly between fear and neutral stimuli ($t(33) = 3.89$, $p < 0.0001$), fear and joy stimuli ($t(33) = 3.76$, $p < 0.0001$), and between joy and neutral stimuli ($t(33) = 9.14$, $p < 0.0001$).

Joy ratings were lowest for fear stimuli, and highest for joy stimuli, with ratings for neutral stimuli being in between. Joy ratings differed significantly between fear and neutral stimuli ($t(33) = 5.63$, $p < 0.0001$), fear and joy stimuli ($t(33) = 21.49$, $p < 0.0001$), and between joy and neutral stimuli ($t(33) = 12.72$, $p < 0.0001$).

Correspondingly, fear ratings were highest for fear stimuli, lowest for joy stimuli, with ratings for neutral stimuli being in between. Fear ratings differed significantly between fear and neutral stimuli ($t(33) = 10.80$, $p < 0.0001$), fear and joy stimuli ($t(33) = 18.28$, $p < 0.0001$), and between joy and neutral stimuli ($t(33) = 5.34$, $p < 0.0001$). Independent samples t-tests showed that the ratings given to the stimuli belonging to each emotion condition did not differ between the two scanning groups (p > 0.15).

To test whether interaction effects between scanner noise and emotion are observable on the behavioral level, a fixed effects ANOVA item analysis was performed on the average ratings of the stimulus set. The results revealed significant interaction effects between scanner noise and emotion reflected on the

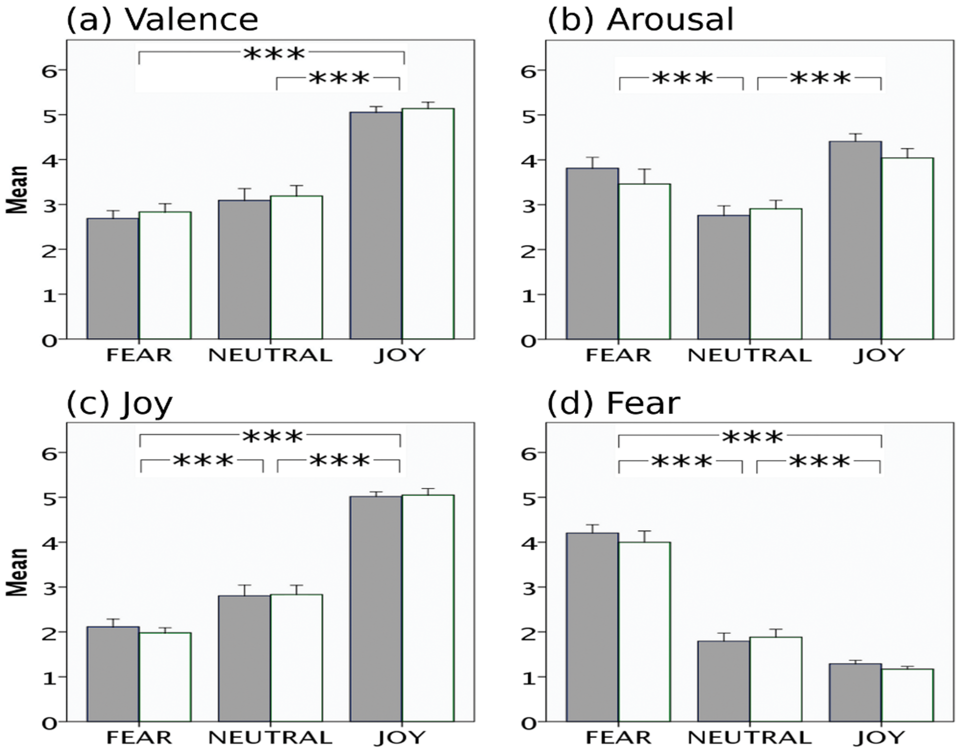

Figure 5.2: Behavioral ratings of participants on the four emotion scales used. (a) valence, (b) arousal, (c) joy, and (d) fear. Ratings are depicted separately for each stimulus category (fear, neutral, joy). White bars represent the sparse scanning group and grey bars represent the continuous scanning group. Note that there were no significant differences in ratings between the two groups. Overall, joy stimuli were rated as more pleasant than fear and neutral ones (valence/pleasantness ratings of fear and neutral did not differ). Arousal ratings of joy and fear stimuli did not differ (and both joy and fear stimuli were rated as more arousing than neutral stimuli).

average ratings of arousal F(2, 42) = 10.34, $p < 0.001$ and fearfulness F(2, 42) = 4.11, $p < 0.05$ but not on the average ratings of valence and joy ($p > 0.05$) (see also Figure 2). Post-hoc t-tests showed that joy and fear stimuli were rated as more arousing, and more fearful by the continuous group, whereas neutral stimuli were rated as more arousing and more fearful by the sparse group ($p < 0.05$; corrected for multiple comparisons – for detailed descriptive statistics see Supplemental Table 2).

Average familiarity ratings did not differ significantly between joy and fear stimuli, fear and neutral stimuli, nor between joy and neutral stimuli ($p > 0.20$). The average ratings of familiarity did not differ between the two scanning groups for the joy stimuli, nor for the neutral stimuli or the fear stimuli ($p > 0.25$).

Each participant's valence, arousal, and familiarity ratings were used in the fMRI data analysis as regressors of no interest (see Data Analysis). Therefore, variance related to these variables (valence, arousal, and familiarity) did not contribute to the fMRI results presented in the following.

5.3.2 fMRI data

The statistical parametric maps of the interaction Group x Emotion (corrected for multiple comparisons, $p < 0.05$) revealed significant interaction effects in the auditory cortex bilaterally, and in the visual cortex medially centered around the calcarine sulcus (see Table 1a and Figure 3a). The interaction in the auditory cortex covered auditory core, belt, and parabelt regions bilaterally, extending in the right hemisphere into the retro-insular cortex. This interaction effect was due to the effect of emotion being stronger in the sparse temporal scanning group than in the continuous scanning group. The opposite was observed in the visual cortex in the left calcarine sulcus; the peak voxel was located with 70% probability in area 17, according to probabilistic brain maps (Eickhoff et al. 2005), where the effect of emotion was significantly stronger for the continuous scanning group.

To clarify the nature of these interactions, post-hoc comparisons between the three emotion conditions were performed for each scanning group separately. Results are summarized in Table 1(b-f). During continuous but not during sparse temporal scanning, fMRI activity differences between joy and fear were significant in the calcarine sulcus and greater during joy. During continuous but not during sparse temporal scanning, fMRI activity differences between joy and neutral were significant in the left auditory cortex and greater during joy. During sparse but not during continuous scanning, fMRI activity differences between joy and fear were significant in bilateral auditory cortex and greater during joy. Activity differences between fear and neutral were also significant in bilateral auditory cortex, only during sparse temporal scanning, and greater during fear. Figure 3(b-e) and Table 1(g-j) show conjunction results between the z-map of the interaction effect and the significant clusters from each post-hoc comparison.

The interaction effect localized in the auditory cortex was related to affective processes, rather than reflecting any difference between the two groups in psychoacoustic processing. Inspection of the z−maps calculated for each of the ten psychoacoustic regressors that differed between stimulus categories showed that none of these psychoacoustic factors interacted with scanner noise, neither within, nor in the vicinity of the auditory cortex.

Table 5.1: fMRI results. (a) Results of general linear model interaction between scanning group and emotion (fear, neutral, joy), corrected for multiple comparisons ($p < 0.05$). (b-f) Results of post-hoc comparisons between emotion conditions, performed separately for each scanning group. No difference was observed for the contrast Fear>Neutral in the continuous scanning group. (g-j) Results of conjunction between interaction effect z-map and z-maps from post-hoc comparisons.

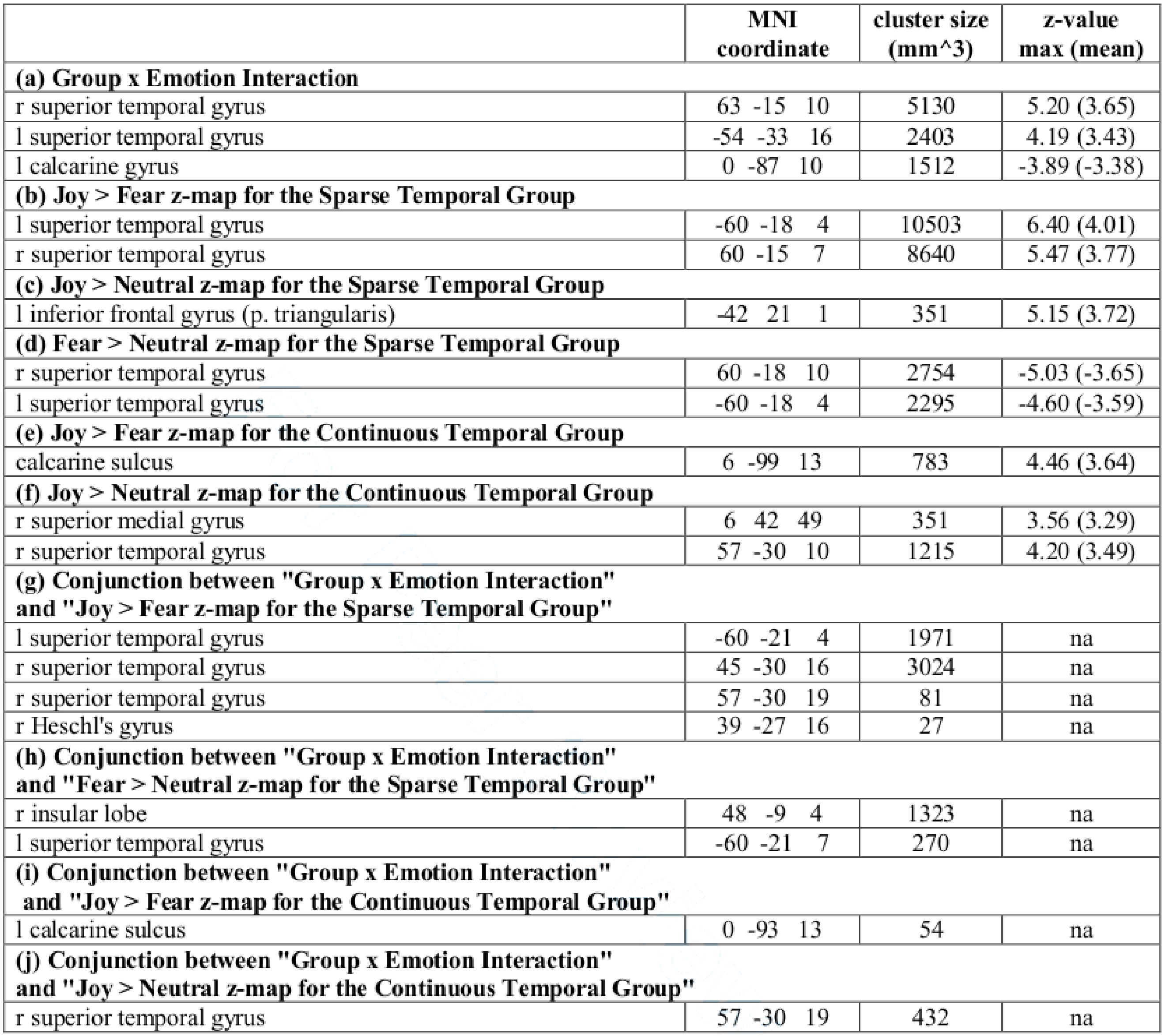

	MNI coordinate	cluster size (mm^3)	z-value max (mean)
(a) Group x Emotion Interaction			
r superior temporal gyrus	63 -15 10	5130	5.20 (3.65)
l superior temporal gyrus	-54 -33 16	2403	4.19 (3.43)
l calcarine gyrus	0 -87 10	1512	-3.89 (-3.38)
(b) Joy > Fear z-map for the Sparse Temporal Group			
l superior temporal gyrus	-60 -18 4	10503	6.40 (4.01)
r superior temporal gyrus	60 -15 7	8640	5.47 (3.77)
(c) Joy > Neutral z-map for the Sparse Temporal Group			
l inferior frontal gyrus (p. triangularis)	-42 21 1	351	5.15 (3.72)
(d) Fear > Neutral z-map for the Sparse Temporal Group			
r superior temporal gyrus	60 -18 10	2754	-5.03 (-3.65)
l superior temporal gyrus	-60 -18 4	2295	-4.60 (-3.59)
(e) Joy > Fear z-map for the Continuous Temporal Group			
calcarine sulcus	6 -99 13	783	4.46 (3.64)
(f) Joy > Neutral z-map for the Continuous Temporal Group			
r superior medial gyrus	6 42 49	351	3.56 (3.29)
r superior temporal gyrus	57 -30 10	1215	4.20 (3.49)
(g) Conjunction between "Group x Emotion Interaction" and "Joy > Fear z-map for the Sparse Temporal Group"			
l superior temporal gyrus	-60 -21 4	1971	na
r superior temporal gyrus	45 -30 16	3024	na
r superior temporal gyrus	57 -30 19	81	na
r Heschl's gyrus	39 -27 16	27	na
(h) Conjunction between "Group x Emotion Interaction" and "Fear > Neutral z-map for the Sparse Temporal Group"			
r insular lobe	48 -9 4	1323	na
l superior temporal gyrus	-60 -21 7	270	na
(i) Conjunction between "Group x Emotion Interaction" and "Joy > Fear z-map for the Continuous Temporal Group"			
l calcarine sulcus	0 -93 13	54	na
(j) Conjunction between "Group x Emotion Interaction" and "Joy > Neutral z-map for the Continuous Temporal Group"			
r superior temporal gyrus	57 -30 19	432	na

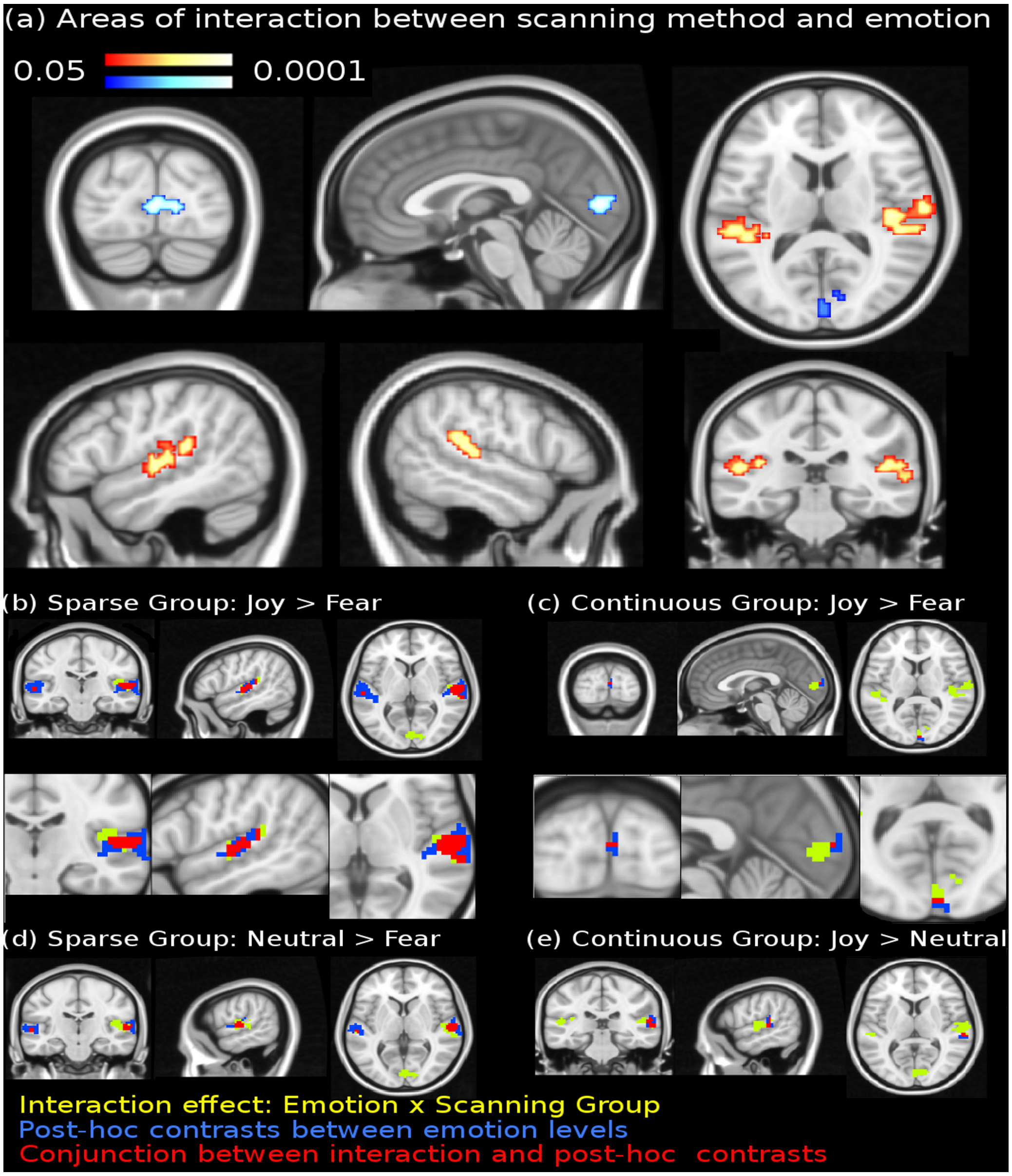

Figure 5.3: fMRI results. (a) Results of general linear model interaction between scanning group and emotional expression of stimuli (fear, neutral, joy), corrected for multiple comparisons ($p < 0.05$). The red scale marks clusters where the activity correlated with increases in emotion (from fear to joy) to a greater extent for the sparse scanning group and the blue scale marks the cluster where the activity correlated with increases in emotion to a greater extent for the continuous scanning group. (b) Conjunction between interaction effects and significant clusters of joy>fear for the sparse scanning group. (c) Conjunction between interaction effects and significant clusters of joy>fear for the continuous scanning group. (d) Conjunction between interaction effects and significant clusters of neutral>fear for the sparse scanning group. (e) Conjunction between interaction effects and significant clusters of joy>neutral for the continuous scanning group. Yellow color marks regions significant only in the z-map of the emotion by scanning group interaction. Blue color marks regions significant only in the contrast between two emotion conditions for a particular scanning group (e.g. joy>fear for the sparse scanning group; see sub-headers). Red color marks regions significant in a conjunction between the interaction effects and the z-map from a specific contrast between two emotion conditions for a particular scanning group (e.g. joy>fear for the sparse scanning group; see sub-headers).

5.4 Discussion

Interaction effects between emotion and scanning group were observed in the auditory and visual cortices. The interaction shows that auditory cortex activity correlates with increases towards the joy end of the fear-joy emotion spectrum, to a greater extent during sparse than during continuous scanning. Significant increases in auditory cortex activity were observed between all emotion levels (fear, neutral, joy), only in the sparse scanning group. The interaction also shows that visual cortex activity correlates with increases towards the joy end of the fear-joy spectrum, to a greater extent for the continuous group and that this is mostly due to the significant increase of visual cortex activity during joy, compared to fear, in the continuous group. These results are plausible and most likely to reflect interference by scanner noise on affective neural functioning.

The auditory cortex plays an important role in affective processing of acoustic stimuli. Differences in activity of auditory cortex between the stimulus categories were not due to psychoacoustic differences between the stimuli because these had been thoroughly controlled for during both the processes of stimulus selection/design and fMRI data analysis. Moreover, no interactions were observed in the auditory cortex between scanning group and any psychoacoustic factor. Increases in auditory cortex activity that are not due to psychoacoustic differences in the stimuli may reflect increases in the level of acoustical analysis performed and the detail of mental representations formed following increases in voluntary attention (Jäncke et al. 1999). Results from several previous studies using the same or similar stimuli corroborate this view (Plichta et al. 2011; Koelch et al. 2005). The interaction effect between scanner noise and emotion, observed in the auditory cortex, probably reflects that the scanner noise interferes with neural processes related to attention and detailed acoustical feature analysis, by means of its unpleasant, masking and distracting contribution to the overall acoustic percept. The continuous scanning group was exposed to more scanner noise, which blurred the perceptual borders between emotion levels. This interpretation is in line with all previous research on the effects of scanner noise on auditory cortex activity (for reviews see McJury and Frank, 2000; Amaro et al 2002) and implies that increases of scanner noise impair the ability to distinguish affective differences in acoustic stimuli. The identified cluster of activity centered in the auditory cortex also covered part of the insula which is involved, amongst other processes and functions, in affective functions during cognitively demanding tasks and in emotion induction by recall and imagery (Phan et al. 2002). The latter insular function provides a functional link with the visual cortex, additionally to well-established anatomical and functional connections between auditory and visual cortices (Bizley et al. 2007).

The visual cortex also plays an important role in emotion processing, though usually of visual stimuli. Emotion induction by visual stimuli leads to increases of activity mainly in the occipital cortex and the amygdala (Phan et al. 2002). Particularly areas of the calcarine fissure have been reported to be more responsive, in terms of activated cluster size, to emotional compared to neutral stimuli from the International Affective Picture System (Lang et al. 1997,1998). These findings are further corroborated by a reported violation of a linear response during playback of recordings of fMRI scanner noise (Mazard et al.

2002). This violation was found in a positron emission tomography study that documented a strong negative correlation between activity in the anterior calcarine cortex and accuracy in a mental imagery task. The observed correlation was present only in the absence of scanner noise. Visual imagery is considered as one basic emotion-evoking principle during music listening (Juslin and Vastfjall, 2008) and anatomical studies indicate that auditory core, belt and parabelt regions project to V1 and V2 of the visual cortex, and that neurons in V2 project back into these auditory regions (Smiley et al. 2007). Note that the eyes-closed requirement of the experimental task used in the present study was motivated by evidence suggesting that affective activity is enhanced when the eyes are closed (Lerner et al. 2009), a condition that practically minimizes any vision-specific sensory contributions to visual cortex activity.

Based on the existing literature on the topic, the most plausible interpretation of the findings related to visual cortex activity is that they reflect interference due to scanner noise on the mental imagery constituents of affective processing. In the context of the experimental task used for the present study, which required extensive emotional ratings after each stimulus, the continuous scanner noise may have forced the participants belonging to the continuous scanning group to rely more on visualization for perceiving the emotion differences in the music. That is, some of the affective functionality of the visual cortex may have been recruited in the continuous group to compensate for the diminished activity in the auditory cortex. A complementary perspective, in line with previous findings, suggests that since the activity in the calcarine cortex correlates negatively with concentration and performance (Mazard et al. 2002), the continuous scanning group was less concentrated due to the distracting effects of the greater amount of scanner noise it was exposed to.

No interaction effects were observed in any limbic structures, commonly associated with emotions, such as the amygdala, ventral striatum and hippocampal formation. There are two factors that might be contributing to this. Firstly, as previously demonstrated (Mueller et al. 2011), activity in these structures is sensitive to scanner noise and becomes observable only under optimized conditions. Secondly, sensitivity to changes of activity in limbic structures improves with increasing field strength (Krasnow et al. 2003). The present study was conducted with a field strength of 1.5 tesla, which may not have allowed for the detection of interaction effects in limbic structures using the particular stimulus set.

Another methodological matter that is relevant to the present study relates to the difference in the number of statistical measurements obtained for each of the two scanning groups. In comparison to the continuous scanning group, there were three times fewer volumes acquired for the sparse scanning group which could result in decreased statistical power and lead to artifacts. However, the number of observations are sufficient in estimating the necessary statistics for both groups and the fact that z-values in the auditory cortex are larger for the sparse group confirms that undersampling is not the reason the presented results were observed. Moreover, the findings observed in the calcarine sulcus consolidate related findings in the existing literature (Mazard et al. 2002; Lang et al. 1998), suggesting that all reported results reflect true interaction effects.

Overall, the observed data suggest scanner noise to be a more significant confound for fMRI research than previously believed. In addition to scanner noise effects on the responsiveness of the auditory cortex, the presented data show that scanner noise interacts with affective processes. Thus, scanner noise affects practically all aspects of brain functioning: from sensory aspects (Cho et al, 1998; Zhang et al. 2005; Mazard et al. 2002; Ludwig et al. 1999; Loenneker et al. 2001), to cognitive domains such as attention (Tomasi et al. 2005) and memory (Novitski et al. 2003; Tomasi et al. 2005), as well as motor function (Cho et al. 1998) and emotion, as suggested previously (Mueller et al. 2011) and evidenced by the present study.

Such findings were expected because it has been long known that exposure to noise is associated with annoyance reactions (Tarnopolsky et al. 1978), hypertension, cardiovascular disease, catecholamine secretion, psychological symptoms, impaired reading comprehension, impaired memory skills (for a review see Clark and Stansfeld, 2007) and possibly prevalence of psychiatric disorder (Stansfeld, 1992). Extensions of the presented work would caution one to the implications that long-lasting exposure to similar types of noise can have on the neural functioning of a population at large (see also Kraus and Canlon, 2012).

Minimizing noise exposure during fMRI scanning is of major importance, especially in obtaining accurate readings of affective neural processes. To this end, many modifications to the usual scanning implementation have been proposed, including software optimization, active noise-reduction technologies and hardware enhancements.

With regards to software optimization, modified acquisition sequences such as Stimulated Echo Acquisition Mode (STEAM; Moelker and Pattynama, 2003; Crémillieux et al. 1997; Hennig and Hodapp, 1993; Frahm et al. 1985); Simultaneous Multislice Excitation (SIMEX) combined with Fast Low Angle Shot (FLASH) or spiral imaging (Moelker and Pattynama, 2003; Ludwig et al. 1999; Loenneker et al. 2001); Functional Burst Imaging (FBI; Schlaug et al. 2005); Sensitivity-Encoded Echo-Planar Imaging (SENSE-EPI; de Zwart et al. 2002); Interleaved Silent Steady State imaging (ISSS; Schwarzbauer et al. 2006); SWeep Imaging with Fourier Transformation (SWIFT; Idiyatullin et al. 2006); and others varying the projection reconstruction method while optimizing gradient pulsing (Moelker and Pattynama, 2003) or minimizing the empty space in the field of view and volume acquisition time through interleaved spiral trajectory k-space imaging (Oesterle et al. 2001) are representative of progress in scanner noise reduction.

Monitoring scanner noise with microphones while simultaneously generating and adding the inverse soundwave to the output of the stimulus-presentation headphones is an application instance of a technology known as Active Noise Cancellation (Goldman et al. 1989; Chen et al. 1999; McJury et al. 1997). An extension of the theory behind active noise cancellation has led to Active Structural Acoustic Control that uses panels featuring vibro-acoustic sensors and active actuators to introduce anti-vibrations on solid materials (Berry, 1999).

With regards to hardware enhancements, using vacuum-enclosed heavy gradient coils, heavy mounting to the floor to maximize vibrational absorption (Moelker and Pattynama, 2003; Katsunuma et al. 2001) and implementing active Lorentz force balancing applied to gradient coil design (Mansfield et al. 1994, 1998; Bowtell and Mansfield, 1995) have been suggested to decrease scanner noise (Moelker and Pattynama, 2003). Hardware customizations implemented in “bench-top prototype two-coil systems” (Mansfield et al. 1994), research scanners featuring high noise reduction and commercial “quiet MR-systems” (Price et al. 2001, Katsunuma et al. 2001; Edelstein et al. 2002) make scanners less noisy and their cost estimates are reasonable in comparison to the cost of the fMRI experiments that are being conducted on more than 20000 fMRI scanners worldwide (Blamire, 2008) offering results that are susceptible to noise interference and should be treated with caution. Considering that most of these solutions have been in place for over a decade and that there has been little development in this field since that time, it is in the interest of valid scientific practice to treat the elimination of scanner noise as a pressing issue of high priority.

5.5 Conclusion

It has been demonstrated experimentally that scanner noise interactions with affective neural processes can occur in the auditory, retro-insular and visual cortices during emotional music listening. Such interactions are likely to reflect involuntary changes in levels of attendance to auditory stimuli and to be related to processes of visual imagery.

5.6 References

Achten E, Jackson G, Cameron J, Abbott D, Stella D, Fabinyi G (1999) Presurgical evaluation of the motor hand area with functional mr imaging in patients with tumors and dysplastic lesions. Radiology 210: 529–538.

Amaro E, Williams S, Shergill S, Fu C, MacSweeney M, Picchioni M, Brammer M, McGuire P (2002): Acoustic noise and functional Magn Reson Imaging: current strategies and future prospects. J Magn Reson Imaging 16: 497–510.

Bandettini P, Jesmanowicz A, Van Kylen J, Birn R, Hyde J (2005) Functional mri of brain activation induced by scanner acoustic noise. Magn Reson Med 39: 410–416.

Beck A, Steer R (1993) Beck depression inventory manual. San Antonio: Psychological Corporation.

Berry A (1999) Advanced sensing strategies for the active control of vibration and structural radiation. Proceedings of Active 99. Florida, USA: Inst of Noise Control Engineer:73-90

Bizley JK, Nodal FR, Bajo VM, Nelken I, King AJ (2007) Physiological and anatomical evidence for multisensory interactions in auditory cortex. Cereb Cortex 17: 2172–2189.

Blamire A (2008) The technology of mri the next 10 years? Br J Radiol 81: 601–617.

Bowtell R, Mansfield P (1995) Quite transverse gradiant coils: Lorentz force balanced designs using geometrical similitude. Magn Reson Med 34: 494–497.

Bowtell R, Peters A (1999) Analytic approach to the design of transverse gradient coils with co-axial return paths. Magn Reson Med 41: 600–608.

Bublak P, Redel P, Finke K (2006) Spatial and non-spatial attention deficits in neurodegenerative diseases: Assessment based on bundesen's theory of visual attention (tva). Restor Neurol Neurosci 24: 287–301.

Chen C, Chiueh T, Chen J (1999) Active cancellation system of acoustic noise in mr imaging. IEEE Trans Biomed Eng 46: 186–191.

Chesney M, Darbes L, Hoerster K, Taylor J, Chambers D, Anderson D (2005) Positive emotions: Exploring the other hemisphere in behavioral medicine. Int J Behav Med 12: 50–58.

Cho Z, Chung S, Lim D, Wong E (1998) Effects of the acoustic noise of the gradient systems on fmri: a study on auditory, motor, and visual cortices. Magn Reson Med 39: 331–335.

Cho Z, Park S, Kim J, Chung S, Chung S, Chung J, Moon C, Yi, J, Sin C, Wong E (1997) Analysis of acoustic noise in mri. Magn Reson Imaging 15: 815–822.

Clark C, Stansfeld S (2007) The effect of transportation noise on health and cognitive development: A review of recent evidence. Int J Comp Psychol 20: 145-158

Cohen S, Pressman S (2006) Positive affect and health. Curr Dir Psychol Sci 15(3):122–125.

Connan F, Campbell I, Katzman M, Lightman S, Treasure J (2003) A neurodevelopmental model for anorexia nervosa. Physiol Behav 79: 13–24.

Counter S, Olofsson A, Grahn H, Borg E (2005) Mri acoustic noise: sound pressure and frequency analysis. J Magn Reson Imaging 7: 606–611.

Crémillieux Y, Wheeler-Kingshott C, Briguet A, & Doran S (1997) Steam-burst: A single-shot, multi-slice imaging sequence without rapid gradient switching. Magn Reson Med 38: 645–652.

de Zwart J, van Gelderen P, Kellman P, Duyn J (2002) Reduction of gradient acoustic noise in mri using sense-epi. Neuroimage 16: 1151–1155.

Deichmann R, Gottfried J, Hutton C, Turner R (2003) Optimized epi for fmri studies of the orbitofrontal cortex. Neuroimage 19: 430–441.

Deichmann R, Josephs O, Hutton C, Corfield D, Turner R (2002) Compensation of susceptibility-induced bold sensitivity losses in echoplanar fmri imaging. Neuroimage 15: 120–135.

Edelstein W, Hedeen R, Mallozzi R, El-Hamamsy S, Ackermann R, Havens T (2002) Making mri quieter. Magn Reson Imaging 20: 155–163.

Edmister W, Talavage T, Ledden P, Weisskoff R, et al. (1999) Improved auditory cortex imaging using clustered volume acquisitions. Hum Brain Mapp 7: 89–97.

Eickhoff S, Stephan K, Mohlberg H, Grefkes C, Fink G, Amunts K, Zilles, K. (2005) A new spm toolbox for combining probabilistic cytoarchitectonic maps and functional imaging data. Neuroimage 25: 1325–1335.

Fox N (1991) If it’s not left, it’s right: Electroencephalograph asymmetry and the development of emotion. Am Psychol 46: 863.

Frahm J, Merboldt, K, Hänicke W, Haase A (1985) Stimulated echo imaging. J Magn Reson 64: 81–93.

Friston KJ, Stephan K (2007) Modelling brain responses. In: Friston KJ, Ashburner JT, Kiebel SJ, Nichols EN, Penny WD, editors. Statistical parametric mapping: The analysis of functional brain images. 1st ed. London:Elsevier. pp 17-31.

Gaab N, Gabrieli J, Glover G (2007a) Assessing the influence of scanner background noise on auditory processing. i. an fmri study comparing three experimental designs with varying degrees of scanner noise. Hum Brain Mapp 28: 703–720.

Gaab N, Gabrieli J, Glover G (2007b) Assessing the influence of scanner background noise on auditory processing. ii. an fmri study comparing auditory processing in the absence and presence of recorded scanner noise using a sparse design. Hum Brain Mapp 28: 721–732.

Gabrielson A, Juslin P (2003) Emotional expression in music. In Davidson R, Scherer K, Goldsmith H,
editors. Handbook of Affective Sciences. New York: Oxford University Press. pp 503–534.

Goldman A, Gossman W, Friedlander P (1989) Reduction of sound levels with anti-noise in mr imaging. Radiology 173:549–550.

Goldman R, Greenberg L, Angus L (2006) The effects of adding emotion-focused interventions to the client-centered relationship conditions in the treatment of depression. Psychother Res 16: 537–549.

Hall D, Haggard M, Akeroyd M, Palmer A, Summerfield, A., Elliott, M., Gurney, E., Bowtell, R., et al. (1999) Sparse temporal sampling in auditory fmri. Hum Brain Mapp 7: 213–223.

Hennig J, Hodapp M (1993) Burst imaging. MAGMA 1: 39–48.

Hoekert M, Kahn R, Pijnenborg M, Aleman A (2007) Impaired recognition and expression of emotional prosody in schizophrenia: review and meta-analysis. Schizophr Res 96: 135–145.

Idiyatullin D, Corum C, Park J, Garwood M (2006) Fast and quiet mri using a swept radiofrequency. J Magn Reson 181: 342–349.

Jakob P, Schlaug G, Griswold M, Lovblad K, Thomas R, Ives J, Matheson J, Edelman R (2005) Functional burst imaging. Magn Reson Med 40: 614–621.

Jäncke L, Mirzazade S, Joni Shah N (1999) Attention modulates activity in the primary and the secondary auditory cortex: a functional Magnetic Resonance Imaging study in human subjects. Neurosci Lett 266: 125–128.

Johnstone T, OresWalsh K, Greischar L, Alexander A, Fox A, Davidson R, Oakes T (2006) Motion correction and the use of motion covariates in multiple-subject fmri analysis. Hum Brain Mapp 27: 779–788.

Juslin P Vastfjall D (2008) Emotional responses to music: The need to consider underlying mechanisms. Behav Brain Sci 31: 597-598.

Kamio S, Nakagome K, Murakami T, Kasai K, Iwanami A, Hiramatsu K, Hata A, Watanabe A, Fukuda M, Honda M, et al. (2001) Impaired suppression of processing in schizophrenic patients suggested by erps obtained in a selective attention task. Schizophr Res 49: 213–221.

Kang J, Namkoong K, Yoo S, Jhung K, Kim S (2012) Abnormalities of emotional awareness and perception in patients with obsessive–compulsive disorder. J Affect Disord. 141: 286-293.

Katsunuma A, Takamori H, Sakakura Y, Hamamura Y, Ogo Y, Katayama R (2001) Quiet mri with novel acoustic noise reduction. MAGMA 13: 139–144.

Koelsch S, Fritz T, Müller K, Friederici A, et al. (2005) Investigating emotion with music: an fmri study. Hum Brain Mapp 27: 239–250.

Koelsch S, Skouras S, Fritz T, Herrera P, Bonhage C, Kuessner M, Jacobs A (2013) The roles of superficial amygdala and auditory cortex in music-evoked fear and joy. Neuroimage, 81:49-60

Kramer, D (1984) Basic principles of Magnetic Resonance Imaging. Radiol Clin North Am 22(4):765.

Krasnow B, Tamm L, Greicius M, Yang T, Glover G, Reiss A, Menon V, et al. (2003) Comparison of fmri activation at 3 and 1.5 T during perceptual, cognitive, and affective processing. Neuroimage 18: 813–826.

Kraus K, Canlon B (2012) Neuronal connectivity and interactions between the auditory and limbic systems. Effects of noise and tinnitus. Hear Res 288: 34–46.

Lang P, Bradley M, Cuthbert B (1997) International affective picture system (iaps): Technical manual and affective ratings.

Lang P, Bradley M, Fitzsimmons J, Cuthbert B, Scott J, Moulder B, Nangia V (1998) Emotional arousal and activation of the visual cortex: an fmri analysis. Psychophysiology 35: 199–210.

Langers D, Van Dijk P, Backes W (2004) Interactions between hemodynamic responses to scanner acoustic noise and auditory stimuli in functional Magnetic Resonance Imaging. Magn Reson Med 53: 49–60.

Leppänen J (2006) Emotional information processing in mood disorders: a review of behavioral and neuroimaging findings. Curr Opin Psychiatry 19: 34-39.

Lerner Y, Papo D, Zhdanov A, Belozersky L, Hendler T (2009) Eyes wide shut: amygdala mediates eyes-closed effect on emotional experience with music. PLoS One 4:e6230.

Loenneker T, Hennel F, Ludwig U, Hennig J (2001) Silent bold imaging. MAGMA 13: 76–81.

Lohmann G, Müller K, Bosch V, Mentzel H, Hessler S, Chen L, Zysset S, Von Cramon D (2001) Lipsia new software system for the evaluation of functional magnetic resonance images of the human brain. Comput Med Imaging Graph, 25: 449–457.

Lohmann G, Neumann J, Müller K, Lepsien J, Turner R (2008) The multiple comparison problem in fmri - a new method based on anatomical priors. In: Proceedings of the First Workshop on Analysis of Functional Medical Images, p 1–8.

Ludwig U, Loenneker T, Hennel F, Hennig J (1999) Getting rid of acoustic noise: functional MRI with silent simultaneous multislice excitation gradient-echo (SIMEX) sequences. Proceedings of the 7th Annual Meeting of the International Society of Magnetic Resonance in Medicine, Philadelphia, PA. p 1662.

Mannie Z, Bristow G, Harmer C, Cowen P (2007) Impaired emotional categorisation in young people at increased familial risk of depression. Neuropsychologia 45: 2975–2980.

Mansfield P, Glover P, Beaumont J (1998) Sound generation in gradient coil structures for mri. Magn Reson Med 39: 539–550.

Mansfield P, Glover P, Bowtell R (1994) Active acoustic screening: design principles for quiet gradient coils in mri. Meas Sci Technol 5:1021.

Mathiak K, Rapp A, Kircher T, Grodd W, Hertrich I, Weiskopf N, Lutzenberger W, Ackermann H (2002) Mismatch responses to randomized gradient switching noise as reflected by fmri and whole-head magnetoencephalography. Hum Brain Mapp 16: 190–195.

Mazard A, Mazoyer B, Etard O, Tzourio-Mazoyer N, Kosslyn S, Mellet, E. (2002) Impact of fmri acoustic noise on the functional anatomy of visual mental imagery. J Cogn Neurosci 14: 172–186.

McJury M, Frank G (2000) Auditory noise associated with mr procedures: a review. J Magn Reson Imaging 12: 37–45.

McJury M, Stewart R, Crawford D, Toma E (1997) The use of active noise control (anc) to reduce acoustic noise generated during mri scanning: some initial results. Magn Reson Imaging 15: 319–322.

Moelker A, Pattynama P (2003) Acoustic noise concerns in functional Magn Reson Imaging. Hum Brain Mapp 20: 123–141.

Moelker A, Vogel M, Pattynama P (2003) Efficacy of passive acoustic screening: Implications for the design of imager and mr-suite. J Magn Reson Imaging 17: 270–275.

Mueller K, Mildner T, Fritz T, Lepsien J, Schwarzbauer C, Schroeter M, Möller H (2011) Investigating brain response to music: A comparison of different fmri acquisition schemes. Neuroimage 54: 337–343.

Mueller W, Yetkin F, Hammeke T, Morris III G, Swanson S, Reichert K, Cox R, Haughton V (1996) Functional Magnetic Resonance Imaging mapping of the motor cortex in patients with cerebral tumors. Neurosurgery 39: 515.

Novitski N, Anourova I, Martinkauppi S, Aronen H, Näätänen R, Carlson S (2003) Effects of noise from functional Magnetic Resonance Imaging on auditory event-related potentials in working memory task. Neuroimage 20: 1320–1328.

Oesterle C, Hennel F, Hennig J (2001) Quiet imaging with interleaved spiral read-out. Magn Reson Imaging 19: 1333–1337.

O’Mara S (2005) The subiculum: what it does, what it might do, and what neuroanatomy has yet to tell us. J Anat 207: 271–282.

Panksepp J (2005) The varieties of emotional systems in the brain: Theories, taxonomies, and semantics. In: Panksepp J, author. Affective neuroscience: The foundations of human and animal emotions. 1st ed. New York:Oxford University Press. pp 41-58.

Phan K, Wager T, Taylor S, Liberzon I, et al. (2002) Functional neuroanatomy of emotion: a meta-analysis of emotion activation studies in pet and fmri. Neuroimage 16: 331-348.

Plevier C, Mooy J, de Mheen P, Stouthard M, Visser M, Grobbee, D, Gunning-Schepers L (2001) Persistent impaired emotional functioning in survivors of a myocardial infarction? Qual Life Res 10: 123–132.

Plichta M, Gerdes A, Alpers G, Harnisch W, Brill S, Wieser M, Fallgatter A (2011) Auditory cortex activation is modulated by emotion: A functional near-infrared spectroscopy (fnirs) study. Neuroimage 55: 1200–1207.

Price D, De Wilde J, Papadaki A, Curran J, Kitney R (2001) Investigation of acoustic noise on 15 mri scanners from 0.2 t to 3 t. J Magn Reson Imaging 13: 288–293.

Schwarzbauer C, Davis M, Rodd J, Johnsrude I (2006) Interleaved silent steady state (ISSS) imaging: a new sparse imaging method applied to auditory fmri. Neuroimage 29: 774–782.

Shah N, Jäncke L, Grosse-Ruyken M, Mueller-Gaertner H, et al. (1999) Influence of acoustic masking noise in fmri of the auditory cortex during phonetic discrimination. J Magn Reson Imaging 9: 19–25.

Smiley J F, Hackett T A, Ulbert I, Karmas G, Lakatos P, Javitt DC, Schroeder C E (2007) Multisensory convergence in auditory cortex, i. cortical connections of the caudal superior temporal plane in macaque monkeys. J Comp Neurol 502: 894–923.

Stansfeld SA (1992) Noise, noise sensitivity and psychiatric disorder: epidemiological and psychophysiological studies. Psychol Med 22:1–44.

Steptoe A, Wardle J, Marmot M (2005) Positive affect and healthrelated neuroendocrine, cardiovascular, and inflammatory processes. Proc Natl Acad Sci U S A 102: 6508–6512.

Sunaert S, Yousry T (2001) Clinical applications of functional Magnetic Resonance Imaging. Neuroimaging Clin N Am 11:221.

Talavage T, Edmister W (2004) Nonlinearity of fmri responses in human auditory cortex. HUM BRAIN MAPP 22: 216–228.

Tarnopolsky A, Barker S, Wiggins R, McLean E (1978) The effect of aircraft noise on the mental health of a community sample: a pilot study. Psychol Med 8: 219–233.

Tomasi D, Caparelli E, Chang L, Ernst T (2005) fmri-acoustic noise alters brain activation during working memory tasks. Neuroimage, 27: 377–386.

Tosevski D, Milovancevic M (2006) Stressful life events and physical health. Curr Opin Psychiatry 19: 184–189.

Voets N, Matthews P (2005) Clinical applications of functional Magnetic Resonance Imaging. Imaging Decis MRI 9: 16–22.

Vuilleumier P, Armony J, Driver J, Dolan R, et al. (2001) Effects of attention and emotion on face processing in the human brain: an event related fmri study. Neuron 30: 829–841.

Warner-Schmidt J, Duman R (2006) Hippocampal neurogenesis: opposing effects of stress and antidepressant treatment. Hippocampus 16: 239–249.

Warren J, Sauter D, Eisner F, Wiland J, Dresner M, Wise R, Rosen S, Scott S (2006) Positive emotions preferentially engage an auditory–motor mirror system. J Neurosci 26: 13067–13075.

Weiskopf N, Hutton C, Josephs O, Turner R, Deichmann R (2007) Optimized epi for fmri studies of the orbitofrontal cortex: compensation of susceptibility-induced gradients in the readout direction. MAGMA 20: 39–49.

Weniger G, Lange C, Sachsse U, Irle E (2009) Reduced amygdala and hippocampus size in trauma-exposed women with borderline personality disorder and without posttraumatic stress disorder. J Psychiatry Neurosci 34:383.

Zhang N, Zhu X, Chen W (2005) Influence of gradient acoustic noise on fmri response in the human visual cortex. Magn Reson Med, 54: 258–263.

5.7 Supplementary Material

Supplemental Table 1: Behavioral Ratings. Descriptive statistics of behavioral data (mean, with standard deviation in parentheses). For statistical tests see main text.

	Fear	**Neutral**	**Joy**
Valence	2.43 (0.20)	2.69 (0.48)	4.84 (0.21)
Arousal	3.97 (0.21)	3.03 (0.22)	4.05 (0.21)
Joyfulness	1.62 (0.16)	2.40 (0.29)	4.83 (0.42)
Fearfulness	4.02 (0.23)	2.22 (0.30)	1.31 (0.17)
Familiarity	1.44 (0.11)	1.17 (0.10)	2.01 (0.42)

Supplemental Table 2: Detailed Statistics. Descriptive statistics of behavioral ratings for each scanning group and emotion category (mean, with standard deviation in parentheses). For statistical tests see main text.

	Joy		**Neutral**		**Fear**	
	Sparse **mean (SD)**	**Continuous** **mean (SD)**	**Sparse** **mean (SD)**	**Continuous** **mean (SD)**	**Sparse** **mean (SD)**	**Continuous** **mean (SD)**
Valence	5.14 (0.23)	5.06 (0.19)	3.19 (0.24)	3.09 (0.18)	2.83 (0.18)	2.69 (0.20)
Arousal	4.04 (0.25)	4.41 (0.26)	2.91 (0.23)	2.76 (0.18)	3.46 (0.15)	3.81 (0.34)
Joyfulness	5.05 (0.31)	5.02 (0.36)	2.83 (0.23)	2.80 (0.21)	1.98 (0.16)	2.11 (0.19)
Fearfulness	1.17 (0.12)	1.29 (0.22)	1.88 (0.20)	1.79 (0.20)	4.00 (0.20)	4.20 (0.31)

Supplemental Table 3: List of Stimuli.

Composer / artist	Title	ASIN Nr.
Joy-evoking		
Joël Francisco Perri	El Canto de Mi Antara	B002BEXEHO
Craobh Rua	The Luck Penny	B000003NHN
Scotch Mist	Shetland Tune	n/a
Alfredo de Angelis	Pregonera	B001P5LDTQ
Orchestra Paraschiv Oprea	Batuta de la Adancata	B00000DTI6
Louis Armstrong	St. Louis Blues	B006CBVRJY
Niccolò Paganini	Violin Concerto No. 1, 3rd movement	B000001GHC
Jonathan Richman	Egyptian Reggae	B00580D1IU
Fear-evoking		
Danny Elfman	The Killing	B00000JC9R
Michael Giacchino	Monsters Are Such Interesting People (from: Lost)	B000EHSVDM
Michael Giacchino	Just Another Day on the Beach (from: Lost)	B000I2IQ9M
Michael Giacchino	Charlie's Dream (from: Lost)	B000I2IQ9M
Takeshi Miura et al.	Pulsating Right Arm (from: Biohazard Code)	B00005HWMB
Seiko Kobuchi	Boss Battle (from: Biohazard Zero)	n/a
Masami Ueda & Saori Maeda	Cold Sweat (from: Biohazard 3)	B000058A7Y
Akihiko Matsumoto et al.	Freezer Burn (from: Resident Evil Outbreak)	B00019257G

Neural correlates of emotional personality: A structural and functional magnetic resonance imaging study

Stefan Koelsch, Stavros Skouras, Sebastian Jentschke

Published in PloS one, 8(11), e77196

http://dx.doi.org/10.1371/journal.pone.0077196

6.0 Abstract

Studies addressing brain correlates of emotional personality have remained sparse, despite the involvement of emotional personality in health and well-being. This study investigates structural and functional brain correlates of psychological and physiological measures related to emotional personality. Psychological measures included neuroticism, extraversion, and agreeableness scores, as assessed using a standard personality questionnaire. As a physiological measure we

used a cardiac amplitude signature, the so-called Eκ value (computed from the electrocardiogram) which has previously been related to tender emotionality.

Questionnaire scores and Eκ values were related to both functional (*eigenvector centrality mapping*, ECM) and structural (*voxel-based morphometry*, VBM) neuroimaging data. Functional magnetic resonance imaging (fMRI) data were obtained from 22 individuals (12 females) while listening to music (joy, fear, or neutral music). ECM results showed that agreeableness scores correlated with centrality values in the dorsolateral prefrontal cortex, the anterior cingulate cortex, and the ventral striatum (nucleus accumbens). Individuals with higher Eκ values showed higher centrality values in the subiculum of the right hippocampal formation. Structural MRI data from an independent sample of 67 individuals (34 females) showed that neuroticism scores correlated with volume of the left amygdaloid complex. In addition, individuals with higher Eκ showed larger gray matter volume in the same portion of the subiculum as was observed to differ between groups in the functional data. Our results highlight a role of the amygdala for neuroticism. Moreover, they indicate that a cardiac signature related to emotionality correlates with both function (increased network centrality) and structure (grey matter volume) of the subiculum of the hippocampal formation, suggesting a role of the hippocampal formation for emotional personality. Results are the first to show personality-related differences using eigenvector centrality mapping, and the first to show structural brain differences for a physiological measure associated with personality.

6.1 Introduction

Personality is a construct with substantial emotional components. For example, neuroticism relates to tendencies for the experience of negative emotions such as depression and anxiety, extraversion relates to behaviour of social approach and avoidance, and agreeableness relates to tender-mindedness on the one side, and to emotional coldness on the other. Correspondingly, differences in personality (such as differences in neuroticism, extraversion and agreeableness) have been reported to be related to functional differences in brain structures implicated in emotion, e.g. orbitofrontal cortex (OFC), amygdala, cingulate cortex, insula, and hippocampal formation: Functional neuroimaging studies have suggested associations between neuroticism and neural activity in anterior cingulate cortex (ACC; Eisenberger et al. 2005; Tauscher et al. 2001; Frokjaer et al. 2008; Brück et al. 2011), insula (Paulus et al. 2003; Deckersbach, 2006), anterior fronto-median cortex (Brück et al. 2011; Britton et al. 2007), and amygdala (during fear learning; Hooker et al. 2008). Extraversion has been reported to be related to neural activity in the striatum (Fischer et al. 1997; Canli et al. 2001; Cohen et al. 2005), ACC (Kumari et al. 2004; Canli et al. 2004; Haas et al. 2006), OFC (Paulus et al. 2003; Deckersbach et al. 2006), and amygdala (in response to positive stimuli; Canli et al. 2001; Canli et al. 2002; Vaidya et al. 2007). Consistent findings for other personality dimensions (agreeableness, openness, and conscientiousness) are rather sparse, except that agreeableness is perhaps linked to activity in the right lateral prefrontal cortex (PFC; taken to be related to emotion regulation; Haas et al. 2007), and that openness has been linked to executive functions of the prefrontal cortex (DeYoung et al. 2005) as well as to serotonergic activity within the striatum (Kalbitzer et al. 2009). For an overview see Table 1A.

Correspondingly, anatomical differences in these brain structures were reported to be associated with personality (see also Table 1B): Extraversion has been associated with volume (DeYoung et al. 2010; Cremers et al. 2011) and cortical thickness of the OFC (Rauch et al. 2005); other studies have associated extraversion with volume of the right amygdala (Cremers et al. 2011) or gray matter concentration of the left amygdala (Omura et al. 2005), and with cortical thickness of the right dorsolateral prefrontal cortex (DLPFC; Wright et al. 2007). Moreover, extraversion and reward-dependence (which is conceptually related to extraversion) have been reported to be negatively correlated with volume of the caudate nucleus (Forsman et al. 2012; Gardini et al. 2009). Neuroticism and harm avoidance (which is conceptually related to neuroticism) have also been associated with volume (Gardini et al. 2009) and cortical thickness (Wright et al. 2006) of the OFC. In addition, neuroticism has been associated with volume of the left amygdala in females (Iidaka et al. 2006) and the right amygdala (Omura et al. 2005). Similarly, a study by Barros-Loscertales et al. (2006) reported increased right amygdalar volume (as well as increased left entorhinal volume) in individuals with increased sensitivity to punishment (as measured with the Behavioural Inhibition System). Furthermore, a study by DeYoung et al. (2010) found an association between neuroticism and mid-cingulate volume, a study by Yamasue et al. (2008) reported that grey matter volume in the (right) hippocampal formation was negatively related to harm avoidance, and Schutter et al. (2012) observed that neuroticism correlated negatively with cerebellar volume. Only few studies have reported relations between brain structure and agreeableness, openness and conscientiousness. Agreeableness was observed to be related to DLPFC volume (taken to be related to the processing of intentions and mental states of others; DeYoung et al. 2010) and cerebellar volume (Hu et al. 2011). Openness has been linked to orbitofrontal and (dorsal) ACC volume (Hu et al. 2011), and conscientiousness has also been linked to DLPFC volume (taken to be related to processes of executive control; DeYoung et al. 2010).

The mentioned studies reporting relations between personality and both activity and morphology of limbic/paralimbic brain structures appear to support the notion of a tight association between personality and emotionality. Note, however, that the replicability of the findings of the mentioned studies is relatively low (for an illustration see Table 1). One reason for such relatively low replicability might be that the mentioned studies assessed personality using subjective measures (questionnaires). Such psychological measures have the advantage of a direct semantic relation between the questionnaire items and the construct of a personality factor. The subjectivity of these measures, however, also bears the problem of potential biases such as socially desirable responding, inaccuracies in self-perception, self-favouring tendencies, self-deception, and moralistic bias (Costa, McCrae 1992; Paulhus, 1986; Barrick, Mount, 1906; Paulhus, John, 1998; Pauls, Stemmler, 2003). Moreover, it cannot be guaranteed that the inner states described by emotion-words in questionnaires (such as “very happy”) refer to the same subjective experience in different individuals, or even in the same individual at

Table 6.1: Overview of personality-related functional (A) and structural (B) brain differences reported in studies using subjective measures of personality. The studies listed in the outermost left column used five factor personality inventories (neuroticism, extraversion, openness, agreeableness, conscientiousness), except those highlighted in light grey (which assessed similar constructs). The second left column indicates the sample size. Only brain structures reported by at least two studies are listed. Note the relatively low replicability of findings. Abbreviations: OFC: orbitofrontal cortex, amyg: amygdala; CC: cingulate cortex; hipp: hippocampal formation; aFMC: anterior fronto-median cortex; PFC: prefrontal cortex; cer: cerebellum.

Study	n	OFC	amyg	CC	hipp	insula	striatum	aFMC	PFC	cer
A: functional studies										
Eisenberger et al. 2005[1]	17			N					E, N	
Tauscher et al. 2001	19			N						
Frokjaer 2008	83			N						
Brück et al. 2011	24		N	N				N		
Paulus et al. 2003	17					N				
Deckersbach et al. 2006	20	E				N				
Britton et al. 2007	12							N		
Hooker et al. 2008[2]	12		E, N		N					
Fischer et al. 1997[2]	30						E			
Canli et al. 2001	14		E	E			E		N	
Cohen et al. 2005	17	E					E			
Kumari et al. 2004[3]	11			E					E	
Canli et al. 2004	12			E						
Haas et al. 2006	26			E						
Canli et al. 2002[2]	15		E							
Vaidya et al. 2007	12		E							
Haas et al. 2007	48								A	
Kalbitzer et al. 2009	50						O			
B: structural studies										
DeYoung et al 2010	116	E		N,A	N		N	N	N,A,C	
Cremers et al. 2011	65	E	E							
Rauch et al. 2005[4]	14	E								
Omura et al. 2005	41		E, N							
Wright et al. 2007	29								E	
Forsman et al. 2012[5]	34						E		E	
Gardini et al. 2009[6]	85	N, E					E			
Wright et al. 2006	28	N						N	E	
Iidaka et al. 2006[6]	56		N				E			
Barros-Loscertales et al 2006[7]	63		N		N					
Yamasue et al. 2008[6]	183				N				N	
Schutter et al. 2012[8]	38									N
Hu et al. 2011	62	O, A		O						A

[1] Only neuroticism, extraversion, and self-consciousness were assessed

[2] Only neuroticism and extraversion were assessed

[3] Only neuroticism, extraversion, and psychoticism were assessed

[4] Only neuroticism and extraversion were evaluated

[5] A five-factor model of Cattel's 16 Personality Factor questionnaire was used

[6] Cloniger's Three-dimensional Personality Questionnaire was used, including harm avoidance (which is conceptually related to neuroticism) and reward-dependence (which is conceptually related to extraversion)

[7] Only the Sensitivity to Punishment scale (which is conceptually related to neuroticism) of the Behavioral Inhibition System was used

[8] Only neuroticism-subscales (anxiety, depression) were assessed

different points in time (see also Wittgenstein’s arguments against the idea of a “private language”; Wittgenstein 1984).

6.1.1 Physiological measures of personality

In addition to subjective measures of personality (obtained with a standard personality questionnaire), the present study also obtained a physiological measure taken to reflect emotional personality. A substantial amount of research associating personality with biological parameters such as levels of neurotransmitters, hormones, and autonomic activity (Canli, 2006; Cloninger, 2000; Davidson, 2001; Eysenck, 1967; Irwin, 2008; Wolkowitz, Rothschild, 2003; Zuckerman, 1991) opens the interesting possibility of using identified biomarkers as indices of personality. Such physiological markers have the advantage that they are not dependent on subjective ratings. However, a disadvantage is that physiological measures can be biased by factors unrelated to personality (such as general health status, inflammation, current mood, or circadian rhythm). Moreover, they have the disadvantage that there is no direct semantic link between a physiological measure and a personality construct. Hence, it is arguable to which degree a physiological personality measure is actually indicative of a specific personality trait.

As a physiological index of emotional personality, we used a cardiac amplitude signature (psychological factors modulating regional cardiac activity are summarized in Box 1). This cardiac amplitude signature is characterized by the relation of four amplitude values of the electrocardiogram (ECG, see also Figure 1).

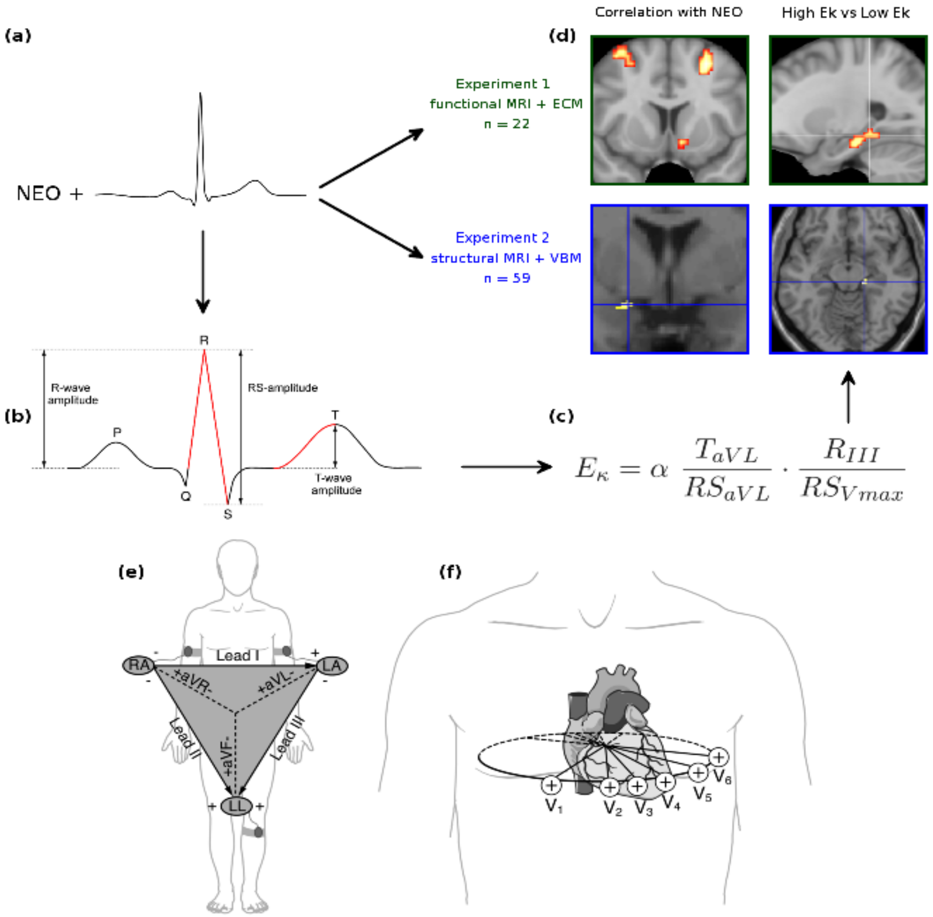

Figure 6.1. Illustration of procedure and data analysis. (a) From each of *n*=81 participants (22 in experiment 1, and 59 in experiment 2), NEO scores as well as a 12-lead rest electrocardiogram (ECG) were obtained. **(b)** From each ECG, absolute values of mean R-, RS-, and T-wave amplitudes were measured electronically (separately for the leads aVL, RIII, and all chest leads), and then computed according to the equation shown in **(c)**, resulting in a single value for each participant: values were computed using the absolute amplitude values of the T-wave of aVL (T_{aVL}), the RS-wave of aVL (RS_{aVL}), the R-wave of III (R_{III}) and the maximal RS-wave measured at any of the chest leads (RS_{Vmax}); for better readability, values were scaled with a factor of $\alpha = 10$. **(d)** Functional magnetic resonance (MR) images were obtained from the participants of experiment 1, and structural MR images were acquired from the participants of experiment 2. In experiment 1, Eigenvector Centrality Maps (ECMs) were computed for each participant. ECMs were then correlated with NEO scores of participants (upper left panel of **d**), and compared between groups of individuals with higher and lower values (upper right panel of **d**). Likewise, structural data obtained in Experiment 2 were correlated with NEO scores (lower left panel of **d**), and compared between groups of individuals with higher and lower values (lower right panel of **d**). he bottom panel illustrates standard ECG leads: The six extremity leads (I, II, III, aVL, aVR, aVF) record voltage differences by means of electrodes placed on the limbs (**e**). The triangle shows the spatial relationships of the extremity leads, which record electrical voltages onto the frontal plane of the body. The six chest leads (V1 - V6) record voltage differences by means of electrodes placed on the chest wall (**f**). The oval indicates spatial relationships of the six chest leads, which record electrical voltages transmitted onto the horizontal plane.

The computation of these amplitude values according to the equation shown in Figure 1c results in a value for each individual, referred to as Eκ value. This Eκ measure has previously (Koelsch et al. 2007) been obtained using discriminant function analysis on ECG amplitude data to differentiate groups of individuals with higher and lower scores of “*tender emotionality*” (as indicated by interviews and self-reports). The construct of tender emotionality refers to the tendency to experience positive emotions (including feelings of joy and happiness), attachment-related emotions (such as love), compassion and empathy. Persistent lack of tender positive emotion (also referred to as emotional coldness, or flattened affect) is a clinically relevant symptom in schizoid personality disorder and schizophrenia. In that study (Koelsch et al. 2007) data from two functional neuroimaging experiments showed stronger BOLD responses to emotional stimuli in amygdala and hippocampal formation in individuals with high Eκ (compared to low Ek).

The notion that Eκ reflects aspects of the emotional personality of an individual was supported by a subsequent study (Koelsch et al. 2012) in which individuals with higher Eκ (assumed to reflect higher tender emotionality) had lower neuroticism scores, higher scores of positive emotion, and tended to have higher extraversion scores (personality scores were measured using the NEO-FFI and NEO-PI-R inventories (Costa, McCrae, 1992). Note that, because there is no direct semantic link between tender emotionality and Eκ, it would be problematic to simply equate the two (as outlined above). Nevertheless, in the present study we tested whether Eκ as a physiological index of emotional personality would show relations to brain function and brain structure.

Box 1: Modulatory influence of psychological factors on regional cardiac activity

The rationale for utilizing ECG amplitude ratios as an index of personality is manifold: ECGs provide multidimensional information about regional cardiac function such as conduction of excitation, conduction velocity, contractile force, coronary circulation, as well as aspects of cardiac valve function (Armour, Kember, 2004). Regional cardiac function is modulated by neurons in intrathoracic extracardiac and intrinsic cardiac ganglia (Horackova 2004). These ganglia represent the final common pathway through which the diverse, extrinsic neural signals to the heart are modified before being transmitted to the effector tissues (Adams, Cuevas, 2004). The neurons of these ganglia form the cardiac nerve plexus, a system of nerve cells within and around the heart which integrates and modifies sensory input and cardiac output (Adams, Cuevas, 2004). Importantly, intrathoracic ganglia are not merely relay stations for autonomic efferent neuronal control of the heart, but integrate various sensory inputs, as well as inputs from central sympathetic/parasympathetic nerve fibres (Adams, Cuevas 2004). We have previously described (Koelsch et al. 2012) that activity of neurons within the cardiac nerve plexus (and thus regional heart activity) is directly and indirectly modulated by several psychological factors: (1) *Emotion and affective traits are accompanied by autonomic activity*, which is transmitted into the cardiac nerve plexus by both parasympathetic and sympathetic nerve fibres (Chechetto, 2004). (2) *Limbic/paralimbic forebrain structures such as amygdala, insular cortex, and (medial) orbitofrontal cortex modulate the efferent autonomic outflow to the heart* (Chechetto, 2004; Critchley, 2005; Critchley et al. 2011; Gray et al. 2007; Gray et al. 2009). As reviewed in the main text, these structures show both functional and structural associations with the personality of an individual. (3) *The left and right hemispheres of the human forebrain have different associations with particular emotions and affective traits* (Craig 2005), probably due to an asymmetrical representation of homeostatic activity that originates from asymmetries in the peripheral autonomic nervous system (Chechetto, 2004; Sander, Klingelhöfer, 1995; Zamrini, 1990; Critchley, 2005). Correspondingly, different emotional states and affective traits exert asymmetric autonomic outflow that modulates regional heart activity: While the right cardiac nerve innervates the anterior surface of the heart (including the sinoatrial node, the atrioventricular node, and the anterior surfaces of the right and left ventricles), the left cardiac nerve innervates the posterolateral surface of the heart, including the atrioventricular node and the posterior surfaces of the right and left ventricles (Lane, Schwartz 1987; Cardinal, Pagé 2004). (4) *Activity of neurons within intrathoracic autonomic ganglia is modulated by circulating hormones* (in particular circulating adrenalin and angiotensin II), as well as by other sensory information (such as vascular information, information about blood pressure, electrolytic balance, and blood gases) (Ardell, 2004). Due to the effects of particular emotions and affective traits on circulating hormones (including adrenalin), blood pressure and blood gases (due to breathing frequency and breathing depth), emotions and affective traits indirectly also modulate regional heart activity. Note that, in clinical populations, the diverse effects of affective traits on the heart have been demonstrated by a plethora of clinical and experimental evidence implicating anger, hostility, depression and anxiety in the occurrence of arteriosclerosis, coronary artery disease, hypertension, myocardial ischemia and infarction, cardiac arrhythmia formation, and sudden cardiac death (Gagnon et al. 2004).

6.1.2 The present study

In the present study, we used both psychological and physiological measures related to emotional personality as independent variables to investigate neural correlates of emotional personality in both functional and structural magnetic resonance imaging (MRI) data (Figure 1). Psychological measures included the *neuroticism*, *extraversion* and *agreeableness* scales of the Neuroticism-Extraversion-Openness Five Factor Inventory (NEO-FFI) (Costa, McCrae, 1992), the extraversion-facets *positive emotion* and *warmth*, as well as the agreeableness-facet *tender-mindedness* (as obtained with the revised version of the NEO Personality Inventory; NEO-PI-R) (Costa, McCrae, 1992). As physiological measure we used the Eκ index. In experiment 1, subjects participated in a functional neuroimaging session, and functional data were then correlated with both psychological and physiological personality measures. In experiment 2, structural brain scans were obtained from an independent sample of subjects, and data were then correlated with both psychological and physiological personality measures. This enabled us (a) to compare consistency between functional and structural findings, (b) to determine the replicability of previous results with regard to psychological and physiological measures, (c) to relate the physiological data to the psychological data, and (d) to compare neurological results obtained with psychological or physiological data as independent variables.

Functional MRI data of experiment 1 were analysed using *Eigenvector Centrality Mapping* (ECM; Lohmann et al. 2010), a new method for determining centrality values across voxels in functional neuroimaging data. ECM attributes a centrality value to each voxel in the brain such that a voxel receives a large value if it is strongly correlated with many other nodes that are themselves central within the network (Google's Page-Rank algorithm is a variant of eigenvector centrality). ECM thus exploits small-world properties of the human brain (Sporns, Honey, 2006), and indicates "computational hubs" of neural networks distributed across different macroscopic brain structures (Tomasi, Volkow, 2011). For example, a previous study with a within-subjects design compared data of resting state scans of subjects when they were in states of hunger or satiety (Lohmann et al. 2010; that study reported that centrality values were higher during the hungry state in the posterior cingulate cortex and the precuneus). ECM is thus reminiscent of resting-state fMRI (Chen et al. 2008), except that ECM can be computed on any functional neuroimaging data (i.e., not necessarily resting state data). In experiment 2, brain-structural differences were analysed using *Voxel-Based Morphometry* (VBM).

Regarding our hypotheses, we expected that individuals with higher Eκ values would have lower neuroticism scores, higher extraversion scores, and higher scores of positive emotion than individuals with lower Eκ values (as in our previous study (Koelsch et al. 2012). Because warmth and tender-mindedness are conceptually related to the construct of tender emotion, we hypothesized that scores of these facets, as well as of agreeableness, would be higher in individuals with higher Eκ values than in individuals with lower Eκ values. With regard to correlations between NEO scores and functional neuroimaging data (experiment 1), we hypothesized (based on the most consistent findings, as reviewed above) that extraversion scores would correlate with neural activity in the striatum (Fischer et al. 1997; Canli et al.

2001; Cohen et al. 2005) and the ACC (Kumari et al. 2004; Canli et al. 2004; Haas et al. 2006). Moreover, we tested whether neuroticism would also correlate with activity in the ACC (Eisenberger et al. 2005; Tauscher et al. 2001; Frokjaer et al. 2008; Brück et al. 2011). Based on our previous study (Koelsch et al. 2007), in which individuals with low Eκ showed reduced neural activity in amygdala and hippocampal formation (in response to emotion-evoking music stimuli), we aimed to test in the present study whether individuals with lower Eκ would show lower centrality values in hippocampal formation and amygdala.

6.2 Experiment 1

Functional MRI using Eigenvector Centrality Mapping

6.2.1 Materials and Methods

6.2.1.1 Participants

Data were obtained from 22 individuals (aged 19 – 31 years, *M*=23.50, *SD*=3.36, 12 females). Exclusion criteria were left-handedness, consumption of alcohol or caffeine exceeding one litre during the 24 hours prior to testing, poor sleep during the previous night, past diagnosis of a neurological, audiological or psychiatric disorder (according to self-report), and abnormal brain anatomy (as diagnosed by a radiologist). All subjects gave written informed consent. The study was conducted according to the Declaration of Helsinki and approved by the ethics committee of the School of Life Sciences and the Psychology Department of the University of Sussex.

6.2.1.2 Experimental procedure

Psychological (NEO) measures.

From each participant, we obtained scores of the personality scales *Neuroticism*, *Extraversion*, and *Agreeableness* (each with 12 Items) from the German translation of the NEO Five Factor Inventory (NEO-FFI; Borkenau, Ostendorf 1993; Costa, McCrae 1992). Moreover, scores of the personality facets *warmth*, *positive emotion* and *tender-mindedness* (each with 8 Items) from the German translation of the revised version of the NEO Personality Inventory (NEO-PI-R; Ostendorf, Angleitner 2004; Costa, McCrae, 1992) were obtained. *Warmth* and *positive emotion* are facets of the extraversion scale, and *tender-mindedness* is a facet of the agreeableness scale. These facets were used because they are more closely related to the construct of tender positive emotionality than other NEO-PI-R facets: *positive emotion* is related to a tendency to experience positive emotions, *tender-mindedness* is related to an attitude of sympathy for others, and *warmth* is related to interest in and friendliness towards others (Costa, McCrae, 1992). The number of items amounted to 54 Items (note that because the NEO-FFI is a short version of the NEO-PI-R, twelve items of the used NEO-FFI scales are identical to those of the used NEO-PI-R facets).

Physiological (cardiac) measures.

A 12-leads resting ECG (2-3 min duration) was acquired from each participant in supine position under standard conditions (Malik et al. 1996). ECGs were recorded (with disposable electrodes) with high resolution (sampling rate: 1000 Hz, resolution: 22 bit, without on-line filtering) using a cardio 100 system (Custo Med GmbH, Ottobrunn, Germany). ECGs and NEO data were obtained directly before the functional neuroimaging experiment.

Functional neuroimaging experiment.

For the functional neuroimaging session we employed an experiment on music and emotion using joy, fear and neutral musical stimuli (joy and fear stimuli are listed in Supplementary Table 1). We chose an emotion experiment for data acquisition to specify in which brain structures personality-related functional differences were dependent on the emotional state of subjects. Joy and fear were chosen because they represent basic emotion categories motivating approach and avoidance behaviours.

Each experimental stimulus had a duration of 30 s, and there were 8 stimuli of each emotion category (joy, fear, neutral; for details see Supplementary Methods). Prior to the fMRI session, participants were presented with short (12 s) versions of each stimulus to obtain familiarity ratings: Participants rated their familiarity with each piece on a four-point scale (ranging from "To my knowledge I have never heard this piece before", to "I know this piece, and/or I know who composed, or performed it"). Participants were then trained on the emotion-rating procedure used in the functional neuroimaging experiment (using 12 s long excerpts of musical pieces that did not belong to the stimulus set used in the fMRI scanning session): At the end of each excerpt, participants indicated how they felt with regard to valence (pleasant/unpleasant), arousal (calm/excited), joy and fear. That is, participants provided ratings about how they felt, and not about which emotion they thought each song was supposed to express (for the importance of this see Gabrielson, Juslin, 2003). Ratings were obtained with 6-point Likert scales (ranging from "not at all" to "very much"), and the time interval for each rating was 3 s (amounting to a duration of the entire rating procedure of 12 s).

In the actual fMRI experiment, stimuli were pseudorandomly intermixed so that no more than two stimuli of each stimulus category (joyful, fearful, neutral) followed each other. Moreover, the entire stimulus set was presented twice (i.e. 16 stimuli per category were presented). Participants were asked to listen to the musical stimuli with their eyes closed. Each musical stimulus was followed by an interval of 2 s in which a beep tone signalled participants to open their eyes and to commence the emotion-rating procedure (as described above). Each rating period was followed by a 4 s rest period, amounting to a total length of 48 s per trial, and a total duration of the functional neuroimaging experiment of about 39 min.

Musical stimuli were presented using Presentation (version 13.0, Neurobehavioral systems, Albany, CA, USA) via MRI compatible headphones (under which participants wore earplugs). Instructions and rating screens were delivered through MRI compatible liquid crystal display goggles with an integrated eyetracker (Resonance Technology Inc., Northridge, CA, USA). The eyetracker was used by the experimenters to control that participants followed the instructions regarding opening and closing their eyes.

6.2.1.3 MR Scanning

Scanning was performed with a 3T Siemens Magnetom Trio scanner (Siemens Medical Systems, Erlangen, Germany). Continuous Echo Planar Imaging (EPI) was used with a TE of 30 ms and a TR of 2,000 ms. Slice-acquisition was interleaved within the TR interval. The matrix acquired was 64x64 voxels with a Field Of View (FOV) of 192 mm, resulting in an in-plane resolution of 3 mm. Slice thickness was 3 mm with an interslice gap of 0.6 mm (37 slices, whole brain coverage). The acquisition window was tilted at an angle of 30 degrees relative to the AC-PC line in order to minimize susceptibility artifacts in the orbitofrontal cortex (Deichmann et al. 2002; Deichmann et al. 2003; Weiskopf et al. 2007).

6.2.1.4 ECG data analysis

ECG-wave detection and measurement of ECG amplitude values was performed electronically using the in-house software package Kardionoon (Koelsch et al. 2007; publicly available at http://sourceforge.net/projects/kardionoon) and visually inspected by the first author. The amplitude measurements are described in detail elsewhere (Koelsch et al. 2007); in short, for each lead of each participant, all P-, R-, S-, and T-wave peaks were identified in the raw ECG, and artifact-free waves were then averaged separately for each lead to obtain ECG waves representative for each participant (i.e. for a 2-min artifact-free ECG of a subject with a heart rate of 60 beats per minute, 120 P-, 120 R-, 120 R-S-, and 120 T-waves were averaged, separately for each wave, and for each of the twelve ECG leads). From these averaged ECG waves, absolute amplitude values of P-, R-, R-S-, and T-waves were measured electronically; R-wave amplitudes were measured with respect to the baseline of the averaged ECG cycle (see also Figure 1b for illustration), T-wave amplitudes were measured with respect to the first plateau-like wave shape preceding the T-wave peak (Koelsch et al. 2007). Moreover, to reduce potential bias introduced by slightly different placement of chest electrodes, the maximal value of each of the four ECG waves (P-, R-, R-S-, and T-wave) measured at any of the chest leads were also computed. Then, the Eκ value was computed for each subject according to the equation shown in Figure 1c. All ECG analyses were carried out blinded, that is, without knowledge about the NEO scores nor (f)MR images of any participant.

6.2.1.5 Functional MRI data analysis

Functional MRI data were processed using LIPSIA 2.1 (Lohmann et al. 2001). Data were corrected for slicetime acquisition and normalized into MNI-space-registered images with isotropic voxels of 3 cubic millimetres. A temporal highpass filter with a cutoff frequency of 1/90 Hz was applied to remove low frequency drifts in the fMRI time series, and a spatial smoothing was performed using a 3D Gaussian kernel and a filter size of 6 mm FWHM.

Eigenvector Centrality Maps (ECMs) were first computed on each participant’s entire fMRI dataset, treating the entire functional session as one time period of interest (that is, the entire experiment was calculated as one single trial for the ECM analysis, and only one ECM image was calculated for each participant). Neuroticism, extraversion, and agreeableness scores were then used as regressors of interest (with age and gender as covariates of no interest) in a second level design matrix that served for regressions with the NEO variables. Regressions were used because NEO scores did not deviate from a standard normal distribution (as indicated by Shapiro-Wilk-Tests, see Supplementary Table 2). By contrast, Eκ values significantly deviated from a normal distribution ($p = 0.02$ according to the Shapiro-Wilk Test of Normality). Therefore, Eκ values were dichotomized using a median-split, and eigenvector centrality maps were compared between the resulting two groups (11 individuals with higher, and 11 individuals with lower). Age and gender were used as covariates of no interest in the second level design matrix for a voxel-wise two-samples *t*-test. All second-level results were corrected for multiple comparisons by the use of cluster-size and cluster-value thresholds obtained by Monte Carlo simulations with a significance level of $p<0.05$ (Lohmann et al. 2008). The voxel-wise threshold before applying the Monte Carlo simulation was $z = 2.326$.

To specify whether (a) correlations between brain activations and personality scores and (b) differences in brain activation between Eκ groups were independent of the emotional state of subjects, we also computed ECMs separately for each music epoch (and for each participant). Thus, 16 ECMs per emotion category (joy, fear, neutral) were computed per participant. Then, for each emotion category the 16 ECMs were averaged into an average ECM per participant (that is, for each participant one average ECM was computed for joy, another one for fear, and a third one for neutral). Subsequently, the neuroticism, extraversion, and agreeableness scores were used as regressors of interest (with age and gender as covariates of no interest) for the average ECMs of each emotion (joy, fear, neutral) in a second level design matrix. In additional second-level analyses, the average ECMs of each emotion condition (joy, fear, neutral) were compared between Eκ groups. Finally, the maximal *z*-values were extracted for those structures in which the first second-level ECM analyses (which used the entire fMRI session as one single trial per participant) indicated significant personality effects. Thus, group results were first obtained with ECMs calculated for the entire fMRI session, and then these results were further investigated using ECMs calculated separately for each emotion condition (joy, fear, neutral).

6.2.1.6 Comparison of NEO and ECG data

In addition to comparing the functional neuroimaging brain data between groups with higher and lower Eκ, we also compared NEO scores between these two groups. For all six NEO scores we had directed hypotheses: individuals with higher values were expected to show lower neuroticism, higher extraversion, higher agreeableness, as well as higher positive emotion, tender-mindedness and warmth (see also Introduction). Thus, the significance level for Bonferroni-corrected one-sided tests was 0.05 / 6 * 2 = 0.017.

6.2.2 Results

6.2.2.1 Relations between cardiac and psychological data

NEO scores were compared between groups of individuals with high and low Eκ values (i.e., Eκ values above and Eκ values below the median) according to the directed hypotheses stated in the Introduction and Methods. Individuals with higher Eκ had significantly (Bonferroni-corrected) higher extraversion scores compared to those with lower Eκ (t=2.5, p=.01). Moreover, individuals with higher Eκ had significantly (Bonferroni-corrected) higher scores of positive emotion (t=2.5, p=.01, for details and complete data see Supplementary Table S3).

6.2.2.2 Relations between behavioral ratings and ECG/NEO data

During the experiment, subjects rated at the end of each music stimulus how they felt with regard to valence, arousal, joy, and fear (see *Methods*). To investigate how these emotion ratings were influenced by the different stimulus categories (joy, fear, neutral), an ANCOVA was computed with the within-subjects factor stimulus category (joy, fear, neutral). This analysis indicated main effects of valence ($F(2, 20) = 83.76$, $p < 0.001$), arousal ($F(2,20) = 20.92$; $p < 0.001$), joy ($F(2, 20) = 196.88$, $p < 0.001$), and fear ($F(2,20) = 84.97$, $p < 0.001$). These results reflect that the stimulus material evoked distinct emotional effects in our participants.

To investigate whether emotion ratings differed between the Eκ groups (i.e., between individuals with Eκ values above and Eκ values below the median), an

ANCOVA was carried out with the within-subjects factor stimulus category (joy, fear, neutral) and Eκ group as between-subjects factor. Results indicated main effects of Eκ group for arousal (F(1,20) = 6.34, p = 0.020), and fear (F(1,20) = 5.95, p = 0.024). These main effects originated from arousal and fear ratings being higher in the group of individuals with higher values.

Finally, to investigate whether emotion ratings were modulated by the NEO scores, an ANCOVA was computed with factor stimulus category, and NEO scores as covariates (neuroticism, extraversion, agreeableness). Results indicated a main effect of extraversion scores for joy ratings (F(1,18) = 5.40, p = 0.032), resulting from lower joy ratings for the fear and neutral stimuli in participants with high extraversion. A main effect of neuroticism scores was marginally significant (F(1,18) = 3.04, p = 0.098) for fear ratings, resulting from fear ratings being higher in participants with higher neuroticism scores. No main effect of agreeableness was observed. Nevertheless, there were interactions of emotion category with the agreeableness scores for arousal (F(2,17) = 4.26, p = 0.032), valence (F(2,17) = 11.91, p = 0.001), and joy (F(2,17) = 8.55, p = 0.003), reflecting that ratings of participants with higher agreeableness scores were more in accordance with the stimulus categories (e.g. they gave higher joy ratings for joy stimuli, and lower joy ratings for fear stimuli, compared to individuals with low agreeableness scores).

6.2.2.3 Psychological (NEO) measures and ECM data

Results of voxel-wise correlations between Eigenvector Centrality Maps (ECMs, computed for the entire fMRI session, see Methods) and scores of each of the NEO scales are listed in Table 2 and shown in Figure 2a. Significant positive correlations with agreeableness scores were observed in the right ventral striatum / nucleus accumbens, ACC, the rostral cingulate zone extending into the pre-SMA of area 6, and dorsolateral prefrontal cortex bilaterally (posterior superior frontal sulcus and superior frontal gyrus, BA 8). Significant negative correlations were found in the central sulcus (face area of either area 3b or area 4).

To investigate whether these correlations were dependent on the emotional states of subjects, we also computed average ECMs for each emotion condition separately (see *Methods*). Correlations between these ECMs and agreeableness scores showed that, in all structures listed in Table 2, the significance values of the observed correlations were similar for joy, fear, and neutral (see Table 2 for details; note that all significance values were above $z = 1.96$, corresponding to $p = .05$).

The ECMs computed for the entire fMRI session did not show significant correlations (corrected for multiple comparisons, $p<.05$) with neuroticism, nor with extraversion. However, when testing our directed hypotheses (stated in the Introduction) using uncorrected regression analyses (thresholded at $p=.001$ and a voxel extent of 10 voxels), we found a correlation between neuroticism and centrality values in the cingulate sulcus at the border of the rostral and caudal cingulate zone (MNI coordinate: -2, 7, 43; $z = 3.4$).

Table 6.2: Results of agreeableness regression. The table shows results of voxel-wise regressions between Eigenvector Centrality Maps (ECMs, controlled for age and gender) and agreeableness scores, corrected for multiple comparisons ($p < .05$). MNI-coordinates, cluster sizes, and *z*-values refer to the analysis in which one single ECM per participant (calculated for the entire fMRI session) entered the second-level analysis. The three columns on the right indicate maximum *z*-values in the respective structures when ECMs were computed separately for each emotion condition (joy, fear, and neutral, see Methods). Abbreviations: l: left; r: right; post.: posterior; ACC: anterior cingulate cortex; MNI: Montreal Neurological Institute; NAc: nucleus accumbens; SFG: superior frontal gyrus; SFS: superior frontal sulcus; SMA: supplementary motor area.

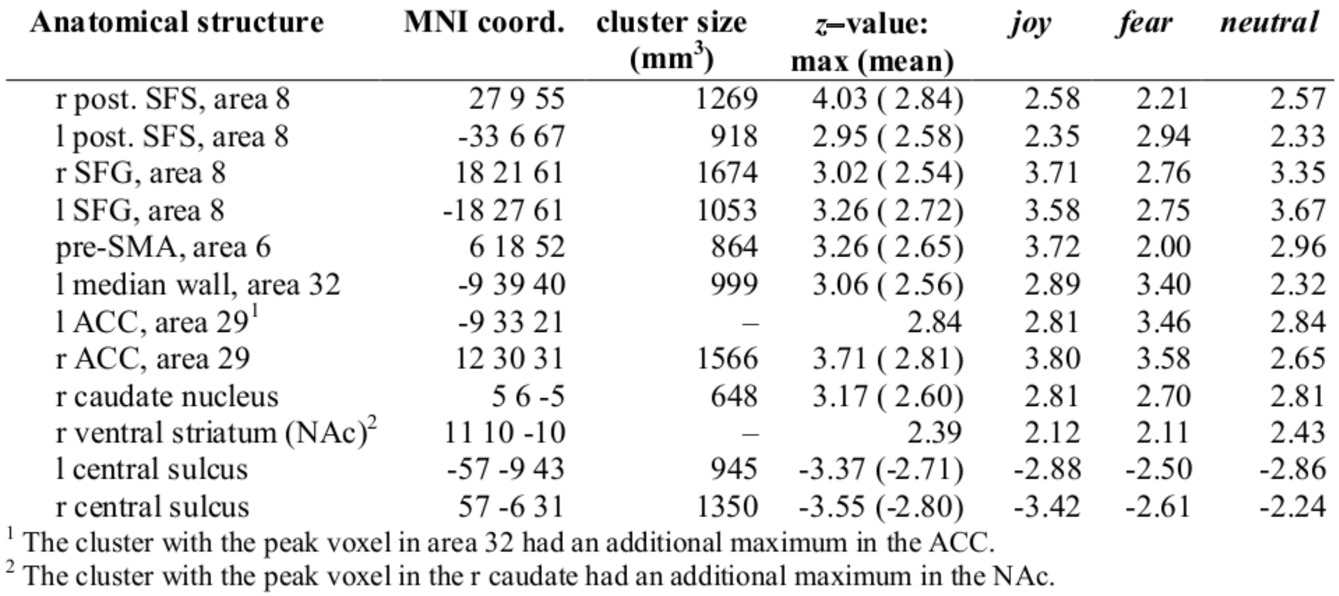

Anatomical structure	**MNI coord.**	**cluster size (mm^3)**	***z*–value: max (mean)**	***joy***	***fear***	***neutral***
r post. SFS, area 8	27 9 55	1269	4.03 (2.84)	2.58	2.21	2.57
l post. SFS, area 8	-33 6 67	918	2.95 (2.58)	2.35	2.94	2.33
r SFG, area 8	18 21 61	1674	3.02 (2.54)	3.71	2.76	3.35
l SFG, area 8	-18 27 61	1053	3.26 (2.72)	3.58	2.75	3.67
pre-SMA, area 6	6 18 52	864	3.26 (2.65)	3.72	2.00	2.96
l median wall, area 32	-9 39 40	999	3.06 (2.56)	2.89	3.40	2.32
l ACC, area 29[1]	-9 33 21	–	2.84	2.81	3.46	2.84
r ACC, area 29	12 30 31	1566	3.71 (2.81)	3.80	3.58	2.65
r caudate nucleus	5 6 -5	648	3.17 (2.60)	2.81	2.70	2.81
r ventral striatum (NAc)[2]	11 10 -10	–	2.39	2.12	2.11	2.43
l central sulcus	-57 -9 43	945	-3.37 (-2.71)	-2.88	-2.50	-2.86
r central sulcus	57 -6 31	1350	-3.55 (-2.80)	-3.42	-2.61	-2.24

[1] The cluster with the peak voxel in area 32 had an additional maximum in the ACC.

[2] The cluster with the peak voxel in the r caudate had an additional maximum in the NAc.

Table 6.3: Results of the ECM constrasts high vs low. In the left column, percentages in brackets following anatomical structures refer to anatomical probabilities according to the SPM Anatomy Toolbox (Eickhoff et al. 2005). The next columns provide MNI-coordinates, cluster sizes, and *z*-values of maxima indicated by the analysis in which one single ECM per participant (calculated for the entire fMRI session) entered the second-level analysis. Results were corrected for multiple comparisons ($p < .05$). The three remaining columns on the right indicate maximal *z*-values in the respective structures when ECMs were computed separately for each emotion condition (joy, fear, and neutral, see Methods). Abbreviations: aFMC: anterior fronto-median cortex; g.: gyrus; l: left; parahipp.: parahippocampal; post.: posterior; r: right; ACC: anterior cingulate cortex; ECM: Eigenvector Centrality Mapping; IFG: inferior frontal gyrus; LGB: lateral geniculate body of the thalamus; MTG: middle temporal gyrus; Rol.operc.: Rolandic operculum; STG: superior temporal gyrus; SUB: subiculum of the hippocampal formation; Th-visual: visual thalamic nuclei; V1: primary visual cortex; WM: white matter.

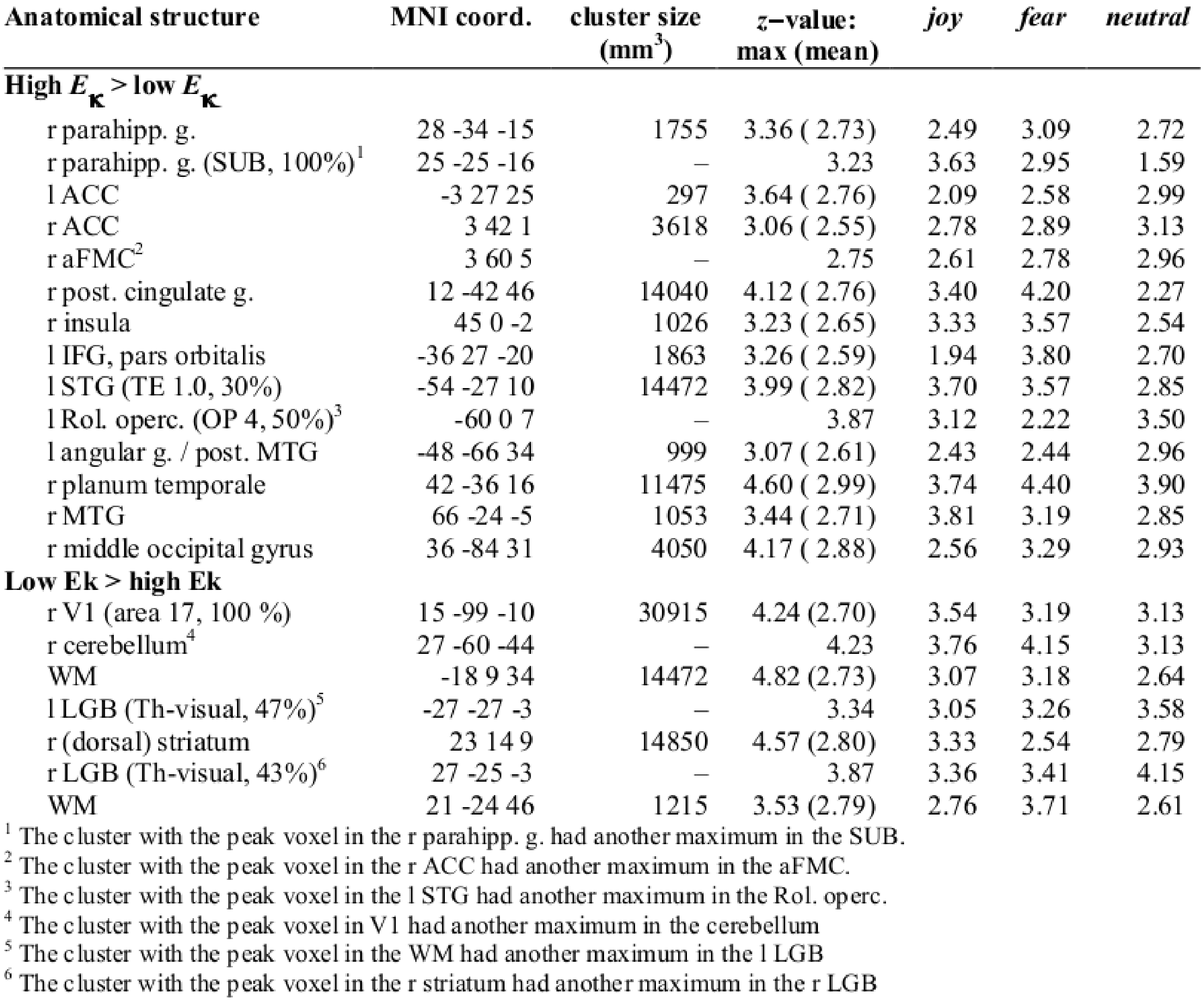

Anatomical structure	**MNI coord.**	**cluster size (mm^3)**	***z*–value: max (mean)**	***joy***	***fear***	***neutral***
High E_κ > low E_κ						
r parahipp. g.	28 -34 -15	1755	3.36 (2.73)	2.49	3.09	2.72
r parahipp. g. (SUB, 100%)[1]	25 -25 -16	–	3.23	3.63	2.95	1.59
l ACC	-3 27 25	297	3.64 (2.76)	2.09	2.58	2.99
r ACC	3 42 1	3618	3.06 (2.55)	2.78	2.89	3.13
r aFMC[2]	3 60 5	–	2.75	2.61	2.78	2.96
r post. cingulate g.	12 -42 46	14040	4.12 (2.76)	3.40	4.20	2.27
r insula	45 0 -2	1026	3.23 (2.65)	3.33	3.57	2.54
l IFG, pars orbitalis	-36 27 -20	1863	3.26 (2.59)	1.94	3.80	2.70
l STG (TE 1.0, 30%)	-54 -27 10	14472	3.99 (2.82)	3.70	3.57	2.85
l Rol. operc. (OP 4, 50%)[3]	-60 0 7	–	3.87	3.12	2.22	3.50
l angular g. / post. MTG	-48 -66 34	999	3.07 (2.61)	2.43	2.44	2.96
r planum temporale	42 -36 16	11475	4.60 (2.99)	3.74	4.40	3.90
r MTG	66 -24 -5	1053	3.44 (2.71)	3.81	3.19	2.85
r middle occipital gyrus	36 -84 31	4050	4.17 (2.88)	2.56	3.29	2.93
Low Ek > high Ek						
r V1 (area 17, 100 %)	15 -99 -10	30915	4.24 (2.70)	3.54	3.19	3.13
r cerebellum[4]	27 -60 -44	–	4.23	3.76	4.15	3.13
WM	-18 9 34	14472	4.82 (2.73)	3.07	3.18	2.64
l LGB (Th-visual, 47%)[5]	-27 -27 -3	–	3.34	3.05	3.26	3.58
r (dorsal) striatum	23 14 9	14850	4.57 (2.80)	3.33	2.54	2.79
r LGB (Th-visual, 43%)[6]	27 -25 -3	–	3.87	3.36	3.41	4.15
WM	21 -24 46	1215	3.53 (2.79)	2.76	3.71	2.61

[1] The cluster with the peak voxel in the r parahipp. g. had another maximum in the SUB.

[2] The cluster with the peak voxel in the r ACC had another maximum in the aFMC.

[3] The cluster with the peak voxel in the l STG had another maximum in the Rol. operc.

[4] The cluster with the peak voxel in V1 had another maximum in the cerebellum

[5] The cluster with the peak voxel in the WM had another maximum in the l LGB

[6] The cluster with the peak voxel in the r striatum had another maximum in the r LGB

(a) Functional (ECM): correlation with agreeableness

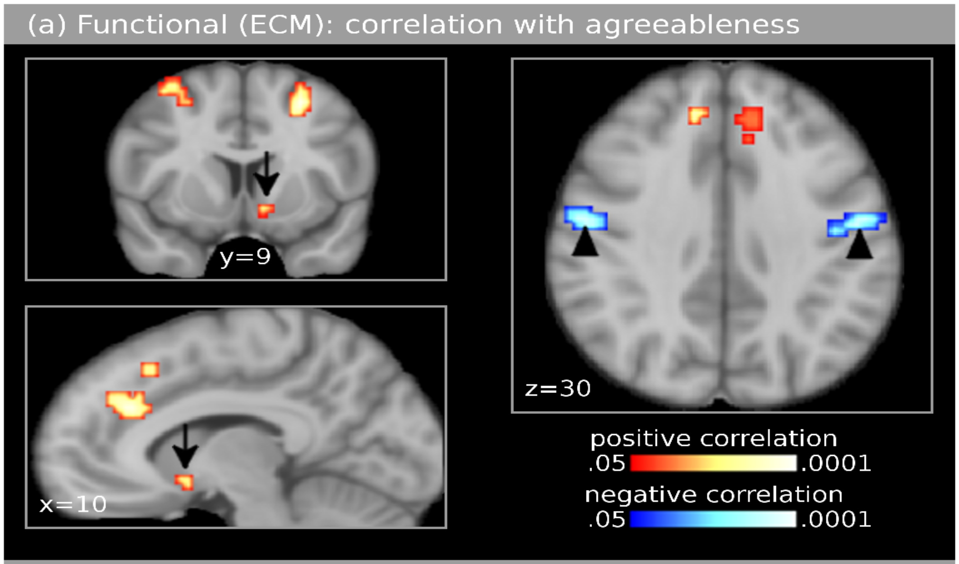

(b) Functional (ECM): high Ek vs low Ek

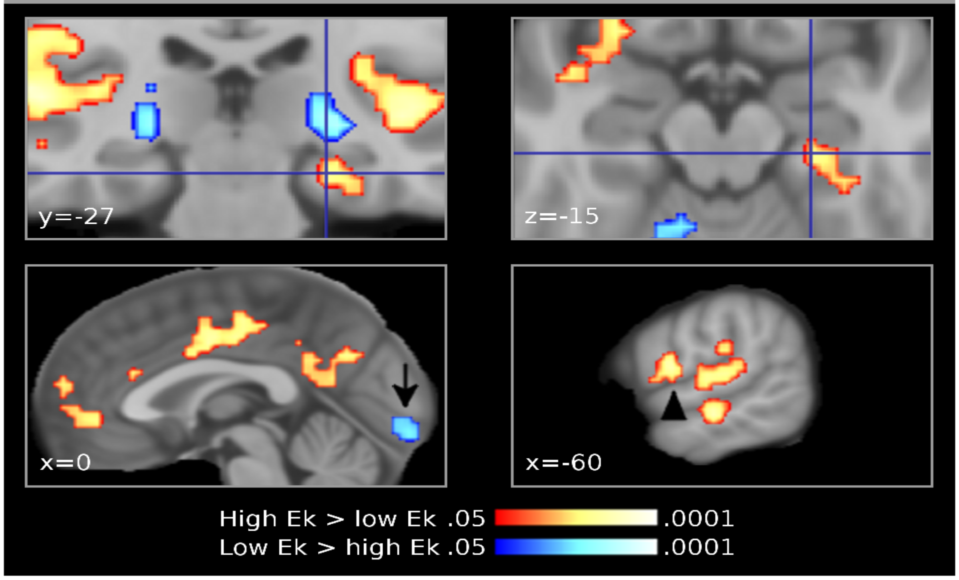

Figure 6.2. Experiment 1: Functional neuroimaging data (Eigenvector Centrality Mapping). Images are shown in neurological convention, all results were corrected for multiple comparisons (p<.05). **(a)** Results of correlations of Eigenvector Centrality Maps (ECMs) with agreeableness scores. For each participant, one ECM was computed for the entire fMRI session. Positive correlations (shown in red-yellow colours) were found in the posterior superior frontal sulcus bilaterally (upper left image), the ventral striatum / nucleus accumbens (arrows in left upper and lower image), and in anterior cingulate cortex (lower left image). Negative correlations (shown in blue) were observed in the central sulcus (arrowheads in right image). **(b)** Comparison of ECMs between groups of participants with higher and lower Eκ values. Individuals with higher Eκ showed higher centrality values in the subiculum of the right hippocampal formation (crosshairs in upper images), in the auditory cortex bilaterally, in both anterior and posterior cingulate cortex (lower left image), the anterior fronto-median cortex (lower left image), and the Rolandic operculum (arrowhead in lower right image). The group with lower Eκ showed higher centrality values in the lateral geniculate body bilaterally (blue clusters in upper left image) as well as in the visual cortex (V1, blue cluster in lower left image).

6.2.2.4 Physiological (cardiac) measures and ECM data

For the comparison of ECMs between individuals with high and low Eκ, subjects were split into two groups based on a median split of Eκ values (i.e., Eκ values above and Eκ values below the median). Group differences were first investigated using the ECMs computed for the entire fMRI session. The results of this comparison are listed in Table 3 and shown in Figure 2b (data were controlled for age and gender, and results were corrected for multiple comparisons, $p<.05$). A difference between groups was found in the subiculum of the right hippocampal formation (MNI coordinate: 23, -27, -15, 90% probability for subiculum according to the cytoarchitectonic maps provided by Amunts et al. (2005), in which centrality values were significantly higher in the group with higher Eκ compared to the group with lower Eκ (see crosshair in Figure 2b). Figure 2b also shows significantly higher centrality values in the group with higher Eκ in the auditory cortex bilaterally, both anterior and posterior cingulate cortex, the anterior fronto-median cortex, and the Rolandic operculum (for full list see Table 3). The group with lower Eκ showed higher centrality values in the lateral geniculate body bilaterally as well as in the visual cortex (V1).

To investigate whether these differences were dependent on the emotional states of subjects, we also computed average ECMs for each emotion condition separately (see Methods). Comparisons between Eκ groups showed that, in almost all structures listed in Table 3, the significance values of the observed correlations were similar for joy, fear, and neutral (see Table 3 for details), except in the right subiculum (in which neutral stimuli did not evoke significant effects) and the left pars orbitalis (in which joy stimuli did not evoke significant effects).

6.2.3 Discussion

6.2.3.1 Functional MR data and psychological (NEO) measures

The ECM data showed a correlation between centrality values and agreeableness scores in the DLPFC bilaterally. Separate clusters were observed bilaterally in both the posterior superior frontal sulcus (SFS, see left upper panel of Figure 2a), and the superior frontal gyrus (all clusters were located in area 8, (Petrides, Pandya, 1999). The SFS clusters closely resemble results reported by Haas et al. (2007), in which agreeableness correlated with activity in the (right) DLPFC (crown of the right medial frontal gyrus) during the processing of fearful faces. The authors of that study (Haas et al. 2007) presumed that, because agreeableness is associated with the tendency to avoid interpersonal conflict, highly agreeable individuals engaged neural mechanisms of affect regulation when facing conflict-related signals. This notion is also consistent with the recent observation that DLPFC is involved in impulse control (Steinbeis et al. 2012). To investigate whether ECM clusters observed in the present study in the DLPFC were driven by the fearful musical stimuli only, we computed ECMs for each experimental condition (joy, fear, neutral music), and correlated the ECMs with agreeableness scores. Local maxima at virtually identical coordinates in the DLPFC were observed for all three conditions (although with lower statistical significance), and these local maxima had comparable *z*-values for fear and joy conditions. This renders it unlikely that only threatening stimuli led to the activation of computational hubs in the DLPFC correlating with agreeableness. Perhaps agreeableness is associated with executive functions in DLPFC due to the organization of behaviour in regard to cooperation and social harmony in any given situation with social relevance, but this remains to be specified.

Centrality values also correlated positively with agreeableness scores in the ventral striatum / nucleus accumbens (NAc). This is perhaps related to agreeableness representing a tendency toward pro-social behaviour (including altruism and cooperation). Note that the musical stimulus used in the functional experiment probably evoked a number of music-related social functions such as social cognition, communication, and premotor coordination of movements (Koelsch 2010; Steinbeis, Koelsch, 2008). Engagement in such functions has been proposed to lead to feelings of reward (Koelsch et al. 2010a), involving dopaminergic activity in the ventral striatum (Salimpoor et al. 2011), and such music-evoked social functions are possibly activated more strongly in individuals with higher agreeableness scores, resulting in increased reward-related brain activity.

No correlations between extraversion and ECMs were observed, perhaps because potential results have been missed due to the relatively small sample size of n = 22 (Yarkoni, 2009). Also note that, due to the sample size, the significant effects we observed might not be as selective as it appears (Yarkoni, 2009).

6.2.3.2 Functional MR data and physiological Eκ measure

The group with higher Eκ values (taken to reflect higher tender emotionality) showed higher centrality values in the subiculum of the right hippocampal formation (the implications of this finding are discussed in the General Discussion). This observation is consistent with results of two previous fMRI experiments, in which fMRI data also showed differences within the hippocampal formation between individuals with high and low Eκ (Koelsch et al. 2007). In that study (Koelsch et al. 2007), which used the traditional general linear model approach (GLM), the main group difference was located in the cornu ammonis. Note that the present study used ECM, thus calculating computational hubs that are central in networks consisting of different brain structures. In contrast to the cornu ammonis, which primarily receives projections from the dentate gyrus and projects to the subiculum (Nieuwenhuys et al. 2008), the subiculum is interconnected with a large array of cortical and subcortical structures: In addition to converging input from the cornu ammonis, it has bidirectional projections with entorhinal, perirhinal and prefrontal cortices, as well as with many subcortical structures (in particular numerous hypothalamic nuclei; O’Mara, 2005). Thus, it is likely that GLM contrasts are better suited to reveal functional differences in the cornu ammonis, whereas ECM is better suited to reveal such differences in the subiculum.

The group with higher Eκ also showed higher centrality values in the ACC. Due to the relation between Eκ and NEO-scores of extraversion, this finding is consistent with studies showing correlations with extraversion and ACC activity (Kumari et al. 2004, Canli et al. 2004, Haas et al. 2006). The cingulate cortex is involved in emotional processes, in particular with regard to autonomic regulation and the production of subjective feelings (Craig, 2009; Medford, Critchley, 2010). In addition, the cingulate cortex has been implicated in the coordination, and synchronization of autonomic activity, behaviour, motor expression, as well as cognitive processes in response to emotionally salient stimuli (Medford, Critchley, 2010, Koelsch et al. 2010b). In the *component process model* of emotion by Scherer (2000), an emotion is even defined as synchronization of these emotion components. The observation that centrality values in the ACC are higher in individuals with high Eκ is thus likely to reflect stronger, or more frequent, synchronization processes in the ACC due to more dynamic emotion-related activity in the “biological subsystems of emotion” (Scherer, 2000). Interestingly, the cluster observed in the ACC also extended into the anterior fronto-median cortex (in which individuals with higher Eκ values also showed higher centrality values). This possibly reflects that individuals with higher tender emotionality engage more strongly in social information processing, including understanding and evaluating emotions of other individuals.

Another interesting result is that the group with lower Eκ values showed higher centrality values in the lateral geniculate body (LGB) bilaterally as well as in the primary visual cortex (V1). Note that both groups had their eyes closed during stimulation (this was controlled via an eyetracker, see *Methods*), and that activation of V1 and LGB with closed eyes is consistent with activation patterns during visual imagery (Chen et al. 1998). Although not included in our hypotheses, this pattern thus indicates increased visual imagery in individuals with low Eκ (compared to individuals with high Eκ). As mentioned in the Introduction, reduced tender emotionality, i.e. emotional coldness and reduced affect, is taken to be reflected in low Ek. In a clinically relevant form, emotional coldness and reduced affect are the prime symptoms of schizoid personality disorder according to the International Classification of Diseases (F60.1 of the ICD-10), which lists as further characteristics preoccupation with fantasy and introspection. Because fantasy involves visual imagery, our results support the notion that, in healthy individuals, low Eκ may reflect subclinical symptoms of schizoid personality disorder, including reduced tender positive emotion (i.e., increased emotional coldness) and increased tendency for fantasy and introversion. Notably, this is also reflected in the lower extraversion scores of individuals with low Ek.

6.2.3.3 Emotion-specificity of ECM results

In addition to ECMs computed for the entire fMRI session, we also computed ECMs for each stimulus condition separately (joy, fear, neutral) to investigate to which degree personality-characteristic brain activity might have been dependent on the emotional states of subjects. Results showed that effects observed in the analysis of the entire fMRI session (pooling the data of all music stimuli and emotion ratings) were also observed in each of the stimulus conditions (joy, fear, neutral). This indicates that the reported ECM findings were largely independent of the emotional states of subjects and that the ECM results on emotional personality are not specific to any particular emotion. It is also unlikely that the observed associations between personality and brain activity are limited only to emotional states involving musical stimulation. Future studies might investigate whether the differences observed in experiment 1 can also be observed in non-emotional experimental paradigms.

6.3 Experiment 2

Structural MRI using Voxel Based Morphometry

Experiment 1 investigated personality-characteristic differences in brain function. In experiment 2, we aimed at investigating whether such differences correspond to differences in brain structure. For this purpose, the same psychological (NEO) and physiological (cardiac) measures were acquired from an independent sample of subjects and used as independent variables to explain variance in structural neuroimaging data. In addition, we hypothesized (based on the most consistent findings reported in previous studies, see Table 1B) positive correlations between neuroticism and OFC volume (Gardini et al. 2009; Wright et al. 2006) as well as between neuroticism and amygdalar volume (Omura et al. 2005; Iidaka et al. 2006; Barros-Loscertales et al. 2006). Likewise, we aimed to test for positive correlations between extraversion and OFC volume (DeYoung et al. 2010; Cremers et al. 2011; Rauch et al. 2005) as well as amygdalar volume (Cremers et al. 2011; Omura et al. 2005), and to test for a negative relation between extraversion and volume of the caudate nucleus (Forsman et al. 2012; Gardini et al. 2009).

6.3.1 Materials and Methods

6.3.1.1 Participants

Data were acquired from 67 individuals (aged 20 – 31 years, *M*=24.15, *SD*=2.40, 34 females). None of the subjects participated in experiment 1. Exclusion criteria were left-handedness, past diagnosis of a neurological or psychiatric disorder, and abnormal brain anatomy. All subjects gave written informed consent. The study was conducted according to the Declaration of Helsinki and approved by the ethics committee of the School of Life Sciences and the Psychology Department of the University of Sussex.

6.3.1.2 Experimental procedure

Acquisition and analysis of psychological (NEO) measures and physiological (cardiac) measures was identical to experiment 1, except that ECG and NEO data were obtained within three weeks before or after the structural imaging session, and that ECG data were acquired using a Refa-system (Twente Medical Systems, Enschede, NL).

6.3.1.3 MR Scanning

Scanning was performed with a 3T Siemens Magnetom Trio scanner (Siemens Medical Systems, Erlangen, Germany). Whole-brain structural scans were acquired using a 3D Fast Low Angle Shot (FLASH) sequence using a 12-channel birdcage head coil. For each subject, 176 sagittal partitions with an image matrix of 240 x 256 and an isotropic spatial resolution of 1 mm, a TE = 4 ms, $\alpha = 10°$ and total scan time of about 8 min were acquired.

6.3.1.4 Structural MRI data analysis

Processing of structural MRI scans was carried out using SPM8 (Ashburner 2009) running on Matlab 2009a (The Mathworks, Natick, MA, USA). All images were checked for artefacts and manually aligned so that the origin of the coordinate system was located at the anterior commissure. Using the *New Segmentation* procedure of SPM8 (Ashburner, Friston, 2009), which is an extension of the default unified segmentation procedure (Ashburner, Friston, 2005), the images were segmented into grey matter (GM), white matter (WM) and cerebrospinal fluid (CSF). For each subject, this resulted in two sets of 3 images: One set was in the same space as the original T1-weighted image in which each voxel was assigned a probability of it being GM, WM and CSF; another set contained the segmented images rigid-body-aligned into MNI space. Spatial normalization employed DARTEL, an algorithm for diffeomorphic image registration (Ashburner, 2007) that provides an improved anatomical precision (Bergouignan et al. 2009; Klein et al. 2009; Yassa, Stark, 2009) compared to previously used methods (Ashburner, Friston, 2005; Ashburner, Friston, 1999). DARTEL was used to optimally warp the rigid-body aligned GM, and WM segments into a new reference space representing an average of all the participants. The method iteratively creates an increasingly fine-grained set of group-specific templates and the deformation fields required to warp the data from each subject. Each subject's specific deformation field is used to warp the corresponding GM and WM segments into the new reference space, with re-sampling at 1.5 mm isotropic voxels using trilinear interpolation. Then, the warped GM and WM segments were affine transformed into MNI space. The probability values were scaled by the Jacobian determinants of the deformations to account for the local compression and stretching that occurs as a consequence of the warping and affine transformation (a process referred to as *modulation;* Good et al. 2001). Finally, the GM probability values were smoothed using a 4 mm FWHM Gaussian kernel.

The GM volumetric data were then correlated voxel-wise with each of the (standardized) NEO scores (extraversion, neuroticism, agreeableness) with an FWE-correction for multiple comparisons ($p < .05$; NEO-scores did not deviate from a standard normal distribution as indicated by a Shapiro-Wilk-Test, see Supplementary Table 2). As in the functional experiment, Eκ values deviated from a normal distribution ($p = 0.001$ according to the Shapiro-Wilk Test of Normality). Therefore, Eκ values were dichotomized using a median-split, and GM volumetric data were compared between the resulting two groups (33 individuals with higher, and 34 individuals with lower Ek) using voxel-wise *t*-tests and an FWE-correction for multiple comparisons (*p* < .05). In cases were we had directed hypotheses (see Introduction of experiment 2), we also computed uncorrected SPMs (thresholded at *p*=.001 and a voxel extent of 10 voxels). In all analyses, we controlled for differences in age, gender and total brain volume (sum of GM and WM volume) by including these variables as covariates of no interest.

6.3.2 Results

6.3.2.1 Relations between ECG and NEO data

As in the functional experiment, NEO scores were compared between groups with high and low Eκ values (i.e., Eκ values above and Eκ values below the median of each experiment) according to the directed hypotheses stated in the Introduction. There was a trend for individuals with higher Eκ showing higher extraversion scores compared to those with lower Eκ (*t*=1.7, *p*=.047, one-tailed). Contrary to the functional experiment, individuals with higher Eκ did not show significantly higher scores of positive emotion (for details and complete data see Supplementary Table S3).

6.3.2.2 Psychological (NEO) measures and VBM data

In a whole-brain-analysis, voxel-wise correlations between the structural brain data (controlled for total brain volume, age and gender) and each of the NEO scales did not indicate any significant correlation in the FWE-corrected statistical parametric maps (SPMs). Inspecting the uncorrected SPMs (based on our directed hypotheses) we observed a positive correlation between neuroticism and tissue density in the left amygdala (Figure 3a). When applying a small volume correction, using the amygdala volume as region of interest (extracted from the Anatomy Toolbox for SPM; Eickhoff et al. 2005) this correlation was significant at the FWE-corrected threshold ($p<.05$ on both cluster and peak level). The voxel with the maximum z-value (3.61) was located at MNI coordinates [-18, 1, -17].

6.3.2.3 Physiological (cardiac) measures and VBM data

In another whole-brain analysis, we computed a voxel-wise comparison of structural brain data (controlled for total brain volume, age and gender) between the two Eκ groups (Eκ values above and Eκ values below the median). The FWE-corrected SPM of this comparison did not indicate any significant group difference. Again, inspecting the uncorrected SPMs (driven by our directed hypothesis) to investigate possible group differences in amygdala and hippocampal formation, we observed that the largest cluster in the comparison high > low Eκ was located in the subiculum of the right hippocampal formation (Figure 3b), in part overlapping with the cluster that was observed to differ between groups in the functional data. This volume difference between groups was significant after FWE-correction ($p<.05$ on the cluster level, and $p<.006$ on the peak level) when using the volume of the subiculum as region of interest (subiculum volume was extracted from the Anatomy Toolbox for SPM; Eickhoff et al. 2005). Even when using the entire hippocampal volume (bilaterally) as region of interest, the difference between groups was significant on the peak level ($p<.05$, FWE-corrected). The voxel with the maximum z-value (3.75) was located at MNI-coordinates [18, -26, -12] (90% probability for

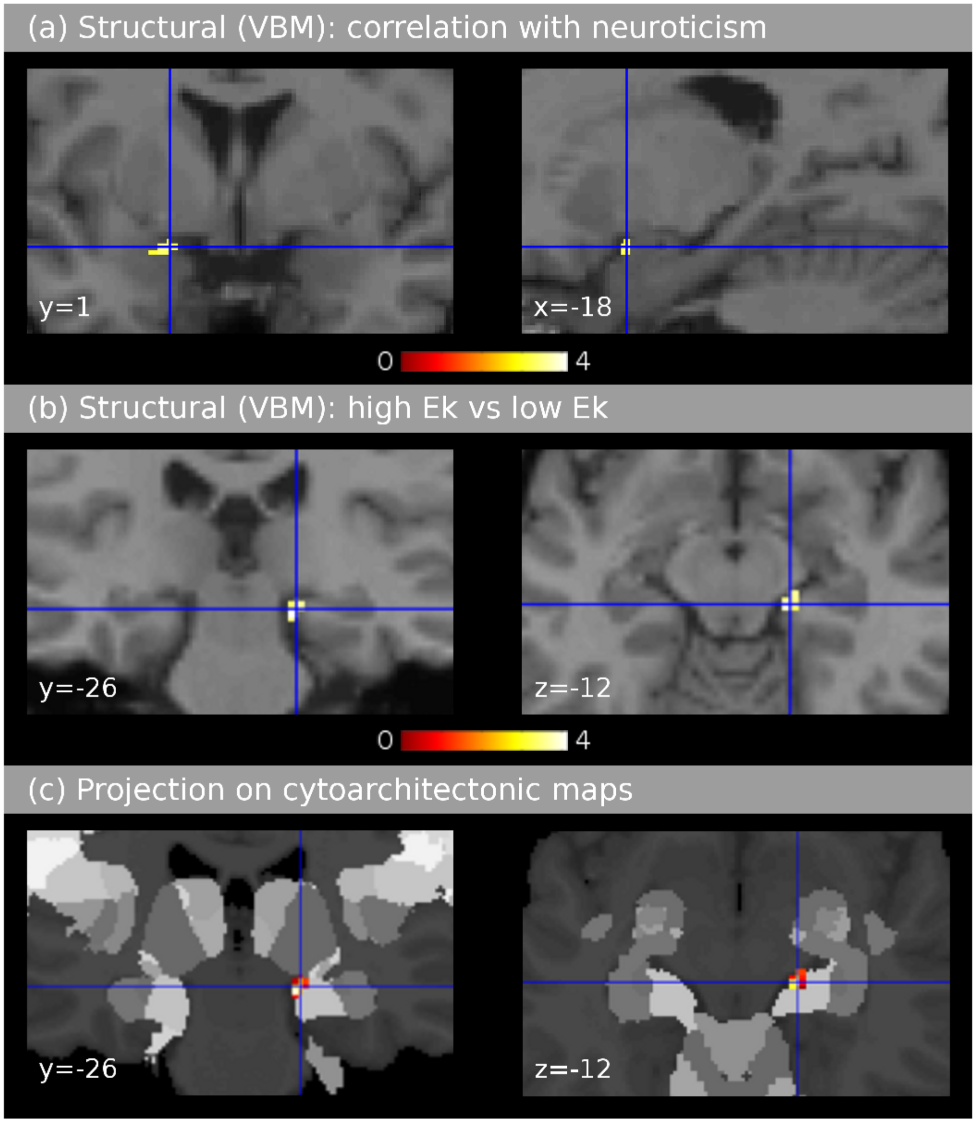

Figure 6.3. Experiment 2: Structural neuroimaging data (voxel-based morphometry). Images are shown in neurological convention. **(a)** Results of correlations of grey matter volume with neuroticism scores (uncorrected data with a threshold of *p*<.001 and a minimum cluster size of 10 voxels). The crosshair indicates a positive correlation in the left amygdaloid complex (significant when applying a region of interest analysis, *p*<.05, FWE-corrected). The left image shows a coronal section, the right images shows a sagittal section (left of the image is anterior). **(b)** Comparison of structural data between groups of participants with higher and lower Eκ values (uncorrected data with a threshold of *p*<.001 and a minimum cluster size of 10 voxels). A difference between groups was found in the subiculum of the right hippocampal formation (significant when applying a region of interest analysis, *p*<.05, FWE-corrected). Gray matter volume was larger in the group of participants with higher Eκ values. Note the consistency with the group difference observed in the left subiculum in the functional data (Figure 2). The left image shows a coronal section, the right image an axial section. **(c)** Shows the same results as (b), projected on the cytoarchitectonic probability map of the hippocampal formation provided by Amunts et al. 2005 using the Anatomy Toolbox provided by Eickhoff et al. 2005. The group difference is located with 90% probability in the subiculum.

subiculum of the hippocampal formation according to the cytoarchitectonic maps provided by Amunts et al. 2005), see also Figure 3c. The opposite uncorrected contrast (low > high Eκ values) did not yield any significant volume differences between groups.

6.3.3 Discussion

6.3.3.1 Structural MR data and psychological (NEO) measures

The positive correlation between neuroticism and volume of the left amygdala corroborates findings of a previous study showing a correlation between neuroticism and amygdalar volume (in females; Iidaka et al. 2006). Another previous finding of an association between neuroticism and right amygdalar volume (Omura et al. 2005) was not supported by our study. It is well established that the amygdala is involved in fear responses (LeDoux, 2000), and the correlation between neuroticism and amygdalar volume might thus reflect structural changes in the amygdala due to the increased tendency to experience anxiety. Corroboratingly, the amygdaloid complex (and related orbitofrontal cortical areas) is centrally involved in mood disorders such as major depressive disorder, bipolar disorder, and pathological anxiety (Prince, Drevets, 2012; Sylvester, 2012). However, substantial evidence indicates that the amygdala also plays a role for positive emotions (Murray, 2007). Therefore, while amygdalar nuclei involved in negative emotion might have greater volume in individuals with high neuroticism, one could also expect greater volume in nuclei involved in positive emotion in individuals with low neuroticism, or high agreeableness. Perhaps negative emotions lead to more pronounced structural changes in the amygdala than positive emotions, but this remains to be specified. No correspondence between functional (experiment 1) and structural results (experiment 2) was observed with regard to the neuroimaging analyses involving NEO measures, substantiating that consistency of neuroimaging results using self-report (questionnaire) measures or personality as independent variables is rather low (see also Table 1).

6.3.3.2 Structural MR data and physiological Eκ measure

The group with higher Eκ (compared to the group with lower Ek) showed larger volume in the subiculum of the right hippocampal formation. These are the first results showing a relation between a cardiac amplitude signature and brain morphometry. Both structural and functional results correspond remarkably well with each other: Effects were partly overlapping, and the maximal effects were located in close vicinity across Experiments 1 and 2. This provides strong evidence for an association between the hippocampal formation and cardiac amplitude signatures in humans. Because the associations between NEO scores and Eκ corroborate a relation between Eκ and emotional personality, these structural data are also the first to show that emotionality-related differences as assessed with a peripheral physiological measure correlate with brain morphology.

6.4 General Discussion

6.4.1 Summary of results

The group with higher Eκ values had higher extraversion scores in both the functional and the structural experiment. In the functional experiment, scores of positive emotion were higher in the group with higher Eκ values. The functional data indicated a significant positive correlation between centrality values and agreeableness in the right ventral striatum (probably nucleus accumbens, NAc), ACC, the rostral cingulate zone extending into the pre-SMA, and dorsolateral prefrontal cortex (DLPFC) bilaterally. Significant negative correlations were found in the central sulcus. The comparison of the functional data between the two Eκ groups showed a difference between groups for the subiculum of the right hippocampal formation, in which centrality values were higher for the group with higher Eκ values. Moreover, significantly higher centrality values in the group with higher Eκ values were indicated in the auditory cortex bilaterally, both anterior and posterior cingulate cortex, the anterior fronto-median cortex, and the Rolandic operculum. The group with lower Eκ values showed higher centrality values in the lateral geniculate body bilaterally as well as in the visual cortex (V1). The analysis of the structural brain data showed a positive correlation between neuroticism and volume of the left amygdala in a ROI analysis of the amygdala. A comparison of the structural data between individuals with high and low Eκ values revealed a group difference in the right subiculum of the hippocampal formation (individuals with high Eκ values had larger grey matter volume).

6.4.2 Relations between cardiac and NEO measures

In each experiment the group with higher Eκ values had higher extraversion scores. This replicates results of a previous experiment (Koelsch et al. 2012), thus up to now data from three independent samples show higher extraversion scores in individuals with higher Eκ values. In addition, as in our previous study, scores of positive emotion (a facet of extraversion) were higher in the group with higher Eκ values in experiment 1 (although not in experiment 2). These findings support the notion that Eκ reflects aspects of the emotional personality of an individual. This notion is also corroborated by the behavioral ratings about the emotional states of participants (obtained after each stimulus in experiment 1), which showed that Eκ was related to felt arousal and fear. However, as a note of caution, the relation between Eκ and neuroticism observed in our previous study (Koelsch et al. 2012) was not replicated by the present results, and contrary to our hypotheses, our results did not show relations between Eκ values and tender-mindedness, nor between Eκ values and warmth (although these two NEO facets are conceptually related to tender emotionality). Hence, Eκ does not reflect the constructs of “friendliness towards others”, and “sympathy for others” as measured with the NEO-PI-R facets of warmth and tender-mindedness. Moreover, the present results call the relation between Eκ and neuroticism (as previously observed; Koelsch et al. 2012) into question. To further investigate to which degree Eκ actually reflects tender emotionality, future studies might thus better use questionnaires that are more specifically designed to assess positive emotion, attachment-related emotions, compassion and empathy.

As outlined in Box 1, personality-specific modulation of regional cardiac activity is likely to be due to the influence of psychological factors on activity of neurons within the cardiac nerve plexus. Such influence includes (a) autonomic activity and sympathovagal balance (a major reaction component of emotion, and thus of emotional personality), (b) limbic/paralimbic modulation of efferent autonomic outflow to the heart, (c) hemispheric weighting of emotional activity and corresponding asymmetric autonomic outflow, as well as (d) central nervous system processes that regulate circulating hormones (Armour, Ardell, 2004). The exact mechanisms involved in psychological modulation of regional heart activity are yet unknown.

Notably, compared to personality questionnaires, the cardiac measure used in the present study does not face the problem of potential subjective bias such as socially desirable responding, inaccuracies in self-perception, self-favouring tendencies, self-deception, and moralistic bias (Costa, McCrae, 1992; Paulhus, 1986; Barrick, Mount, 1996; Paulhus, John, 1998; Pauls, Stemmler, 2003) although, on the other hand, it may well be influenced by biological factors unrelated to personality, as mentioned in the Introduction. Therefore, combinations of biomarkers such as the cardiac measure used in the present study, or similar cardiac indices (Koelsch et al. 2012), with standardized personality questionnaires might lead to a substantial improvement in the assessment of personality and in the investigation of neural correlates of emotional personality. To investigate a possible gain from combining questionnaire and ECG measures of personality, future studies could obtain data from healthy controls and from patients (e.g. from individuals with depression, or with a personality disorder such as schizoid personality disorder) and investigate whether the combination of NEO and ECG scores (as compared to using either only ECG or only NEO scores) significantly increases the discrimination of the two groups.

6.4.3 The functional significance of the hippocampal formation for emotional personality

The present results reveal a link between regional cardiac activity on the one hand, and both function as well as structure of the subiculum of the hippocampal formation on the other. Regional cardiac activity was reflected in the Eκ values, i.e. in the relations of ECG amplitudes recorded at different ECG leads (cf. Figure 1). It is unlikely that the relations of amplitudes as captured in Eκ are simply due to different levels of cardiovascular stress: body mass index (BMI) was in both groups within the normal range (mean BMI, averaged across all participants of Experiments 1 and 2, was 21.8 (SD = 2.9) in the group with higher Eκ, and 23.0 (SD = 3.0) in the group with lower Eκ values, with no significant difference between groups), and both groups consisted of young adults without cardiovascular disease. This also renders it likely that blood pressure did not differ between groups (similar to our previous study (Koelsch et al. 2007), although blood pressure was not obtained in the present study. In addition, our previous investigations (Koelsch et al. 2007) indicated that Eκ values do not correlate with serum concentrations of N-terminal pro-brain natriuretic peptide (and are thus not related to left-ventricular hypertrophy). Hence, the association between Eκ values and hippocampal activity does not appear to originate simply from different levels of cardiovascular stress. Instead, in light of the associations between Eκ values and personality measures observed in the present as well as in previous studies, the present data corroborate the notion that the hippocampal formation plays a role for emotional personality.

In cognitive neuroscience, the hippocampus is best known for its role for learning and memory (Moscovitch et al. 2006), as well as for novelty and expectedness (Nadel, 2008). In addition, however, a plethora of evidence shows that the hippocampus also plays an important role for emotional processes: For example, the hippocampus is substantially involved in the regulation of the hypothalamic-pituitary-adrenal (HPA) axis stress response (Jacobson, Sapolsky, 1991), and hippocampal neurons are uniquely vulnerable to emotional stressors (Warner-Schmidt, Duman, 2006). Particularly the subiculum is substantially involved in the regulation of HPA axis activity, and profoundly affected by emotional stress (O’Mara, 2005). The fact that the subiculum has dense connections to numerous hypothalamic nuclei (in addition to connections with many other subcortical and cortical structures; O’Mara 2005) makes it highly likely that the subiculum has modulatory influence on cardiac activity via endocrine and autonomic neurons located in the hypothalamus. Therefore, physiology lends plausibility to the notion that, in humans, emotional personality is at least in part associated with hippocampal activity, and that such activity modulates regional heart activity. The notion that the hippocampal formation is a neural substrate involved in tender emotion is consistent with the view that the hippocampal formation generates attachment-related affects that are perceived by humans as tender feelings (Koelsch, 2010a). Attachment-related behaviour includes kissing, caressing, hugging, softly touching, softly vocalizing, and in animals behaviours such as licking, grooming, nest-building, and pup retrieval. Several lines of evidence point to the involvement of the hippocampus in attachment-related emotions: (1) Lesions of the hippocampus lead to impairment of maternal behaviour in rats as indexed by less frequent and less efficient nursing, poorer nest building, increased maternal cannibalism, poorer pup retrieving, and fewer pups surviving to weaning (Kimble et al. 1967). On the other hand, increased pup licking, grooming and nursing by rat mothers leads to increased hippocampal glucocorticoid receptor messenger RNA expression in the offspring (Liu et al. 1997), influences hippocampal synaptic development in the offspring (Meaney, 2001), and alters the offspring epigenome at a glucocorticoid receptor gene promoter in the hippocampus (Weaver et al. 2004). (2) The hippocampus is damaged by chronic emotional stressors, particularly by helplessness and despair (Warner-Schmidt, Duman, 2006). The hippocampus is unique in its vulnerability to emotional stressors, and presumably the only brain structure in which severe emotional stress can lead to the death of neurons (in addition to neuronal death, the volume reduction of the hippocampus in response to severe chronic emotional stress is due to reduced neurogenesis in the dentate gyrus of the hippocampal formation). (3) Dysfunction and structural damage of this structure has been observed in individuals suffering from post-traumatic stress disorder (PTSD) such as Vietnam veterans who witnessed extreme violence or committed extremely violent acts (Brenner, 1999); similar findings have been reported for individuals that were sexually abused during childhood (Stein et al. 1997). Moreover, both dysfunction and volume reduction of the hippocampal formation has been observed in depressive patients (Videbech, Ravnkilde, 2004). Our results show that even in healthy, non-clinical individuals, hippocampal volume and hippocampal activity is related to regional heart activity as reflected in Eκ values (and, thus, presumably to tender emotionality). Whether the group differences in hippocampal volume are due to subclinical trauma in individuals with low Eκ, or due to use-dependent hippocampal plasticity in individuals with higher Eκ, remains to be specified. (4) Numerous functional neuroimaging studies with healthy adults indicate signal changes in the hippocampal formation in response to pleasurable, joyful music (Koelsch, 2010). This association between hippocampal activity and music-evoked feelings of joy has been linked in part to the social functions of music, such as communication, cooperation, and social cohesion, thus to functions that serve the formation of interindividual attachments.

Group differences in the hippocampal formation were observed in the right hemisphere, in both functional and structural experiments of the present study, as well as in two previous functional neuroimaging experiments (Koelsch et al. 2007). As mentioned in the Introduction, the left and right hemispheres of the human forebrain have different associations with particular emotions and affective traits (Craig, 2005), probably due to an asymmetrical representation of homeostatic activity that originates from asymmetries in the peripheral autonomic nervous system (Chechetto, 2004; Sander, Klingelhöfer, 1995; Zamrini et al. 1990). Lesion studies indicate a right-hemispheric dominance for sympathetic efferent neuronal effects, and stimulation of the right anterior insular cortex elicits increases in heart rate and blood pressure (whereas left anterior insular stimulation decreases heart rate; Chechetto, 2004; Sander, Klingelhöfer, 1995; Zamrini et al. 1990). Thus, the right-lateralization of hippocampal activity possibly originates from a more dynamic emotional activity involving increased sympathetic tone in individuals with high Eκ.

This notion is supported by two previous experiments showing higher heart-rate variability in individuals with high Eκ (compared to individuals with low Eκ; Koelsch et al. 2007; Koelsch et al. 2012), indicating a stronger tone of the sympathetic branch of the autonomic nervous system in individuals with high Ek.

6.4.4 Limitations

Although the present results corroborate relations between Eκ and psychological (NEO) measures of personality (in both experiments, individuals with higher Eκ had higher extraversion scores, as in previous studies), it remains arguable to which degree Eκ is a valid measure of tender emotionality. This could, for example, be investigated further in studies that perform diagnostic interviews, conducted by independent raters, to test whether a classification based on Eκ corresponds to the interview-based classification.

Moreover, it has previously been noted (Yarkoni 2009) that in experiments with relatively small sample sizes (such as $n = 22$, as in our functional experiment), only a fraction of the effects that really exist might be detected, and that results might promote the illusion of highly selective activations. Thus, as noted above, the effects we observed in the functional experiment might not be as selective as observed, and there might be more potential results that have been missed due to the relatively small sample size.

6.5 Conclusions

This study has three main conclusions: *First*, our data are the first to show personality-characteristic computational hubs in the brain (identified using Eigenvector Centrality Mapping). Results substantiate previous studies reporting associations between agreeableness and function of the DLPFC, as well as between tender (positive) emotionality and (right) hippocampal function. In addition, they reveal an association between agreeableness and function of the ventral striatum (including nucleus accumbens), possibly related to the rewarding nature of altruism and cooperation. *Second*, the structural data substantiate associations between neuroticism and amygdalar volume, and are the first to show an association between volume of the hippocampal formation and regional cardiac activity taken to reflect emotional personality. The latter association was revealed in virtually the same aspect of the right subiculum as in the functional data. Thus, along with previous reports on this issue, there is substantial convergence and replicability of functional and structural associations between a cardiac measure related to emotional personality and the hippocampal formation. This indicates a new role of the hippocampal formation in human emotional personality (in addition to its well-known role for cognition). Previous studies showed associations between structure and function of the hippocampal formation in clinical populations (such as patients with depression, PTSD, or borderline personality disorder). Our results indicate that in healthy individuals function and structure of the hippocampal formation is associated with human emotional personality. *Third*, results demonstrate that based on a cardiac measure, consistent and replicable results can be obtained in the analysis of functional as well as structural neuroimaging data, in addition to replicable associations between this cardiac measure and extraversion (and, in part, positive emotion as obtained with the NEO inventory). This substantiates that ECG amplitude relations are useful biomarkers for effects of emotional personality on regional heart activity. The replicability and consistency of results obtained with the cardiac index used in the present study (as compared with results obtained using personality questionnaires) thus motivates to investigate further cardiac indices of personality, and to combine both psychological and physiological measures of emotional personality.

6.6 Acknowledgment

The authors would like to thank Corinna Bonhage and Ronny Enk for their help during data acquisition.

6.7 References

Adams D, Cuevas J (2004) Electrophysiological properties of intrinsic cardiac neurons. In: Armour J, Ardell J, editors, Basic and clinical neurocardiology, Oxford University Press. pp.

1–60.

Amunts K, Kedo O, Kindler M, Pieperhoff P, Mohlberg H, et al. (2005) Cytoarchitectonic mapping of the human amygdala, hippocampal region and entorhinal cortex: intersubject variability and probability maps. Anatomy and embryology 210: 343–352.

Ardell J (2004) Intrathoracic neuronal regulation of cardiac function. In: Armour J, Ardell J, editors, Basic and clinical neurocardiology, Oxford University Press. pp. 118–152.

Armour J, Kember G (2004) Cardiac sensory neurons. In: Armour J, Ardell J, editors, Basic and clinical neurocardiology, Oxford University Press. pp. 79–117.

Ashburner J, Friston KJ (1999) Nonlinear spatial normalization using basis functions. Human brain mapping 7: 254–66.

Ashburner J, Friston KJ (2005) Unified segmentation. NeuroImage 26: 839–51.

Ashburner J (2007) A fast diffeomorphic image registration algorithm. NeuroImage 38: 95–113.

Ashburner J (2009) Computational anatomy with the SPM software. Magnetic resonance imaging 27: 1163–74.

Ashburner J, Friston KJ (2009) Computing average shaped tissue probability templates. NeuroImage 45: 333–41.

Barrick MR, Mount MK (1996) Effects of impression management and self-deception on the predictive validity of personality constructs. Journal of Applied Psychology 81: 261–272.

Barros-Loscertales A, Meseguer V, Sanjuan A, Belloch V, Parcet M, et al. (2006) Behavioural inhibition system activity is associated with increased amygdala and hippocampal gray matter volume: a voxel-based morphometry study. Neuroimage 33: 1011–1015.

Bergouignan L, Chupin M, Czechowska Y, Kinkingnéhun S, Lemogne C, et al. (2009) Can voxel based morphometry, manual segmentation and automated segmentation equally detect hippocampal volume differences in acute depression? NeuroImage 45: 29–37.

Borkenau P, Ostendorf F (1993) NEO-Fünf-Faktoren-Inventar:(NEO-FFI) nach Costa und McCrae. Hogrefe Göttingen.

Bremner J (1999) Does stress damage the brain? Biological Psychiatry 45: 797–805.

Britton J, Ho S, Taylor S, Liberzon I (2007) Neuroticism associated with neural activation patterns to positive stimuli. Psychiatry Research: Neuroimaging 156: 263–267.

Brück C, Kreifelts B, Kaza E, Lotze M, Wildgruber D (2011) Impact of personality on the cerebral processing of emotional prosody. NeuroImage 58: 259–268.

Canli T, Zhao Z, Desmond J, Kang E, Gross J, et al. (2001) An fMRI study of personality influences on brain reactivity to emotional stimuli. Behavioural neuroscience 115: 33.

Canli T, Sivers H, Whitfield S, Gotlib I, Gabrieli J (2002) Amygdala response to happy faces as a function of extraversion. Science 296: 2191.

Canli T, Amin Z, Haas B, Omura K, Constable R (2004) A double dissociation between mood states and personality traits in the anterior cingulate. Behavioural Neuroscience 118: 897.

Canli T (2006) Biology of personality and individual differences. The Guilford Press.

Cardinal R, Pagé P (2004) Neuronal modulation of atrial and ventricular electrical properties. In: Armour J, Ardell J, editors, Basic and clinical neurocardiology, Oxford University Press. pp. 315–339.

Chechetto D (2004) Forebrain control of healthy and diseased hearts. In: Armour J, Ardell J, editors, Basic and clinical neurocardiology, Oxford University Press. pp. 220–251.

Chen W, Kato T, Zhu X, Ogawa S, Tank D, et al. (1998) Human primary visual cortex and lateral geniculate nucleus activation during visual imagery. Neuroreport 9: 3669–3674.

Chen S, Ross T, Zhan W, Myers C, Chuang K, et al. (2008) Group independent component analysis reveals consistent resting-state networks across multiple sessions. Brain research 1239: 141.

Cloninger C (2000) Biology of personality dimensions. Current Opinion in Psychiatry 13: 611.

Cohen M, Young J, Baek J, Kessler C, Ranganath C (2005) Individual differences in extraversion and dopamine genetics predict neural reward responses. Cognitive Brain Research 25: 851–861.

Costa P, McCrae R (1992) Revised neo personality inventory (NEO PI-R) and neo five-factor inventory (NEO-FFI). Psychological Assessment Resources Odessa, FL.

Craig A (2005) Forebrain emotional asymmetry: a neuroanatomical basis? Trends in Cognitive Sciences 9: 566–571.

Craig A (2009) How do you feel–now? The anterior insula and human awareness. Nat Rev Neurosci 10: 59–70.

Cremers H, van Tol M, Roelofs K, Aleman A, Zitman F, et al. (2011) Extraversion is linked to volume of the orbitofrontal cortex and amygdala. PloS one 6: e28421.

Critchley H (2005) Neural mechanisms of autonomic, affective, and cognitive integration. The Journal of Comparative Neurology 493: 154–166.

Critchley H, Taggart P, Sutton P, Holdright D, Batchvarov V, et al. (2005) Mental stress and sudden cardiac death: asymmetric midbrain activity as a linking mechanism. Brain 128: 75.

Critchley H, Nagai Y, Gray M, Mathias C (2011) Dissecting axes of autonomic control in humans: insights from neuroimaging. Autonomic Neuroscience 161: 34–42.

Davidson R (2001) Toward a biology of personality and emotion. Annals of the New York Academy of Sciences 935: 191–207.

Deckersbach T, Miller K, Klibanski A, Fischman A, Dougherty D, et al. (2006) Regional cerebral brain metabolism correlates of neuroticism and extraversion. Depression and anxiety 23: 133–138.

Deichmann R, Josephs O, Hutton C, Corfield D, Turner R (2002) Compensation of susceptibility-induced bold sensitivity losses in echo-planar fMRI imaging. Neuroimage 15: 120–135.

Deichmann R, Gottfried J, Hutton C, Turner R (2003) Optimized EPI for fMRI studies of the orbitofrontal cortex. Neuroimage 19: 430–441.

DeYoung C, PETerson J, Higgins D (2005) Sources of openness/intellect: Cognitive and neuropsychological correlates of the fifth factor of personality. Journal of personality 73: 825–858.

DeYoung C, Hirsh J, Shane M, Papademetris X, Rajeevan N, et al. (2010) Testing predictions from personality neuroscience. Psychological Science 21: 820.

Eerola T, Toiviainen P (2004) Mir in matlab: The midi toolbox. In: Proceedings of the International Conference on Music Information Retrieval. Citeseer, pp. 22–27.

Eickhoff S, Stephan K, Mohlberg H, Grefkes C, Fink G, et al. (2005) A new spm toolbox for combining probabilistic cytoarchitectonic maps and functional imaging data. Neuroimage 25: 1325–1335.

Eisenberger N, Lieberman M, Satpute A (2005) Personality from a controlled processing perspective: An fMRI study of neuroticism, extraversion, and self-consciousness. Cognitive, Affective, & Behavioural Neuroscience 5: 169–181.

Eysenck H (1967) The biological basis of personality. Transaction Pub.

Fischer H, Wik G, Fredrikson M (1997) Extraversion, neuroticism and brain function: A PET study of personality. Personality and Individual Differences 23: 345–352.

Forsman L, de Manzano Ö, Karabanov A, Madison G, Ullén F (2012) Differences in regional brain volume related to the extraversion-introversion dimension–a voxel based morphometry study. Neuroscience Research : 59-67.

Fritz T, Jentschke S, Gosselin N, Sammler D, Peretz I, et al. (2009) Universal recognition of three basic emotions in music. Current Biology 19: 573–576.

Frokjaer V, Mortensen E, Nielsen F, Haugbol S, Pinborg L, et al. (2008) Frontolimbic serotonin 2a receptor binding in healthy subjects is associated with personality risk factors for affective disorder. Biological psychiatry 63: 569–576.

Gabrielson A, Juslin P (2003) Emotional expression in music. In: Davidson R, Scherer K, Goldsmith H, editors, Handbook of Affective Sciences, New York: Oxford University Press. pp. 503–534.

Gagnon C, Ramachandruni S, Bragdon E, Sheps D (2004) Psychological aspects of heart disease. In: Armour J, Ardell J, editors, Basic and clinical neurocardiology, Oxford University Press. pp. 393–418.

Gardini S, Cloninger C, Venneri A (2009) Individual differences in personality traits reflect structural variance in specific brain regions. Brain research bulletin 79: 265–270.

Good CD, Johnsrude IS, Ashburner J, Henson RN, Friston KJ, et al. (2001) A voxel-based morphometric study of ageing in 465 normal adult human brains. NeuroImage 14: 21–36.

Gray M, Harrison N, Wiens S, Critchley H (2007) Modulation of emotional appraisal by false physiological feedback during fMRI. PLoS One 2: e546.

Gray M, Rylander K, Harrison N, Wallin B, Critchley H (2009) Following one's heart: cardiac rhythms gate central initiation of sympathetic reflexes. The Journal of Neuroscience 29: 1817–1825.

Haas B, Omura K, Amin Z, Constable R, Canli T (2006) Functional connectivity with the anterior cingulate is associated with extraversion during the emotional stroop task. Social Neuroscience, 1: 16–24.

Haas B, Omura K, Constable R, Canli T (2007) Is automatic emotion regulation associated with agreeableness? Psychological Science 18: 130–132.

Hooker C, Verosky S, Miyakawa A, Knight R, D'Esposito M (2008) The influence of personality on neural mechanisms of observational fear and reward learning. Neuropsychologia 46: 2709–2724.

Horackova M (2004) Colocalization of Multiple Neurochemicals in Mammalian Intrathoracic Neurons. In: Armour J, Ardell J, editors, Basic and clinical neurocardiology, Oxford University Press. pp. 61–75.

Hu X, Erb M, Ackermann H, Martin J, Grodd W, et al. (2011) Voxel-based morphometry studies of personality: Issue of statistical model specificationâ”effect of nuisance covariates. Neuroimage 54: 1994–2005.

Iidaka T, Matsumoto A, Ozaki N, Suzuki T, Iwata N, et al. (2006) Volume of left amygdala subregion predicted temperamental trait of harm avoidance in female young subjects. a voxel-based morphometry study. Brain research 1125: 85–93.

Irwin M (2008) Human psychoneuroimmunology: 20 years of discovery. Brain, Behavior, and Immunity 22: 129–139.

Jacobson L, Sapolsky R (1991) The role of the hippocampus in feedback regulation of the hypothalamic-pituitary-adrenocortical axis. Endocrine reviews 12: 118–134.

Kalbitzer J, Frokjaer V, Erritzoe D, Svarer C, Cumming P, et al. (2009) The personality trait openness is related to cerebral 5-HTT levels. Neuroimage 45: 280–285.

Kimble D, Rogers L, Hendrickson C (1967) Hippocampal lesions disrupt maternal, not sexual, behavior in the albino rat. Journal of Comparative and Physiological Psychology 63: 401–407.

Klein A, Andersson J, Ardekani BA, Ashburner J, Avants B, et al. (2009) Evaluation of 14 nonlinear deformation algorithms applied to human brain MRI registration. NeuroImage 46: 786–802.

Koelsch S, Fritz T, Cramon DY, Müller K, Friederici AD (2006) Investigating emotion with music: An fMRI study. Human Brain Mapping 27: 239–250.

Koelsch S, Remppis A, Sammler D, Jentschke S, Mietchen D, et al. (2007) A cardiac signature of emotionality. European Journal of Neuroscience 26: 3328–3338.

Koelsch S (2010) Towards a neural basis of music-evoked emotions. Trends in Cognitive Sciences 14: 131–137.

Koelsch S, Offermanns K, Franzke P (2010a) Music in the Treatment of Affective Disorders: An Exploratory Investigation of a New Method for Music-Therapeutic Research. Music Perception 27: 307–316.

Koelsch S, Siebel WA, Fritz T (2010b) Functional neuroimaging of emotion with music. In: Juslin P, Sloboda J, editors, Handbook of Music and emotion: Theory, Research, Applications, 2nd ed., Oxford: Oxford University Press Oxford. pp. 313–346.

Koelsch S, Fuermetz J, Sack U, Bauer K, Hohenadel M, et al. (2011) Effects of music listening on cortisol levels and propofol consumption during spinal anesthesia. Frontiers in Psychology 2: 1-9.

Koelsch S, Enge J, Jentschke S (2012) Cardiac signatures of personality. PloS one 7: e31441.

Kumari V, Williams S, Gray J, et al. (2004) Personality predicts brain responses to cognitive demands. The Journal of neuroscience 24: 10636–10641.

Lane R, Schwartz G (1987) Induction of lateralized sympathetic input to the heart by the cns during emotional arousal: A possible neurophysiologic trigger of sudden cardiac death. Psychosomatic medicine 49: 274–284.

LeDoux J (2000) Emotion circuits in the brain. Ann Rev Neurosci 23: 155 – 184.

Liu D, Diorio J, Tannenbaum B, Caldji C, Francis D, et al. (1997) Maternal care, hippocampal glucocorticoid receptors, and hypothalamic-pituitary-adrenal responses to stress. Science 277: 1659–1662.

Lohmann G, Müller K, Bosch V, Mentzel H, Hessler S, et al. (2001) Lipsia - a new software system for the evaluation of functional magnet resonance images of the human brain. Computerized Medical Imaging and Graphics 25: 449–457.

Lohmann G, Neumann J, Müller K, Lepsien J, Turner R (2008) The multiple comparison problem in fMRI – a new method based on anatomical priors. In: Workshop on Analysis of Functional Medical Images, New York University.

Lohmann G, Margulies D, Horstmann A, Pleger B, Lepsien J, et al. (2010) Eigenvector Centrality Mapping for Analyzing Connectivity Patterns in fMRI Data of the Human Brain. PLoS-one 5: e10232.

Malik M, Bigger J, Camm A, Kleiger R, Malliani A, et al. (1996) Task Force of the European Society of Cardiology and the North American Society of Pacing and Electrophysiology. Heart rate variability: standards of measurement, physiological interpretation, and clinical use. Circulation 93: 1043.

Meaney M (2001) Maternal care, gene expression, and the transmission of individual differences in stress reactivity across generations. Neuroscience 24.

Medford N, Critchley H (2010) Conjoint activity of anterior insular and anterior cingulate cortex: awareness and response. Brain Structure and Function 214: 535–549.

Moscovitch M, Nadel L, Winocur G, Gilboa A, Rosenbaum R (2006) The cognitive neuroscience of remote episodic, semantic and spatial memory. Current Opinion in Neurobiology 16: 179–190.

Murray E (2007) The amygdala, reward and emotion. Trends in cognitive sciences 11: 489–497.

Nadel L (2008) Hippocampus and context revisited. In: Mizumori S, editor, Hippocampal place fields: relevance to learning and memory, New York: Oxford University Press. pp. 3–15.

Nieuwenhuys R, Voogd J, Huijzen CV (2008) The Human Central Nervous System. Berlin: Springer.

O’Mara S (2005) The subiculum: what it does, what it might do, and what neuroanatomy has yet to tell us. Journal of anatomy 207: 271–282.

Omura K, Todd Constable R, Canli T (2005) Amygdala gray matter concentration is associated with extraversion and neuroticism. Neuroreport 16: 1905.

Ostendorf F, Angleitner A (2004) NEO-Persönlichkeitsinventar (NEO-PI-R) nach Costa und McCrae. Göttingen: Hogrefe .

Pauls C, Stemmler G (2003) Substance and bias in social desirability responding. Personality and Individual Differences 35: 263–275.

Paulhus D (1986) Self-deception and impression management in test responses. Personality assessment via questionnaire : 143–165.

Paulhus D, John O (1998) Egoistic and moralistic biases in self-perception: The interplay of self-deceptive styles with basic traits and motives. Journal of personality 66: 1025–1060.

Paulus M, Rogalsky C, Simmons A, Feinstein J, Stein M (2003) Increased activation in the right insula during risk-taking decision making is related to harm avoidance and neuroticism. Neuroimage 19: 1439–1448.

Petrides M, Pandya D (1999) Dorsolateral prefrontal cortex: comparative cytoarchitectonic analysis in the human and the macaque brain and corticocortical connection patterns. European Journal of Neuroscience 11: 1011–1036.

Price J, Drevets W (2012) Neural circuits underlying the pathophysiology of mood disorders. Trends in cognitive sciences 16: 61–71.

Rauch S, Milad M, Orr S, Quinn B, Fischl B, et al. (2005) Orbitofrontal thickness, retention of fear extinction, and extraversion. Neuroreport 16: 1909.

Salimpoor V, Benovoy M, Larcher K, Dagher A, Zatorre R (2011) Anatomically distinct dopamine release during anticipation and experience of peak emotion to music. Nature neuroscience 14: 257–262.

Sander D, Klingelhöfer J (1995) Changes of circadian blood pressure patterns and cardiovascular parameters indicate lateralization of sympathetic activation following hemispheric brain infarction. Journal of neurology 242: 313–318.

Scherer KR (2000) Emotions as episodes of subsystem synchronization driven by nonlinear appraisal processes. In: Lewis M, Granic I, editors, Emotion, development, and self-organization: Dynamic systems approaches to emotional development, Cambridge Univ. Press. pp. 70–99.

Schutter D, Koolschijn P, Peper J, Crone E (2012) The cerebellum link to neuroticism: A volumetric MRI association study in healthy volunteers. PLoS ONE 7: e37252.

Sporns O, Honey C (2006) Small worlds inside big brains. Proceedings of the National Academy of Sciences 103: 19219.

Stein M, Koverola C, Hanna C, Torchia M, McClarty B (1997) Hippocampal volume in women victimized by childhood sexual abuse. Psychological Medicine 27: 951–959.

Steinbeis N, Koelsch S (2008) Understanding the intentions behind man-made products elicits neural activity in areas dedicated to mental state attribution. Cerebral Cortex 19: 619-623.

Steinbeis N, Bernhardt B, Singer T (2012) Impulse control and underlying functions of the left dlpfc mediate age-related and age-independent individual differences in strategic social behavior. Neuron 73: 1040–1051.

Sylvester C, Corbetta M, Raichle M, Rodebaugh T, Schlaggar B, et al. (2012) Functional network dysfunction in anxiety and anxiety disorders. Trends in Neurosciences .

Tauscher J, Bagby R, Javanmard M, Christensen B, Kasper S, et al. (2001) Inverse relationship between serotonin 5-HT1A receptor binding and anxiety: a [11C] WAY-100635 PET investigation in healthy volunteers. American Journal of Psychiatry 158: 1326–1328.

Tomasi D, Volkow N (2011) Association between functional connectivity hubs and brain networks. Cerebral Cortex 21: 2003–2013.

Vaidya J, Paradiso S, Andreasen N, Johnson D, Ponto L, et al. (2007) Correlation between extraversion and regional cerebral blood flow in response to olfactory stimuli. American Journal of Psychiatry 164: 339–341.

Videbech P, Ravnkilde B (2004) Hippocampal volume and depression: a meta-analysis of MRI studies. American Journal of Psychiatry 161: 1957-1966.

Warner-Schmidt J, Duman R (2006) Hippocampal neurogenesis: opposing effects of stress and antidepressant treatment. Hippocampus 16: 239–249.

Weaver I, Cervoni N, Champagne F, D'Alessio A, Sharma S, et al. (2004) Epigenetic programming by maternal behavior. Nature neuroscience 7: 847–854.

Weiskopf N, Hutton C, Josephs O, Turner R, Deichmann R (2007) Optimized epi for fMRI studies of the orbitofrontal cortex: compensation of susceptibility-induced gradients in the readout direction. Magnetic Resonance Materials in Physics, Biology and Medicine 20: 39–49.

Wittgenstein L (1984) Philosophische Untersuchungen. Frankfurt: Suhrkamp.

Wolkowitz O, Rothschild A (2003) Psychoneuroendocrinology: the scientific basis of clinical practice. American Psychiatric Pub.

Wright C, Williams D, Feczko E, Barrett L, Dickerson B, et al. (2006) Neuroanatomical correlates of extraversion and neuroticism. Cerebral Cortex 16: 1809–1819.

Wright C, Feczko E, Dickerson B, Williams D (2007) Neuroanatomical correlates of personality in the elderly. Neuroimage 35: 263–272.

Yamasue H, Abe O, Suga M, Yamada H, Inoue H, et al. (2008) Gender-common and-specific neuroanatomical basis of human anxiety-related personality traits. Cerebral Cortex 18: 46–52.

Yarkoni, T. (2009). Big correlations in little studies: Inflated fMRI correlations reflect low statistical power – Commentary on Vul et al.(2009). Perspectives on Psychological Science, 4(3), 294-298.

Yassa MA, Stark CEL (2009) A quantitative evaluation of cross-participant registration techniques for MRI studies of the medial temporal lobe. NeuroImage 44: 319–27.

Zamrini E, Meador K, Loring D, Nichols F, Lee G, et al. (1990) Unilateral cerebral inactivation produces differential left/right heart rate responses. Neurology 40: 1408–1408.

Zuckerman, M. (1991). *Psychobiology of personality* (Vol. 10). Cambridge University Press.

6.8 Supplementary Material

Supplemental Table S1: List of Stimuli

Composer / artist	Title	ASIN Nr.
Joy-evoking		
Joël Francisco Perri	El Canto de Mi Antara	B002BEXEHO
Craobh Rua	The Luck Penny	B000003NHN
Scotch Mist	Shetland Tune	n/a
Alfredo de Angelis	Pregonera	B001P5LDTQ
Orchestra Paraschiv Oprea	Batuta de la Adancata	B00000DTI6
Louis Armstrong	St. Louis Blues	B006CBVRJY
Niccolò Paganini	Violin Concerto No. 1, 3rd movement	B000001GHC
Jonathan Richman	Egyptian Reggae	B00580D1IU
Fear-evoking		
Danny Elfman	The Killing	B00000JC9R
Michael Giacchino	Monsters Are Such Interesting People (from: Lost)	B000EHSVDM
Michael Giacchino	Just Another Day on the Beach (from: Lost)	B000I2IQ9M
Michael Giacchino	Charlie's Dream (from: Lost)	B000I2IQ9M
Takeshi Miura et al.	Pulsating Right Arm (from: Biohazard Code)	B00005HWMB
Seiko Kobuchi	Boss Battle (from: Biohazard Zero)	n/a
Masami Ueda & Saori Maeda	Cold Sweat (from: Biohazard 3)	B000058A7Y
Akihiko Matsumoto et al.	Freezer Burn (from: Resident Evil Outbreak)	B00019257G

Supplemental Table S2: Descriptive statistics of questionnaire scores. Abbreviations: M: arithmetic mean; SEM: standard error of mean; PR: percentile rank of the scores; p: probability of deviation from normality tested using Shapiro-Wilk test.

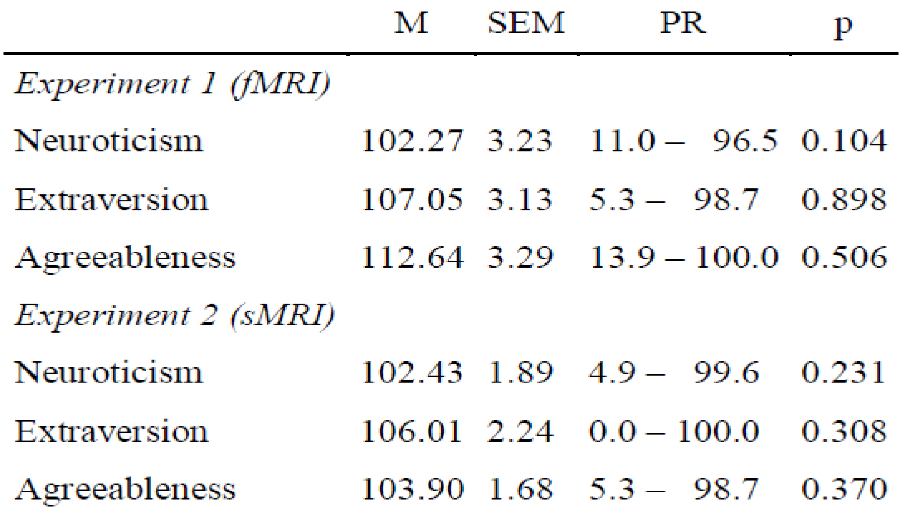

	M	SEM	PR	p
Experiment 1 (fMRI)				
Neuroticism	102.27	3.23	11.0 – 96.5	0.104
Extraversion	107.05	3.13	5.3 – 98.7	0.898
Agreeableness	112.64	3.29	13.9 – 100.0	0.506
Experiment 2 (sMRI)				
Neuroticism	102.43	1.89	4.9 – 99.6	0.231
Extraversion	106.01	2.24	0.0 – 100.0	0.308
Agreeableness	103.90	1.68	5.3 – 98.7	0.370

Supplemental Table S3. Statistics of NEO scales (neuroticism, extraversion, agreeableness) and NEO facets (warmth, positive emotion, tender-mindedness). Data are shown separately for the groups with higher and lower values, and separately for the structural experiment (Exp. 1) and the functional experiment (Exp. 2). Scores of neuroticism, extraversion, and agreeableness are standard scores. Scores of warmth, positive emotion, and tender-mindedness are T-scores. The outermost right column shows t values (with p values in parentheses) for the comparison between groups with higher and lower values. Degrees of freedom for the group comparisons were 57 in Exp. 1, and 20 for Exp. 2.

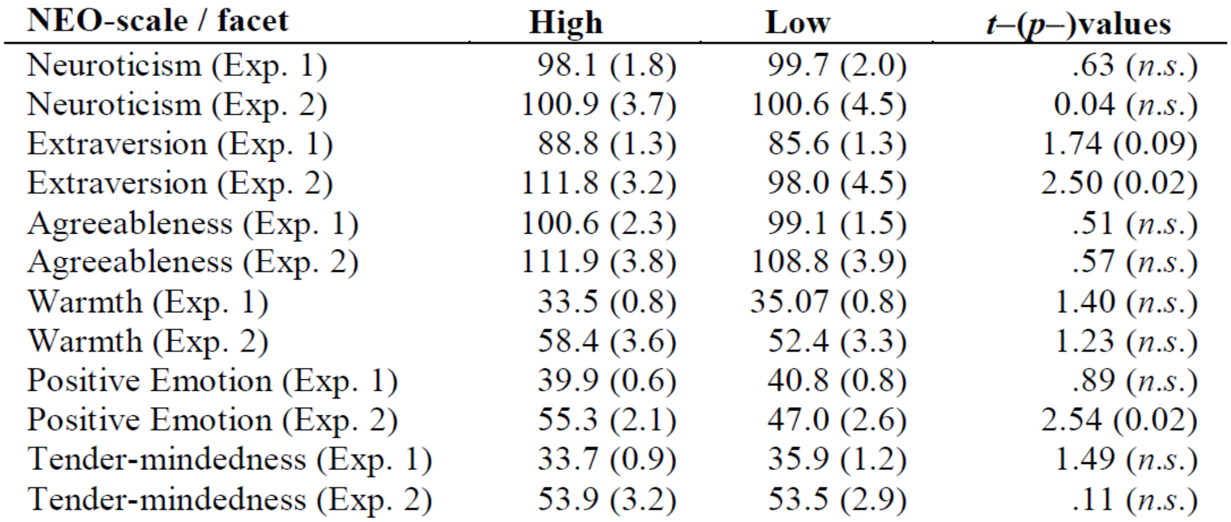

NEO-scale / facet	**High**	**Low**	***t*–(*p*–)values**
Neuroticism (Exp. 1)	98.1 (1.8)	99.7 (2.0)	.63 (*n.s.*)
Neuroticism (Exp. 2)	100.9 (3.7)	100.6 (4.5)	0.04 (*n.s.*)
Extraversion (Exp. 1)	88.8 (1.3)	85.6 (1.3)	1.74 (0.09)
Extraversion (Exp. 2)	111.8 (3.2)	98.0 (4.5)	2.50 (0.02)
Agreeableness (Exp. 1)	100.6 (2.3)	99.1 (1.5)	.51 (*n.s.*)
Agreeableness (Exp. 2)	111.9 (3.8)	108.8 (3.9)	.57 (*n.s.*)
Warmth (Exp. 1)	33.5 (0.8)	35.07 (0.8)	1.40 (*n.s.*)
Warmth (Exp. 2)	58.4 (3.6)	52.4 (3.3)	1.23 (*n.s.*)
Positive Emotion (Exp. 1)	39.9 (0.6)	40.8 (0.8)	.89 (*n.s.*)
Positive Emotion (Exp. 2)	55.3 (2.1)	47.0 (2.6)	2.54 (0.02)
Tender-mindedness (Exp. 1)	33.7 (0.9)	35.9 (1.2)	1.49 (*n.s.*)
Tender-mindedness (Exp. 2)	53.9 (3.2)	53.5 (2.9)	.11 (*n.s.*)

Experiment 1: Description of stimuli

Musical stimuli were selected to evoke (a) feelings of joy, (b) feelings of fear, or (c) neither joy nor fear (henceforth referred to as neutral stimuli). There were n=8 stimuli per category, and each stimulus was presented twice during the experiment. The complete list of joyful and fearful stimuli is provided in Supplementary Table S1. Behavioral data showed that musical stimuli evoked the intended feelings in our study population: Mean joy ratings (with standard deviation in parentheses), on a scale from 1 = “evokes no joy at all” to 6 = “evokes very strong joy”, were 4.90 (0.43) for joy stimuli, 2.45 (0.29) for neutral stimuli, and 1.68 (0.16) for fear stimuli. Mean fear ratings (with standard deviation in parentheses), on a scale from 1 = “evokes no fear at all” to 6 = “evokes very strong fear”, were 3.92 (0.21) for fear stimuli, 2.26 (0.32) for neutral stimuli, and 1.26 (0.16) for joy stimuli.

Joyful stimuli had been used in previous studies (Koelsch et al. 2010; Fritz et al. 2009; Koelsch et al. 2011) and consisted of CD recorded pieces from various epochs and styles (classical music, Irish jigs, jazz, reggae, South American and Balkan music). Fearful musical stimuli were excerpts from soundtracks of suspense movies and video games.

To increase the fear-evoking effect of the fear stimuli, their relatively high acoustic roughness was further increased by creating dissonant versions, where each musical excerpt was audible in three different pitches simultaneously (original pitch, one semitone higher, and a tritone lower; Fritz et al. 2009; Koelsch et al. 2006). The pitch-shifted, additional counterparts of each excerpt were created so that only their pitch differed, while their tempo remained equal. The original excerpt together with the two pitch-shifted counterparts was then rendered as a single wav-file using Ableton Live (version 8.0.4, Ableton Inc., New York, USA). Neutral stimuli were sequences of isochronous tones, for which the pitch classes were randomly selected from a pentatonic scale. Tone sequences were coded in MIDI (musical instrument digital interface) and generated using the MIDI toolbox for Matlab (Eerola et al. 2004). Importantly, for each joyful-fearful stimulus pair, a neutral control stimulus was generated that matched joyful and fearful stimuli with regard to tempo, F0 (i.e. fundamental frequency) pitch range, and instrumentation (using the two respective main instruments or instrument groups of the respective joyful-fearful pair). To create stimuli that sounded like musical compositions played with real instruments (similar to the joyful and fearful stimuli), the tones from the MIDI sequences were set to trigger instrument samples from a high quality natural instrument library (X-Sample Chamber Ensemble, Winkler & Stahl GbR, Detmold, Germany) and from the Ableton Instrument library (Ableton Inc., New York, USA). Stimuli were then rendered as wav-files using Ableton Live. Using Praat (version 5.0.29; Paul Boersma & David Weenink, 2009, Praat: doing phonetics by computer, http://www.praat.org), all excerpts (joyful, fearful, and neutral) were edited so that they all had the same length (30 s), 1.5 s fade-in/fade-out ramps, and the same RMS power.

Importantly, joyful and fearful stimuli were chosen such that each joyful excerpt had a fearful counterpart that matched with regard to tempo (beats per minute), mean F0 pitch, F0 pitch variation, pitch centroid value, spectral complexity, and spectral flux. This was confirmed by an acoustic analysis of the stimuli using Essentia, a library for extracting acoustical and music features from audio files (http://mtg.upf.edu/technologies/essentia). The Essentia software was also used to test for differences between stimuli with regard to other acoustical factors: 177 acoustical descriptors were extracted frame-by-frame (frame length = 21.5 ms, 50% overlap), averaged along the entire duration of the file, and then compared between conditions (joyful, neutral, fearful) using one-way ANOVAs. Significant effects of condition (Bonferroni-corrected significance-level was p<.001) were indicated for the following acoustic factors (with F values in parentheses, degrees of freedom: 2, 21): (a) Mean (72.3) and variance (13.8) of F0 salience (this measure is highest for single tones, intermediate for chords, and lowest for noises; note that mean F0 and variance of F0 did not differ between joyful, fearful, and neutral stimuli). The mean F0 salience was highest for neutral, intermediate for joyful, and lowest for fearful stimuli (p<.001 in all pairwise comparisons). This reflects that both joyful and fearful (but not neutral) stimuli contained numerous harmonies, and that fearful (but not joyful) stimuli contained numerous percussive sounds, as well as hissing and whooshing noises. (b) Mean (41.3) and variance (28.0) of sensory dissonance. Sensory dissonance was lowest for neutral, intermediate for joyful, and highest for fearful stimuli. Mean sensory dissonance differed significantly between joyful and neutral (p<.001), between fearful and neutral (p<.001), and between joyful and fearful stimuli (p<.05). (c) Mean chord strength (25.2) and key strength (14.7); these factors measure how strongly a sound resembles the sound of a chord, and how clearly the sounds of a stimulus can be attributed to a key. Chord strength was larger for joyful compared to fearful, as well as for joyful compared to neutral sounds ($p<.001$ in each test), whereas fearful and neutral stimuli did not differ significantly from each other. Key strength was larger for joyful compared to fearful ($p<.001$), and for neutral compared to fearful sounds ($p=.01$); joyful and neutral stimuli did not differ significantly from each other ($p>.15$). (d) Mean (30.0) and variance (16.4) of spectral flux, mean spectral crest (30.0) and mean spectral complexity (10.6). Mean spectral flux, spectral crest, and spectral complexity were lowest for neutral stimuli (with significant differences between neutral and joyful, as well as between neutral and fearful stimuli, $p<.05$ in each test), and did not differ significantly between joyful and fearful stimuli ($p>.2$ in each test).

Appendix

Selbständigkeitserklärung

Hiermit versichere ich, dass ich die vorgelegte Arbeit selbständig verfasst habe. Andere als die angegebenen Hilfsmittel habe ich nicht verwendet. Die Arbeit ist in keinem früheren Promotionsverfahren angenommen oder abgelehnt worden.

Berlin, den 28. June 2013

Stavros Skouras

Publications related to this thesis

* authors with equal contribution

Koelsch S*, Skouras S*, Fritz T, Herrera P, Bonhage C, Küssner MB, Jacobs AM (2013). The roles of superficial amygdala and auditory cortex in music-evoked fear and joy. NeuroImage 81:49-60. http://dx.doi.org/10.1016/j.neuroimage.2013.05.008

Koelsch S*, Skouras S* (2013). Functional centrality of amygdala, striatum and hypothalamus in a “small-world” network underlying joy: An fMRI study with music. Human Brain Mapping. http://dx.doi.org/10.1002/hbm.22416

Skouras S, Gray M, Critchley H, Koelsch S (2013). fMRI Scanner Noise Interaction with Affective Neural Processes. PloS one, 8(11), e80564. http://dx.doi.org/10.1371/journal.pone.0080564

Koelsch S, Skouras S, Jentschke S (2013). Neural correlates of emotional personality: A structural and functional magnetic resonance imaging study. PloS one, 8(11), e77196. http://dx.doi.org/10.1371/journal.pone.0077196

Skouras S, Gray M, Critchley H, Koelsch S (under revision for NeuroImage). Superficial Amygdala and Hippocampal Activity During Affective Music Listening at 3 T but not 1.5 T fMRI.

For reasons of data protection, the Curriculum vitae is not published in the online version.